DOWNSTREAM CHANGE IN THE PROCESSES OF RIVERBANK EROSION ALONG THE RIVER SWALE, UK

by

James Robin Grove

A thesis submitted to
The University of Birmingham
for the degree of
DOCTOR OF PHILOSOPHY

School of Geography and Environmental Sciences
University of Birmingham
Edgbaston
Birmingham
UK

November 2000

ABSTRACT

This study was designed to test the hypothesis that riverbank erosion processes altered with increasing distance from a river source. The River Swale, northern England, was monitored at nine sites throughout its 109-km length, from December 1995 – March 1998. Erosion pins, bank-edge surveying, and Photo-Electronic Erosion Pins (PEEPs) were used to determine rates and timings of erosion. The rates were compared against a range of environmental variables based on temperature, river stage, and precipitation at 14-day intervals for erosion pins and 15-minute intervals for PEEPs. This allowed processes of erosion to be inferred.

Catchment erosion rates were modelled using quadratic equations, simulating a mid-basin peak of 3.58 m a^{-1}. Rates of erosion were low upstream, 0.07 m a^{-1}, and also downstream, 0.12 m a^{-1}. Subaerial processes, especially frost action, dominated upstream. Fluvial entrainment was most influential mid-catchment. Mass failures were most efficient downstream, but were more frequent mid-catchment. Piping, sapping and cantilever failures did not follow the same trends and were modelled separately. The length of the erosion season increased downstream as the number of active processes increased.

ACKNOWLEDGEMENTS

I would like to thank NERC for funding my studentship GT4/95/20/F, and the Centre for Ecology and Hydrology (CEH) for being CASE sponsors. The Environmental Change Network, British Atmospheric Data Centre, Environment Agency, CEH, and Yorkshire Dales National Park Authority all efficiently provided essential data and information. The landowners that let me dig up and tramp over their land are much appreciated.

Damian Lawler, Graham Leeks, and John Gerrard all supervised this project. Damian helped getting the project started, especially with advice on PEEPs. He provided comprehensive corrections on drafts of Chapters 2-7, despite numerous mental and physical illnesses. John allowed much needed opportunities to discuss concepts and valuable moral support. I hope Graham is pleased with the results. Colin Thorne and Chris Bradley gave an educational viva, entertaining corrections, and a lot of relief to me by approving this work.

All fellow postgraduates, and the support staff at the School of Geography and Environmental Science, Birmingham University are thanked especially my office mates for putting up with my mess. Neil Harris' fantastic work was a guide in the darkness and he is remembered for his help and kindness. Everyone at the Department of Geography, University of Durham, especially Bob Allison, office mates Toru-Matt-Dave, postgraduates, and housemates should get medals. Louise Bull deserves sainthood for her understanding of my plight, and for acting as a surrogate supervisor.

My sister (Sarah), Adam Sawyer, John Couperthwaite, John Livesey, Iqbal Hamaddudin, Sharon Woodruffe, Dave Tickner, Jenny Clayman, Conor, and Barney were all dragged to the beautiful Yorkshire Dales to get covered in mud. On my way round the country Chris, Laura, Frances, and Clay offered a roof over my head and a counselling service. You are all stars.

Yvette Parkes has managed to put up with permanent Ph.D. crises, after 3 years of B.Sc. moaning. She has been a constant support, and provider of food, especially through all my little *accidents*. Caroline and Yvette deserve awards for managing the fort whilst I was in intensive care, and for finding Bangor Hospital in the end.

I owe my life to Kirsty Jones, plus an unknown climber and his mobile phone, and the Mountain Rescue team at Cader Idris. Words cannot describe my thanks to you all and everyone who put me back together at Bangor Hospital, I also thank the Physios and Dermatologists at Cirencester and Dryburn Hospitals, Oral and Maxillofacial Dept. at Cheltenham Hospital, A+E at Selly Oak and Sheffield Hospitals, my dentist, and the Infectious and Tropical Diseases Dept. at Heartlands Hospital.

To the *special* people on BSES Svalbard Spring '96, and Greenland '98 especially Sally Mackay, Christina Hennessey, Tim Stott, and Frobisher Fire, I love you all. Richard Burt managed to keep me out of Birmingham and sane for a multitude of weekends, without falling off anything. Bob Allison and Graham Philip on the other hand had the brilliant idea of sending me to Syria and Jordan where I could do nothing in my *spare time* but Ph.D. work. Thank-you.

Finally, to my parents and Oonagh the dog. Despite never quite understanding exactly what I was doing you have always been there. What more could I ask.

" Facts may lead to truth just as bricks may finally produce a wall. Facts are to truth what traffic lights and the red tape of government are to order – they are necessities, a cause of more bookkeeping, often way out of proportion to the ends to be gained and a reason why men grow old before their time."

(Talcott, 1936, p.173)

" Every particle of hitherto unknown information obtained in any direction whatever is supposed to, and undoubtedly can if properly pieced together, further the advance of science. But in turn, let me ask, of what use is science except as a means to further the enjoyment of life?

I wonder in this connection who it is who really comes closest to the final truth - the man who ecstatically watches the flight of a bird for the sheer sensation of pleasure derived from the way it banks its corners (and is not that the essence of scientifically apportioned effort?) or the man who cannot afford time to enjoy the sight in his nervous haste to run and fetch a book? – a book that will tell him what the bird's name is, how many toes it has and where else it is known to breed."

(Talcott, 1936, p.172)

" Exploration is the physical expression of the Intellectual Passion.

And I tell you, if you have the desire for knowledge and the power to give it physical expression, go out and explore. If you are a brave man you will do nothing, for none but cowards have need to prove their bravery. Some will tell you that you are mad, and nearly all will say, 'What is the use?' For we are a nation of shopkeepers, and no shopkeeper will look at research which does not promise him a financial return within a year. And so you will sledge nearly alone, but those with whom you sledge will not be shopkeepers: that is worth a good deal. If you march your Winters Journeys you will have your reward, so long as all you want is a penguin's egg."

(Cherry-Garrard, 1994, p.597-598)

CONTENTS

LIST OF FIGURES PAGE N°

CHAPTER 1

CHAPTER 2

PAGE N°

PAGE N°

PAGE N°

PAGE N°

PAGE N°

PAGE N°

PAGE N°

PAGE N°

PAGE N°

PAGE N°

LIST OF TABLES PAGE N°

CHAPTER 1

CHAPTER 2

CHAPTER 3

PAGE N°

PAGE N°

CHAPTER 5

CHAPTER 6

PAGE N°

PAGE N°

CHAPTER 8

LIST OF PLATES PAGE N°

CHAPTER 3

CHAPTER 5

PAGE N°

PAGE N°

CHAPTER 2

THEORETICAL AND EMPIRICAL STUDIES OF BANK EROSION PROCESSES

2.1 INTRODUCTION

The work by Wolman (1959) was the starting point for a suite of different studies that monitored the way in which riverbanks erode. Comprehensive reviews of these erosion process studies are provided by Thorne (1982), Harris (1996), and Lawler *et al.* (1997). This chapter does not seek to repeat these reviews but to introduce and explain the processes of relevance to this study. The model formulated by Lawler (1992a; 1995) (Section 1.1.2) was essentially based around a humid river catchment. The erosion processes identified within these types of systems will be emphasised. The critical conditions needed for erosion process initiation, and the potential variations within a rivers longitudinal profile will also be highlighted.

The five process categories subaerial (including erosion and preparation), fluid entrainment, and mass failures (including fluvial/mass failure and mass failure) (Table 1.1) will be used as subsections within the chapter in order to simplify the complex interactions of processes. The influences of vegetation and anthropogenic activity on erosion processes at a catchment scale are also considered.

2.2 SUBAERIAL PROCESSES

2.2.1 Introduction

"Processes of weakening and weathering act on intact bank material to reduce its strength and decrease bank stability" (Thorne, 1982, p. 228)

Processes that directly erode sediment (subaerial erosion) and those that weaken the bank in preparation for other processes (subaerial preparation) will be considered within this section. The subaerial processes may be divided into three main areas:

1. Cryergic processes: including needle ice growth; ice lens growth; thermo-erosional niching; and snow-melt;
2. Pore water associated processes: including desiccation; slaking; piping and sapping; and gravel lens washout;
3. Rainsplash processes: including raindrop impact; rilling; and gullying.

2.2.2 Cryergic Processes

Needle Ice Growth

Needle ice consists of the growth of fine crystals perpendicular to the bank surface; the ice may incorporate bank sediment during ice nucleation in the bank surface. The crystals are usually around 1 mm in diameter and up to 80-100 mm in length (Outcalt, 1971). Three conditions are needed for needle ice development (Lawler, 1988b, p. 295; adapted from Outcalt, 1971):

1. An approximately low equilibrium surface temperature (T_{es}) to initiate ice nucleation;
2. A sufficiently low soil water tension (W_t) for ice segregation to take place (i.e. a sufficiently high moisture content);
3. A sufficiently fast migration of unfrozen moisture to the freezing front, in order to match the rate of latent heat loss at the plane of segregation and so prevent the *in situ* freezing of pore water.

Near perfect growth conditions, of high soil moisture contents and soil surface temperatures of –1 to –4 ^{o}C, mean that the freezing front may not descend into the bank. This results in clear, none erosive, ice formation. If the freezing front does enter into the bank surface then sediment may be incorporated into the ice in several mechanisms (Branson *et al.*, 1992, p. 361):

A. As distinct bands of soil within the needle ice, producing multi-tiered crystals;
B. Dispersed throughout the crystal, producing dirty needle ice;
C. As a soil cap pushed up by the ice needles;
D. As aggregates pushed up between dispersed needle-ice crystals.

Dirty ice (B) results from the crystal growth being stressed due to the freezing front moving into the bank surface. This may be caused by a limitation in moisture supply or a sharp decrease in the soil moisture content. The capping of the ice (C) occurs when there is a 15-25 % soil moisture content, not enough for needle ice growth only for *in situ* nucleation. After this a period of sufficient soil moisture conditions will elevate the cap so sits on top of the ice crystal growth.

In terms of sediment erosion from the bank surface four different delivery mechanisms were identified by Lawler (1993b, p. 104-105) (Figure 2.1):

1. Direct particle fall.
2. Sediment laden rivulets.
3. Needle ice sliding failure.
4. Needle ice toppling failure.

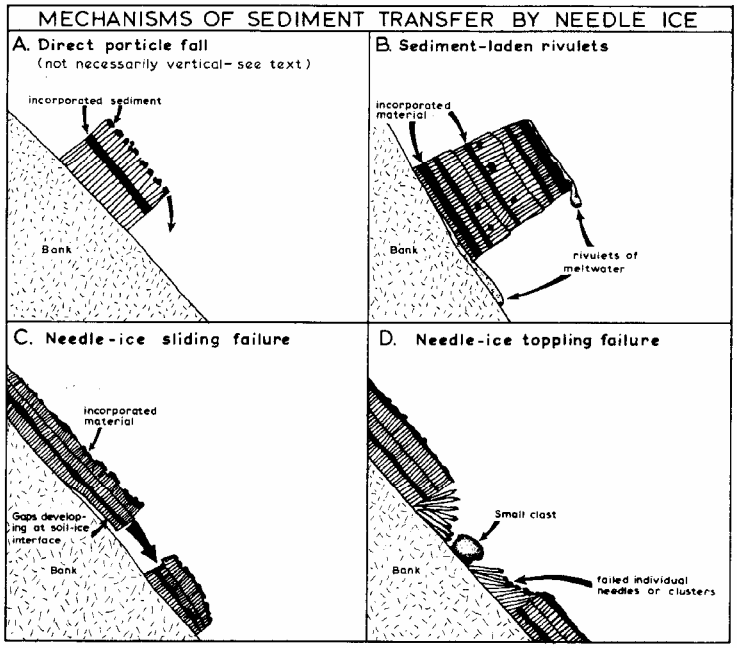

Figure 2.1 Mechanisms of sediment transport by needle ice: (**A**) direct particle fall; (**B**) sediment-laden rivulets; (**C**) sliding failure; (**D**) toppling failure (Lawler, 1993b, p. 104).

The sediment released by needle ice heaving can either fall directly into the river, as subaerial erosion, or be left on the surface of the bank as a layer of reduced shear strength material, subaerial preparation. The removal of the residue by fluvial entrainment produces notches or trim lines, where the material below the maximum stage height is removed.

Examining the relationship between needle ice and sediment production statistically, Lawler (1986) found that 92.4% of the variation in erosion rates, measured on erosion pins (Section 3.4.3), were explained by the air frost frequency. Estimates of sediment production from needle ice were made using the length of sub-zero temperatures, grass minimum temperatures and the Antecedent Precedent Index (Section 2.3.2) at a catchment in South Wales (Lawler, 1993b). The sediment yield from needle ice, during a 834 day study period, was estimated as 23.6 kg m^{-2} or 32.04 kg m^{-2} from the different methods. This equated to needle ice accounting for 32 % or 43 % of the pin measured erosion rate. Stott (1997) also found frost to be significant in the Balquidder catchments, Scotland; however afforestation was found to reduce amount of frost occurrence (Section 2.5).

The length of time the bank is frozen, and the texture of the riverbank sediment, may affect the longitudinal variation of frost action within a catchment. The particle size distribution of the bank sediment will control its moisture retention characteristics, as the bank sediment becomes coarser its ability to retain water is reduced (Meentemeyer and Zippin, 1981). Fine grained soils, such as clays, may not be able to transport water fast enough to maintain needle ice growth due to their high suction and low permeability (Derbyshire *et al.*, 1980).

Thermo-Erosional Niching

Freezing of the whole bank profile followed by river flow inundation can result in the lower bank 'defrosting'. This means that the upper bank maintains a high shear strength whilst it remains frozen but the lower bank becomes weaker and prone to preferential erosion by fluvial entrainment. As the upper bank becomes undercut the potential for overhangs and mass failures occurs. Scott (1978) found cohesive material in Alaska more susceptible to niching than non-cohesive sediment, whilst Miles (1976) observed removal of basal gravel creating an unstable upper gravel layer in Arctic Canada.

Although a mechanism mainly found in permafrost areas of the higher latitudes, the potential for thermo-erosional niching may occur to a limited extent in areas with prolonged sub-zero temperatures in the U.K. Low banks in the colder upper catchment may be susceptible, due to the reduced freezing depth needed.

Snow Melt

Miles (1976) found that snowmelt and sloughing in Arctic Canada delivered fine material into the channel from the riverbanks. Melting of the interstitial ice in the bank sediment reduces the shear strength of the material by increasing the pore water pressure, and lowering the interstitial strength provided by the freezing of pore water. The angle of the slope will influence the amount of sediment eroded; a steep slope would increase the potential for sediment to become incorporated into the semi-melted, or melted, snow due to the increased potential energy. Vertical, or near vertical, slopes would not accumulate snow so are less likely to be prone to this process.

2.2.3 Pore Water Associated Processes

Desiccation

The drying of the bank face can alter the physical structure of the sediment. The creation of void spaces, once occupied by pore water, can leave a friable structure. Expansive clays containing sodium montmorillionite are particularly prone to desiccation due to the comparatively large change in volume between saturated and unsaturated states. In wet conditions the clay expands, absorbing the pore water, on the drying the structure becomes crumb-like with lower aggregate cohesion and a larger roughness surface. Extremes of moisture content will therefore aid the efficacy of this process, such as those found in semi-arid regions.

There is a paucity of research into desiccation processes and their effects on bank erosion rates. Direct soil fall caused by drying of the sediment on the base of overhanging blocks has been observed (Duysings, 1986). The weakened desiccated material may act as store of prepared material ready to be removed by another process (Bello *et al.*, 1978). Abam (1997) found that

preferential drying within the bank profile created strata with decreased shear strengths allowing preferential erosion.

High summer temperatures in the Sieve catchment, Italy, caused intense desiccation and cracking leading to the formation of slabs partially detached (Rinaldi and Casagli, 1999). Clay material alongside drier conditions during the summer months would be expected in the lower catchment region.

Slaking

The rate at which the bank wets up on the rising limb of the flood hydrograph can produce pressure differences in the sediment. Preceding the wetting front there is a wave of increased pressure due to the evacuation of air from the void spaces as they become filled with water. This pressure wave may push/explode the surface sediment off the bank face (Thorne, 1982). This process can be difficult to identify in the field as the following flood wave could entrain the failed material, which maybe why there are few published articles on the subject.

Piping and Sapping

Seepage exfiltration from the riverbank that is competent enough to entrain the bank sediment may be able to erode a tube like structure, this process is termed piping (Hagerty, 1991a). If the seepage is over a larger area the term sapping may be used. Initiation of piping and sapping involves a complex interactions of processes (Jones, 1981) however there needs to be the potential for seepage, which could be created from infiltration during high flows, recharge from ground water, surface infiltration, or throughflow. Alluvial material is particularly suited to piping initiation because of the interbedding of sand and clay layers, resulting in preferential flow through the more porous sand (Hagerty *et al.*, 1981). The decreasing hydraulic conductivity of a soil with depth, due to compaction, also aids piping and sapping caused by the creation of lateral flow through the bank face.

The eroded material from the bank surface may accumulate in front of the zone of exfiltration, blocking the flow, lowering the seepage potential, and therefore the amount of erosion that can take place as well. The cavities produced by the removal of sediment may make the upper bank

unstable (Figure 2.2), producing the conditions for mass failures (Section 2.4). The failure of overlying material may again block the seepage from the bank and also hide the evidence of the piping, or sapping.

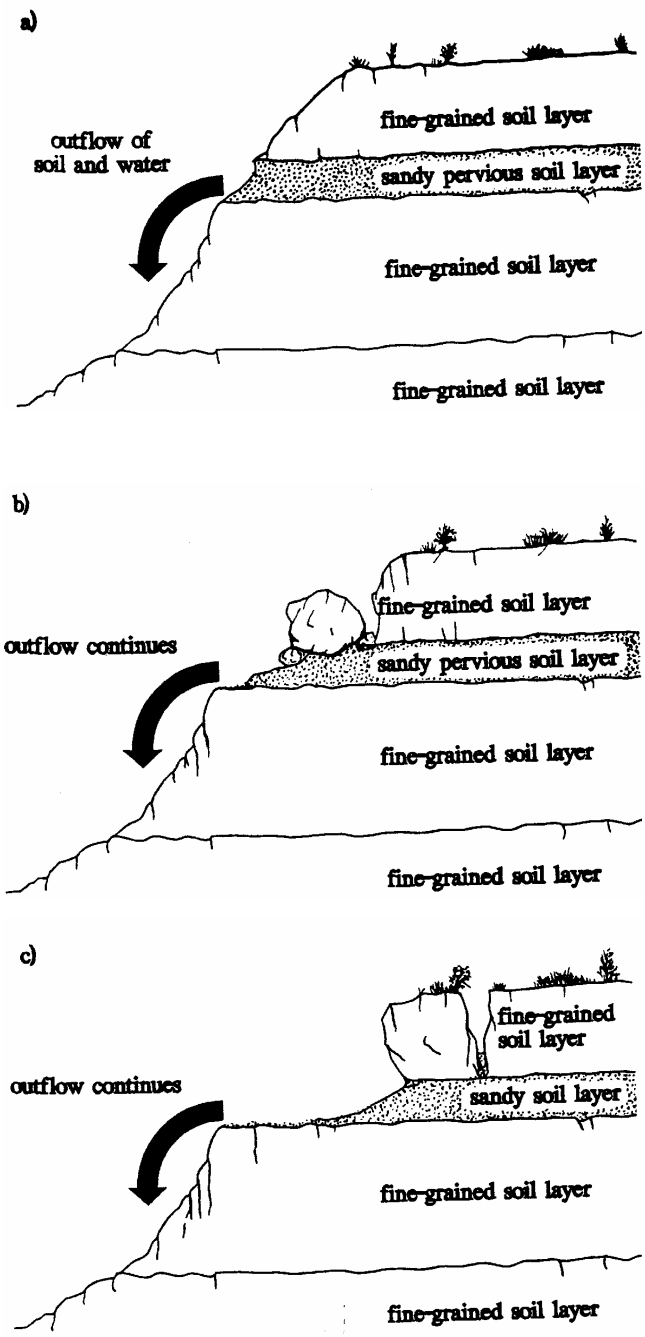

Figure 2.2 Piping and sapping failure. (**A**) Bank erosion by piping/sapping with subsequent collapse: seepage outflow initiates soil loss. (**B**) Bank erosion by piping/sapping with subsequent collapse: undermined upper layer fails, blocks detached. (**C**) Bank erosion by piping/sapping with subsequent collapse: failed blocks topple or slide (Hagerty, 1991a, p.993).

Burial by soil fall, confusion with animal burrows or bird nests, and flood inundation after failure make the piping process difficult to identify in the field. Because of this Hagerty (1991b) provides the following identification hints:

1. Cavities may be up to 1 m in diameter, and from 0.3 – 6 cm in depth;
2. A debris fan may be formed at the base of the seepage area if the material is not removed;
3. Discolouration of the bank surface where elluviation has occurred;
4. Cusp shaped debris flows (Section 2.4.6) formed in thick loose pervious layers. These may also be due to increased pore pressures;
5. Multiple scarp faces caused by piping removing underlying sandy areas. The scarp faces may appear like those formed by wave action but can be differentiated by being less regular in form.

The likelihood of piping and sapping will be maximised in catchment regions that contain banks consisting of clay and sand layers. The bank height would also have to be sufficient to allow enough potential energy to build in the saturated material forcing out the exfiltrating fluid.

Gravel Lens Washout

The deposition of large waterborne vegetation, Coarse Woody Debris (CWD), acting in conjunction with a gravel lens in the bank to undermine the banktop (Davis and Gregory, 1994). The CWD redirects the flow structure in the river by causing an obstruction, leading to impinging flow into the gravel lens. The gravel is entrained preferentially, leaving the more cohesive upper bank unsupported. The destabilised banktop then has the potential to fail by slow subsidence of a mass failure (Figure 2.3).

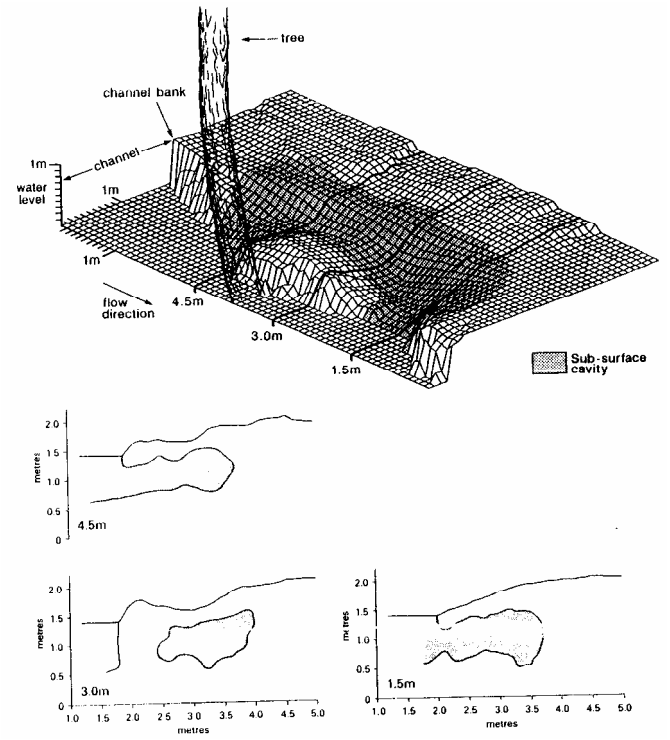

Figure 2.3 A three-dimensional representation of the subsiding bank in August, showing the extent of the sub-surface cavity and selected cross-sections across the feature in relation to the position of the tree (Davis and Gregory, 1994, p. 7).

2.2.4 Rainsplash Processes

Rainsplash or Raindrop Impact Erosion

Direct impact of raindrops on to a soil surface may lift the surface particles moving them downslope. The process may be cumulative with the falling particles hitting, and initiating movement in, other particles. The process is most effective on slopes with angles of 33-45°, and is affected by rainfall intensity (Figure 2.4), drop size distribution, and the terminal velocity of the falling drops (Salles and Poesen, 2000). It is not until the ground surface is covered by a depth of water of around three raindrop diameters that it is protected from impact erosion (Moseley, 1973).

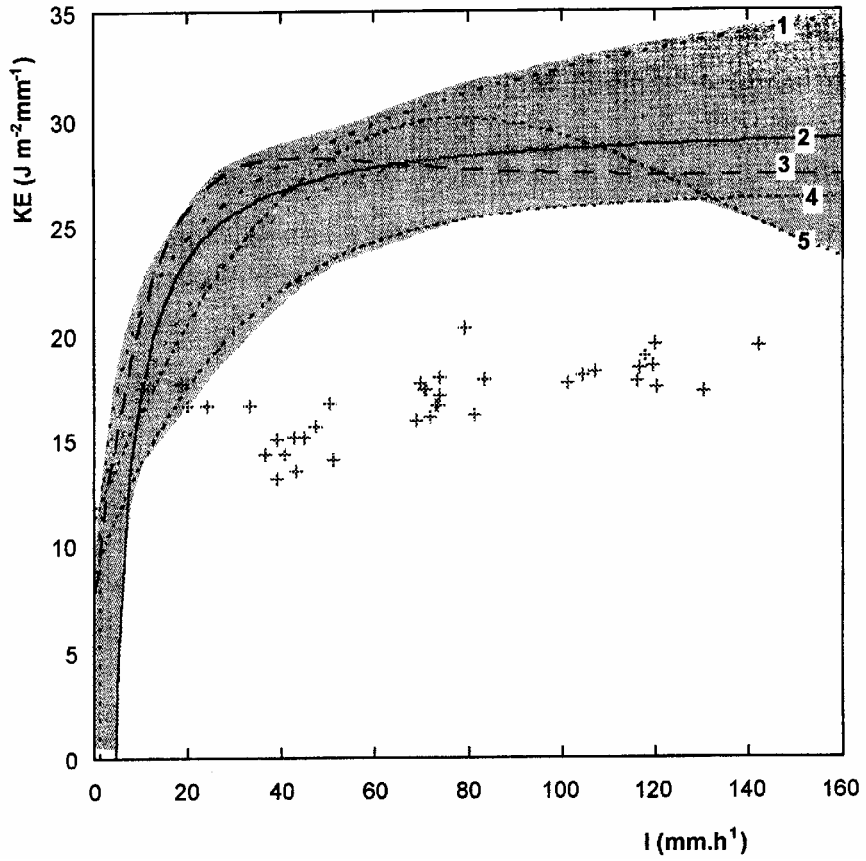

Figure 2.4 The kinetic energy (KE) of the raindrop size distributions produced by a four-nozzle rain simulator versus rain intensity (I). The grey area indicates the different relationships between KE and I given in the literature; (1) Zanchi and Torri (1978) in Italy; (2) Hudson (1965) in Rhodesia; (3) McGregor and Mutchler (1976) in the USA (Mississippi); (4) Rosewell (1986) in Australia; (5) Carter et al., (1974) in the south central USA (Salles and Poesen, 2000, p. 275).

The percentage of the surface exposed to direct rainfall, slope angle, organic carbon content, and proportion of fine sand (50-250 μm) controlled the amount of rainsplash erosion in the Schrondweilerbaach catchment, Luxembourg (Duysings, 1986). The high intensity rainfall during summer thunderstorms produced a summer peak in the amount of eroded material from raindrop impact. This may have been aided by the fact that soil surface had dried, therefore becoming more susceptible to particle detachment (Bello *et al.*, 1978). This may be more likely to occur in the lower catchment regions where the rainfall may be sporadic during the summer months, allowing the soil to dry but still supplying intense rainfall.

2.3 FLUID ENTRAINMENT

2.3.1 Introduction

The process of fluid entrainment under consideration is the incorporation of material from a river channel boundary into solution, suspension, or bedload due to fluid forces. Bank erosion is controlled by both the composition of the bank sediment and the interacting fluid (Grissinger, 1982). The processes important in these two factors will be discussed alongside the eight factors indicated by Lawler *et al.* (1997, p. 150) that influence fluvial processes (Table 1.2).

2.3.2 Sediment Influences on Entrainment

Bank sediment may be divided into two main sub-classes in terms of its entrainment mechanics: cohesive and non-cohesive (Thorne, 1982).

The entrainment of non-cohesive sediment is better understood than for cohesive materials, with sand and gravel have resisting forces resulting from their immersed weight. Laboratory testing of riverbed entrainment has resulted in empirical relationships between flow velocities and sediment movement, into suspension, saltation or bedload (Richards, 1982). A non-cohesive grain on the riverbed will have a fluid force and lift force that will be resisted by the force of gravity (Figure 2.5) (Morisawa, 1985). Once the force of gravity is exceeded by these factors entrainment will commence.

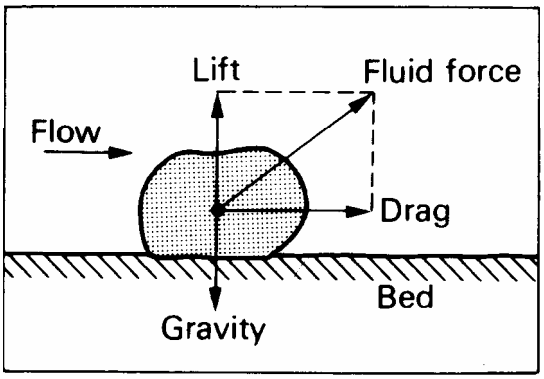

Figure 2.5 Forces acting on a grain lying loose on the channel bed (Morisawa, 1985, p. 43).

An additional consideration for riverbank modelling, from this simple case, is the downslope component of the channel side slope (Figure 2.6). The equation (Equation 2.1) developed to model fluid entrainment of a non-cohesive bank (Task Committee on Sedimentation; cited in Thorne, 1982, p. 229) includes this term but does not account for packing modes, such as imbrication, in coarse sediment that would increase the shear stress needed for entrainment (Thorne *et al.*, 1998a). The lift force is also not included (Thorne, 1982) however the empirical basis of the formula will cause these factors to be intrinsic within the model to a degree, they are however not considered separately.

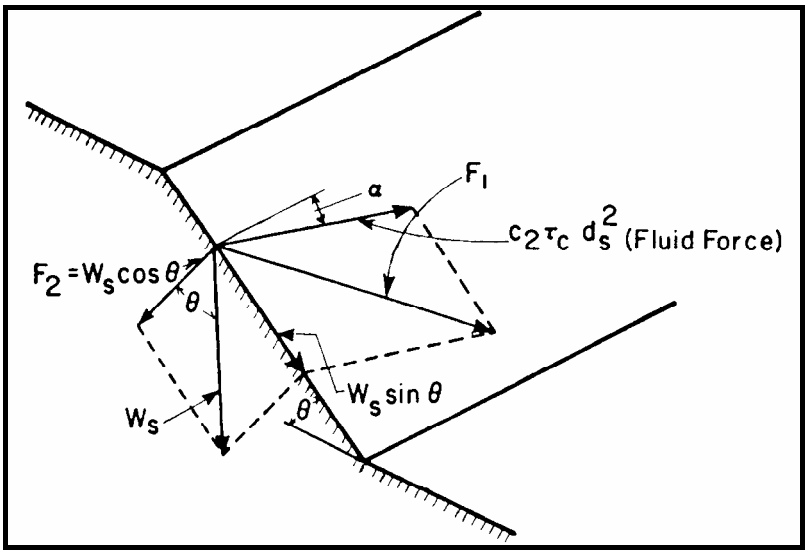

Figure 2.6 Forces on a particle at the surface of a submerged non-cohesive bank (Thorne, 1982, p. 230).

$$\tan\phi = \left[\frac{F_1}{F_2}\right] = \left(\frac{c_2^2\tau_c^2 d_s^4 + W_s \sin^2\theta + 2c_2\tau_2 d_s^2 W_s \sin\theta \sin\alpha}{w_s \cos\theta}\right)^{0.5} \qquad (2.1)$$

Where:

F_1 = disturbing force;
F_2 = restoring force;
d_s = grain size;
W_s = submerged weight of grain;
c_2 = a constant such that the effective surface area = $c_2 d_s^2$;
θ = bank angle;
α = flow angle to longstream direction;
ϕ = friction angle;
τ = critical boundary shear stress.

Cohesive sediments, usually clay sized material, have electromechanical forces that bind the particles together. When subjected to a stress, such as from boundary fluid forces, the particles may not be removed individually but as aggregates. These particle clusters will have a proportion of void space within their structure, making them less dense than a single unit of quartz. This results in a lower force being needed to lift them off the bed/bank than a solid particle of the same dimensions (Richards, 1982; Lawler *et al.*, 1997). The past conditions that the sediment has been subjected to will alter the degree of cohesion, which makes exact prediction of shear stresses needed for entrainment difficult. The stability of the cohesive sediment may be affected by (Grissinger, 1982, p. 276):

1. Mean particle size;
2. Clay and organic matter content;
3. Type of clay;
4. Bulk density or void ratio;
5. Solution phase/exchangeable ionic strength and composition.

Solute fluxes within cohesive material may increase the pore water pressures in-between both aggregates and particles, reducing the effective cohesion and its resistance to entrainment. The chemical composition and temperature of the pore water may also weaken the cohesive forces, increasing the sodium ion content will reduce the shear resistance of the sediment (Osman and Thorne, 1988). If this does occur then the mineral could be leached out of the soil in solution, or elluviation may wash fines though the sediment horizon. These processes all lower the effective strength of the sediment, thus increasing the potential for entrainment.

The boundary shear stress on the sediment surface will be affected by the surface roughness. A completely homogeneous smooth surface would create little drag and therefore be less prone to entrainment as the particles would be contained in the laminar sublayer (Knighton, 1998). The layering within alluvial sediments can lead to more heterogeneous material, with preferential erosion of certain layers. The surface would become uneven, leading to conditions of enhanced roughness (Grissinger, 1982).

The amount of water entering the sediment may be influenced by the preceding precipitation (Hooke, 1979). The moisture content, not including the input from river inundation, may be simply modelled using the Antecedent Precipitation Index (API) (Equation 2.2) (Gregory and Walling, 1973).

$$API_d = (API_{d-1} \times 0.9) + P_d \quad (2.2)$$

Where:

API_d = the API for the day under consideration;
API_{d-1} = the previous days index;
P_d = the precipitation on the day under consideration.

The constant 0.9 is a decay constant reflecting the drying of the catchment moisture, so if it is set near to 1 it relates to a poorly drained catchment such as those containing peat bogs.

2.3.3 Entrainment Fluid Dynamics

The prevalence of erosion during high flow events (Thorne and Abt, 1993) has resulted in research to determine how fluid forces interact with the bank sediment. The velocity distribution over the bank surface indicates where the forces of drag and lift may be maximised, and therefore where the maximum potential for entrainment exists. In practical terms it is difficult to measure the boundary velocities at the channel margin due to the fact that the instrumentation will often disrupt the flow structure creating a false reading, although this has been overcome (to some extent) by the acoustic Doppler velocimeter (Lane *et al.*, 1998).

In spite of the measurement problems Osman and Thorne (1988) adapted the equation used to predict average shear stress (Equation 2.3) using empirical data to model the rate of cohesive bank lateral erosion. On gravel channel margins Pizzuto (1990) used Equation 2.4 (Figure 2.7) to predict the shear stress distribution on gently curved riverbanks, in order to model channel widening.

$$\tau_o = \rho g R S \tag{2.3}$$

Where:

τ_o = reach-mean average shear stress (N m^{-2});
ϱ = fluid density (1000 kg m^{-3});
g = gravitational acceleration (9.81 m s^{-2});
R = hydraulic radius (m);
S = channel slope (m m^{-1}).

$$\tau_o = \rho g S \frac{dA}{dP} + \frac{d}{dP}\int_0^{D_N} \tau_{\eta x} d\eta \tag{2.4}$$

τ_o = local boundary shear stress ;
dA = area between normals to the bed;
dP = wetted perimeter above dA;
D_N = distance along a normal from the bed to the water surface;
η = a spatial coordinate along normals to the bed;
$\tau_{\eta x}$ = local downstream-directed shear stress induced by turbulence which acts on the normals.

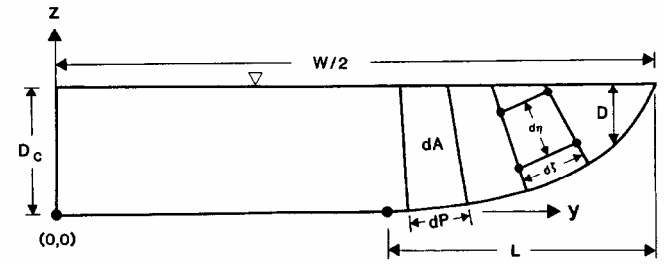

Figure 2.7 The coordinate system and variables used to describe local boundary shear stresses for a gravel channel calculated using Equation 2.4. The spacing between normals and grid points along normals is greatly exaggerated (Pizzuto, 1990, p. 1972).

The preceding theorems have been based around a flow component in the downstream direction. Secondary flow may be created in the channel, due to boundary effects. The force may be in the plane normal to the local axis of the primary flow. In a meander bend the outer bank cell created by secondary currents may produce an increased shear stress on the channel boundary increasing the potential for entrainment.

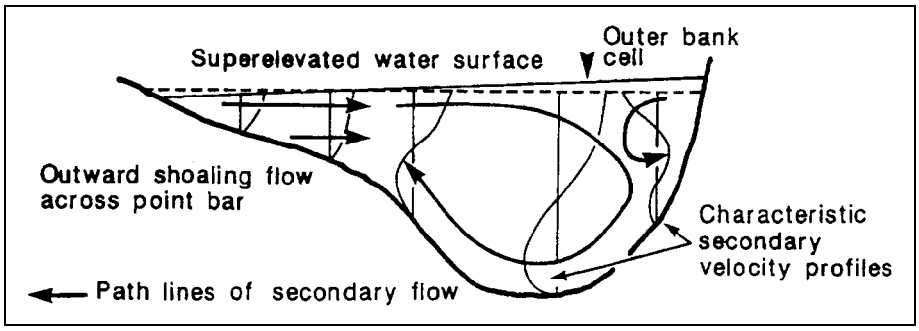

Figure 2.8 Secondary circulation pattern at a river bed cross-section, showing the main circulation cell restricted to the deepest part of the section, the cell of reverse circulation at the outside bank and shoaling-induced outward flow over the point bar at the inside bank (Markham and Thorne, 1992; cited in Bathurst, 1997, p. 74).

The changing distribution of velocities during a flood event may alter the pattern of entrainment in the channel, this is especially true in a meander bend. The position of the maximum shear stress/impinging flow may move downstream during a high flow event (Hooke, 1995) if the meander bends are not tightly spaced together (Parker *et al.*, 1983). This may result in meanders not growing laterally but migrating downstream instead.

The problems involved in estimating the boundary shear stresses in a channel due to the variations in flow structure (Mosselman, 1992), and non uniform bank topography, have led to the use of stream power as a fluvial entrainment predictive tool (Lawler, 1992a: 1995; Annandale, 1995; Annandale and Parkhill, 1995). To investigate the changing potential of the river to entrain at a catchment scale an approximation of the energy available in channel cross-sections, or reaches, may be made (Equation 2.5) (Bagnold, 1960). The nomenclatures used for different stream power scales of measurement are described by Rhoads (1987) (Table 2.1).

$$\Omega = \rho g Q S \quad (\text{kg m s}^{-3}) \tag{2.5}$$

Where:

ρ = fluid density (kg m^{-3});
g = acceleration due to gravity (m s^{-2});
Q = discharge (m^3 s^{-1});
S = energy slope (m m^{-1}).

TERM	SYMBOL	FUNCTIONAL FORM	DEFINITIONAL FORM	SI DERIVED UNITS	SI BASE UNITS
Total Stream Power	ρ	$\rho gQSX$ ($\int_x \rho gQS\, dx$)	Power of a defined reach of a stream channel	Watts	Kg m^2 s^{-1}
Cross-sectional Stream Power	Ω	ρgQS	Power per unit length of a defined reach	Watts/m	Kg m s^{-1}
Mean Stream Power	ω	$\rho gRVS$	Power per unit wetted area of a defined reach	Watts/m^2	Kg s^{-1}
Unit Stream Power	vs	VS	Power per unit weight of water	Watts/ Newton	m s^{-1}

Table 2.1 Standardised stream power nomenclature (Rhoads, 1987, p. 194). Where: (X) is the length of the flow reach (m); (R) is the hydraulic radius (m); (V) is the mean velocity (m s^{-1}).

To predict where in a longitudinal profile stream power is maximised, and therefore entrainment as well if the two variables are connected, Lawler (1992a) used the variations in discharge (Q) and slope (S) at a catchment scale. Discharge was proposed to vary as an exponential function of the distance downstream (Equation 2.6), and slope as a negative exponential function of distance downstream (Equation 2.7).

$$Q = kL^m \tag{2.6}$$

Where:

Q = Bankfull discharge (m^3 s^{-1});
L = Channel length (km).

$$S = S_o e^{-rL} \tag{2.7}$$

Where:

S_o = initial slope at some upstream reference section (m m^{-1});
r = coefficient of slope reduction.

Variations in both the discharge and slope, from a river's source to its estuary, have been found to cause peaks in stream power (Lewin, 1982; Lawler, 1992a; 1995; Lecce, 1997; Abernethy and

Rutherfurd, 1998; Knighton, 1999). The stream power peaks are mainly found mid-catchment (Section 1.1.2), as the slope may be maximised upstream but the discharge is at a peak downstream. Constrictions of the channel, both natural and anthropogenic, may not allow the channel to attain its minimum stream power dimensions (Chang, 1979). This would raise the stream power relative to its surrounding 'natural' geomorphology.

2.3.4 Basal Endpoint Control

Modelling the effectiveness of removal of basal sediment by entrainment gives an indication of the general 'state' of stability of the bank. Three states have been identified (Thorne and Osman, 1988):

1. Impeded Removal

Inputs of sediment, from stream and bank, are higher than the volume being removed. Net accumulation results, which lowers the bank angle and height.

2. Unimpeded Removal

Inputs of sediment are balanced with outputs of sediment. This is therefore a state of equilibrium. The bank may retreat by parallel retreat if the sediment load at the bank base is above zero.

3. Excess Basal Capacity

Inputs of sediment are lower than the outputs. Basal retreat, and lowering, occurs increasing the bank angle, and height. The retreat results in increased bank erosion due to instabilities.

The state of the bank is not fixed. The three states of basal capacity will therefore interchange and over time in theory unimpeded removal should result, as long as there are no external inputs to the system.

2.4 MASS FAILURE PROCESSES

2.4.1 Introduction

The downslope movement of a unit of sediment (or rock) due to the internal strength becoming lower than gravitationally induced stresses is known as mass movement/failure/wasting. The failures are not directly caused by ice, water and air but are frequently aided by these variables (Selby, 1982). The exceedence of the shear strength of the soil by the stresses of the overlying material weight, or seepage forces, may be quantified using the 'factor of safety' (Equation 2.8) (Hemphill and Bramley, 1989).

$$F_s = \frac{soil\ shear\ strength}{shear\ stress\ imposed\ on\ the\ soil} = \frac{s}{\tau} \tag{2.8}$$

When the value of F_s reaches unity a failure is imminent, lower values indicate decreasing stability, whilst values less than one should not exist in reality as a failure should have already occurred. Internal shear strengths of the sediment are usually related to the cohesion and friction of the sediment. Undercutting of the bank toe, seepage, and high pore water pressures will all reduce the soil strength (Figure 2.9).

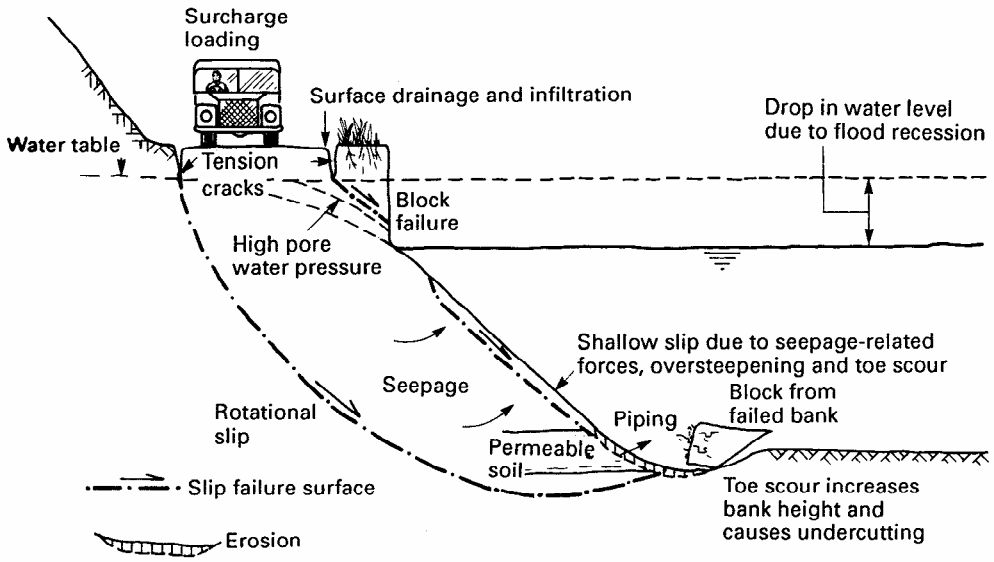

Figure 2.9 Channel cross-section illustrating processes responsible for mass failure (Hemphill and Bramley, 1989, p. 27).

The different types of mass failure are basically described by their morphology. Cantilever, planar, pop-out/draw-down, and rotational failures will all be discussed as well as sediment flows.

2.4.2 Cantilever Failures

The undercutting of a riverbank by the removal of basal material can lead to instabilities in the upper bank profile. The mechanism often cited is the removal of basal gravel by entrainment, leaving an unsupported cohesive sediment layer (Thorne and Lewin, 1979; Rinaldi and Casagli, 1999). The upper layer of sediment may be more resistant to erosion because of their higher shear strength, provided by the cohesion of fine sediment or the root strength from vegetation (Sidle, 1991). Lower non-cohesive sediment may lose strength by winnowing of interstitial material, reducing the angle of internal friction (Carson, 1971). The potential for entrainment may also be raised in the basal area due to the increased number of flows that encroach on the lower bank, when compared against the upper bank (Thorne and Tovey, 1981; Hickin and Nanson, 1984).

The bank does not necessarily need to be composite in nature for cantilever development. Abam (1997) found that in the Niger Delta the differing moisture regimes in the bank profile produced heterogeneity in homogenous sediment. The wetting and drying sequence of lower layers increased pore water pressures and allowed desiccation processes (Section 2.2.3) to occur at depth, whilst on the surface the vegetation bound the soil (Section 2.5).

A block of overhanging sediment may fail by several different mechanisms, of which Thorne and Tovey (1981) identified 3 main processes (Figure 2.10):

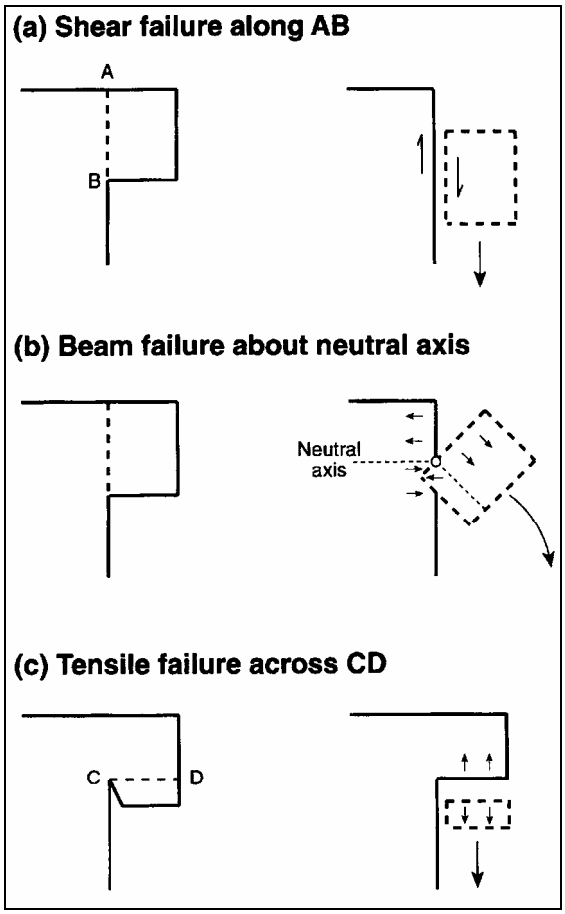

Figure 2.10 Modes of cantilever failure on composite river banks (Thorne and Tovey, 1981, p. 475).

1. **Shear failure** (Figure 2.10A). A vertical shear plane is developed, possibly along an interped fissure: the block then fails due to an increase in weight or a decrease in the coherency of the soil. These failures most often occur in sandy soils, which have an inherent low cohesion. A lack of vegetation to bind the soil also aids this failure.

2. **Beam failure** (Figure 2.10B). A block of soil has a neutral axis where forces of tension above are being balanced by compression below. Increasing the weight of the block unbalances the opposing forces allowing the cantilever to fall forward. This is the most common of the cantilever failure mechanisms.

3. **Tensile failure** (Figure 2.10C). The base of an overlying block may develop a horizontal failure plane across the unit. When the tensile strength is less than the stresses produced by the weight of the material under gravity then the soil beneath the failure plane may fall. The failure is facilitated by the formation of a tension crack at the bottom of the overhang,

between the block and bank face. This crack may be formed by expansion when the block is exposed on its upstream or downstream sites. The removal of overburden material, creating a change in the effective pressure, allows the material to move always from the bank surface. Desiccation (Section 2.2.3) may also aid the formation of the crack by drying and shrinking aggregates.

2.4.3 Planar Failures

A planar failure plane often found in steep (>60°) relatively low banks may lead to a wedge of slab failure (Osman and Thorne, 1988). The basic bank profile, and the controlling factors, used in the consideration of a planar failure are shown in Figure 2.11.

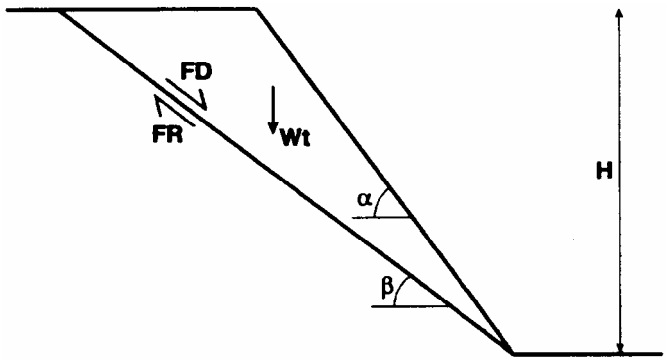

Figure 2.11 Idealised bank profile used in simplified bank stability analyses. Symbols: β = failure plane angle, a = uneroded bank angle, W_t = weight of failure block, FD = driving force, FR = resisting force, H = total bank height (Darby *et al.*, 2000).

Long shallow planar failures, of around 1-4 m in depth, may be termed translational failures (Selby, 1982). The shallow depth does not require the same deep percolation of water experienced in other failures, the infiltration of heavy rainfall is sufficient to trigger the collapse. A combination of blocks sliding and/or debris flows (Section 2.4.6), depending on the variability in moisture content, may distinguish this failure.

Failures, often found in steep alluvial material on the outside of meander bends, may be modelled using the Culmann analysis (Selby, 1982):

$$H_c = \frac{4c}{\gamma} \frac{\sin\alpha \cos\phi}{[1-\cos(\alpha-\phi)]} \quad (2.9)$$

Where:

H_c = critical height of slope for stability (m);
c = internal cohesion of the soil (kPa);
γ = unit weight of soil or rock at a natural moisture content (kN m^{-3});
β = angle of the surface slope (^{o});
ϕ = angle of internal friction (^{o}).

This model is based around the total stress on the sediment, not including the pore pressures within the sediment, and so should be applied to permeable soils. The failure is considered to take place at the same time over the whole failure plane. In fact the elasticity and heterogeneity of riverbank sediment has the potential to fail at different times along the failure plane (Lohnes and Handy, 1968; Little *et al.*, 1982). The tension cracking at the back of the failure will alter the position of the failure plane and so the model may be re-written to include a tension crack that extends to around one-half of the total bank height (Thorne, 1982):

$$H_c^{'} = \left(\frac{2c}{\gamma}\right) \tan\left(45 + \frac{\phi}{2}\right) \quad (2.10)$$

Even including tension cracks there are still problems in applying Equation 2.10, these are summarised by Darby *et al.* (2000, p. 177).

1. The failure plane is constrained to pass through the toe of the bank. Field observations indicate this is sometimes unrealistic (Simon *et al.*, 1991).
2. The effects of soil pore water pressures and the hydrostatic confining pressure of water in the channel are usually either ignored, or characterised by a simplified pore pressure ratio term (Simon *et al.*, 1991).
3. Application of the planar failure analysis is restricted to very steep banks (Taylor, 1948; Millar and Quick, 1997).

In response a computer program has been developed for stability analysis of steep, cohesive riverbanks. The model used to create the computer program is summarised by Figure 2.12.

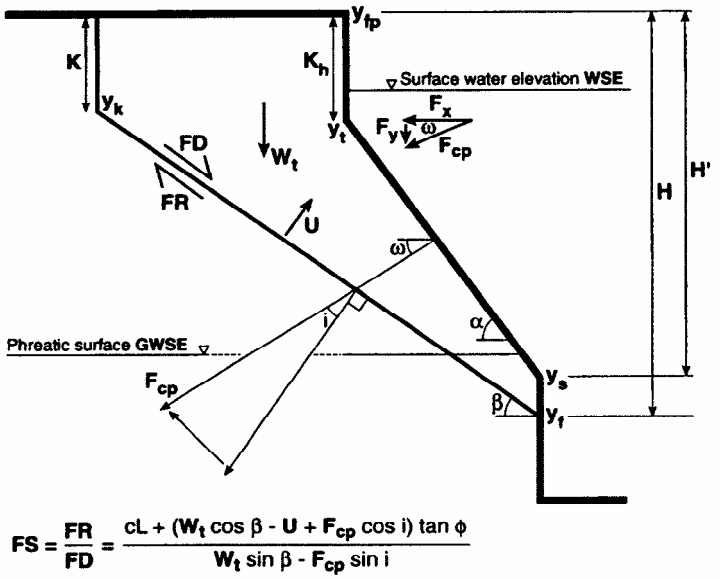

Figure 2.12 Definition diagram for the Darby-Thorne bank stability analysis (modified after Darby and Thorne, 1996). Symbols: K = tension crack depth, K_h = relic tension crack depth, i = angle between resultant of hydrostatic confining force and normal to failure plane, β =failure plane angle, U = hydrostatic uplift force, F_{cp} = hydrostatic confining force, ω = angle at which the resultant of the hydrostatic confining force is directed, α = uneroded bank angle, GWSE = groundwater surface elevation, WSE = surface water elevation, W_t = failure block weight, FD = driving force, FR = resisting force, y_{fb} = floodplain elevation, y_t = base of 'vertical face', y_s = elevation of base of uneroded bank slope (base of 'upper bank'), y_f = elevation of base of failure plane, y_k = elevation of base of tension crack, H = total bank height, H' = uneroded bank height, L = length of failure plane. The terms 'vertical face' and ' upper bank' are defined and used by Simon and Hupp (1992) (Darby *et al.*, 2000, p. 176).

In his suggested model of downstream changes in bank erosion Lawler (1992a; 1995) used Equation 2.10 to estimate the critical height at which bank of known sediment cohesion (c), saturated bulk unit weight (γ), and friction angle (ϕ), will fail. Models of channel geometry throughout a river's longitudinal profile (Leopold and Maddock, 1953; Prestegaard, 1988) mean that for a given bank sediment the critical point within the catchment for planar failures to be initiated can be identified when the channel exceeds the critical failure height (H_c).

These models of channel geometry usually predict sediment fining downstream resulting in higher banks formed by more cohesive sediment. The models of channel geometry are probably based around straight channel reaches with a 'predictable' geometry, rather than areas with riffles and pools. This could cause an underprediction of bank heights. The model (Lawler, 1992a) also

assumes the catchment to have a single sediment type, bank angle, riparian vegetation and channel-margin hydrology.

The model has the ability to predict the regions within a catchment that are of a sufficient bank height to fail by a slab or wedge failure mechanism. It is suggested (Lawler, 1992a) that the technique could be extended to predict the critical point in the catchment for other types of mass failure to occur. Implicit within the model (Figure 1.1) is the assumption that once the critical height for a failure has been reached the failures downstream will become larger or more frequent, and therefore have a greater efficacy, as the bank height increases.

2.4.4 Pop-out or Draw-down Failures

The failure processes needed for pop-out failures are similar to those needed in sapping and piping erosion (Section 2.2.3). Seepage concentrated at the base of a steep bank may result in a failure plane at the bank base. Rather than removing individual particles of sediment a block, or blocks, of material are eroded. The increased cohesion of the upper bank sediment, basal position of a single sandy preferential flow path, or elevated seepage potential due to a higher bank and/or rapidly receding hydrograph falling limb, may all cause a mass failure as opposed to piping or sapping.

An alcove shaped cavity remains in the bank after the failure has occurred, this is a distinctive means of identification (Thorne, 1993). The upper soil is then left overhanging, probably due to the greater shearing strength provided by the root zone. This unsupported material then has the potential to fail as a cantilever failure (Section 2.4.2).

Relatively little research has been undertaken on the mechanisms that cause pop-out failures, probably because of their rapid nature, and the difficulty in prediction. Understanding/monitoring the distribution of pore water pressures in the bank during the failures would be useful.

2.4.5 Rotational Failures

Physically a rotational failure can often be identified in the field by the deep seated, curved failure scars; back-tilted towards the intact bank failure blocks; and arcuate shape of the intact bank line behind the failure mass (Thorne, 1993). High, gently angled (<60°) slopes are needed in a cohesive material in order to attain the shear stresses need to initiate the failure. Cohesive materials, such as clay, have increasing shear stresses with depth that can become higher than the shear strength. The frictional forces in non-cohesive sediment increase with depth, and so limit the ability for a failure plane to develop.

The stability of a bank with respect to rotational failures may be modelled using the Bishop's simplification of the method of slices (Bishop, 1955), cited in Selby (1982) and Thorne (1991). The analysis involves a two dimensional analysis of the cross-section of the failure. The section is divided up into segments that are analysed individually and then summed together (Figure 2.13).

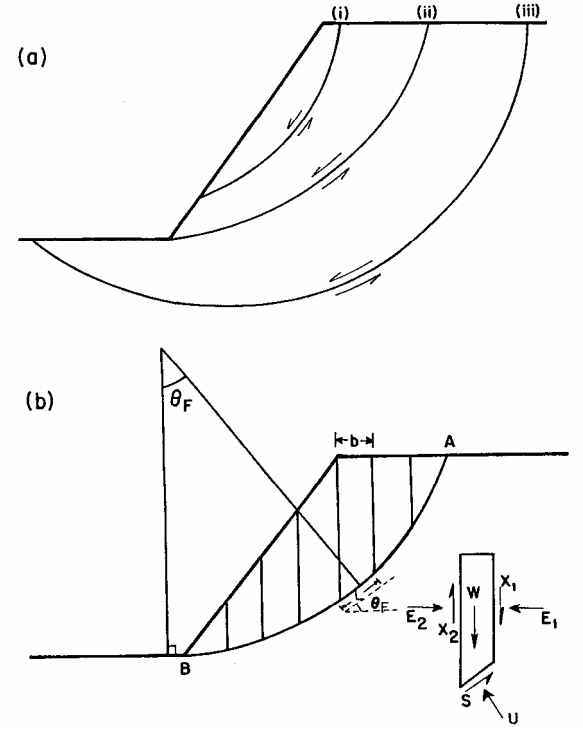

$$F_s = \sum_B^A \left\{ \frac{[c'b + (W - ub)\tan\phi]\sec\theta_F}{1 + (\tan\theta_F \tan\phi')/F_s} \frac{1}{W \sin\theta_F} \right\}$$

Where:

F_s = factor of safety with respect to a rotational slip;

c' = apparent cohesion;

W = weight of a slice;

ø' = apparent friction angle.

Figure 2.13 Slices method of analysis for rotational failures (Thorne, 1982, p. 239).

The requirements of high, gently sloping, cohesive banks are not often met in U.K. catchments. Thorne (1978) did identify a rotational failure in the mid-catchment on the River Swale, U.K. This was, however active on an artificial embankment. Larger drainage basins, such as those found in the Americas (Laury, 1971; Brunsden and Kesel, 1973; Kesel and Baumann, 1981; Pizzuto, 1982; 1984; Simon, 1989), may be more likely to attain high cohesive banks naturally in their downstream reaches.

2.4.6 Sediment Flows

There are three different flow typologies:

1. Debris flow;
2. Earth flow;
3. Mud flow.

These categories correspond to the liquefaction of coarse debris, fine grained soil and clay respectively (Selby, 1982). The loss of coherence of the soil to cause the flow may be facilitated by:

1. Soils having been remoulded after a landslide has disturbed it;
2. The presence of clays with high liquid limits in regions of high rainfall;
3. The presence of clays with low liquid limits in regions of low rainfall;
4. Soils with relatively open fabrics, due to flocculation during deposition or thawing of soil ice;
5. The collapse of material at the head or sides of the failure, loading the sediment beneath and creating high pore pressures.

There is a paucity of work identifying flows as a mechanism of bank erosion. This may be because they form near to larger failures, such as rotational failures, which are more prominent. They are included within this work as they were observed to be active at the monitoring sites in this study.

2.5 THE INFLUENCE AND VARIABILITY OF RIPARIAN VEGETATION

"… vegetation effects are complex, and vegetation cannot be classed simply as a benefit or liability to bank stability without detailed consideration of other factors including the processes responsible for retreat or advance, bank material properties and bank geometry, and the type, age, density and health of the vegetation." (Thorne, 1990, p. 125)

Some of the main influences that vegetation exerts on bank erosion process are summarised in Tables 2.2 and 2.3. There are a few processes of erosion, such as fluid entrainment (Haslam, 1978; Murgatroyd and Ternan, 1983) that have been found to be both enhanced and inhibited by vegetation. Caution must therefore be applied when considering the effects that vegetation will have on bank erosion.

The seasonal growth patterns of vegetation in temperate climates create differing vegetational effects over an annual cycle. Typically perennial plants die back during the winter in the U.K. leaving the bank surface free from vegetation during the period of greatest flood frequency (Haslam, 1978). During the same period the loss of leaves on deciduous trees will reduce their susceptibility to windthrow. The regrowth of perennial vegetation may mean that more flexible vegetation is introduced at the bank face, rather than the continued growth of 'woody' annual species. This could result in the annual regrowth of vegetation with the ability to reduce boundary shear stresses.

To reduce 'snagging' (increasing channel boundary shear stresses) vegetation that regrows on the channel margin has been removed as a catchment management tool (Gurnell and Sweet, 1998) (Section 2.2.3). Without the protection of plants the amount of bank erosion may be increased, due to the higher boundary shear stresses, resulting in a wider channel. This change in channel morphology may further increase boundary shear stress due to a less efficient hydraulic radius (Section 4.4.2) (Thorne, 1990).

In terms of spatial distribution of vegetational effects on bank erosion Dunaway *et al.* (1994) researched the effect of different substrates on vegetation growth and fluvial entrainment. The resistance of clay soils to fluvial entrainment was found to decrease with the presence of vegetation. This may be because of the poor drainage and aeration conditions in the clay

restricting the root growth, and in the root zone the cohesion of the soil is reduced by rhizome growth. This has implications for the downstream distribution of entrainment. If clay material is prevalent in the lower river reaches of a catchment the upper root zone may be preferentially eroded in these areas.

ENHANCED EROSION PROCESSES	**VEGETATION INFLUENCE**
Subaerial Preparation *(Piping)*	If large woody roots are present they may break up imbrication and soil structure. If the vegetation dies then the degradation of roots may result in preferential flow pathways, leading to piping erosion (Section 2.2.3) (Thorne, 1990).
Fluvial Entrainment	If the bank vegetation is woody and fibrous its flexibility will be limited. Isolated trees can affect the flow structure during inundation leading to local scouring effects (Pizzuto and Meckelnburg, 1989). Afforestation may reduce grass growth, decreasing root cohesion shear strengths (Murgatroyd and Ternan, 1983).
Mass Failure *(Cantilever Failure)*	The greater cohesion in the rooting zone (Smith, 1976) can lead to preferential erosion in the basal bank areas. This results in overhanging material than can collapse as a cantilever failure (Section 2.4.2).
Mass Failure *(Windthrow)*	The force of wind on the above ground surface sections of trees can lead to disruption of the soil matrix. Weakening of the shear strength by vibrations may precede a complete collapse of the tree, and the associated sediment around the root mass (Abernethy and Rutherfurd, 1998). The surcharging of the bank by increasing vegetation weight may also contribute.

Table 2.2 A description of the processes of erosion that are enhanced by riparian vegetation.

INHIBITED EROSION PROCESSES	VEGETATION INFLUENCE
Subaerial Preparation *(Frost Action)*	The microclimate provided by the vegetation canopy could potentially reduce the incidence of ground frost. Stott (1997) found that erosion was reduced on forested streams compared with a moorland stream in the same catchment (Section 2.2.2).
Subaerial Preparation *(Desiccation)*	Shading provided by riparian vegetation can reduce the temperature extremes in the summer months, and hence the maximum temperature on the soil surface. The lower evaporation on the surface can reduce both direct desiccation erosion, and the enlargement of tension cracks.
Fluvial Entrainment	Flexible plant stems can reduce the boundary shear stress at the inundated bank surface. The resistance of the plant to breaking and tearing will determine the effectiveness of the plant during high flows. Stems breaking may reduce the amount of erosion, as drag is reduced, however the roots will still bind the sediment together (Haslam, 1978).
Mass Failure	Interception, evapotranspiration, and increased soil suction reduce the amount of water effectively reaching the soil (Thorne, 1978). This may reduce likelihood of soil saturation leading to mass failures.

Table 2.3 A description of processes of erosion that are inhibited by riparian vegetation.

2.6 ANTHROPOGENIC INFLUENCES ON EROSION PROCESSES

Human impact on bank erosion may be both deliberate, in terms of bank stabilisation, and accidental due to an alteration in land-use or water abstractions upstream. The capacity of the channel geometry to transport high flows may be altered by removing vegetation (Thorne, 1990) (Section 2.5), protecting the banks with hard or soft protection, or by straightening or embanking the channel (Hemphill and Bramley, 1989). These alterations affect both the flow resistance at the channel boundary and alter the strength of the bank material. If hard or soft protection is poorly designed, or built, then it may become ineffective due to fluvial undercutting, or collapse due to mass failure. Undercutting of rip rap and gabions took place on the River Swale, U.K., due to bed elevation lowering and undercutting, and the hard engineering structure lost competence and subsequently failed (Dunnett, 1994).

Altering the sediment input to the channel upstream by mining, reservoir flushing (Leeks and Newson, 1989), and construction work (Trimble, 1995), can change the entrainment potential of the river. The concept of basal endpoint control (Section 2.3.4) may be used to predict the change in channel geometry resulting from altering the sediment input to the system (Simon and Darby, 1997). Schumm (1994) warns that the degree to which these factors alter the natural system may in some cases be overstated.

The geomorphological effects downstream of dams were researched by Brandt (2000), and the cross-sectional changes summarised (Figure 2.14). The worst case, in terms of lateral changes from bank erosion, resulted from the sediment load being less than the flow capacity and the discharge being increased due to the diversion of another watershed into the reservoir. The effect of reservoirs on channel morphology downstream may be limited in the U.K. due to the small size of the affected catchment areas compared to the total drainage area (Petts, 1980).

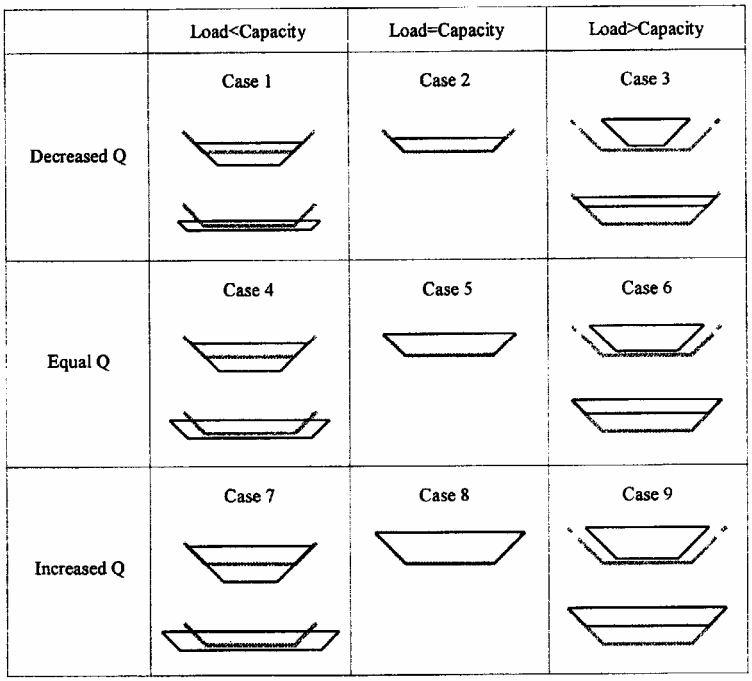

Figure 2.14 Schematic examples of the possible resulting cross-sectional geomorphology, after changes in water discharge, Q, and the relation of sediment load to sediment transport capacity. Grey lines signify cross-sections before the dam construction and black lines after the dam construction. Note that in Case 1, degradation may not occur if the reduced water discharges are not capable of eroding and transporting the bed material, even though the full flow capacity is not used (Brandt, 2000, p. 383).

Increased grazing of the riparian area, with less fallow periods, can reduce the amount of bank-top vegetation. Direct rainfall on to the surface, may increase rainsplash erosion (Section 2.2.4). The amount of desiccation and frost action may also be increased (Sections 2.2.2 and 2.2.3) caused by the microclimatic changes. Deeper root cohesion provided by varied vegetation cover may also decline (Sansom, 1996). Removal of instream and bank surface vegetation due to grazing may therefore reduce the bank cohesion from root growth, and increase the amount of entrainment.

Trampling by cattle can create ramps down to the river, which induce greater turbulence and may self-perpetuate during high flows (Trimble and Mendel, 1995). By sliding down the bank and rubbing against the bank surface cattle can remove surface sediment. Grazing near to the bank edge can create trampled paths that may develop into failure planes for mass failures, whilst failures can be initiated by the weight of animals on the sediment.

2.7 PROCESS COMBINATIONS AND INTERACTIONS

In order to understand the processes that may be active at in a particular situation they have been considered separately (Sections 2.2-2.4). In most cases a combination of processes will occur either together and/or in succession to prepare and erode sediment, examples of these combinations are given in Table 2.4.

PRECONDITIONING PROCESS	SECONDARY PROCESS	INTERACTION MECHANISM
Subaerial Preparation	Fluvial Entrainment	Subaerial processes such as frost action (Section 2.2.2) and desiccation (Section 2.2.3) may weaken the bank material, and relocate it in the bank profile as a bank retreat process. The removal of material from the site, bank erosion, will be dominated by fluvial entrainment (Section 2.3).
Subaerial Preparation	Mass Failure	Tension crack enlargement by subaerial preparation such as frost action (Section 2.2.2) and desiccation (Section 2.2.3) may result in the failure block reaching its critical factor of safety, and subsequently failing. Increases in pore water pressures along the failure surface caused by water infiltrating through tension cracks may have a similar result (Rinaldi and Casagli, 1999).
Piping, Sapping and Pop-out Failures	Mass Failure	Removal of basal material by the preparation processes leaves the upper bank material unstable. This may result in the mass failure of the upper bank (Haggerty, 1991a), for example as a cantilever failure (Section 2.4.2).
Fluid Entrainment	Mass Failure	Removal of basal material by fluvial entrainment, which may have been subaerially prepared, leads to instability in the overlying material. This may prepare the upper bank for a form of mass failure (Davis and Gregory, 1994).
Increasing Pore Water	Frost Action, Fluid Entrainment, Mass Failure	Increased pore water may result in a greater moisture supply to the freezing bank surface, increasing the amount of frost action (Section 2.2.2). Weaking of interparticle forces upon saturation (espectially in cohesive material) means that entrainment (Section 2.3) will be more effective. The increased weight of the bank whilst saturated increases the likelihood of mass failures (Section 2.4).
Mass Failure	Fluvial Entrainment	Bank retreat by mass failure (Section 2.4) may be tranformed into bank erosion by the entrainment of weakened and relocated material.

Table 2.4 The interactions between different processes of erosion.

As well as individual processes creating the conditions for process combinations they may also result from changes in the hydroclimatology of a riverbank. Variations in the river stage alter the level at which entrainment and bank saturation may occur. This can result in a difference in processes during periods of high flow in the spring and low flow in the winter, or at a shorter temporal scale differences before, during, and after a flood event. The seasonal changes in climate also create changes in the type and intensity of different processes. An example of this is frost action being more influential in the colder winter months and desiccation in the drier summer months.

Spatial variations of the bank stratigraphy may cause combinations of processes to be active at the same time. Coarser basal material will erode in a very different manner to overlying cohesive material, both due to the sedimentology and more frequent inundation. Differences in hydraulic conductivity due to varying grain sizes may result in preferential seepage, possibly resulting in piping and sapping in specific regions. The potential for a cantilever to also form is aided by the presence of bank top vegetation increasing the strength of the bank surface and rooting zone.

2.8 SUMMARY

1. Three broad classifications of bank erosion appear explain most of the processes of bank erosion. These are sub-aerial, fluvial entrainment and mass failure processes. There are complex interactions between these three categories making them difficult to differentiate into individual processes in practice. The effects of anthropogenic activity may also alter the processes that are occurring at a site.
2. Many of the processes of erosion described have not been specifically investigated on vertically exposed riverbanks, such as rainsplash erosion (Section 2.2.4) which has more of a research focus in the area of agricultural runoff. Fluid entrainment research has been concentrated on riverbed material rather than bank sediment. There is also a lack of research into the processes of desiccation, ice lens growth, slaking, pop-out failures, and sediment flows. This may be because of the lack of adequate monitoring equipment, or the lower visual impact of these processes after an erosion event due to entrainment.
3. The following chapters seek to research the distribution of these processes spatially and temporally at a catchment scale. Many of the process examples from this chapter are related to specific case studies at differing points spatially in a catchment. Catchment scale models of erosion, and a compilation of rates and processes identified at different DBA by other authors will be discussed in Chapter 7.

CHAPTER 1

INTRODUCTION

1.1 RESEARCH BACKGROUND

1.1.1 The Importance of Bank Erosion in the Fluvial System

Bank Erosion may be defined as:
"Detachment, entrainment and removal of bank material as individual grains or aggregates by fluvial and subaerial processes" (Lawler *et al.*, 1997, p. 148)

The bank can also erode during a *Bank Failure*, which may be defined as:
"Collapse of all or part of the bank *en masse*, in response to geotechnical instability processes" (Lawler *et al.*, 1997, p. 148)

The removal of sediment from the sides of the river channel and its subsequent transport by the river has implications throughout the river system. The supply of sediment into suspension (Walling *et al.*, 1999) can increase the river turbidity affecting inchannel flora, fauna, and anthropogenic abstractions (Haslam, 1978; National Rivers Authority, 1996). Pollutants, both natural and anthropogenic, may be released into the channel as the bank erodes resulting in water supply problems and hazards where sedimentation occurs on bank tops (Lewin *et al.*, 1977; Lecce and Pavlowsky, 1997; Green *et al.*, 1999; Carroll *et al.*, 2000; Sedgewick, 2000). The sediment load may lead to problems of reservoir, or channel, siltation affecting fish spawning grounds (Petts *et al.*, 1993; Pentz and Kostaschuk, 1999) and navigation routes.

The movement of the channel as the bank erodes produces land-use problems. The encroachment of rivers into urban areas, with the potential of large and rapid mass failures, is a costly process (Schumm, 1994). Riparian zones are also often fertile areas supplying land for agricultural use, which may be removed by erosion (National Rivers Authority, 1995a). Amending this problem through engineered structures, both soft and hard, to deflect impinging flow patterns can lead to unsightly structures, which have often proved inadequate because of the lack of understanding of the erosion system (Hemphill and Bramley, 1989). The reshaping of

disturbed channels, through river restoration schemes, could also be managed more effectively with a knowledge of stable bank morphologies (Downs and Thorne, 1998; Richter *et al.*, 1998).

It is apparent that understanding bank erosion can be important in economic, social and environmental terms (Table 1.1). Understanding when, where and how a riverbank is likely to erode, allows the assessment of potential costs involved in mitigating measures.

"One of the main tasks of a geomorphologist is identifying those river basins, or reaches, that may be potentially susceptible to future environmental change and those presently subject to dynamic adjustment to altered channel or climatic conditions" (Macklin and Lewin, 1997, p. 15).

Connectivity within the fluvial hydrosystem and environmental impact
< Quantitative field techniques and surveys enabling sediment sources to be traced.
< Studies of the downstream impacts on river channel morphology of river regulation, channelisation, and river training
< Preliminary equations for catchment sediment yield prediction in relation to land use change (e.g. agriculture, mining, deforestation and urbanisation), and assessment of the impact of change on the downstream fluvial system

Historic legacy, chronology and channel adjustments
< Studies of channel process (e.g. bed and bank erosion and bedload and suspended sediment transport rates)
< Examination of the role of importance of floodplain stratigraphy on channel adjustment
< Quantification of rates and modes of sediment movement within the fluvial system
< Studies of past channel adjustment in relation to climatic and anthropogenic change

Landscape sensitivity
<Qualitative and quantitative field techniques and modelling to identify instability
< Analysis of river channel cross-sections and planform to predict future change
< The influence of large flood events, land use changes and climatic changes

Eco-geomorphology
< Appraisal and design of mitigation and enhancement measures and restoration projects
< Determination of instream flow requirements
< Fluvial auditing and river channel typologies

Table 1.1 A summary of the key aspects of fluvial geomorphology that have direct relevance to river engineering, including research into bank erosion as part of the study of channel adjustment processes (Gilvear, 1999, p.231).

1.1.2 The Influence of Catchment Scale on Bank Erosion

"The main factors controlling channel form are discharge, sediment load, bed and bank material composition, and valley slope. All can vary considerably along and between rivers." (Knighton, 1987, p. 97)

Hooke (1980) found that increasing erosion rates on Devon streams were loosely related to increasing drainage basin area (DBA), and that the rates compared well with a database of different bank erosion studies. The differing rates of erosion may be due to:

1. A change in the efficacy of a single erosion process as the DBA increases;
2. The geographic change in study locations, through alterations in variables such as climate, geology or flow regimes;
3. A change in type, or combination, of erosion processes that are active at different DBA values (Lawler, 1992a; 1995; Brierley and Murn, 1997; Abernethy and Rutherfurd, 1998; Lawler *et al.*, 1999);
4. Varying methods of measurement and length of measurement periods (Hooke, 1980; Lawler, 1993a; Harris, 1996).

Lawler (1992a; 1995) suggested that there was a downstream trend in the distribution of erosion processes at a catchment scale. The trends in process efficacy were suggested to be determined by the fact that variables such as temperature, rainfall, stream power (a product of slope and discharge (Section 2.3.3), and sediment size are related to the longitudinal slope of the river.

The model is sub-divided in three main process categories (Figure 1.1); subaerial preparation processes; fluvial entrainment; and mass failure. The factors that influence these process categories are shown in Table 1.2.

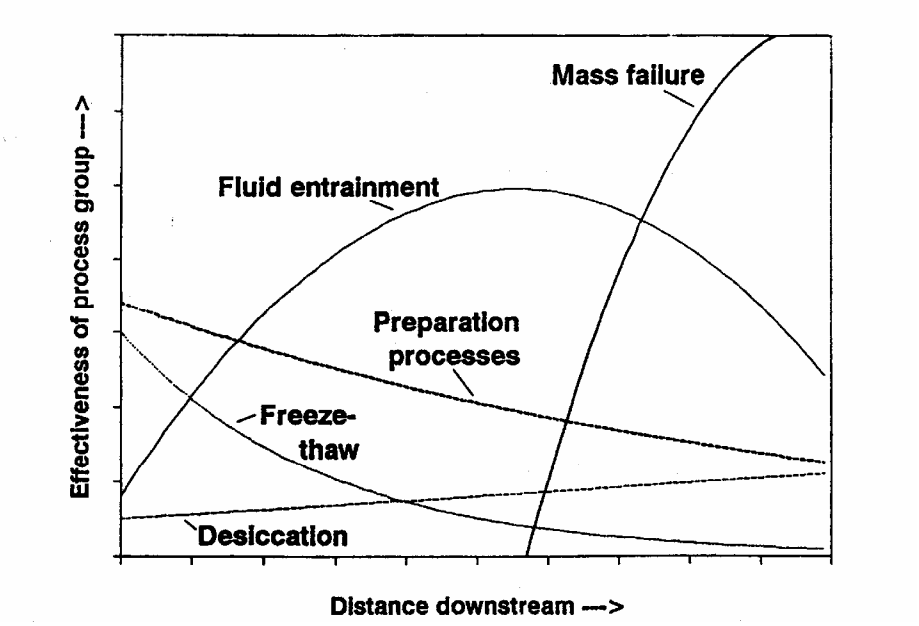

Figure 1.1 A hypothetical model of changing bank erosion process efficacy with distance downstream a river catchment (Lawler, 1995, p.181).

INFLUENTIAL FACTORS IN BANK EROSION SYSTEMS	
Subaerial Processes	Microclimate, especially temperature Bank composition, especially silt/clay percentage
Fluvial Processes	Stream power Shear stress – but actual distribution influenced by position of primary currents Secondary currents Local slope Bend morphology – cs, curvature Bank composition Vegetation Bank moisture content
Mass Failure	Bank height Bank angle Bank composition Bank moisture content or pore water pressure/tension

Table 1.2 Influential factors in bank erosion systems in terms of Preparation Processes, Fluvial Entrainment, and Mass failures (Lawler *et al.*, 1997, p. 150).

Subaerial preparation processes (Section 2.2) were subdivided into frost action and desiccation (Lawler, 1995). The efficacy of frost is thought to decline downstream through the catchment as the temperature increases, alongside decreasing altitude (Lawler, 1988a). Desiccation was proposed to increase in efficacy downstream alongside a reduction in rainfall and an increase in summer air temperatures and associated evapotranspiration rates (Bello *et al.*, 1978). The overall sediment contribution from subaerial preparation processes should stay almost constant due to the increasing influence of desiccation compensating the decline in frost action (Figure 1.1). As

other erosion processes become increasingly important downstream the efficacy of subaerial preparation decreases downstream, even though the sediment production theoretically remains almost constant.

Fluid entrainment (Section 2.3) was thought to follow the same trend as stream power (Section 2.3.3) throughout the catchment. The boundary shear stresses responsible for entraining bank sediment are approximated by stream power, which have been observed/modelled to peak in the mid-catchment region (Graf, 1982; 1983; Lewin, 1982; 1983; 1987; Knighton, 1987; 1999; Couperthwaite, 1997) (Figure 1.1). The bank material may also be more erodible in the middle catchment reaches as coarse material theoretically dominates in the upper reaches (Harris, 1996) whilst downstream the increasing clay content results in greater cohesion (Lewin, 1983).

The retreat of the bank by mass failure was modelled using the modified Culman analysis (Thorne, 1982) (Section 2.4.3). This analysis uses the bank sediment properties of cohesion, unit weight and friction angle to determine the critical vertical bank height required for a wedge/slab failure. Using a model of exponentially increasing bank height downstream (Leopold and Maddock, 1953; Prestegaard, 1988), and a uniform sediment size thoughout the catchment, the region of the catchment that exceeds the critical height for failure can be estimated. This allows a zone of mass failure dominance to be identified; theoretically rising in efficacy as bank height increases downstream.

The overall conclusions reached by constructing the model were that there should be a shift in process dominance downstream, from subaerial preparation upstream, to fluvial entrainment in the mid-catchment, through to mass failure downstream. The conclusions are based around theoretical models and field observations of individual processes; however, no systematic field examination has been undertaken. A field-based validation of the theoretical model would need to meet the following criteria:

1. The geographic location of the monitoring sites would need to be similar, to avoid problems of differing geology, climate and stream power not associated with a rivers longitudinal change. This would be best achieved using a single catchment.

2. Similar measurement methods should be used at each monitoring site to reduce the potential for differing accuracy's to occur, which may have affected the comparisons of different erosion rate studies (Lawler, 1993a).
3. The measurement techniques should be able to infer separate erosion *processes* as opposed to the cumulative *rate* of erosion over a known period, which has often been determined in the past.

"Field studies are required to support investigations of the rates and directions of change in channels with actively adjusting widths and to allow measurements of flow fields and bank material characteristics affecting bank erosion/accretion, bank stability, and processes of bankline retreat and advance." (Thorne *et al.*, 1998, p. 897)

1.1.3 Seasonal Changes in Bank Erosion

Studies into rates of erosion have identified a seasonal trend over the annual erosion cycle. Winter-spring periods have been observed to contain an elevated period of erosion, whilst the summer has relative low erosion rates (Wolman, 1959; Hooke, 1979; Lawler, 1986; Bull, 1997; Stott, 1997). This distribution may be due to the winter-spring maintaining:

1. Higher flood frequencies, resulting in the potential for more entrainment (Hooke, 1979);
2. Increased periods of catchment wetness, reducing the bank shear strength through elevated pore pressures (Thorne, 1982);
3. More frequent rainfall events, directly removing surface material and increasing the catchment wetness (Gregory and Walling, 1973);
4. Longer periods of sub-zero temperatures, with frost action preparing the bank sediment for entrainment, or directly eroding the bank (Lawler, 1986);
5. Decreased vegetation cover, altering the microclimate allowing lower temperatures with more frost action, reduced flow resistance, and more efficient rainfall impacts (Thorne, 1990; Abernethy and Rutherfurd, 1998).

If there is a downstream trend in the processes of erosion efficacy throughout a catchment (Figure 1.1) then the distribution of annual erosion rates may also change with each of the three

process categories (Subaerial preparation, Fluid Entrainment and Mass Failures) having a distinct seasonal erosion pattern (Table 1.3).

EROSION PROCESS CATEGORY	THEORETICAL SEASONAL PROCESS DOMINANCE
Preparation Processes	Frost Action would be expected to dominate during the winter months, with a greater frequency of sub-zero temperatures allowing ice formation on, and in, the bank sediment. Desiccation should increase during the summer months when the bank moisture levels are low due to lower frequency rainfall and flood inundation.
Fluvial Entrainment	Entrainment should dominate during the spring due to increased flood frequencies, and higher stage events (Hooke, 1979; Pizzuto and Meckelnburg, 1989).
Mass Failures	The undercutting of the bank by fluid entrainment and preparation processes should create the conditions for bank instabilities, after their dominant winter/spring activity. This suggests that failures would occur later in the year than fluid entrainment, however, the ability of floods to saturate the bank, resulting in a lower sediment shear strength, means that failures should dominate during the main flood season.

Table 1.3 Theoretical seasonal erosion domains of Subaerial Preparation; Fluvial Entrainment; and Mass Failure Processes.

The result of the temporal distribution of erosion should result in the upper catchment having a winter dominated erosion season due to the dominance of subaerial preparation. However, the subaerial processes prepare the bank for erosion by another mechanism, as well as directly eroding the bank. The process of erosion that removes the weakened material will determine the timing of the actual erosion event. Understanding which is the main 'secondary' erosion agent will have implications on the dominant erosion season.

Further downstream the efficacy of fluvial entrainment should result in the spring floods, after the winter period of frost action, extending the erosion season. The lower catchment should have peak erosion during the main flood season at the same time, or just after, entrainment because of bank saturation and fluvial undercutting. The relative combination of processes throughout the catchment, and their differential efficacy spatially, requires investigation to determine the true temporal and spatial distribution of erosion processes.

1.2 AIMS AND OBJECTIVES

1. To assess, quantify, and explain downstream changes in the seasonality of bank erosion rates at sites throughout a catchment.

2. To examine the timing of erosion at an event timescale in order to identify the magnitude and frequency of individual erosion processes, and the interactions between groups of processes.

3. To investigate the relative influence of catchment characteristics on rates and processes of erosion. This will be achieved by examining a more comprehensive database of physical characteristics than has been used before. This would include catchment changes in bank sedimentology, climate, hydrograph shape, channel dimensions, and stream power.

4. To develop a model of catchment scale downstream change in bank erosion efficacy in terms of rates and processes. This model will be put in context against previous catchment scale models of erosion efficacy, and the rates and processes from other studies.

1.3 THESIS STRUCTURE

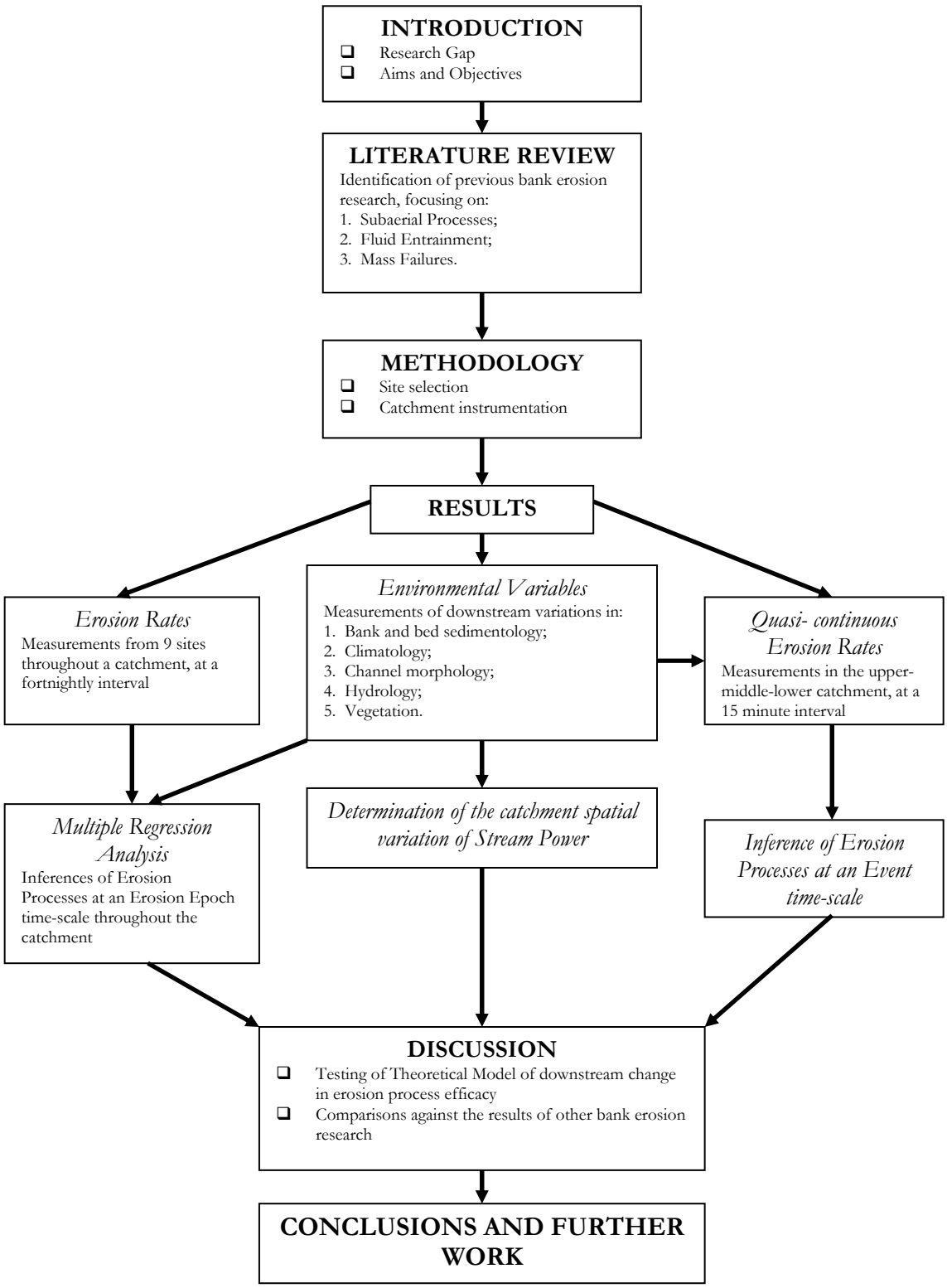

CHAPTER 3

METHODOLOGY

3.1 INTRODUCTION

To test the model presented by Lawler (1992a; 1995) the downstream changes in erosion processes, discussed in Chapter 2, were monitored. The aims of this chapter are to introduce the reasoning behind the selection of the study area, individual monitoring sites and the monitoring regime used. By presenting the study area in terms of geographical position, geology, climate, hydrology, vegetation, and land-use the catchment may be put into context against other studies.

The differing types of instrumentation used within the study are outlined so a cohesive picture of the monitoring framework can be built up. The advantages and disadvantages of the differing techniques used are discussed so that an objective view may be gained of the strengths and weaknesses of each set of data collected.

3.2 STUDY AREA SELECTION

The study area selection was based on the following criteria:

1. The study should be based around a single catchment, rather than a number of studies at different DBA values or distances from the river source. This avoids the inclusion of different hydrologic regimes, and catchment morphologies increasing uncertainty between study sites.

2. An ideal system would be completely 'natural' so that the downstream change in an undisturbed catchment could be identified. This would allow the effects of anthropogenic activity to be assessed, and the effect of altering components of the natural system to be predicted. An example of this would be determining the effect of adding a reservoir to a catchment, and the different changes caused by placing it in different positions in the longitudinal profile.

3. The scale of the chosen catchment should be large enough to encompass all of the bank erosion mechanisms under consideration. If the catchment were not large enough to attain a critical bank height that could initiate mass failures (Section 2.4) then the study would be restricted.

4. Reliable climatic and hydrological background data, such as that collected by the Environment Agency (EA) and Centre for Ecology and Hydrology (CEH), would allow supporting evidence for measurements taken by this study. Longer-term records also allow the monitoring period to be put into context against other hydrological and climatic events.

5. The need for frequent site visits for process observations over a two-year period meant that the chosen catchment needed to be within a reasonable travel distance of Birmingham.

Although both the Severn basin in Wales, and Ouse basin in North Yorkshire (Figure 3.1) fulfilled the selection criteria the Ouse basin was chosen. This enabled an exchange of information with the Natural Environmental Research Council (NERC) funded Land-Ocean Interaction Study (LOIS) (Wilkinson *et al.*, 1997; Stebbing *et al.*, 1998). The monitoring by NERC/LOIS Special Project 231 "Dynamics of bank sediment supply and suspended sediment transport in lower reaches and estuaries" meant that an exchange of data, and resources could be made between projects.

A desktop survey followed by site visits of the least urbanised tributaries of the River Ouse (the rivers Nidd, Wharfe, Ure and Swale) was undertaken (Figure 3.1). All the river catchments contained suitable highly eroding bank erosion sites, however, the River Swale best suited the combination of selection criteria.

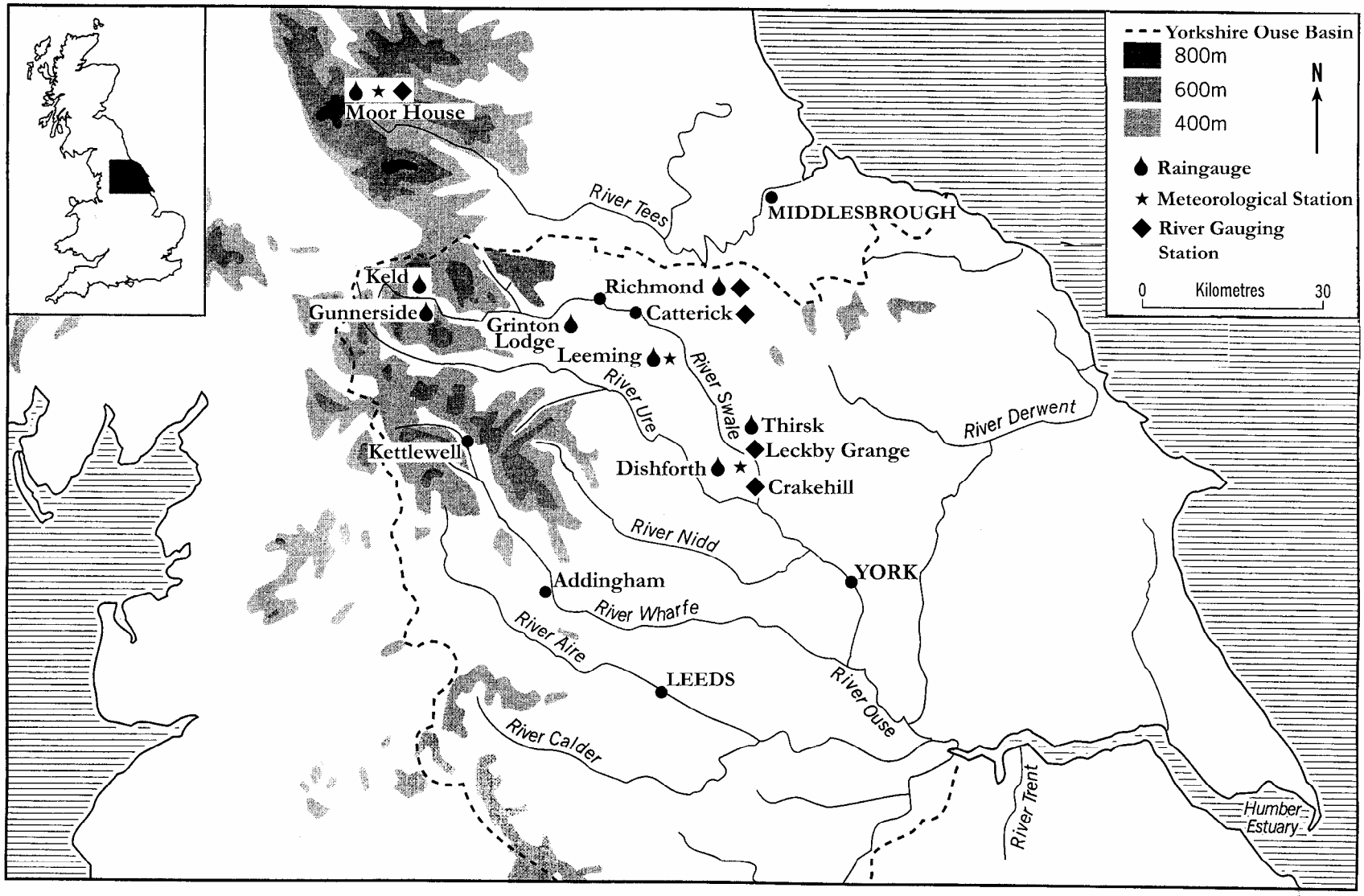

Figure 3.1 A map of the Yorkshire Ouse basin showing the position of rainfall, meteorological, and stage monitoring stations.

3.3 STUDY AREA CHARACTERISTICS

3.3.1 Geology and Pedology

The upper catchment in Swaledale is mainly underlain by Carboniferous Millstone Grit, a sequence of coarse grits, sandstones, and thinly bedded shales (Jarvie *et al.*, 1997) (Figure 3.2). The cap of millstone grit overlies the more erodible Yoredale series, consisting of shales, sandstones and limestones, which outcrop for up to 50 km along the length of the River Swale (Drewitt, 1991; Ainsworth and Goulder, 2000). The lowland region of the River Swale is dominated by Triassic Bunter Sandstone, Mercia mudstone, and Sherwood mudstone until the confluence with the River Ure. The eastern regional dip, due to the great Pennine anticline is responsible for the rocks becoming younger in an easterly direction.

Faulting of the Carboniferous limestone measures has allowed the hydrothermal deposition of metalliferous minerals, such as Pb and Zn (Raistrick, 1975). These deposits have been mined since the Roman era, and there are also phreatic network caves connecting with the mining systems (Ryder, 1975). The boundary between the Viséan and Namurian stages of the Carboniferous near the base of the Main Yoredale Limestone, is the most fissured geological formation. By creating a relatively fast subterranean flow route this may possibly be a factor, along with the valley gradient and high rainfall, in causing the river to be very "spatey" (Environment Agency, 1997).

Glacial deposits of morainic sand and gravel laid down during the Pleistocene dominate the drift geology within the catchment (Law *et al.*, 1997). The morainic material is mostly found in the valley bottoms of mid-Swaledale and consists of both basic (limestone) and acidic (millstone grit) sources.

The weathering of the Millstone Grit and the addition of organic material creates peat soils that dominate the uplands of Swaledale (Wright, 1977; Garcia-Ruiz *et al.*, 1999). In regions underlain by the Yoredale Series the varying rock types allow different types of pedogenesis to occur. The valley bottoms contain drained loam and gley soils providing better grazing vegetation than on the upland peats. In region underlain by Triassic rocks the 'Swale Series' of soils consists of sandy loam alluvium deposits, with a high pH, and calcium carbonate content (Allison and Hartnup, 1981). The resulting bank sedimentologies produced by the geology and pedology within the catchment will be discussed in Section (4.3).

Figure 3.2 The geology map of River Swale catchment, North Yorkshire (Christmas, 1998, p. 70).

3.3.2 Hydrology, Water Quality and Meteorology

The River Swale stretches from its upland source in the Yorkshire Dales National Park, at an altitude of 700 m A.O.D., through to its confluence with the River Ure in the Vale of York (Figure 3.1). The Ure then becomes the River Ouse further down the catchment, downstream of the confluence with the River Nidd (Figure 3.1). The Swale has a main channel length of 109 km, whilst the Ure extends for 111 km and finally the River Ouse flows for 75 km until it reaches the Humber Estuary. The catchment area near the Swale-Ure confluence, at Crakehill (Figure 3.1) is 1363 km^2.

Due to a combination of a steep longitudinal profile in the Swale's upper sections (Section 4.4.2), and steep narrow valley sides, the river tends to be characteristically flashy (Environment Agency, 1997). The river has undergone anthropogenic alterations along its length, mainly due to early settlements (Fleming, 1998), and mining activity (Raistrick, 1975). The more contemporary structural alterations have been focused downstream of Catterick (Figure 3.1), with the building of flood embankments and channel straightening (National Rivers Authority, 1995b). This has left the river in the upper catchment "almost completely natural in formation until it reaches Richmond" (Garcia-Ruiz *et al.*, 1999, p. 1232).

The upland flow regimes were not automatically gauged on the River Swale. Mean flow data were collected from the gauging stations at Richmond, and Crakehill (Table 3.1) (Figure 3.1) (Institute of Hydrology, 1995), however the gauging station at Richmond was decommissioned in 1980. The station resumed measurements and calibration in 1994, 10 km downstream of Catterick (Figure 3.1) (Institute of Hydrology, 1995) and the data were used to supplement the flow data at Low Row (Site 4) and Greystone Farm (Site 8).

AUTOMATIC GAUGING STATIONS SITUATED ON THE RIVER SWALE		
GAUGING STATION NAME	RICHMOND	CRAKEHILL
U.K. Grid Reference	NZ 146 006	SE 425 734
Station Level AOD (m)	107.6	12.6
Catchment Area (km^2)	381	1363
Measurement Period	1961-1980	1955-1994
Mean Flow ($m^3 s^{-1}$)	10.30	19.535
Mean Annual Flood ($m^3 s^{-1}$)	273.3	255.7

Table 3.1 A description of the positions, mean flows and mean annual floods of the automatic river gauging stations within the Swale Catchment (Institute of Hydrology, 1995).

In order to put the Swale's current flow regime in a historical context the long-term flood/flow data at York (Figure 3.1) may be used, representing the changing hydrologic regime within the Ouse basin. The 119 year flow record at York, up to 1996, was described by Longfield and Macklin (1999) (Figure 3.3). The rising trend in flood frequency, and magnitude, over this period is summarised in Table 3.2.

The biological and chemical GQA scores are generally high for the Swale catchment, as shown by the 1995 example (Table 3.3). The General Quality Assessment (GQA) of water quality is based on dissolved oxygen (DO), biological oxygen demand (BOD), and ammonia. The six classes of quality, and their determinate concentrations are shown in Table 3.4. The GQA criteria for biological classification are shown in Table 3.5. Diffuse agricultural sources and effluent cause the reduced quality of the Swale tributary, the River Wiske (Figure 3.5), from Northallerton and Romby sewage treatment works (Environment Agency, 1997).

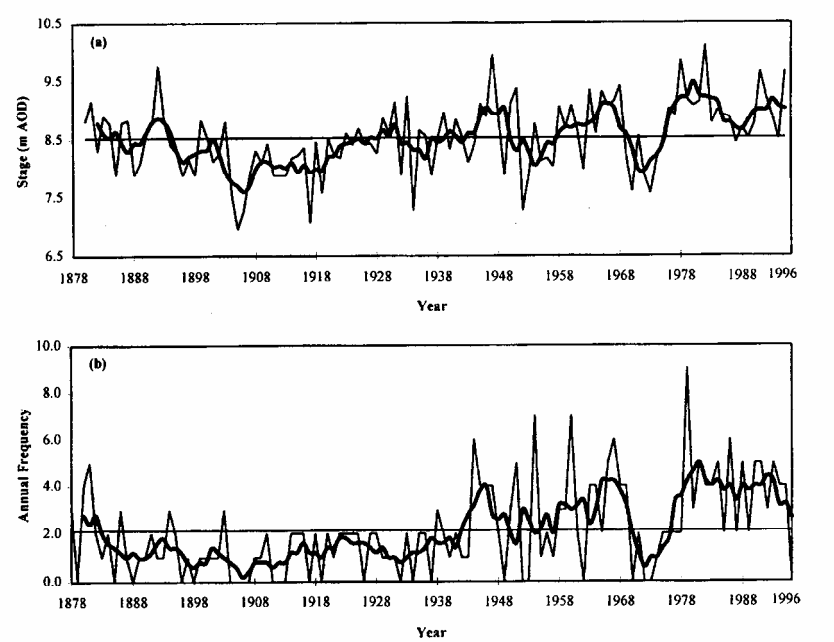

Figure 3.3 (**a**) Annual maximum flood and (**b**) annual flood frequency at York, 1878-1996. The dark line shows the five-year moving average; the horizontal line shows a long-term mean from 1878-1996 (Longfield and Macklin, 1999, p. 1054).

TIME PERIOD	CHANGE IN FLOOD MAGNITUDE AND FREQUENCY
1878-1903	Low flood frequencies and magnitudes close to the long-term means. Fine sediment supply was high in the Yorkshire Dales uplands owing to base metal mining (Macklin *et al.*, 1997), though in the lowlands reversion of arable to grassland is likely to have reduced sediment availability.
1904-1943	Flood frequency further declined and magnitude remained very low. The cessation of base metal mining towards the end of the nineteenth century would have resulted in a marked reduction in contaminant metal and fine sediment supply. It is likely that the sediment and contaminant fluxes were low, probably the lowest in the 119-year record.
1944-1968	Increased sediment supply from both upland gripping and lowland cereal cultivation, together with higher flood frequencies, would have significantly increased sediment fluxes in comparison with the early decades of the twentieth century.
1969-1977	Large-scale drainage in both upland and lowland areas continued, although extremely low flood frequencies and flood magnitudes would have resulted in considerably reduced sediment fluxes.
1978-1996	The most recent period has experienced the highest flood frequencies and magnitudes in the last 119 years. In terms of fine sediment transport, four very large flood events (1978, 1982, 1991, and 1995) are likely to have remobilized considerable volumes of floodplain sediment through bank erosion. Sediment supply is also likely to have increased markedly in this period, associated with rapidly increasing numbers of grazing animals and a switch to winter cereals (cf. Evans and Cook, 1986; Boardman, 1990; 1995; Boardman *et al.*, 1994). The last two decades has probably experienced the highest rates of sediment flux over the past 120 years.

Table 3.2 The change in flood frequency and magnitudes gauged over the past 119 years at York, North Yorkshire (after Longfield and Macklin, 1999).

SITE	DISTANCE FROM RIVER SOURCE (Km)	BIOLOGICAL GQA	CHEMICAL GQA
River Swale at Keld	5.0	A	A
River Swale at Hudswell	38.4	A	A
River Swale at Catterick	49.9	A	A
River Wiske at Kirby Wiske	86.1 (Swale) ~2.5 (Wiske)	C	C
River Swale at Thornton Manor	107.9	A	A

Table 3.3 Biological and chemical General Quality Assessment grade from sites within the Swale catchment, 1995. Data provided by the Environment Agency (cited in Christmas, 1998, p. 74).

Chemical General Quality Assessment (GQA)	DO % saturation 10 percentile	BOD mg L^{-1} 90 percentile	Ammonium-N mg L^{-1} 90 percentile
A-very good	80	2.5	0.25
B-good	70	4	0.6
C-fairly good	60	6	1.3
D-fair	50	8	2.5
E-poor	20	15	9.0
F-bad	<20	>15	>9.0

Table 3.4 General Quality Assessment chemical classification used by the Environment Agency based on the determinants: DO, BOD, and ammonium-N (Environment Agency, 1988, p. 179).

Biological General Quality Assessment (GQA)	Outline Description
A-very good	Biology similar to (or better than) that expected for an average and unpolluted river of this size, type and location. High diversity of groups, usually with several species in each. Rare to find dominance of any one group.
B-good	Biology falls a little short of that expected for an unpolluted river. Small reduction in the number of groups that are sensitive to pollution. Moderate increase in the number of individuals in the groups that tolerate pollution.
C-fairly good	Biology worse than expected for an unpolluted river. Many sensitive groups absent, or number of individuals reduced. Marked rise in numbers of individuals in groups that tolerate pollution.
D-fair	Sensitive groups scarce and contain only small numbers of individuals. A range of pollution tolerant groups present, some with high numbers of individuals.
E-poor	Biology restricted to pollution tolerant species with some groups dominant in terms of the numbers of individuals. Sensitive groups rare or absent.
F-bad	Biology limited to a small number of very tolerant groups such as worms, midge larvae, leeches, and water hoglouse, present in very high numbers. In the worst case, there may be no life present.

Table 3.5 General Quality Assessment biological classification used by the Environment (Environment Agency, 1988, p. 180).

An important variable in determining river flows, catchment moisture, and their associated erosion processes is the frequency and intensity of rainfall. As a rough guide the annual average rainfall has been presented (Table 3.6) to show the distribution of rainfall throughout the catchment. There is a decrease in average annual rainfall in an easterly direction, representing the combination of lower altitudes and prevailing westerly wind direction, in controlling the amount of rainfall. More detail on the frequency and intensity of rainfall during the study period is presented in Section 5.4.1.3.

Downstream ↓	Station Name	National Grid Ref.	Altitude AOD (m)	Average Rainfall 1941-1970 (mm)	Average Rainfall 1996-1998 (mm)
	Keld	NY 892 011	320	1411	1351
	Gunnerside	SD 949 982	240	-	1116
	Grinton Lodge	SE 049 976	259	1019	912.1
	Richmond	NZ 172 016	189	819	758
	Thirsk	SE 438 818	35	640	641
	Leeming	SE 306 890	32	611	646
	Dishforth	SE 383 711	33	-	601

Table 3.6 Decreasing average annual rainfall moving eastward along the River Swale. Long-term annual average data is from 1941-1970 (British Rainfall Organisation, 1989). Monitoring period annual average data is from 1996-1998 (supplied courtesy of the British Atmospheric Data Centre).

3.3.3 Vegetation and Land-use

The Swale was divided up into three main zones based on its physical features and vegetation types by Holmes and Whitton (1977).

1. The upper zone had a rocky substrata and largely bryophtic vegetation population of which the most abundant were: *Chiloscyphus polyanthos, Brachythecium plumosum, Cincildotus fontinaloides, Eurhynchium riparioides, Fontinalis antipyretica, Grimmia alpicola, Hygrohypnum ochraceum, and H. luridum.*
2. The middle zone had unconsolidated substrata and the macrophytic vegetation is relatively sparse.
3. The lower zone was silted and the macrophytic vegetation consisted largely of angiosperms, of which *Potamogeton spp.* was usually dominant.

In the uplands "large-scale gripping was initiated in the Yorkshire Dales in the 1940s, prompted by the introduction of grant-aid and a greater need for livestock production during the Second World War, which continued until the 1960s. Rates of upland drainage increased markedly in the 1970s and declined in the 1980s to very low levels at present (after Robinson, 1990; cited in Longfield and Macklin, 1999, p. 1060). The effect of gripping has been thought to exacerbate downstream flooding within the Swale catchment due to the faster flow routes that it has potentially provided. The distribution and amount of moorland griping in the upper Swale region is shown in Figure 3.4.

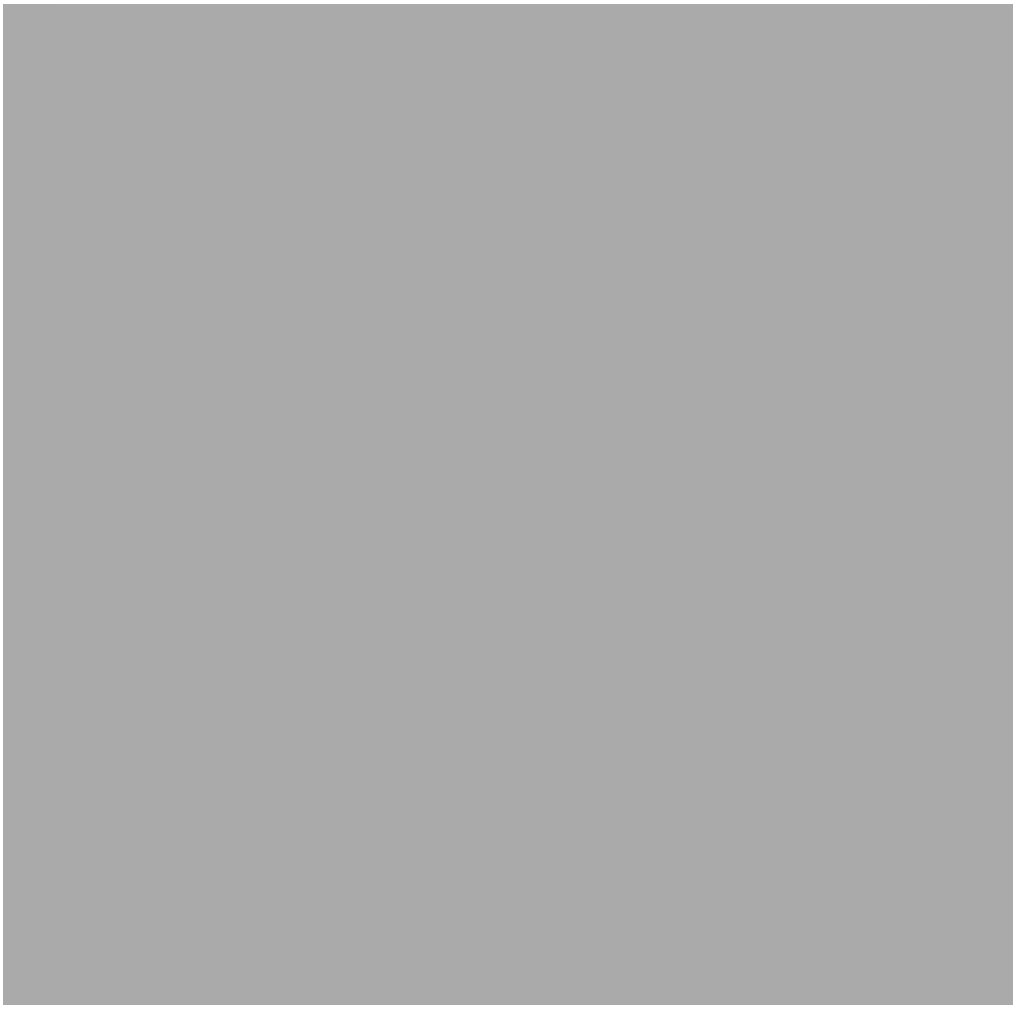

Figure 3.4 Percentage of land upstream of York that has had moorland gripping (after Robinson, 1990 cited in Longfield and Macklin, 1997, p. 1060).

Semi-natural woodlands consisting of self-sown and indigenous tree species occur as small to moderately sized woodlands in Swaledale. The woods are mainly confined to steep valley sides and only make up about of 1.5 % of the catchment area in the Yorkshire Dales National Park (Drewitt, 1991).

Downstream of Reeth the main riparian vegetation is improved grassland. This may be used for sheep grazing or as intensively cropped arable land. *Minuartia verna* established on the north banks of the Swale at Catterick (Figure 3.1) (Radley and Simms, 1971) is a species commonly found on metaliferous mining spoil heaps. This indicates the downstream transport of metal-rich sediment from the upstream gangue deposits.

3.3.4 Anthropogenic Activity

The Swale catchment has in the past been mined for both lead and coal (Raistrick, 1975; Macklin *et al.*, 1994). This has meant that there has been some alteration to the drainage conditions due to past processing works, which may also have the caused the linkage of mining passages with phreatic cave networks (Section 3.3.1). Improved drainage in the upland by griping (Section 3.3.3) may have also altered the runoff times for the upper catchment.

The inclusion of the upper catchment within the Yorkshire Dales National Park has meant that there are prescribed land use and planning restrictions for the region. There is little, or no, heavy industry throughout the Swale catchment at present, and no reservoirs within the system.

There has been a systematic planting of willows along the riverbanks downstream of Catterick (Figure 3.1) in order to stabilise riverbanks and provide better fish habitats (Environment Agency, 1996).

3.4 INSTRUMENTATION

3.4.1 Monitoring Rationale

In an ideal situation all the eroding banks in the selected catchment would be monitored continually. This was not logistically feasible so the alternative was to monitor 'rapidly' eroding sites spaced throughout the catchment. The sites were chosen so that they could be representative of the processes active at the highly eroding regions within each reach. If a random selection of banks had been taken as the study sample, in order to be a representative

sample of the catchment, then the rate of erosion may well have not been sufficient to be able to identify the dominant erosional processes.

In order to observe erosion processes *in situ* and in real time frequent site visits were necessary. The datalogged Photo-Electronic Erosion Pin (PEEP) rates of erosion, air temperatures, bank face temperatures, and stages (Figure 3.15), alongside manual measurements of erosion rates, all allowed inferences to be made about the type of erosion process that were occurring. Comparing these data against field observations meant that ground truthing of logged data process inferences could be undertaken.

An intensive study of bank and bed sediment was not possible due to time constraints; however the importance of these variables in influencing bank erosion was recognised. Data were collected at a less intensive scale than necessary to completely describe the bank and bed surface, but adequate to provide baseline data on these variables.

3.4.2 Site Selection Criteria

In order to determine the position of the individual monitoring sites within the catchment a more detailed survey of the river by foot was undertaken. The selection of suitable sites was based on the following criteria:

1. The riverbank had to be actively eroding in order to give a measurable amount of erosion during the two-year study period. A site was deemed to be actively eroding if there was a sparsely vegetated, usually steep, bank surface. These banks often indicated that the rate of erosion was faster than the growth of vegetation of the bank surface, and so the bank was relatively active. Local observations were often used to collaborate these inferences.

2. A comprehensive coverage of eroding sites throughout the long profile of the river, specifically including upper, middle, and lower catchment reaches.

3. The sites needed to be accessible from the road to enable monitoring to be undertaken efficiently.

4. If at all possible the eroding banks needed to be close to existing I.H. monitoring sites, in order to provide historic and verification data for the study. However, none of the monitoring sites was in very close proximity to a gauging station. This is because the gauging stations had been constructed in relatively stable reaches in order to maintain cross-sectional profiles for stage-discharge relationships.

With all the potential sites tabulated the overall monitoring site structure was created by selecting sites that covered the entire catchment (Figure 3.5). Nine was deemed to be a feasible number of monitoring sites (Plates 3.1-3.9) (Figures 3.6-3.14), optimising costs of both time taken to instrument and measure the sites and financial costs.

One of the variables considered influential on the type of bank erosion was stream power (Section 2.3.3). To incorporate this into the monitoring network a logarithmic spacing of sites was implemented from upstream to downstream (Figure 3.5). It was hoped that this would mirror the theorised logarithmic increase of stream power within the upper catchment (Lewin, 1982; 1983; Couperthwaite, 1997).

The three most downstream sites (Figure 3.1) Morton-on-Swale [7], Greystone [8], and Topcliffe [9] were jointly monitored with the LOIS/NERC Special Project 231.

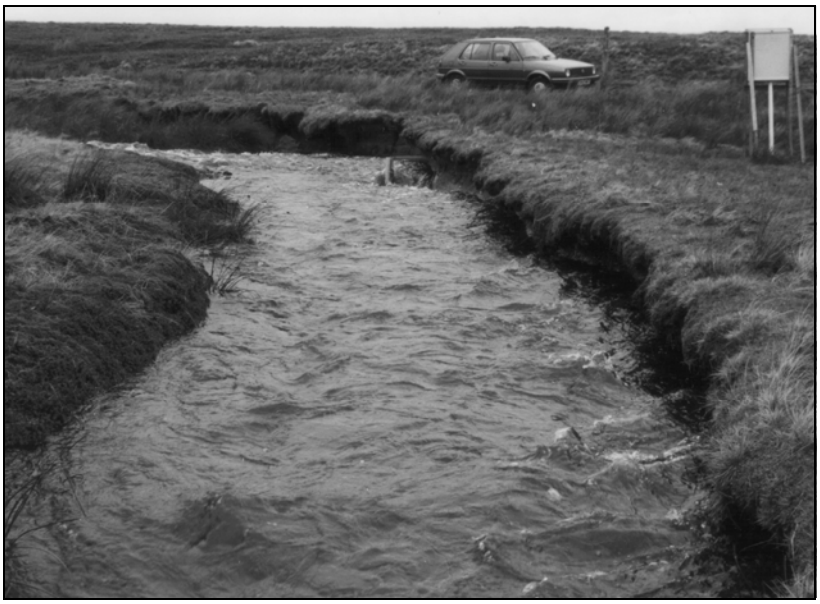

Plate 3.1 Beck Meetings (Site 1), looking upstream during a flood event (10/02/97). The data logger housing is on the right hand side of the frame.

Plate 3.2 Hoggarths (Site 2), looking downstream with collapsed cantilever blocks in the foreground (16/01/97). The rucksack on the banktop is approximately 1 m long.

Plate 3.3 Muker (Site 3), looking upstream (16/01/97). The bank is approximately 1.5 m high.

Plate 3.4 Low Row (Site 4), looking upstream (23/12/96). The pressure transducer housing is in the foreground, approximately 1 m of drainpipe is vertically exposed above the water.

Plate 3.5 Reeth (Site 5) looking downstream (15/01/97). The pinned section is downstream on the right hand half of the frame. The bankface is approximately 2 m high.

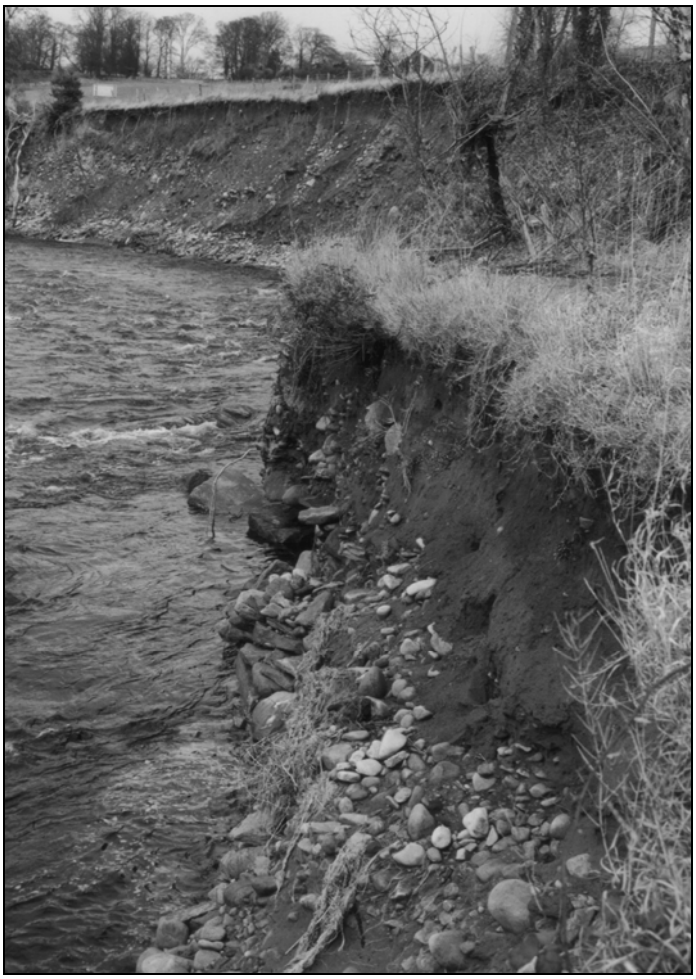

Plate 3.6 Easby (Site 6) looking upstream (13/02/97), the bankface is approximately 4 m high.

Plate 3.7 Morton-on-Swale (Site 7) looking upstream (05/01/97) with snow over part of the bank surface. The bank is approximately 4 m high.

Plate 3.8 Greystone Farm (Site 8) looking upstream (07/03/97). The bank approximately 2 m high.

Plate 3.9 Topcliffe (Site 9) looking downstream (18/11/95), the banks are approximately 4 m high.

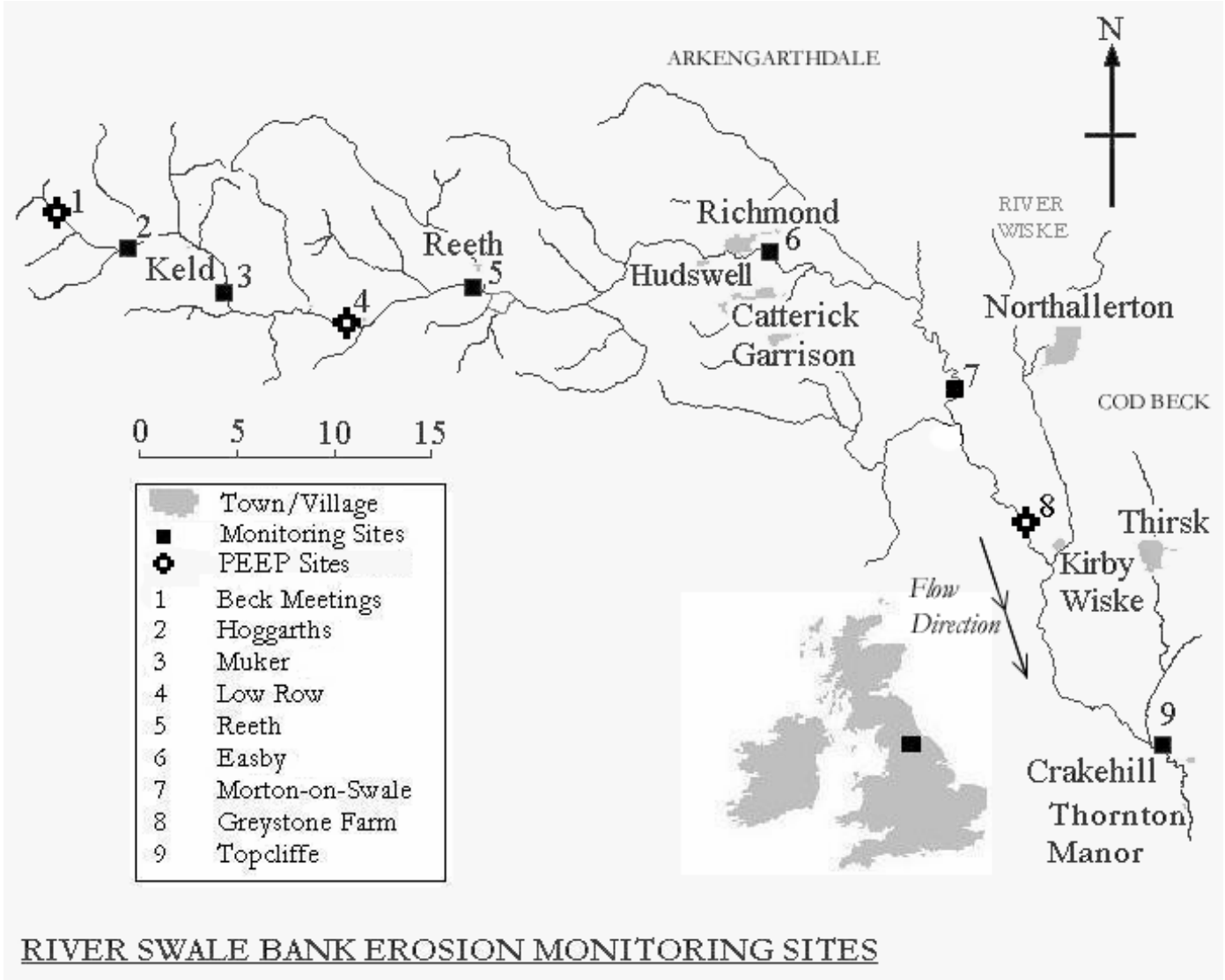

Figure 3.5 A map showing the position of erosion pin and PEEP monitoring sites.

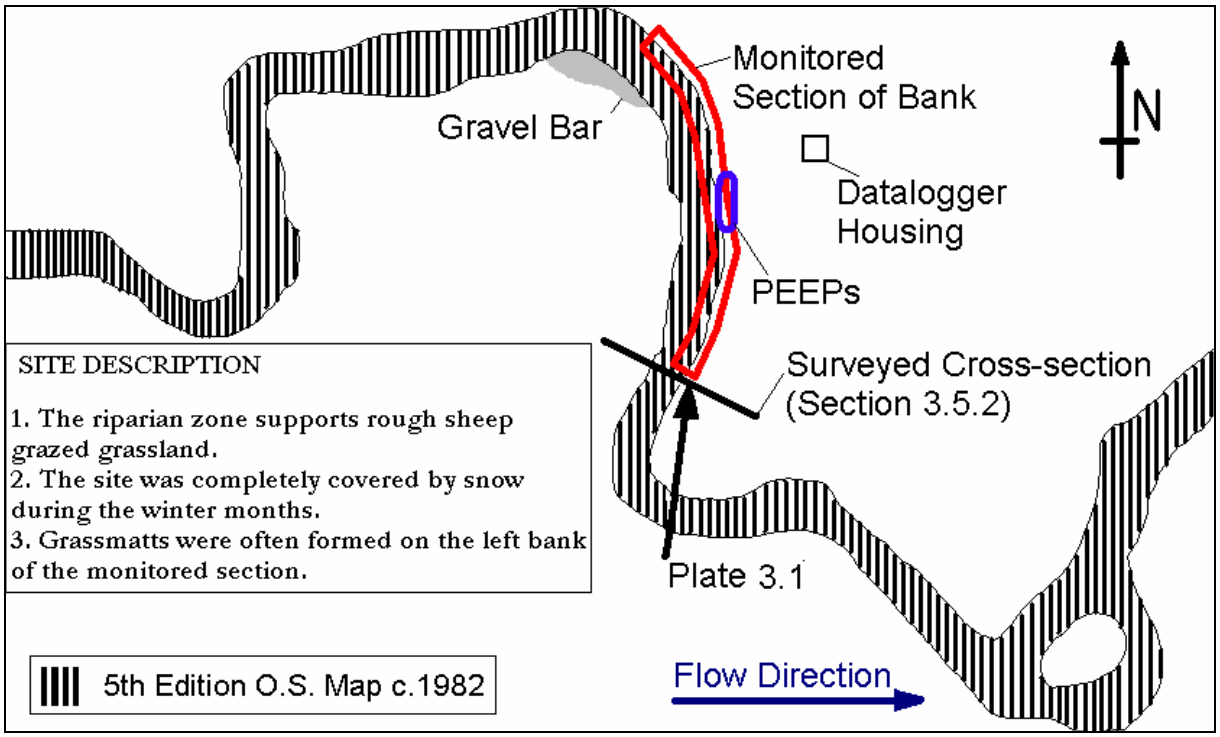

Figure 3.6 A site map of BECK MEETINGS (Site 1) showing the position of the monitored section of the bank, and the position of the channel in 1982.

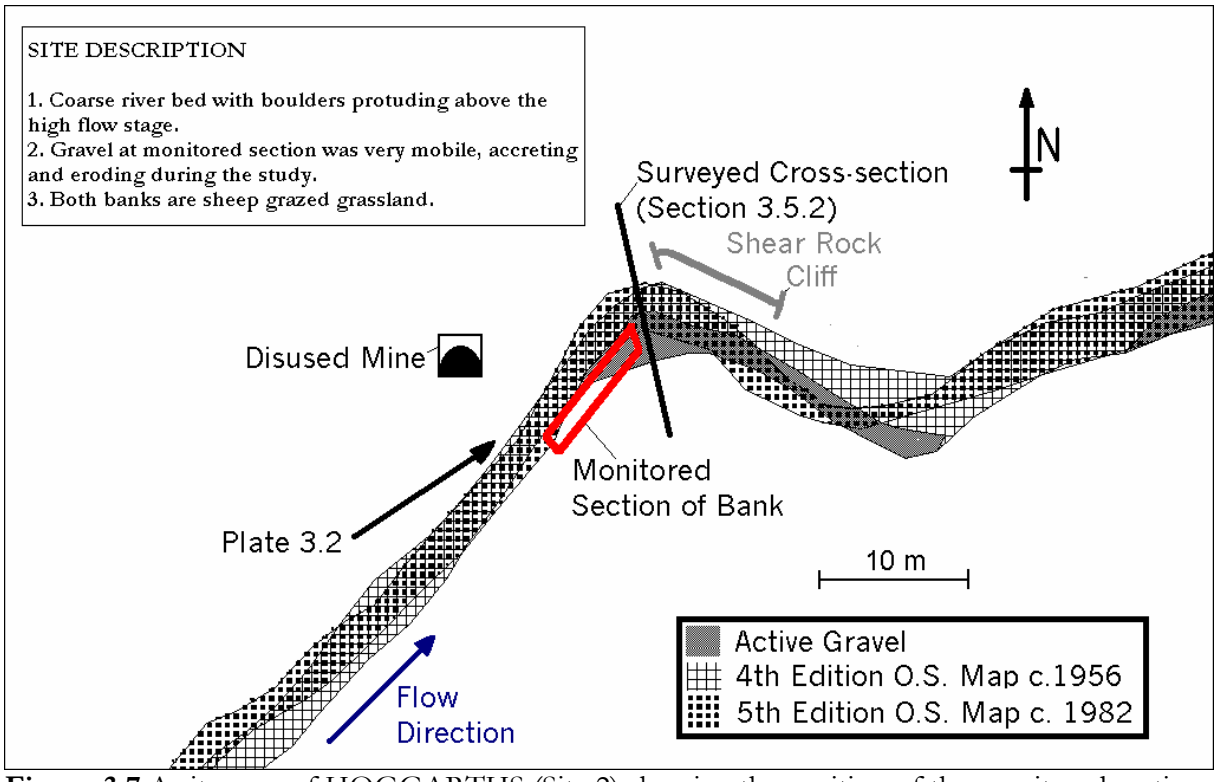

Figure 3.7 A site map of HOGGARTHS (Site 2) showing the position of the monitored section of the bank, and the position of the channel in 1956, and 1982.

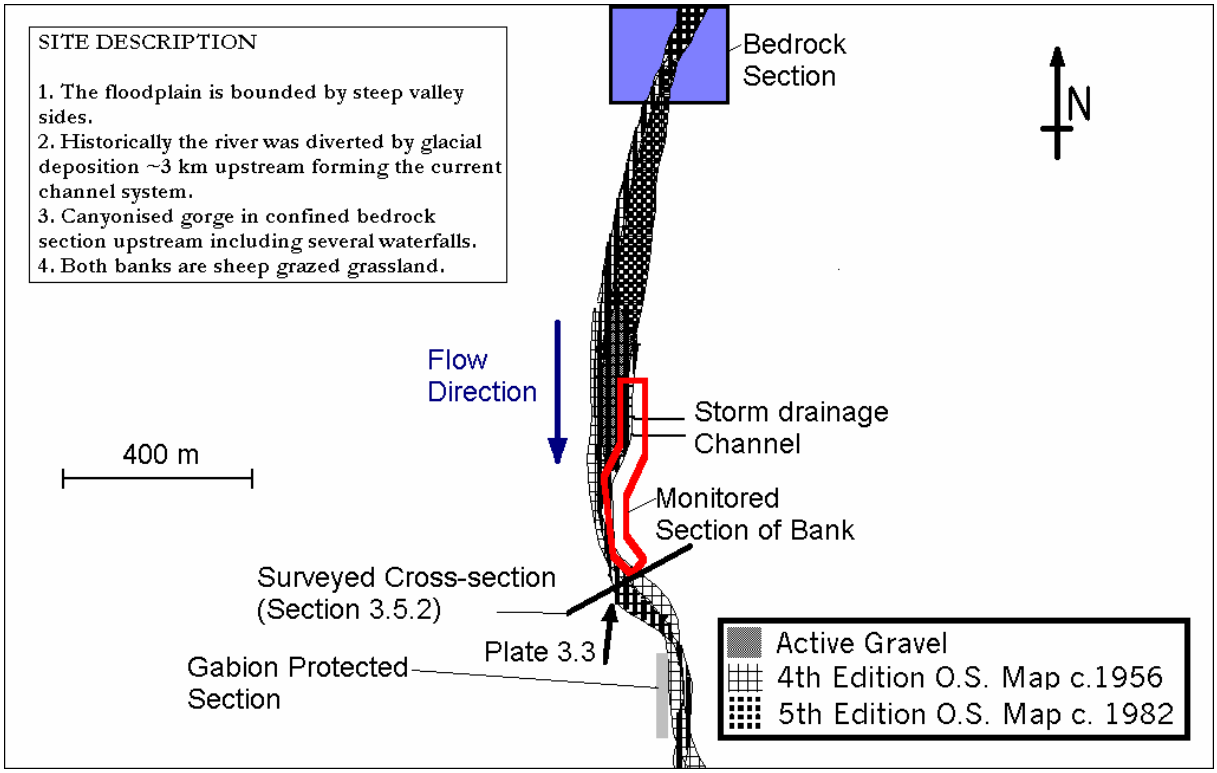

Figure 3.8 A site map of MUKER (Site 3) showing the position of the monitored section of the bank, and the position of the channel in 1956, and 1982.

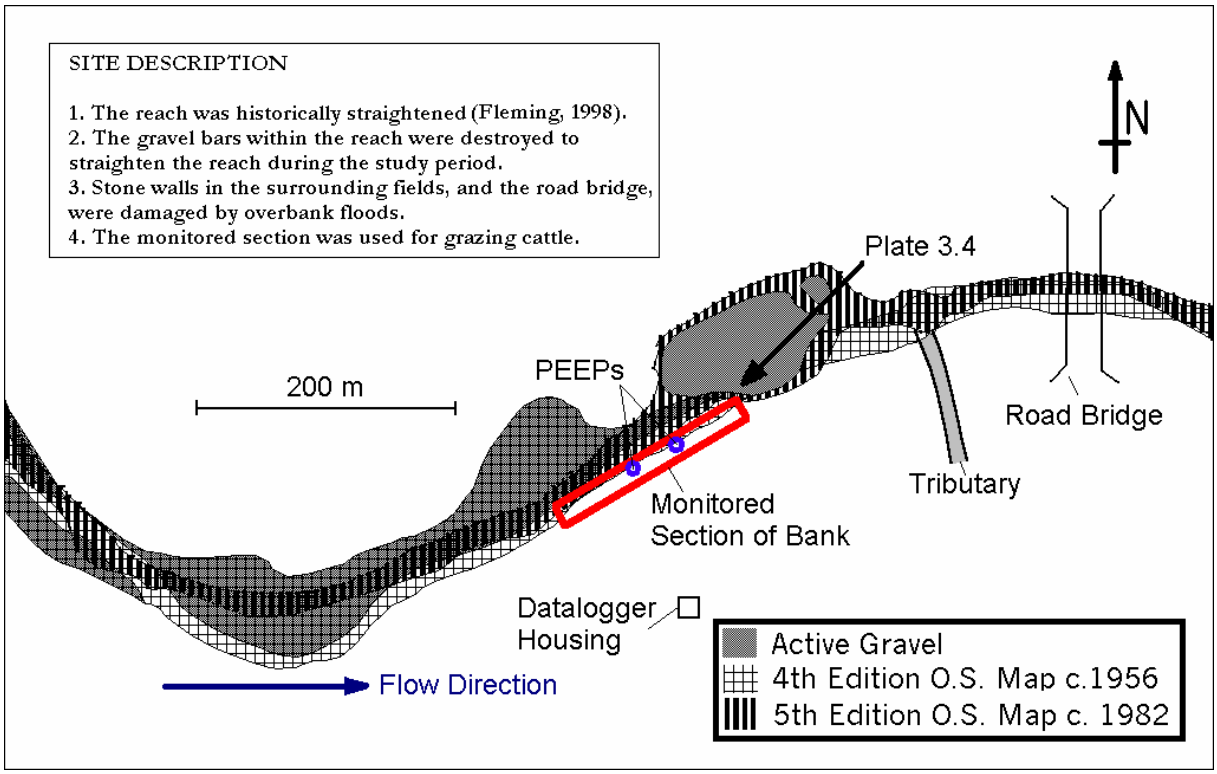

Figure 3.9 A site map of LOW ROW (Site 4) showing the position of the monitored section of the bank, and the position of the channel in 1956, and 1982.

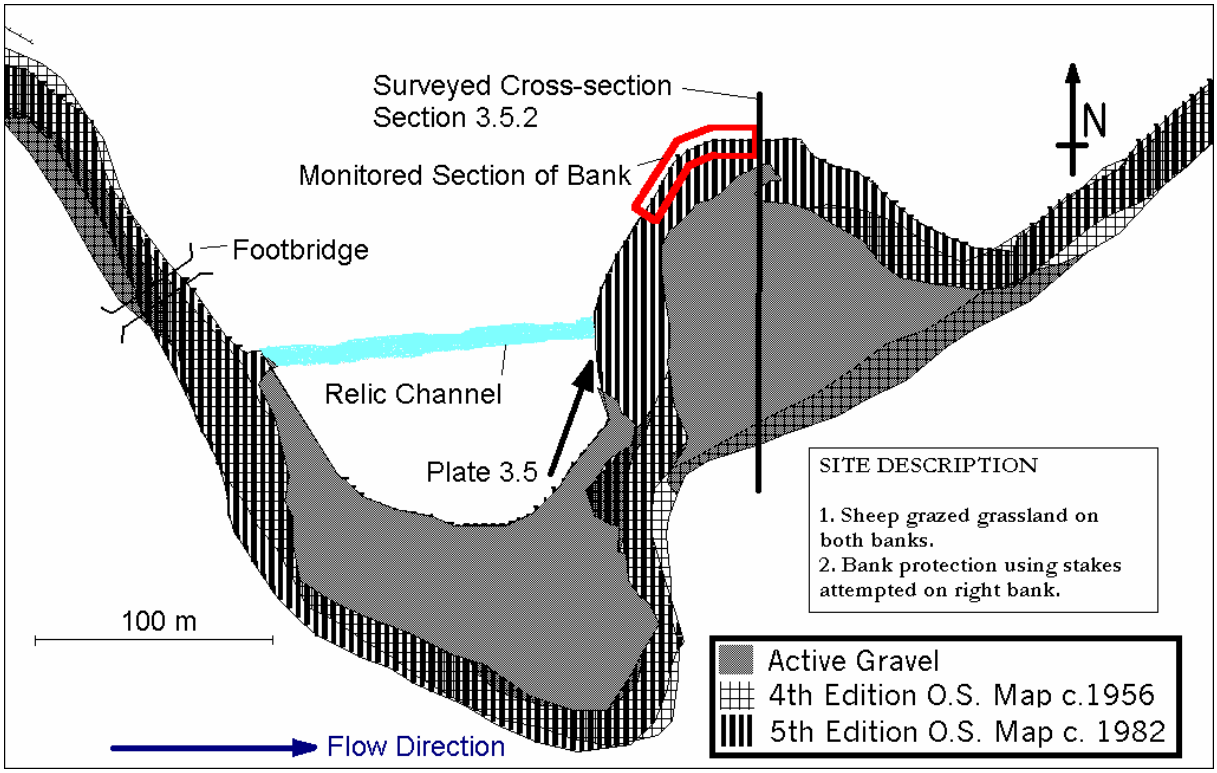

Figure 3.10 A site map of REETH (Site 5) showing the position of the monitored section of the bank, and the position of the channel in 1956, and 1982.

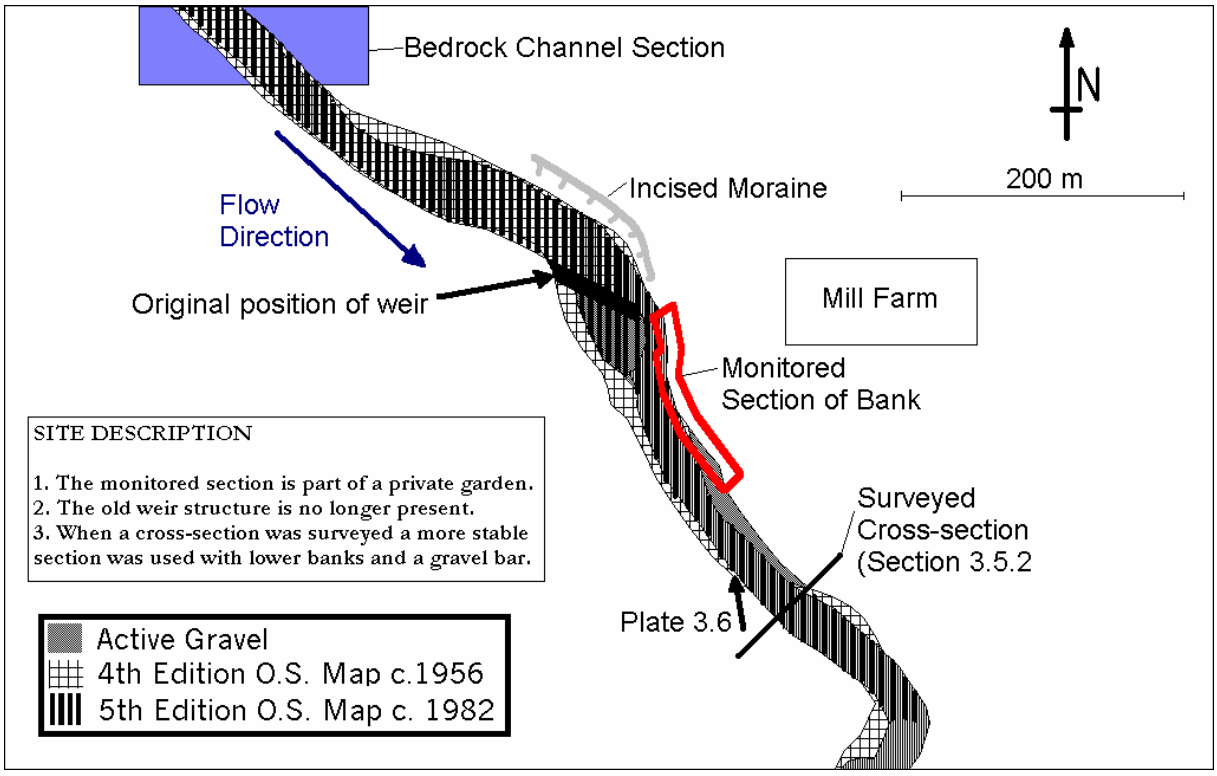

Figure 3.11 A site map of EASBY (Site 6) showing the position of the monitored section of the bank, and the position of the channel in 1956, and 1982.

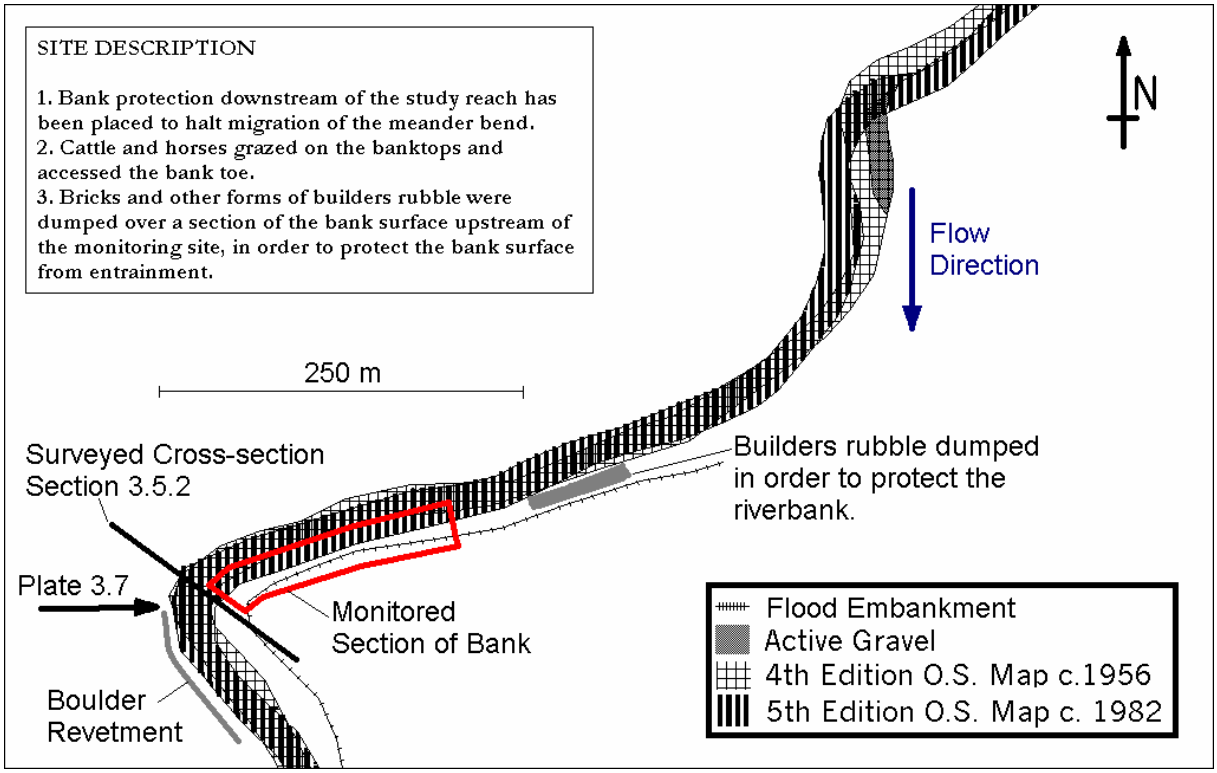

Figure 3.12 A site map of MORTON-ON-SWALE (Site 7) showing the position of the monitored section of the bank, and the position of the channel in 1956, and 1982.

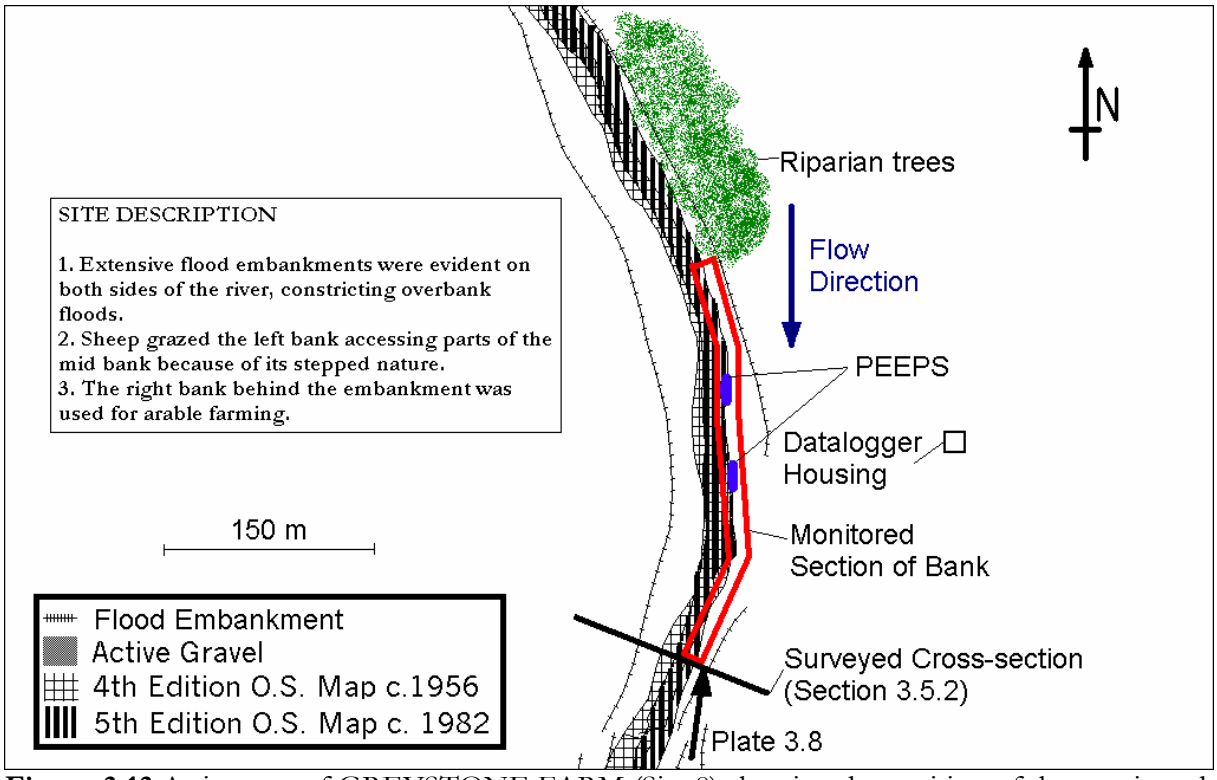

Figure 3.13 A site map of GREYSTONE FARM (Site 8) showing the position of the monitored section of the bank, and the position of the channel in 1956, and 1982.

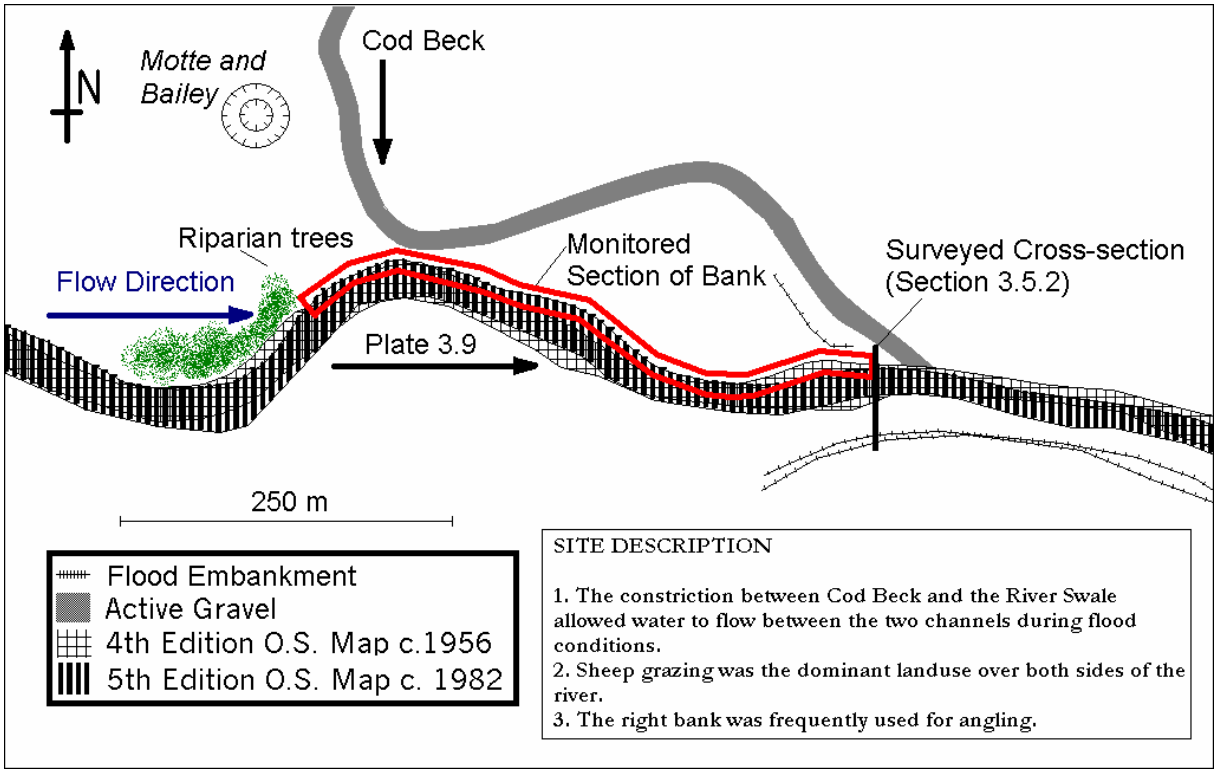

Figure 3.14 A site map of TOPCLIFFE (Site 9) showing the position of the monitored section of the bank, and the position of the channel in 1956, and 1982.

3.4.3 Erosion Pins

The baseline data for the rates of erosion at each monitoring site were provided by erosion pin measurements. Erosion pins are both simple to use and relatively economical, because of this they have been employed in previous bank erosion studies (Wolman, 1959; Hooke, 1980; Thorne, 1981; Lawler, 1986; Stott, 1997). A comprehensive review of the use of pins and their limitations is provided in Lawler (1978: 1993a).

Approximately thirty pins were installed at each monitoring site, except for Easby (Site 6) (Table 3.7) where the bank conditions were unsuitable for pin insertion due to the large clast size. The pins were made of lengths of silicon bronze welding rod, 1.2 mm in diameter and 370 mm or 500 mm in length. The 500 mm long pins were used on the joint LOIS-Ph.D. sites at Morton-on-Swale (Site 7) to Topcliffe (Site 9) (Figure 3.5). The diameter meant there was sufficient strength to allow pin insertion perpendicular to the bank surface with minimal disturbance. The length was chosen so that the pins were not long enough to support potential cantilever failures (Hooke, 1980; Thorne, 1981). One end of the erosion pin was covered with 30 mm of yellow heatshrink

(Lawler, 1989), which was left exposed when the pin was installed. The distinctive colour of the heatshrink allowed easier identification in the field, helping to reduce the number of unrecovered pins in each recording session. The pins were inserted in a grid network at each site, with the gridded area selected so that the entire eroding bank surface was covered (Table 3.7) (Figure 3.15). The exceptions to this were at Beck Meetings (Site 1) and Reeth (Site 5) where the length of the eroding face was too long to be practical, and access difficult. So the most accessible section was used instead of the whole eroding face.

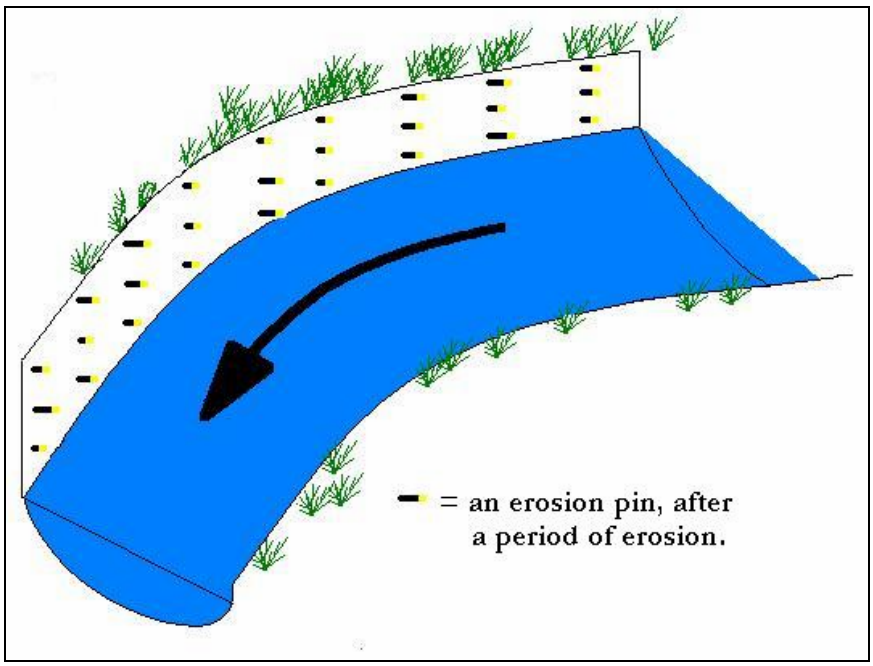

Figure 3.15 A typical erosion pin monitoring site installation, showing variable erosion on the pins. The arrow shows the stream flow direction.

An eighteen-day interval was used between pin readings during the more active winter months; this was extended to approximately monthly readings during the summer. Other studies (Stott *et al.*, 1986; Casagli *et al.*, 1999) have used a much longer interval between measurements, of two to three months. The selected period was chosen to allow the seasonal change in erosion rates to be assessed with confidence whilst being practical in terms of time and money. The summer increase in bank vegetation and lower flows meant that less frequent visits were needed, as often no recordable erosion was identified.

If a pin was clearly buried by eroded debris then it was attributed a value of 0 mm of erosion (Stott, 1999). The same was true if the erosion pin was only partially buried; however a note was also made that the pin had been buried or partially buried. If there was any doubt as to whether

the pin had been eroded out of the bank, buried, or hidden by vegetation, no value of erosion was attributed to the pin. If the pin was re-exposed during the next recording session then the average amount of erosion per day was calculated from the date it was last read. Readings could not be taken during flood inundation, or when they were inaccessible due to ice and snow. The same convention of averaging the unread pins, as used for re-exposed pins, was adopted in these cases.

The pins were read along their exposed length, perpendicular to the bank surface, up to the start of the heatshrink. The vernier callipers used allowed measurements to be recorded to the nearest 0.1 mm, reading the distance along the top of the pin from bank surface to the start of the heatshrunk section. After a measurement had been taken pushing them into the bank so that the heatshrink edge was flush with the sediment surface reset the pins. If an erosion pin was completely eroded out of the bank then a value of 300 mm was recorded for the pins 370 mm in length, and 400 mm for the pins 500 mm in length. This is in accordance with the methodology used by Hooke (1980) and Thorne (1981); which assumed that this was shortest length that the pin would have to be exposed before it was entrained, or removed by gravitational forces.

Stott (1999) randomly measured seven erosion pins using callipers with the same accuracy as those used in this study, standard errors ranged 0.17 to 0.33 mm with a mean of 0.26 mm. Lawler (1993a) suggested that mean erosion rates, derived from a large number of erosion pin measurements, should have their variability represented by $\pm$ 1 standard deviation from the mean.

SITE NUMBER AND NAME	O.S. GRID REFERENCE AND *DISTANCE DOWNSTREAM (KM)*	DATE INSTALLED	NUMBER OF EROSION PINS*	NUMBER OF PEEPS *(INSTALLATION DATE)*	APPROX. BANK HEIGHT (m)	VERTICAL PIN SPACING (m)	HORIZONTAL PIN SPACING (m)
1. Beck Meetings	NY 81750360 *2.6*	09/12/95	30	3 *(29/03/96)*	1	0.4	1.5
2. Hoggarths	NY 87640157 *8.8*	30/11/95	27		1	0.3	0.8
3. Muker	SD 90909892 *15.2*	30/11/95	36		1.5	0.5	3
4. Low Row	SD 97579739 *23.4*	14/01/96	36	4 *(31/10/96)*	1.7	0.7	2
5. Reeth	SE 03459886 *29.9*	30/11/95	28		1.5	0.5	2
6. Easby	NZ 18400040 *49.5*				4		
7. Morton-on-Swale	SE 31859180 *74.7*	16/12/95	31		4	0.7	3
8. Greystone Farm	SE 35408530 *87.4*	29/02/96	61	4 *(31/03/96)*	2.5	0.5	2
9. Topcliffe Manor Farm	SE 41307490 *104.4*	04/02/96	49		4	1	40
Total			288	11			

* Not including Photo-Electronic Erosion Pins.

Table 3.7 Monitoring site locations and the installation dates of erosion pins and PEEPs. The number of PEEPs and erosion pins, including the spacing of rows and columns of erosion pins.

3.3.4 Photo-Electronic Erosion Pins (PEEPs)

Whilst erosion pins are simple and economic, providing a good spatial coverage of the eroding bank surface, the data they provide is limited by the frequency of re-measurements. To overcome this problem, and to aid the identification of individual erosion process by monitoring at an event time-scale, Photo-Electronic Erosion Pins (PEEPs) were used (Lawler, 1991). The sensor consists of an array of ten photo-voltaic cells mounted in a transparent acrylic tube (Figure 3.16). The photo-voltaic cells produce a voltage that is proportional to the amount of light that reaches the sensor. The reference cell (Figure 3.16) has the same voltage output as the other nine photo-voltaic cells (known as the cell series) combined. Changes in sunlight intensity can be accounted for by dividing the reference cell voltage by the cell series (Equation 3.1).

$$L_{expd} = a+b\ R_p \qquad (3.1)$$
$$R_p=(V_{ser}/V_{ref})$$

Where:
L_{expd} = length of PEEP exposed (mm).
a = regression constant derived from calibration.
b = regression constant derived from calibration.
R_p = photovoltaic ratio.
V_{ser} = output from the cell series (mV).
V_{ref} = output from the reference cell.

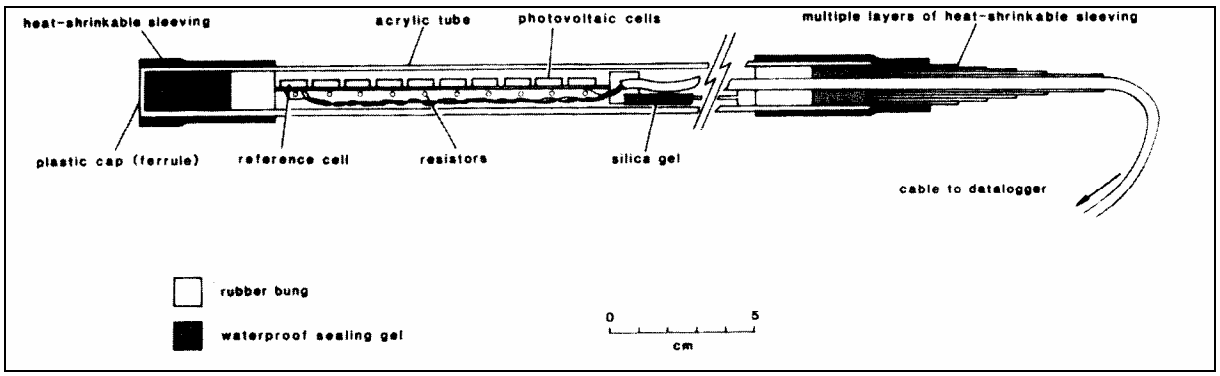

Figure 3.16 The Photo-Electronic Erosion Pin (PEEP) sensor (Lawler, 1991, p. 2126).

The regression constants a and b were calculated by covering the photo-voltaic sensors on each of the PEEP sensors with a sleeve of black tubing, simulating the initial state of the PEEP installed in the riverbank. The cells were exposed at 2 mm intervals for the whole active length of ~100 mm, noting V_{ser} and V_{ref} at the same time. The linear increase of R_p when plotted against L_{expd} allowed the constants to be estimated, alongside the explained variance (R^2) and standard error, for each pin (Table 3.8) (Lawler, 1989). PEEP 11 (version AED12) was industrially manufactured, unlike the other 'homemade' versions, and its own standard calibration equation was used (Table 3.8).

The PEEPs were inserted into the riverbank perpendicular to the bank surface, with their wires taken out of the back of the sensor tubing, through the bank, and out to a data logger (Figure 3.17). Auguring into the bankface and the banktop surface was done with the minimum amount of disturbance to the surrounding sediment to reduce destabilising the bank sediment, especially the bank surface around the PEEP so as not to cause an artificial crater. An unnatural hollow around the sensor could affect the hydrometeorological conditions during monitoring.

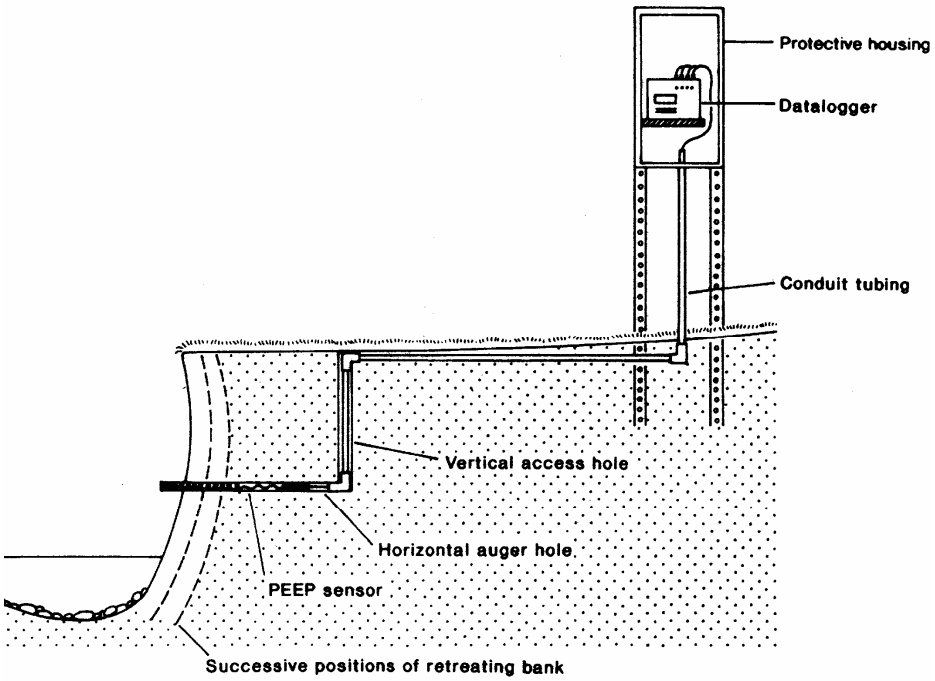

Figure 3.17 Schematic installation of the PEEP at a riverbank site (Lawler, 1992b, p.457).

After the PEEPs were installed the voltages, V_{ref} and V_{ser}, were logged instantaneously at a 15-minute interval. This was a compromise between a temporal resolution that would allow individual processes to be identified, at a hydrological event time scale, and the data storage capability of the data loggers. The loggers used were Grant Instrument Ltd Squirrel 1202 and 1206, or a Campbell Scientific Ltd CR10.

The length of each PEEP exposed was measured along the upper surface of the sensor from the sensor tip to the bank surface. At the same time the voltages V_{ref} and V_{ser} were noted. This allowed a *field* calibration of the instruments, which was subsequently compared to the *laboratory* calibration (Section 6.3.2). If erosion had taken place then the sensor was reset in the bank by pushing the PEEP into the bank surface until the reference cell and part of the first cell in the cell series were exposed, and the new length of exposure, V_{ref} and V_{ser} noted. If deposition had occurred then the sensor was left buried so that the time at which it was re-exposed, by erosion of the surface debris, could be determined. This also limited the amount of disturbance to the bankface. If, however, over a metre of erosion occurred then the bank insertion hole had to be re-augured. The new holes were usually slightly offset from the original ones due to the old remaining vertical holes used to feed the wires (Figure 3.17) which could allow preferential erosion to take place (Plate 3.10).

Plate 3.10 An exposed section of buried cabling for the PEEP system at Greystone Farm (Site 8) showing preferential erosion around the vertically augured hole and PEEP sensor to the right (27/08/97). River flow was from left to right of the frame. Approximately 400 mm of grey tubing was exposed.

PEEP NUMBER (SITE AND POSITION)	LINEAR REGRESSION EQUATION (mm)	CO-EFFICIENT OF DETERMINATION R^2 (%)	STANDARD ERROR (mm)
1 (***Site 1*** *Upper)*	$L_{expd} = 98.34R_p + 46.59$	99.7	2.10
2 (***Site 1*** *Middle*)	$L_{expd} = 109.78R_p + 51.35$	99.8	1.40
3 (***Site 1*** *Lower*)	$L_{expd} = 109.05R_p + 54.02$	99.8	1.36
4 (***Site 8*** *Downstream Lower*)	$L_{expd} = 123.64R_p + 48.42$	99.3	2.31
5 (***Site 4*** *Downstream Lower*)	$L_{expd} = 95.15R_p + 46.08$	99.7	2.09
6 (***Site 4*** *Upstream Upper*)	$L_{expd} = 101.63R_p + 35.31$	99.8	1.65
7 (***Site 4*** *Upstream Lower*)	$L_{expd} = 95.67R_p + 37.19$	99.7	2.01
8 (***Site 8*** *Downstream Upper*)	$L_{expd} = 107.10R_p + 47.41$	98.5	3.50
9 (***Site 8*** *Upstream Lower*)	$L_{expd} = 123.36R_p + 52.64$	99.5	2.22
10 (***Site 8*** *Upstream Upper*)	$L_{expd} = 97.74R_p + 48.34$	99.8	1.39
11 (***Site 4*** *Downstream Upper*)	$L_{expd} = 111.45R_p + 18.32$	99.7	0.632

Table 3.8 PEEP positions, linear regression equations, coefficients of determination and standard errors.

3.3.5 Stage Measurements

The length of time pins and PEEPs were submerged could act as an indicator for the amount of exposure to fluvial entrainment. The amount of time that the banks were inundated could also have implications for the bank moisture content. Thus, automatically logged pressure transducers were used to determine the stage of the River Swale; comparisons were made with these data and IH gauging station data.

The automatically monitored sites at Beck Meetings (Site 1) and Low Row (Site 4) (Figure 3.5) were installed with SH3500 Dynamic Logic Ltd pressure transducers. Before being installed in the field the sensors were calibrated in a water tank, with voltage outputs taken every 20 mm over a 10 to 520 mm depth range. The voltage output (mV) was linearly regressed against the water depth (m). The explained variance (R^2) for the transducer at Beck Meetings was 99.5 %, and at Low Row 99.7 %.

The pressure transducers were installed at the monitoring sites enclosed in a plastic stilling well to protect them from flood debris. The stilling well was placed vertically in the river at approximately a 700 mm perpendicular distance away from the bank surface, with a ruler attached to act as a stage board (Figure 3.18). At Beck Meetings a Dexion structure was sufficient to hold the sensor, with cabling fed along the supports into the bank. The flow velocity at Low Row, combined with the woody debris deposition to a greater degree than at Beck Meetings, meant that the original Dexion structure was not strong enough to support the sensor. To overcome this problem a stronger scaffolding support was installed. The channel cross-section was surveyed, including the position of the transducer base, allowing the stage to be calculated from the arbitrary height recorded.

The data loggers scanned the pressure transducer outputs at a 15-minute interval, at the same time as the PEEP measurements. The logging interval was also timed to coincide with the stage measurements recorded at the IH gauging stations at Catterick and Crakehill (Figure 3.1), which allowed the stage changes at the downstream sites to be estimated. At each downloading session the water level on the stage board was recorded alongside the voltage output, and excitation voltage. This allowed a *field* calibration of the sensor and a confirmation that the excitation voltage had not gone beneath the critical threshold.

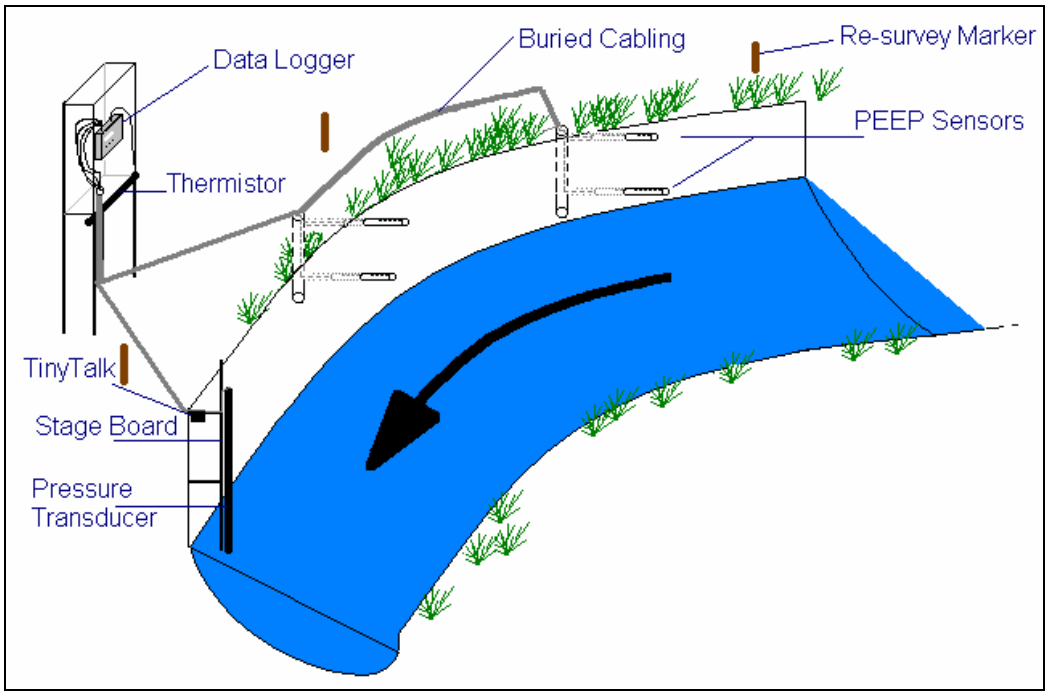

Figure 3.18 A typical installation of equipment at a PEEP monitored site, including data logger, PEEPs, pressure transducer with a stage board, TinyTalk, thermistor, and re-survey markers.

3.3.6 Air and Bankface Temperature

The importance of air temperature as a variable used to model the timing, and magnitude, of bank erosion was shown by Lawler (1986). Rather than using a remote weather station to measure air and bankface temperature *in situ* measurements were taken at Beck Meetings (Site 1), Low Row (Site 4), and Greystone Farm (Site 8). Air temperature was measured using Grant Instruments Ltd mini-thermistors, with a smooth-ended 321 stainless steel probe. The probes were capable of measuring temperature in the range of –50 to + 150 °C. The maximum deviation of the probes from the theoretical resistance/temperature, in the temperature range of 0 to 70 °C, is ± 0.2 °C.

The thermistor probe was housed in a 300 mm length of white plastic tubing, positioned underneath the environmental housing that contained the data logger. The plastic tubing was open ended and perforated with small holes along its length, situated approximately 1.2 m from the ground surface. This arrangement mimicked a standard Stevenson Screen measurement of dry bulb temperature.

The bankface temperature was measured using Gemini Data Loggers (UK) Ltd *Tiny Talk II* data loggers. The thermistors were able to take readings in the temperature range of –10 to +40 °C, with an accuracy of ± 0.2 °C. The data loggers were waterproof to a depth of 15 m, and only 78 x 50 x 34 mm in size. This meant that they could be placed on the bank surface with minimal disturbance to the flow, and no problems due to water ingress during inundation. At each of the sites the sensor was attached to a piece of Dexion 300 mm beneath the bank top, at Beck Meetings and Low Row (Figure 3.5) this was part of the pressure transducer structure (Figure 3.18). The sensor element of the thermistor/logger was situated flush with the bank surface.

Logging at a 15-minute interval meant that an eighteen-day downloading interval was necessary due to memory constraints of the *Tiny Talk II*. During the summer months the logging interval was extended to thirty minutes to lessen the frequency of downloading trips. The advantage of using the *TinyTalk II* was that it did not need any cabling to be laid from the bankface to logger housing, which at Greystone Farm was a distance of ~50 m. Fixing the device to the bank surface did however mean that during periods of high flow the data logger could not be retrieved for downloading, reducing the data recovery for the sensors (Tables 3.9 – 3.11).

3.5 CHANNEL MORPHOLOGY AND VEGETATION ASSESSMENT

3.5.1 Planform Bank-top Re-survey

The erosion pins provided spatial information on the active processes on the bank surface but large-scale failures may completely remove all the erosion pins. Mass failures may also relocate entire sections of the bank over time, moving the erosion pins within the failure, but not registering any erosion on the pins. To overcome these problems, and add a verification mechanism for the pin measurements, the position of the riverbank top was surveyed over time to highlight any large-scale erosional events.

A Zeiss Elta 4 Electromagnetic Distance Meter (EDM) was used to measure the planform position of the bank-top. Survey pegs were inserted at all sites, except Muker (Site 3) (Figure 3.5), where land-use conflicts made this impossible. The pegs were used as reference markers enabling the position of the EDM to be established at each survey date. The function of the surveying was not to produce a detailed map of the bank-top, but rather to highlight any major

changes in planform morphology to an accuracy of approximately ± 0.025 m (Couperthwaite, 1997).

At Easby (Site 6) the gravely nature of the bank material meant that it was not feasible to instrument the bank face with erosion pins. The bank was therefore surveyed with a greater frequency than the other monitoring sites (approximately every 36 days).

3.5.2 Cross-sectional Survey

At each of the monitored sites one cross-sectional profile was measured. The EDM was used to measure the larger cross-sections, whilst at the narrower upstream sites (Beck Meetings (Site 1) and Hoggarths (Site 2)) a fibreglass tape measure and plastic ruler was used (Pugh, 1975). The flow conditions in the channel were observed during two and a half years of monitoring. The bankfull flow conditions had been observed at all the sites, giving confidence to the definition of the bankfull cross-section at the end of the study. The break in slope combined with a loss of vegetation was usually distinct at the bank being monitored at each site (Plates 3.1-3.9). The level of the bank surface on the opposite bank was sometimes less distinct. In all cases the surveyed height from the well distinguished bank top was compared with the height of the opposite bank. The height of point bar structures, changes in vegetation from woody to herbaceous, the level of trash lines, and regions of sedimentation (Petts, 1983) were all then used to verify that the correct height had been used on both sides of the channel.

3.5.3 Vegetational Survey

Instream and bank surface, and bank top vegetation can all affect the type of erosion processes that occur (Section 2.5) (Haslam, 1978; Thorne, 1990). To account for the vegetational influences at each of the monitoring sites a hand survey was used to identify the species along a 3 m wide section parallel to the bank edge, and any bank surface or instream vegetation. The width was selected so that it could encompass the extent of the bank subject to mass failures that would be influenced by vegetation. The length of bank with erosion pins defined the longitudinal extent of the survey. The abundance of each of the species was not measured, as the majority of the sites were uniformly vegetated grazed grassland.

3.6 CHANNEL BOUNDARY SEDIMENT SAMPLING

3.6.1 Bank Sediment Sampling

The proposed downstream change of mass failures (Section 1.) is affected by the composition of the bank sediment, with more cohesive bank material able to attain a greater height. Fluid entrainment is also affected by the grainsize of the bank material, with a proposed increase in erosion in the 0.1 –0.5 mm size range (Shields, 1936).

To describe the properties of the bank sediment at each of the monitoring sites, six samples were taken. The samples were extracted from the top, middle, and bottom of the bank at the same heights as the upper, mid and lower erosion pins. Two columns of samples were taken at the upstream and downstream limits of the pinned section of the bank.

The samples were taken at the end of the monitoring period so that the bank would not be disturbed whilst measurements were being taken. Pre-weighed cylindrical bulk density sampling tins were used to extract 231 cm^3 of sediment at each sampling point. The tins were inserted until they were flush with the surface and then removed by excavating the soil around the tin. So that the moisture content of the sample could be determined the tins were sealed straight away and sealed in plastic bags.

Moisture Content Determination and Loss on Ignition

The samples were weighed after extraction, then placed in an oven at 105 ^{0}C for 12 hours (British Standards Association, 1975), and reweighed after drying. This allowed the moisture content of the sample to be determined. The dried sample was then disaggregated using a pestle and mortar, using as little force as possible to avoid crushing any particles. A pre-weighed part of each sample was placed in a crucible of a known weight, placed in an oven at 105 ^{0}C for 12 hours, to ensure a consistent dried weight, and then placed in a Muffle furnace at 850 ^{0}C for 30 minutes (McRae, 1988). The loss of ignition that is gained from heating the sediment at 850 ^{0}C was a measure of the amount of organic matter within the sample. There may have been other losses during the firing, such as the conversion of $CaCO_3$ to CaO, and the dehydration of amorphous

oxides and clay minerals (McRae, 1988). The technique is best suited to either very peaty, or very sandy, soils to represent the true organic content. There may, therefore, be some differences in the representativeness of this technique between the upland peaty sites and the lowland silty-clay sites.

The British Standards Association (1975) recommends a loss of ignition technique involving a temperature of 440 ± 25 ^{0}C for three hours. From the fifty-one samples extracted ten were selected at random and dried at 440 ^{0}C for three hours, weighed and then returned to the oven for thirty minutes at 850 ^{0}C. The means of the ten samples before and after the 850 ^{0}C treatment showed no significant difference from each other, using a 95 % confidence limit on a students t-test.

Particle Size Determination

The particle size distribution of the samples was determined using two techniques. The coarse fraction, > 250 μm, was sorted using 6 sieves (8 mm, 4 mm, 2 mm, 500 μm, and 250 μm). The pre-dried, at 105 ^{o}C for 12 hours, pre-weighed samples were wet sieved using mechanical agitation for fifteen minutes. The content of each sieve was placed in a pre-weighed container, dried at 105 ^{o}C for 12 hours, and then the weight of the dry sample and container measured. The combined dry weight of the sediment collected on the sieves was subtracted from the original total sample weight. The difference was assumed to equal the collected < 250 μm fraction weight. There is some loss in the system due to particles getting stuck in the sieves, however this was assumed to be negligible.

The fine fraction (<250 μm) was analysed using a Mastersizer Micro particle sizer (Malvern Instruments, 1994). A well-mixed sample of the fine sediment suspended in tap water was diluted in water used as a background measurement standard. The dilute sample was measured twice to check for any drift in the measurements.

The laser diffraction method used in the Mastersizer Micro assumed all the particles to be spherical and of a known density. The scattering of a laser beam by Mie diffraction allows the particle size to be estimated. The percentages of each range of particle sizes were converted into mass ranges by assuming a quartz density of 2.65 kg m^{-3}.

3.6.2 Riverbed Sediment Sampling

The riverbed sediment size distribution allows an estimation of the bankfull flow velocity at each of the monitoring sites (Limerios, 1970; McEwen, 1994) (Section 4.4.4). The velocity could then be used to calculate the bankfull discharge if the cross-sectional area was known, and finally the stream power at points throughout the river catchment (Equation 4.6). Two different methods were used to determine the sediment sizes of the river bed material:

1. A Wolman count (Wolman, 1954) for the larger sediment sizes, > 8 mm (Church *et al.*, 1987).
2. Grab samples were taken on beds with smaller sediment sizes, < 8 mm (Fripp and Diplas, 1993).

The Wolman count involved randomly selecting 100 particles across the riverbed profile. The selected particles were measured along their B axes, using vernier callipers, or a metal tape measure with an accuracy of ± 1 mm.

Where the riverbed sediment was mainly sandy in size i.e. Morton-on-Swale (Site 7), Greystone Farm (Site 8), and Topcliffe (Site 9) (Figure 3.5) the Wolman count was not suitable. The sample was taken by using a plastic bag to 'grab' the sediment from the riverbed. The problem with this technique is that it does not only remove the material in contact with the flow, but also the sediment beneath this layer (Fripp and Diplas, 1993). The velocity in the channel may not have been in contact with the sediment, distorting the estimation of the bankfull discharge. The sampling was also affected by the fact that the grab was spatially limited, not necessarily representative of the whole reach with size distribution differences caused by riffles and pools.

Once collected the grab sample was dried and weighed. It was then analysed in the same way as the riverbank sediment samples (Section 3.5.1) in order to give a size distribution of each sample.

3.7 SUMMARY

1. The Ouse basin was chosen for the study due to the data available from IH, and the potential linkages with the LOIS project. The River Swale was selected for instrumentation because of the good spatial coverage of eroding sites and an almost natural flow regime.
2. Nine monitoring sites were instrumented. Eight had their planform bank edge position re-surveyed to provide gross estimates of bank retreat.
3. Two hundred and eighty-eight erosion pins were distributed over eight monitoring sites, and they were measured at an eighteen-day interval.
4. Three sites; in the upper (Beck Meetings (Site 1)), middle (Low Row (Site 4)), and lower (Greystone Farm (Site 8)) catchment were instrumented with automated monitoring equipment (Tables 3.9 - 3.11) recording at a 15-minute interval.
5. Riverbank morphology, vegetation characteristics, bank sediment size, loss on ignition, and bed sediment size were recorded at each monitoring site in order to model the variables influencing erosion rates and processes. These results, and the rates of erosion provided by the erosion pins, will be present in Chapter 4.

INSTRUMENTATION	MEASUREMENT VARIABLE	MEASUREMENT PERIOD	DATA RECOVERY DURING INSTALLATION PERIOD (%)
PEEP 1 *(Upper)*	Bank Erosion/Deposition	29/03/96 - 23/04/98	68.7
PEEP 2 *(Middle)*	Bank Erosion/Deposition	29/03/96 - 23/04/98	68.7
PEEP 3 *(Lower)*	Bank Erosion/Deposition	29/03/96 - 23/04/98	74.0
Thermistor	Air Temperature	31/10/96 - 23/04/98	97.6
Thermistor	Bank Face Temperature	14/01/97 - 23/04/98	79.1
Pressure Transducer	River Stage	30/11/96 – 23/04/98	86.8

Table 3.9 A summary of automated instrumentation installed upstream at Beck Meetings (Site 1).

INSTRUMENTATION	MEASUREMENT VARIABLE	MEASUREMENT PERIOD	DATA RECOVERY DURING INSTALLATION PERIOD (%)
PEEP 5 (*Downstream Lower*)	Bank Erosion/Deposition	31/10/96 - 19/04/98	93.3
PEEP 7 *(Upstream Lower)*	Bank Erosion/Deposition	31/10/96 - 19/04/98	93.6
PEEP 11 (*Downstream Upper*)	Bank Erosion/Deposition	31/10/96 - 19/04/98	93.3
PEEP 6 *(Upstream Upper)*	Bank Erosion/Deposition	31/10/96 - 19/04/98	93.3
Thermistor	Air Temperature	29/06/96 - 19/04/98	99.7
Thermistor	Bank Face Temperature	23/12/96 - 19/04/98	54.4
Pressure Transducer	River Stage	23/12/96 - 19/04/98	77.2

Table 3.10 A summary of automated instrumentation installed mid-catchment at Low Row (Site 4).

INSTRUMENTATION	MEASUREMENT VARIABLE	MEASUREMENT PERIOD	DATA RECOVERY DURING INSTALLATION PERIOD (%)
PEEP 4 *(Downstream Lower)*	Bank Erosion/Deposition	31/03/96 - 11/03/98	93.3
PEEP 8 *(Upstream Lower)*	Bank Erosion/Deposition	31/03/96 - 19/04/98	93.6
PEEP 9 *(Downstream Upper)*	Bank Erosion/Deposition	31/10/96 - 19/04/98	93.3
PEEP 10 *(Upstream Upper)*	Bank Erosion/Deposition	31/10/96 - 19/04/98	93.3
Thermistor	Air Temperature	31/10/96 - 23/04/98	99.7
Thermistor	Bank Face Temperature	14/01/97 - 23/04/98	54.4
Pressure Transducer	River Stage	30/11/96 – 23/04/98	77.2

Table 3.11 A summary of automated instrumentation installed downstream at Greystone Farm (Site 8).

CHAPTER 4

SPATIAL VARIABILITY IN BANK EROSION RATES AT THE CATCHMENT SCALE

4.1 INTRODUCTION

Consideration of downstream changes in erosion rates at the basin scale can reveal the regions of erosion dominance. A constant rate of erosion throughout the catchment could indicate a single process of erosion maintaining its efficacy. Peaks in erosion rates may be due to the changing efficacy of a single process, an alteration of the type of erosion process, or the combination of several processes. Associated downstream patterns in the catchment sedimentology, channel form, and riparian ecology can aid the prediction of erosion processes.

4.2 DOWNSTREAM CHANGE IN EROSION RATES

4.2.1 Erosion Pin Results

A mid-basin peak in erosion rates was observed when the average rates of erosion at the monitoring sites were considered (Table 4.1) (Figures 4.1 and 4.2).

Downstream →	Site Name	ER9698 Average Rate of Erosion from 29/02/96-13/03/98 (mm a^{-1})	Standard Deviation of Erosion Rates from 29/02/96-13/03/98 (mm a^{-1})	Coefficient of Variation for erosion rates from 29/02/96-13/03/98 (%)	ER9798 Average Rate of Erosion from 16/01/97-13/03/98 (mm a^{-1})	Standard Deviation of erosion rates from 16/01/97-13/03/98 (mm a^{-1})	Coefficient of Variation for erosion rates from 16/01/97-13/03/98 (%)
	1. Beck Meetings	66.1	93.6	141.6	74.7	110.3	147.5
	2. Hoggarths	140.2	242.6	173.0	84.0	115.1	136.9
	3. Muker	257.3	400.2	155.6	272.6	472.8	166.5
	4. Low Row	91.8	124.9	136.1	91.6	140.8	153.8
	5. Reeth	619.6	646.8	104.4	476.0	465.1	97.7
	6. Easby	**No Data**	**No Data**	**No Data**	***3582.2**	***8401.4**	***234.5**
	7. Morton-on-Swale	347.5	454.9	130.9	441.0	537.9	122.0
	8. Greystone Farm	414.4	363.2	87.7	506.0	386.8	76.5
	9. Topcliffe	128.4	160.7	125.2	154.5	186.3	120.6

Table 4.1 Average Pin Erosion and Standard Deviation for the Periods, 29/02/96-13/03/98 and 16/01/97-13/03/98. * = Erosion measured by banktop re-surveys.

The total erosion recorded on each of the erosion pins, at each site, was used to calculate the average rate of erosion for both the whole study period (ER9698) and when all the sites were being monitored simultaneously (ER9798) (Table 4.1). The upstream sites had a low rate of erosion that increased from Beck Meetings (Site 1) to Muker (Site 3) during both the periods under consideration (Figures 4.1 and 4.2). The rate of erosion decreased at Low Row (Site 4), followed by a rise in the erosion rate to a mid-basin peak at Easby (Site 6). The rates of erosion, at the downstream sites for both periods, decreased at Morton-on-Swale (Site 7), increased again at Greystone Farm (Site 8), and finally at Topcliffe (Site 9) were about a quarter of the rate at Greystone Farm (Site 8) (Figures 4.1 and 4.2).

To model the general trend of erosion rates throughout the catchment, so that the optimum points of erosion could be identified, a simple quadratic least-squares function has been fitted to the data (Figure 4.1). The regression equation was of the form:

$$ER9698 = -0.7249DDS^2 + 78.742DDS - 555.26 \quad (4.1)$$

(n = 9, R^2 = 36.9 %, R^2 95 % significance level = 44.3 %, R^2 90 % significance level = 33.9 %)

Where:

ER9698 = site spatially averaged erosion rates from c.29/02/96 – c.13/03/98 (mm a^{-1}).
DDS = distance downstream from the river source (km).

If Easby was excluded from the analysis (Figure 4.1) then the revised regression was of the form:

$$ER9698\text{-}E = -0.1532DDS^2 + 17.287DDS + 5.0867 \quad (4.2)$$

(n = 8, R^2 = 51.8 %, R^2 95 % significance level = 50.0 %, R^2 90 % significance level = 38.7 %)

Where:

ER9698-E = site spatially averaged erosion rates from c.29/02/96 – c.13/03/98 excluding Easby (mm a^{-1}).

For the common monitoring period at all the sites from c.16/01/97-c.13/03/98 (Figure 4.2) the regression equation was:

$$ER9798 = -0.7185DDS^2 + 79.096DDS - 587.46 \quad (4.3)$$

(n = 9, R^2 = 37.2 %, R^2 95 % significance level = 44.3 %, R^2 90 % significance level = 33.9 %)

Where:

ER9798 = site spatially averaged erosion rates from c.16/01/97 – c.13/03/98.

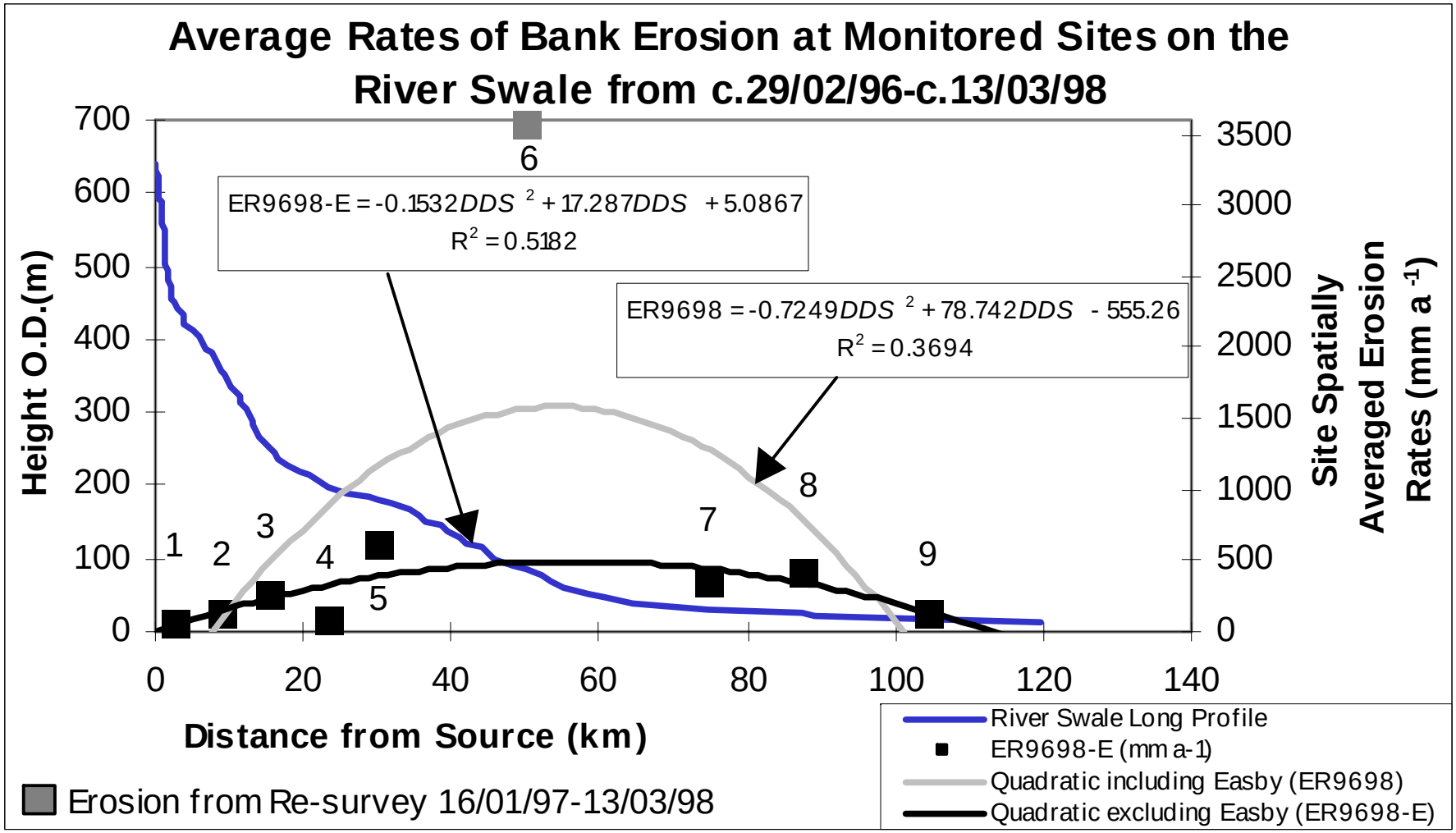

Figure 4.1 Polynomial trend lines for average rates of bank erosion at the monitoring sites from c.29/02/96-c.13/03/98 (ER9698), and for all the monitoring sites excluding the non-erosion pin site Easby (ER9698-E).

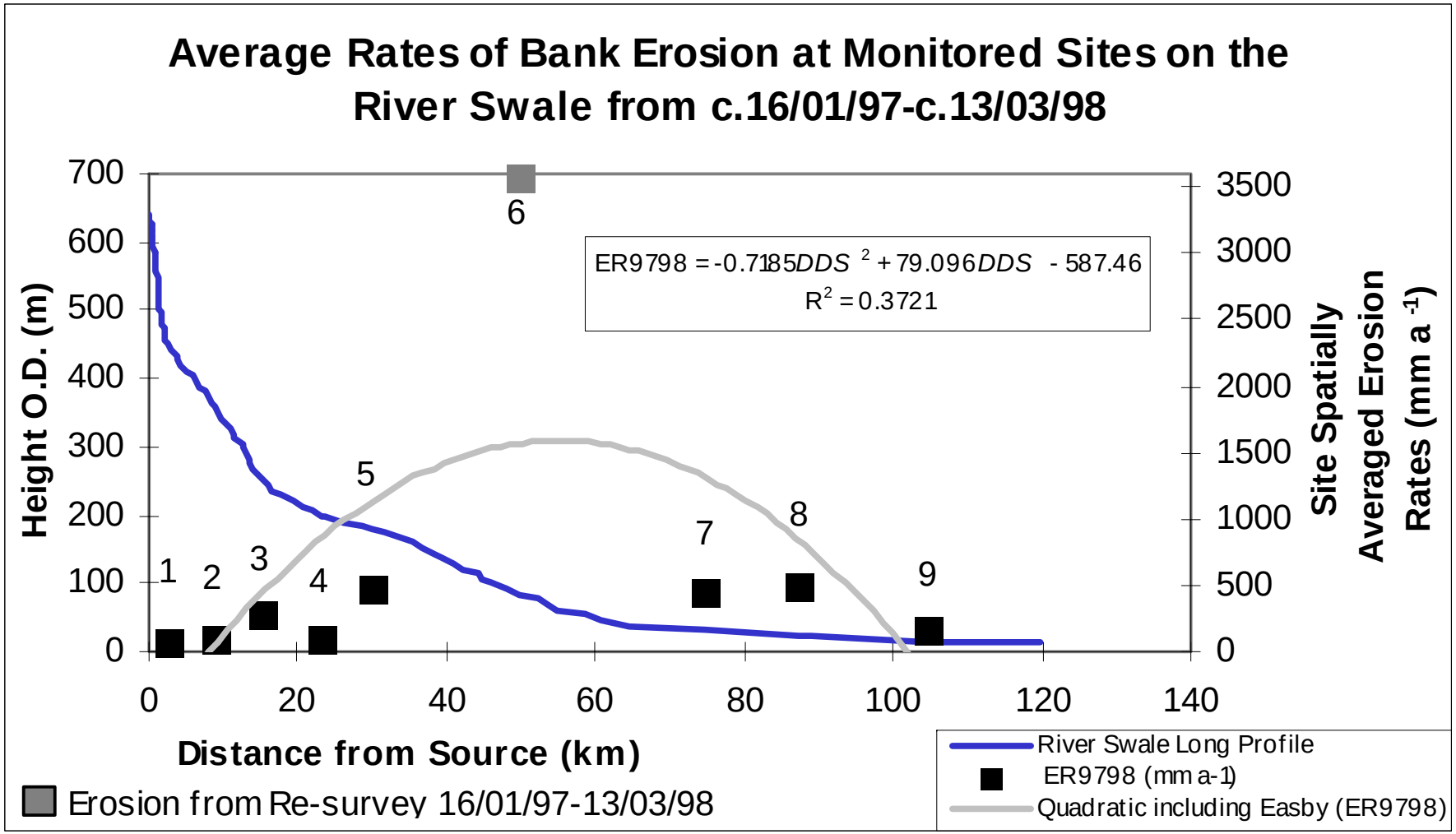

Figure 4.2 A polynomial trend line for average rates of bank erosion at the monitoring sites from c.16/01/96-c.13/03/98 (ER9698).

The standard deviation of the cumulative erosion pin measurements gives an indication of the spread of data around the mean, and may be used to describe the measurement error (Lawler, 1993a). Proportionally the highest variability occurred upstream at Hoggarths during the longer monitoring period (Table 4.1), whilst during the shorter common measurement (ER9798) Muker had a larger standard deviation.

The coefficients of variation (CV) are calculated by dividing the standard deviations by the sample means (Webster and Oliver, 1990). This measure allows the data to be more comparable with each other. Laubel *et al.* (1999) found that the coefficients of variation for their erosion pins were over 100 % due to the high degree of spatial variability. Most of the CVs for the Swale were, as with Laubel *et al.* (1999), above 100% (Table 4.1). The lowest values of CV for the erosion pins were at Reeth and Greystone Farm for both ER9698 and ER9798 (Table 4.1), perhaps indicating more consistent average erosion values during the monitoring period at these sites.

If the monitoring period was divided into two years, from March 96-March 97 and from March 97-March 98, a difference in the annual rates of erosion may be observed (Figure 4.3). This inconsistency in average annual erosion rates may be due to the errors in measurement; however changes in environmental variables such as temperature, rainfall, and stage may also responsible. The variations in erosion rates over time, and the variables that affect the differing rates may be used to understand the processes of erosion at each of the sites. The spatial variability of the channel morphology and sedimentology affecting erosion rates will be presented in Sections 4.3 and 4.4, and their influences on erosion processes will be explored in more detail in Chapter 5.

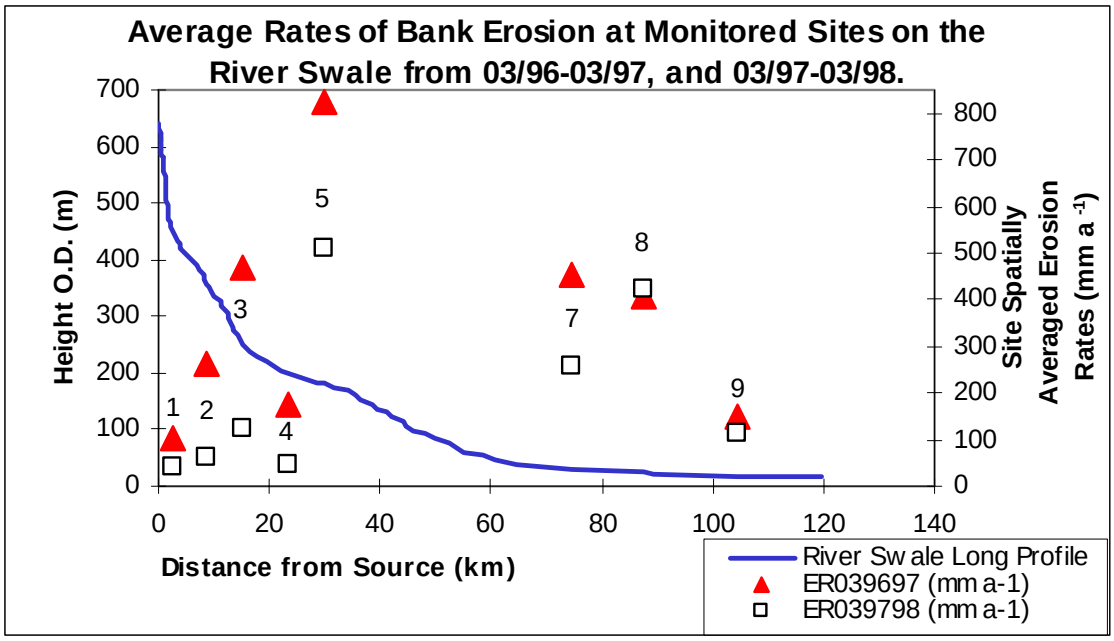

Figure 4.3 A comparison of the rates of average rates of erosion at all of the monitoring sites during the two periods from March 1996 – March 1997, and from March 1997 – March 1998.

4.2.2 Planform Re-survey Results

The change in planform during the study period was measured at five of the monitoring sites: Beck Meetings (Site 1), Hoggarths (Site 2), Low Row (Site 4), Reeth (Site 5), and Easby (Site 6). No erosion pins were used at Easby (Site 6) so the two forms of measurement, erosion pins, and re-survey, could not be compared. At the most downstream LOIS/Ph.D. sites (Sites 7 – 9) insufficient re-survey markers remained at the end of the study to allow an accurate repeat measurement.

The change in the planform does not replicate the erosion pin measurements as only the bank top surface was surveyed (Section 3.4.3), rather than points over the whole bank surface measured by the pins. Similarities between the two forms of measurement would, however, add confidence to the estimates from both measurements on the average rates of erosion. So that the measurements were comparable the re-survey data was plotted, and difference in bank edge positions at ten evenly spaced perpendicular sections was averaged (Table 4.2), similar to reading ten columns of erosion pins. Each surveyed point had an estimated error of 50 mm (Couperthwaite, 1997), and using two surveys to determine the difference in bank edge planform position gave an overall error of 100 mm. One standard deviation from the mean was used to represent the errors in the erosion pin measurements (Lawler, 1993a).

There was a general downstream trend of increasing erosion rates from Beck Meetings (Site 1) to Reeth (Site 5) (Table 4.2). The lowering of erosion rates measured on the erosion pins at Low Row (Site 4), compared to Sites 3 and 5, was not recorded by re-surveying. This difference in measurements indicates that the bank top at Low Row is more active than the average measurements of the whole bank surface, perhaps due to preferential erosion in one bank horizon undercutting the bank top.

Downstream →	MONITORING SITE	AVERAGE RATE OF PLANFORM BANK RETREAT (mm a^{-1})	AVERAGE EROSION PIN RETREAT (mm a^{-1})	MEASUREMENT PERIOD
	1. Beck Meetings	90 ± 100	43.3 ± 15.5	16/01/97-13/03/98
	2. Hoggarths	126 ± 100	64.1 ± 17.8	16/01/97-07/04/98
	3. Low Row	247 ± 100	45.8 ± 15.8	15/01/97-13/03/98
	4. Reeth	454 ± 100	509.3 ± 67.8	15/01/97-07/04/98

Table 4.2 A comparison of erosion rates obtained from re-surveying planform bank edge positions and average erosion pin measurements, from c. Jan. 1997 – c. April 1998.

Using maps of the river channel position over time (Table 4.3) the activity of the channel throughout the catchment, in planform, can be estimated, rather than limited to individual monitoring sites. The accuracy of the data is more limited using this method with changes in the river planform position between maps of over 10 m being considered significant (Sedgwick, 2000).

DATE	SCALE	SERIES
First edition: surveyed c.1854, published c. 1857	1: 10560	County
Second edition: resurveyed c. 1891, published c.1895	1: 10560	County
Third edition: revised c.1910, re-levelled c.1911, published c.1914	1: 10560	County
Fourth edition: revision of c. 1910 with major changes only in c. 1951, published in c.1956	1: 10000	National grid
Fifth edition: surveyed c.1980, published c.1982	1: 10000	National grid

Table 4.3 Archive map evidence used in the analysis of historical planform change on the River Swale (Sedgwick, 2000).

Sedgwick (2000) adapted the channel pattern classification used by Ferguson (1981) to define the Swale into seven different categories of change (Table 4.4) (Figure 4.4). The chosen categories for the reaches containing the monitoring sites from this study are presented in Table 4.5. The upstream sites (Beck Meetings and Hoggarths) and the most downstream site (Topcliffe) were considered to be the most stable, defined as stable confined meanders. Morton-on-Swale was

situated in the most active of the reach classifications, whilst most of the mid-catchment reaches were actively meandering.

Plotting the average erosion pin data against the channel pattern classification (Figure 4.4) allows the representativeness of the monitoring sites to be assessed. The general trend of increasing channel pattern in the mid-catchment is well represented by the spread of the monitoring sites, and the collected data. The classification of *active multi-channel* was considered to be a region of rapid erosion not monitored, although Muker (Site 3) is at the boundary between this zone and a reach of *active confined meandering*.

CHANNEL PATTERN CLASSIFICATION	DESCRIPTION
(7) Active multi-channel/ low-sinuosity	Rivers may be actively modifying their channels whilst not conforming to a classically braided or meandering channel pattern. In these rivers, bank erosion tends to be the result of mid-channel bar evolution during floods that actively transport bedload. At lower discharges bars may be emergent and divide the flow, giving a locally braided channel pattern.
(6) Highly or (5) Moderately active meandering	In unconfined alluvial meandering, erosion of the outer bank is complemented by point bar deposition on the inside of each bend as the meander loop grows or migrates. The lateral erosion at the bends was observed to be highly, or moderately active on the Swale.
(4) Inactive or (3) Active confined meandering	Media, such as narrow valleys may limit meander development, restricting the meander growth to those found in local unconfined valley material. These categories may be identified by (Ferguson, 1981): i) Restricted lateral growth that results in increased down-valley migration. ii) The development of a regular sequence of restricted bends that are typically box-shaped or square-wave form. iii) The creation of a long backwater slough in the wake of the migrating pool at the bend apex. iv) The transformation of an S-bend into a Z-shape lying across, not along, the valley with a hairpin bend at the point of confinement. v) The tendency to hug one or another valley wall for substantial distances. This is especially common where the valley itself is winding. The confined meanders may be classified as inactive or active during the period of study.
(2) Inactive straight (1) Inactive sinuous	There are three main types of inactive channel in Britain: i) Rock-bound channels, common in upland headwaters, which have incised meanders and low sinuosity and are often bounded by boulders. ii) Tree-lined, gravel rivers are common in the middle courses of many upland rivers and the headwaters of some lowland rivers in Britain. The trees may stabilise the riverbank, promoting channel stability. The channel pattern of inactive gravel rivers of this kind may be virtually straight, gently winding, or irregular with straight reaches and occasional fairly sharp bends. iii) Lowland rivers are common and geographically widespread in Britain. The combination of low stream power and cohesive, resistant bank sediments explains the absence of perceptible channel migration. Nevertheless they are not always straight. Some have a zigzag pattern with occasional bends linking straight or gently curved reaches.

Table 4.4 The channel pattern classification criteria used to describe the historic channel change in the River Swale (adapted from Sedgwick, 2000).

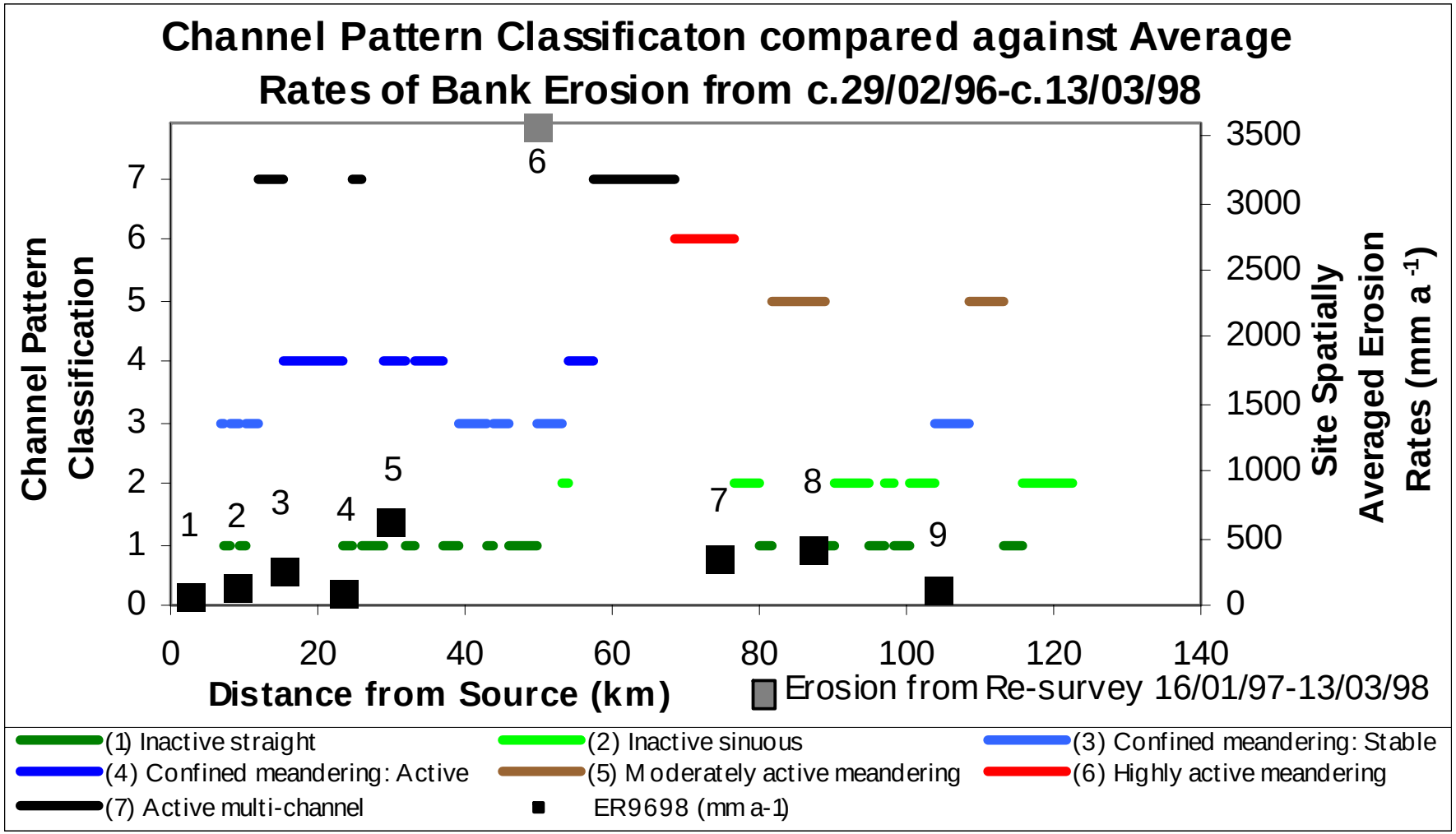

Figure 4.4 Classification of channel morphology and pattern change for the River Swale identified on five editions of OS 1:10 000/1:10560 scale maps covering the period from c.1854 – 1980, plotted against average erosion pin rates from 29/02/96-13/03/98.

MONITORING SITE	CHANNEL PATTERN CLASSIFICATION
1. Beck Meetings	Confined meandering: Stable
2. Hoggarths	Confined meandering: Stable
3. Muker	Confined meandering: Active
4. Low Row	Confined meandering: Active
5. Reeth	Confined meandering: Active
6. Easby	Confined meandering: Active
7. Morton-on-Swale	Highly active meandering
8. Greystone Farm	Moderately active meandering
9. Topcliffe	Confined meandering: Stable

Tables 4.5 The channel pattern classifications by Sedgwick (2000) for the reaches containing erosion pin and re-survey monitoring sites.

4.3 DOWNSTREAM TRENDS IN BANK SEDIMENT PROPERTIES

4.3.1 Introduction

The downstream trends in bank sedimentology directly influence the type of bank erosion processes that are active. Research has been concentrated on the downstream change in riverbed particle size distributions (Ashworth and Ferguson, 1986; Knighton, 1998), decreasing bank sediment sizes may result in higher values of sediment cohesion. This would limit entrainment and increase bank heights, enhancing the conditions for mass failures (Section 2.4) thus affecting mass failure processes.

The bank sediment samples were taken at the same heights as the upper, middle and lower erosion pins (Section 3.5.1). The samples were therefore taken from bank material that was suitable for erosion pin insertion. Thus the very coarse bank material was not sampled, as it was both too large for the sampling technique (Section 3.5.1) and unsuitable for inserting erosion pins.

The general trends in sediment composition throughout the catchment may be identified using the average of the six samples taken at each monitoring site (Section 3.5.1). This is a simplification of the overall sediment composition derived from sequential overbank deposition and encroachment into fluvial and glacial deposits by meandering. It does, however, allow the average bank conditions to be compared against average erosion conditions.

The grain size classification defined by BS 1377 (British Standards, 1975) allows the different size classes to be compared. The averaged data shows a rapid downstream fining, from Beck Meetings to Reeth (Sites 1-5) (Figure 4.5), and then a much shallower decrease in particle size distribution from Easby to Topcliffe (Sites 6-9). The percentages of clay and silt from Sites 1-5 increase from 1.5-5.4 %, and from 21.7-53.0 % respectively. Over the same distance the percentage weight of sand decreases from 75.7-41.6 %. For the more downstream sites (Sites 6-9) the percentage weight of each particle size is around 5 % clay, 40 % silt, and 53 % sand. The distribution of gravel is more variable in a downstream direction, with peaks of 4.2 % and 2.7 % at Muker (Site 3) and Easby (Site 6) respectively. The rest of the catchment has values of at or below 1.1 %.

The downstream trends in sediment composition have been investigated in the upper, middle, and lower bank heights (Sections 4.3.2 – 4.3.4). This allowed one of the variables thought to affect the spatial distribution in erosion rates at the sites to be understood. For each of the size categories (clay, silt, sand, and gravel) a least squares regression was undertaken, finding the strength of the relationship between distance downstream and sediment size percentage weights. Polynomial regression equations explained the most variance between the two variables. The higher order polynomial gave the best values of R^2, however, due to the relatively small sample size (n = 18) it was not considered appropriate to fit curves of greater orders than x^3.

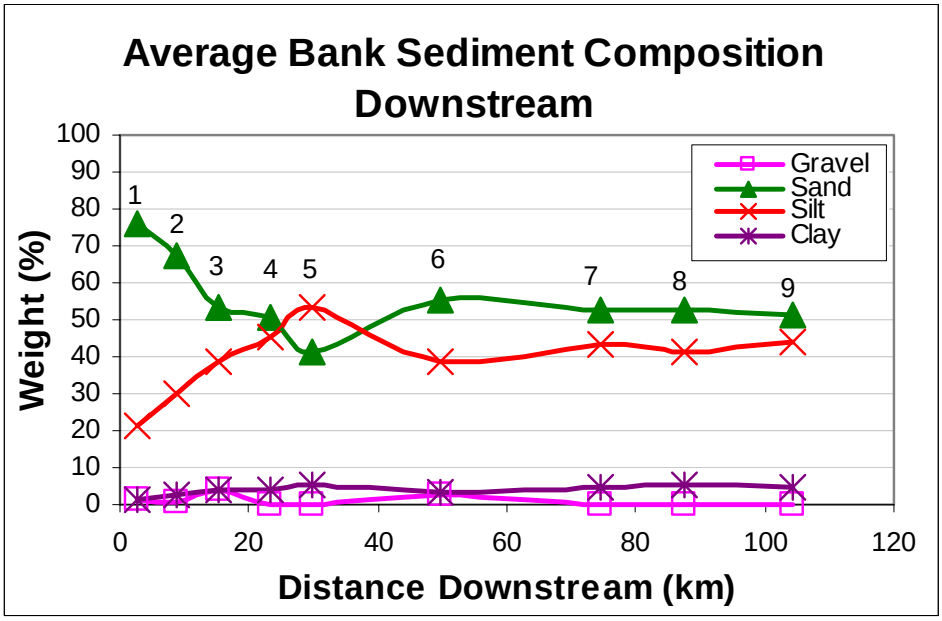

Figure 4.5 The composition of the average of the six bank sediment samples from each monitoring site, showing downstream trends in the percentage weight of gravel, sand, silt, and clay (British Standards, 1975).

4.3.2 Upper Bank Trends

The upper banks contain low percentage weights of gravel throughout the catchment with two peaks at Muker (Site 3) (11.2 %) and Easby (Site 6) (10.1 %) (Figure 4.6A). None of the regression curves fitted to the data were significant above a 95 % confidence level.

The sand fraction in the upper banks was the dominant sediment size in the upper and lower sections of the catchment (Figure 4.6B). A quadratic curve fitted through the data was significant (95% confidence limit) and indicated decreasing sand from Beck Meetings (Site1) (78.2 %) until Easby (Site 6) (41.5 %), before increasing again further downstream.

Silt composition in the upper bank (Figure 4.6C) has the opposite trend to the sand composition. Percentage weights of silt are low in the upper and lower catchment, and peak mid-catchment, this was modelled using a quadratic curve (95 % confidence). The highest percentage weights of silt occurred at Reeth (Site 5) (38.9 % and 53.6 %), decreasing downstream to Topcliffe (Site 9) (36.3%).

Very low clay contents were found throughout the catchment (Figure 4.6D), reaching a maximum at Reeth (Site 5) (4.6 %). The lower catchment did not appear to increase in clay downstream, instead maintaining a reasonably constant level (~3.5 %).

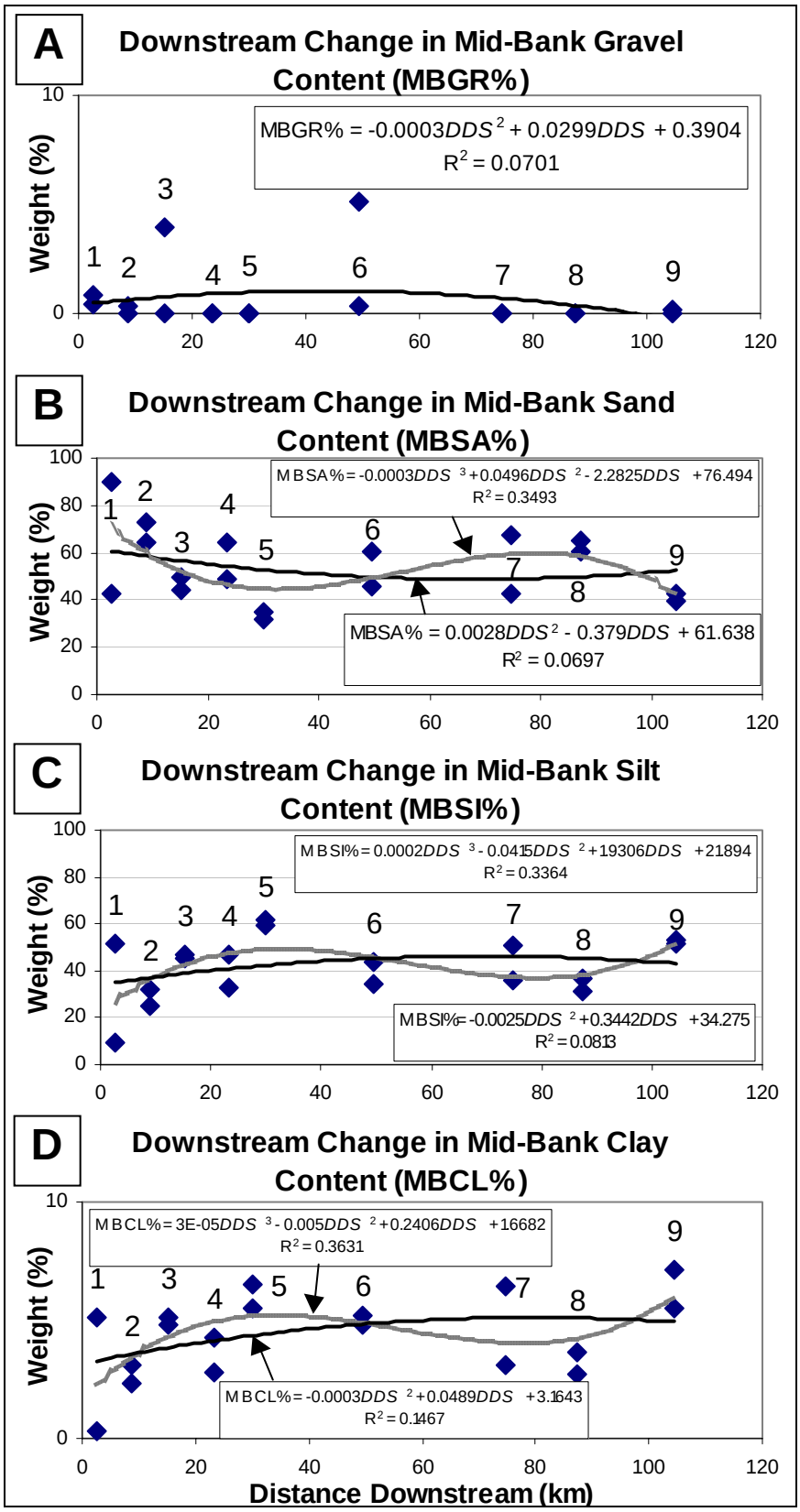

Figure 4.6 Downstream trends in the percentage weight of (**A**) Gravel, (**B**) Sand, (**C**) Silt, and (**D**) Clay in the upper bank (upstream and downstream) at each monitoring site.

4.3.3 Mid-bank Trends

The gravel content of the mid-bank (Figure 4.7A) followed a similar pattern to the upper bank, with low values (<10 %) at all the sites. Two peaks occurred at Muker (Site 3) (3.9 %) and Easby (Site 6) (5.1 %), however ten out of the eighteen samples registered no gravel content. This resulted in a lack of a significant (95 % confidence) downstream trend.

Sand percentage weights, as with the upper bank, accounted for approximately 50 % of the sediment composition (Figure 4.7B). Unlike the upper banks, a quadratic function delineating a mid-basin drop in sand percentage weights was not significant (95 % confidence). A cubic trend more efficiently explained the downstream variation in mid-bank sand contents (R^2 = 34.9 %, 95 % confidence). The downstream trend would appear to be a decline in sand contents from Beck Meetings (Site 1) (89.9 % and 42.7 %) to Reeth (Site 5) (34.9 % and 31.6 %), followed by an increase to a peak at Morton-on-Swale (Site 7) (67.2 % and 49.2 %).

The mid-bank silt compositions (Figure 4.7C) are low upstream, increasing to a peak at Reeth (Site 5) (59.6 % and 61.8 %). The percentage weights decrease until Greystone Farm (Site 8) (36.8 % and 31.3 %) and then increase up to 53.2 % at Topcliffe (Site 9). This trend is modelled by a cubic curve (95 % confidence), rather than a quadratic curve.

Clay contents are low throughout the catchment (< 8 %) (Figure 4.7D). They have a similar trend to the mid-bank silt contents modelled by a cubic equation (95 % confidence). The maximum percentage weight (6.5 %) was measured at Reeth (Site 5), decreasing to 2.7 % at Greystone Farm (Site 8), and rising again up to 7.1 % at Topcliffe (Site 9).

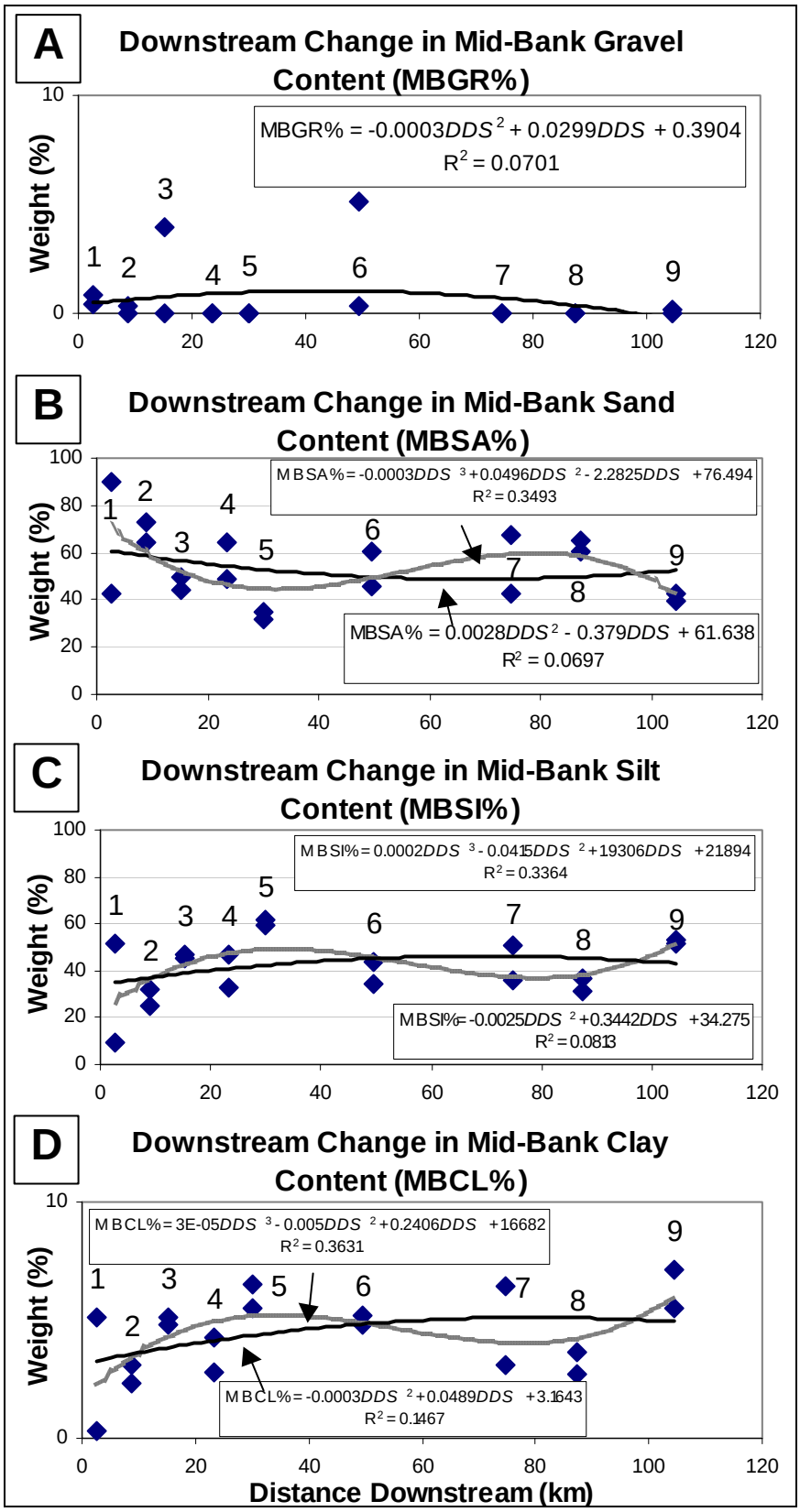

Figure 4.7 Downstream trends in the percentage weight of (**A**) Gravel, (**B**) Sand, (**C**) Silt, and (**D**) Clay in the mid-bank (upstream and downstream) at each monitoring site.

4.3.4 Lower Bank Trends

The lower bank has the potential to be the most susceptible to entrainment processes due to the greater incidence of inundation. Erosion at the bank toe can lead to instabilities in the overlying sediment, increasing erosion rates (Thorne and Osman, 1988). Thus, the susceptibility of the lower bank to flow shear stresses or bank saturation is important in predicting the risk of erosion.

The gravel content of the basal region displays a downstream decline with peaks at Beck Meetings (Site 1) (5.2 %) and Muker (Site 3) (8.8 %) (Figure 4.8A). All other sites have <1 % clay fractions.

Sand composition in the lower bank (Figure 4.8B) follows a similar trend to the upper bank. A mid-basin decrease in sand percentage weights around Easby (Site 6) and Morton-on-Swale (Site 7) was highlighted by the quadratic regression line (R^2 = 32.3 %, 95 % confidence). At Greystone Farm (Site 8) the upstream end of the pinned section had 59.9 % sand, whilst downstream at the site there was only 11.5 %. This indicates the heterogeneity of the sediment in some of the banks, with different sediment layers/structures being sampled. The basal layer values do in general remain broadly consistent with the upper and middle of the bank with approximately 80 % sand upstream reducing to approximately 50 % downstream.

The silt content in the lower bank (Figure 4.8C) had a similar tend to that found in the upper bank with a mid-basin peak of indicated by the quadratic regression equation. The peak silt percentage weight (71.4 %) was measured further downstream at Greystone Farm (Site 8).

Clay contents are again low throughout the catchment, with < 10 % at every site except at the downstream end of Greystone Farm (Site 8) (Figure 4.8D). The increase in clay content downstream is better modelled by a logarithmic regression equation (95 % confidence) as opposed to a quadratic equation.

The most composite bank stratigraphies, with coarse gravel underlying finer silts/sand/clay, were at Muker (Site 3) (Plate 3.3) and Easby (Site 6) (Plate 3.6). There does not appear to be a trend of the banks becoming increasingly composite downstream as found on the River Severn, U.K. (Harris, 1996).

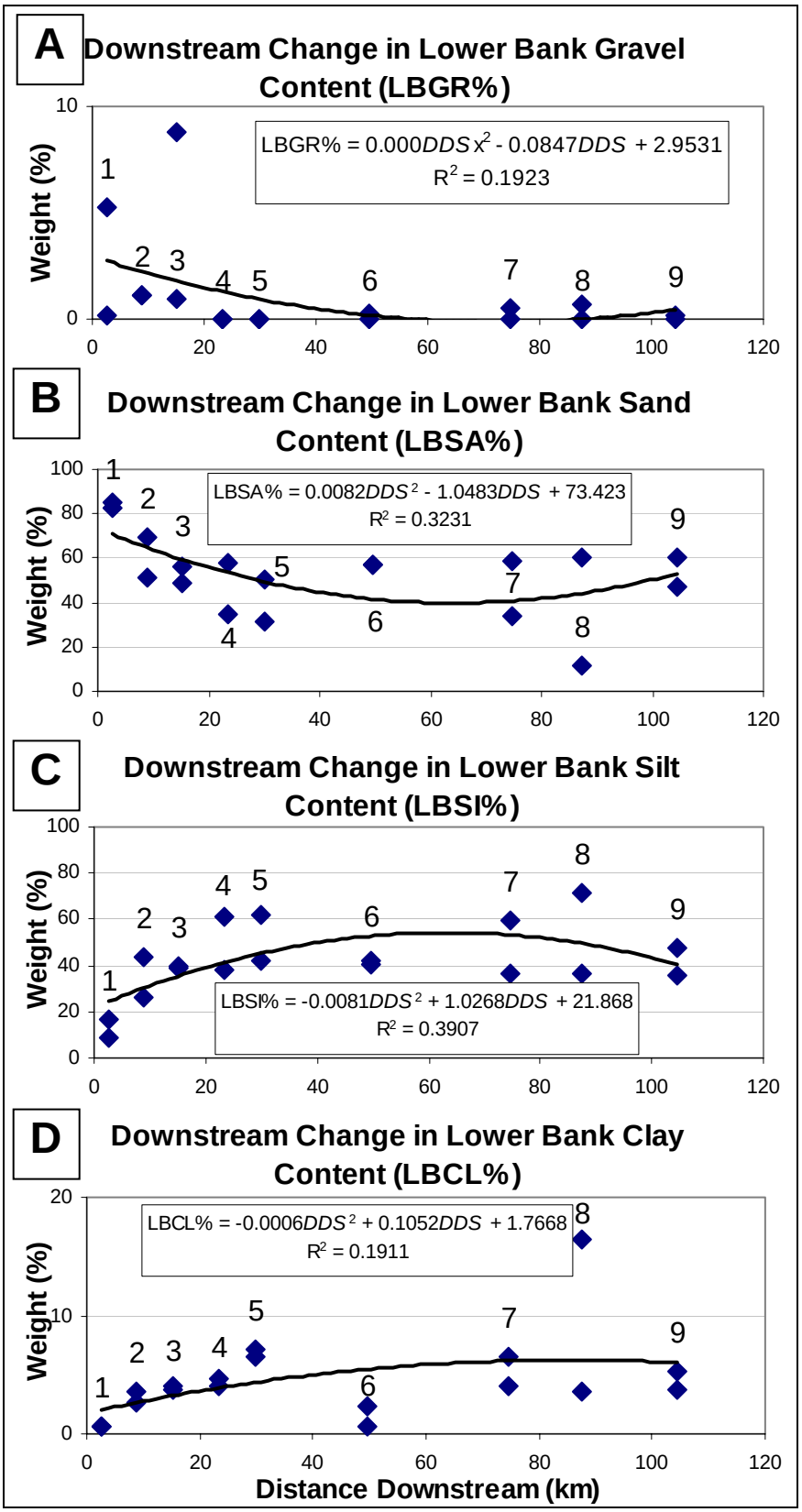

Figure 4.8 Downstream trends in the percentage weight of (**A**) Gravel, (**B**) Sand, (**C**) Silt, and (**D**) Clay in the lower bank (upstream and downstream) at each monitoring site.

4.3.5 Downstream Change in the Organic Content of the Riverbank Sediment

The loss of ignition technique (Section 3.5.1) was used to determine the organic content of both living and dead vegetation within the banks.

The highest values of organic matter content were found in the peaty sediment at Beck Meetings, with up to 53.3 % of the sample weight lost after ignition (Figure 4.9). The rest of the catchment had organic contents of between 2.6-13.0 %. High values of organic material contents were found in the downstream bottom sample at Low Row (13.3 %), the downstream top sample at Reeth (13.0 %), the upstream bottom sample at Easby (11.2 %), and the downstream bottom sample at Greystone Farm (11.1 %). The minimum values were in the lower bank at Reeth (2.6 % and 3.1 %), the upstream mid-bank sample at Easby (2.7 %), and the mid-bank samples at Greystone Farm (3.6 % and 3.9 %).

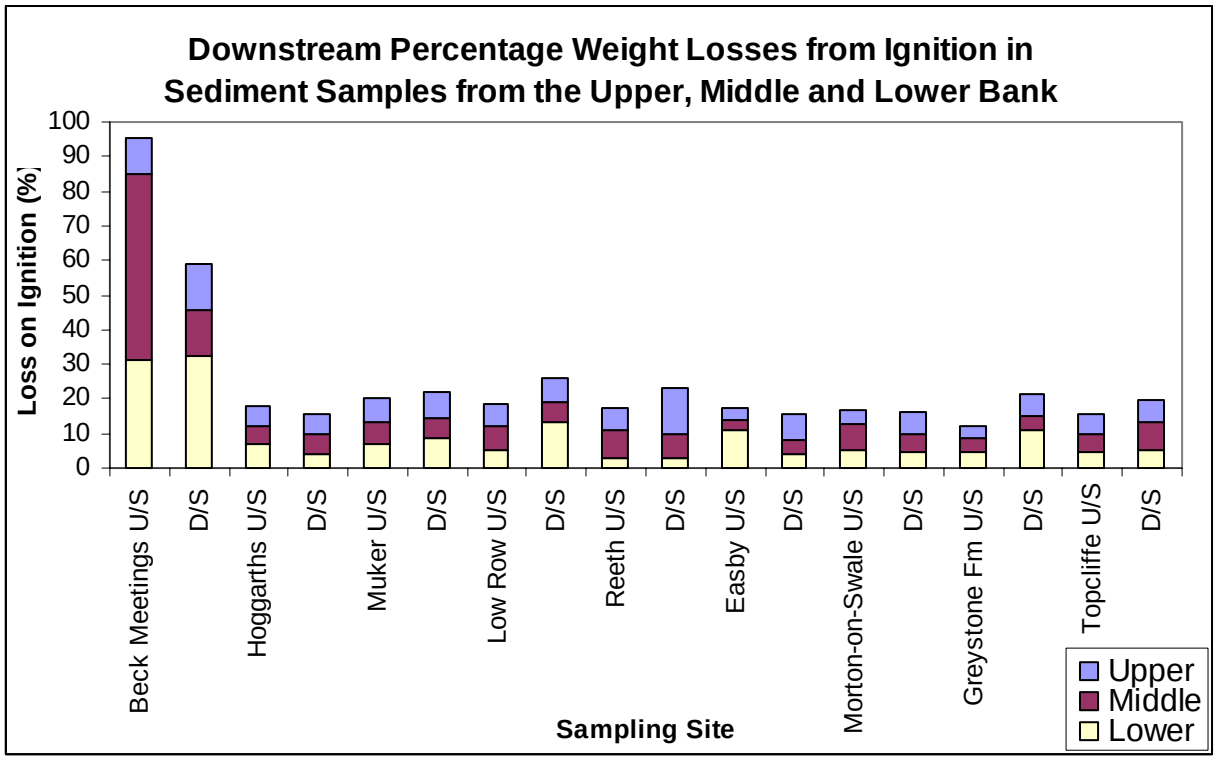

Figure 4.9 Downstream change of loss on ignition in bank sediment from the upper, middle, and lower bank. U/S = upstream end of the erosion pinned section of the montoring site, D/S = downstream end of the erosion pinned section of the montoring site.

4.4 DOWNSTREAM CHANGES IN BANKFULL FLOW EFFICIENCY

4.4.1 Introduction

The present form of the River Swale channel is a reflection of both recent and antecedent processes. The present hydraulic efficiency may be estimated at the monitoring sites using the physical characteristics of the channel i.e. channel dimensions, riverbed sediment characteristics, and vegetation resistance. Understanding how well the channel routes flood discharges, and whether the channel is in regime or under/over sized for the current discharges, allows the current erosion processes to be put into context.

4.4.2 Downstream Variability in Channel Dimensions

The bankfull channel width increased from Site 1 until the mid-catchment region (Site 5) and then decreased to a plateau of ~40 m at Sites 6-9 (Figure 4.10A) (Table 4.6). The overall trend in bankfull depths was a tendency to increase downstream; however, there was a lowering of the depths mid-catchment from Sites 5-7 which disrupted this trend (Figure 4.10A). The width:depth ratio may be a reflection of the adjustments of the channel to its sedimentological characteristics (Simon, 1989). An armoured bed material combined with a weak bank material, such as a silty-sand stratigraphy, may result in a high width:depth ratio. The downstream trend in the width:depth ratio at the monitoring sites reveals an increase from 11.5 at Beck Meetings (Site 1) to 33.6 at Hoggarths (Site 2) (Figure 4.10B) (Table 4.6). The ratio then remained almost constant until Morton-on-Swale (Site 7), apart from a large peak value of 112.1 at Reeth (Site 5). The two most downstream monitoring sites Greystone Farm (Site 8) and Topcliffe (Site 9) have a lower ratio of around 12, close to that found upstream at Beck Meetings (Site 1).

Changes in the channel slope (Figure 4.10C) may also be responsible for the variability in channel dimension downstream, as well at the bed and bank sedimentology. Some of the monitoring sites may not be at an equilibrium state, having only reached an intermediate state of adjustment (Simon and Hupp, 1990). The cross-sectional areas of 73.4 m^2 at Reeth (Site 5) and 51.4 m^2 at Easby (Site 6) do not fit into the general trend of increasing area downstream (Figure 4.10D) (Table 4.6), and Easby does not fit into the downstream trend of decreasing bank slope (Figure

4.10C). The downstream trend of increasing cross-sectional area may be indicative of the channel being at equilibrium with the bankfull discharge. This may mean that the channel at Reeth is too large for the dominant discharges, or at Easby too small. Overbank flows were common at all the sites but Easby was, based on anecdotal evidence from the landowner, particularly prone to flooding over the current channel during high flow events. This would appear to indicate a channel not sufficiently well adjusted to carry the influential flood events occurring within the catchment.

The ability of the channel to transport high flows is affected by the channel dimensions as well as the bed and bank roughness (Darby, 1998). As well as considering the width:depth ratios and the cross-sectional areas the wetted perimeter and hydraulic radius can also be used as descriptive tools of the cross-sectional hydraulic efficiency.

The wetted perimeter increased from 7.5 m at Beck Meetings (Site 1) to a peak of 92.5 m at Reeth (Site 5) and then decreased to a plateau of around 40 m from Sites 6-9 (Figure 4.10E) (Table 4.6). The hydraulic radius increased downstream from the river source (Figure 4.10F) from 0.5 m (Site 1) up to 2.9 m (Site 9). There was a mid-basin dip (Sites 5-7) in the downstream trend of increasing hydraulic radii. This may again be caused by channel adjustments to bed and bank sediment alterations, or changes in slope (Figure 4.10C).

4.4.3 Downstream Trends in Bed Sediment

The b-axis measurements at each of the monitoring sites (Section 3.5.2) had an overall decrease in size from upstream to downstream in the catchment (Figure 4.10G). There were, however, variations from the anticipated downstream decreasing size trend. The sediment size of 86.0 mm at Beck Meetings (Site 1) was lower than the site further downstream, with an average size of 132.2 mm at Hoggarths (Site 2) (Table 4.6). This may be because there is limited source of material upstream of the site, with few colluvial inputs of large clasts into the channel.

Sites 2-4 all decreased in b-axis dimensions downstream, with 84^{th} percentile b-axis measurements from 132.2-124.0 mm. There was then a rapid decrease in bed sediment size at Reeth (Site 5) to 54.5 mm, perhaps caused by storage of sediment upstream as the channel slope decreased (Figure

4.10C) (Table 4.6). The much higher average sediment sizes of 140.8 measured at Easby (Site 6) may be affected by the measurement technique. The Wolman sample (Wolman, 1954) was taken approximately 20 m downstream of the monitoring site due to the unstable nature of the bank. The high flow velocities made sampling the bed material hazardous, even at low flows. To overcome this problem material at the left hand side of the channel was sampled during low flow conditions leading to an overestimation of the bed material size. An alternative explanation from the higher bed material D_{84} value at Easby could be the influence of an upstream source of coarse sediment. Tributaries may inject coarse material into the main Swale channel skewing the general trend of downstream fining. The nearest upstream tributary to Easby was Clapgate Beck, approximately 8 km upstream. Just upstream of the monitoring site the eroding bank was composed of diamicton, produced by till deposition, which also contributed coarse sediment directly into the channel (Plate 3.6).

The downstream sites (7-9) all consisted of fine bed material, from 2.1-13.6 mm. This meant that they were sampled in using a grab sample, rather than a Wolman count (Section 3.5.2). The increase in b-axis D_{84} downstream from Greystone Farm (Site 8) to Topcliffe (Site 9) could be due to the grab sample having been taken in a different geomorphologic unit within the channel. Finer material my have been taken from pool material, as opposed to the coarser riffle sediment.

The hydraulic radius and D_{84} may be used to determine a friction factor for each of the monitoring sites. The friction factor may be a product of four forms of flow resistance: skin (grain) resistance, form resistance of bedforms, internal distortion resistance caused by channel bends, and spill resistance (Richards, 1982). The Darcy-Weisbach friction factor (Equation 4.4) is based around the skin resistance of channels with near uniform flows, or in riffle sections. This allows the resistance to the flow by the bed material to be compared between sites, and therefore comparisons of the energy available to transport sediment at each of the measured cross-sections (Section 4.4.4).

$$f = \frac{1}{1.16 + 2\log\left(\frac{R}{D_{84}}\right)^2} \tag{4.4}$$

Where:

f =Darcy-Weisbach friction factor;
R = Hydraulic radius (m);
D_{84} = 84th percentile of the b-axis measurements of the bed material sample (m).

Channel roughness decreased from 0.138 upstream at Beck Meetings (Site 1) to 0.019 at Greystone Farm (Site 8), 87.4 km downstream (Figure 4.10H). The only exception to this trend was at Easby (Site 6), where the friction factor of 0.12 was considerably higher than the neighbouring values of 0.082 at Reeth (Site 5), and 0.037 at Morton-on-Swale (Site 7) (Table 4.6). A relatively low hydraulic radius and high value of D_{84} were responsible for the high-predicted value of channel roughness at Easby. Inaccuracies in these variables could lead to the overestimation of *f* at the monitoring sites; however observations of the channel indicated high channel roughness as well (Plate 4.6).

There was a slight increase in the friction factor at the most downstream site, Topcliffe (Site 9) (0.028), from the lowest value of 0.019 at Greystone Farm. This is probably a combination of sampling variability and the low bed sediment D_{84} measured at Greystone Farm (Site 8) (Figure 4.10G).

4.4.4 Downstream Variability in Stream Power

The Darcy-Weisbach friction factor (*f*) can be used to estimate the mean velocity at a cross-section during bankfull flows (Equation 4.5) (Limerinos, 1970). The velocity combined with the bankfull cross-sectional area allows the bankfull discharge, with a return period of approximately two years (Petit and Pauquet, 1997), to be determined (Equation 4.6). In combination with the channel slope, water density, and acceleration due to gravity the stream power at each monitoring site could be calculated (Equation 2.5).

$$\hat{\bar{V}}_{bf} = \sqrt{\frac{8gRS}{f}} \tag{4.5}$$

Where:

$\hat{\bar{V}}_{bf}$ = Estimated mean bankfull velocity (m s^{-1});
g = Acceleration due to gravity (m s^{-1});
S = Water surface slope, which in this case was approximated by the banktop slope (McEwen, 1994) (m m^{-1}).

$$Q_{bf} = \hat{\bar{V}}_{bf} \times A_{bf} \quad (4.6)$$

Where:

Q_{bf} = Bankfull discharge (m^3 s^{-1});
A_{bf} = Channel cross-sectional area at bankfull (m^2).

The catchment scale variation in predicted bankfull discharge (Figure 4.10I) reveals an upstream peak in discharge, which is uncharacteristic of a natural hydraulic system. Muker (Site 3) and Low Row (Site 4) had predicted discharges of 237 m^3 s^{-1} and 207 m^3 s^{-1} respectively (Table 4.6). These high discharges represent a large cross-sectional area and hydraulic radius at these sites.

From Easby (Site 6) downstream there was a rise in estimated discharges from 70 m^3 s^{-1}, 49.5 km downstream, up to 253 m^3 s^{-1}, 104.4 km downstream. Further downstream from Topcliffe (Site 9) the IH gauging station at Leckby Grange (Figure 3.1) has a bankfull discharge of 195.0 m^3 s^{-1}, which is of the same order of magnitude as the Q_{bf} of 253 m^3 s^{-1} at Topcliffe. Using the estimated discharge values the gross stream power at each monitoring site could be calculated (Equation 4.7) (Section 2.5).

$$\Omega_{bf} = \rho g Q_{bf} S \quad (4.7)$$

Where:

Ω_{bf} = Bankfull gross stream power (W m^{-1}).

The gross stream power had two peaks in the catchment (Figure 4.10J). The first was upstream at Muker (Site 3), 39081 W m^{-1}, and the other near mid-catchment defined by a single high value of 4521 W m^{-1} at Easby (Site 6) (Table 4.6). This suggests that these are regions of high erosivity within the catchment, due to the potential energy that the river has to expend on entrainment of bank material.

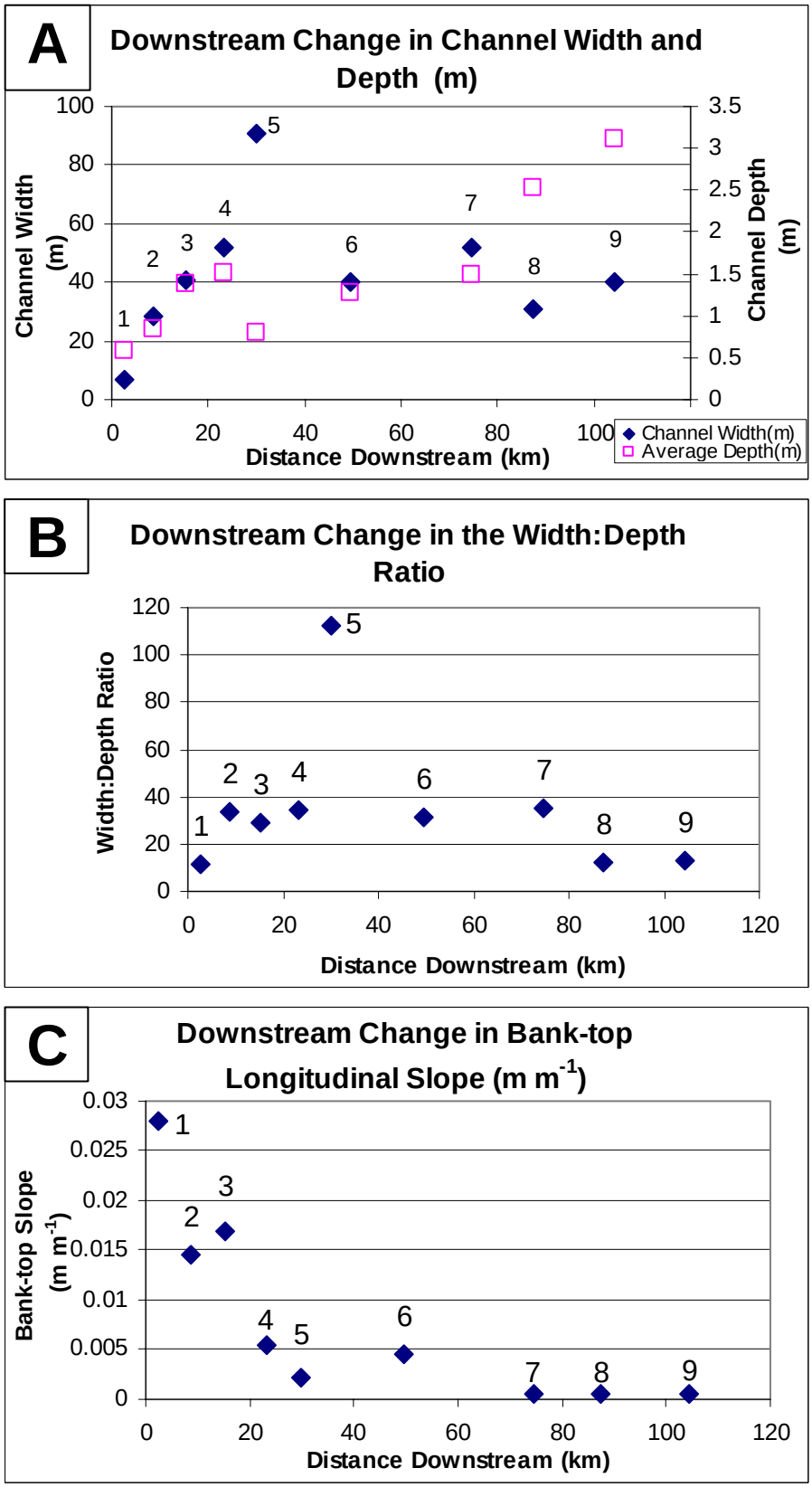

Figure 4.10 Downstream changes in monitoring site (**A**) channel widths and depths, (**B**) width:depth ratios, (**C**) longitudinal slopes.

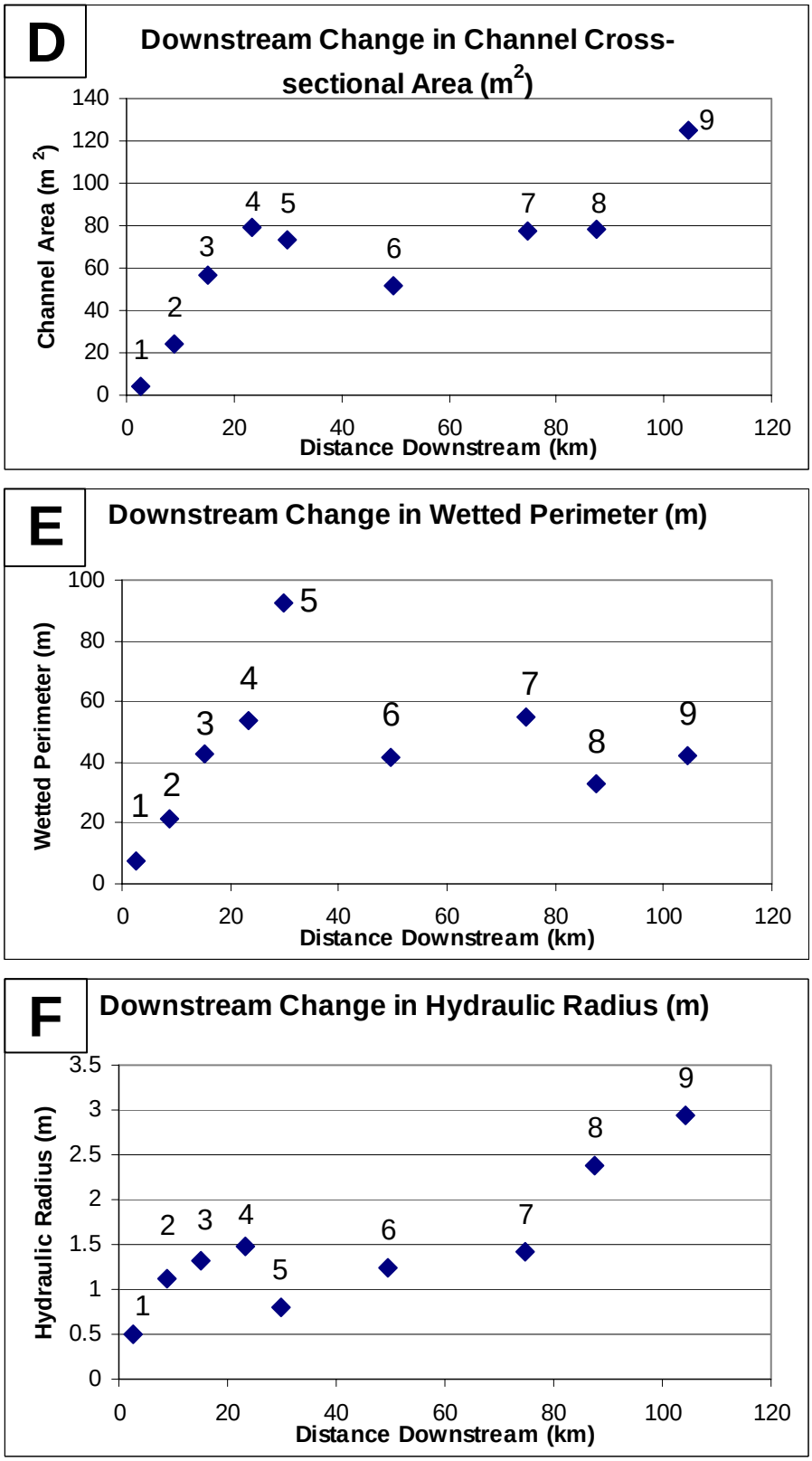

Figure 4.10 continued Downstream changes in monitoring site (**D**) cross-sectional areas, (**E**) wetted perimeters, (**F**) hydraulic radii.

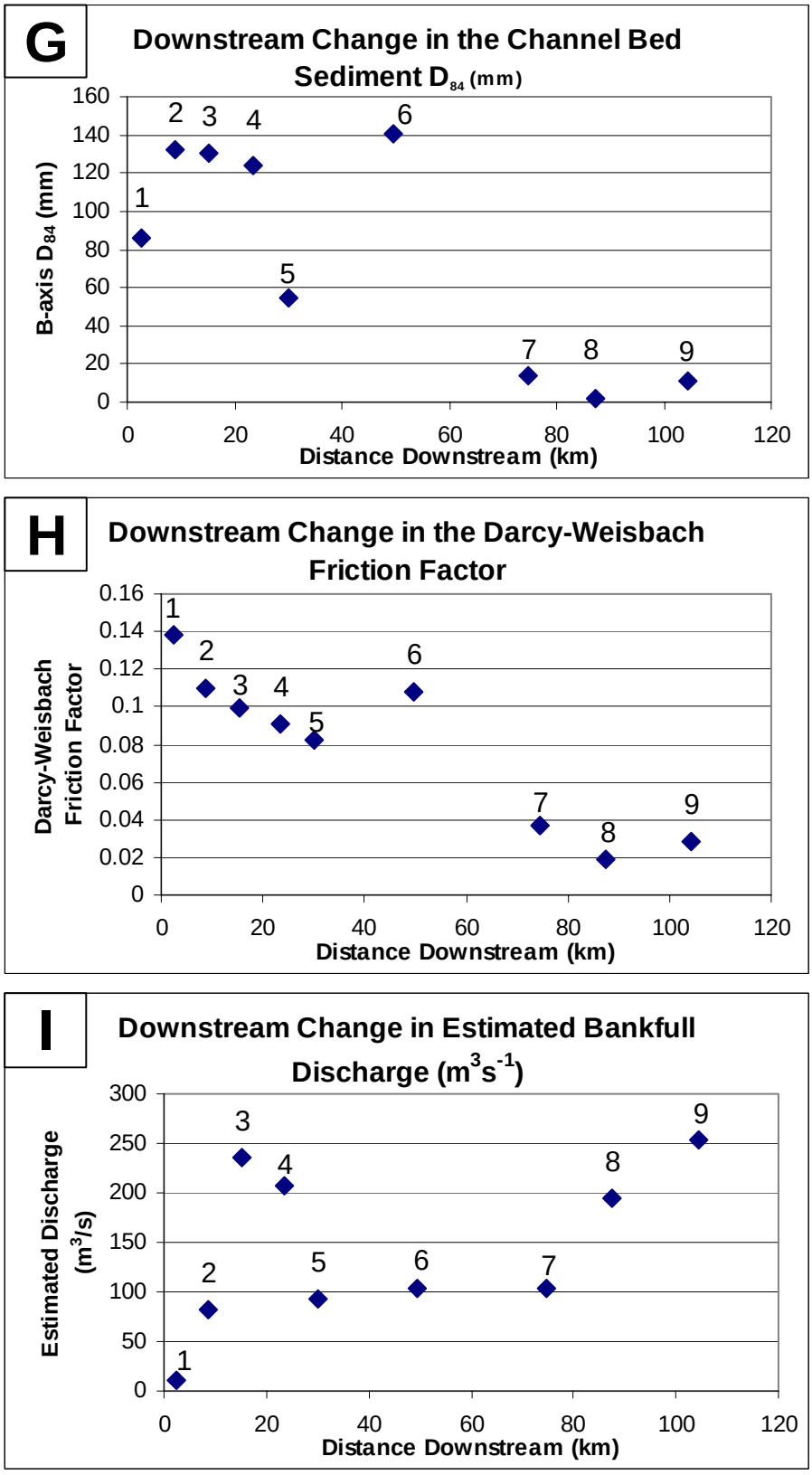

Figure 4.10 continued Downstream changes in monitoring site (**G**) bed-sediment sizes, (**H**) Darcy-Weisbach friction factors, (**I**) estimated bankfull discharges.

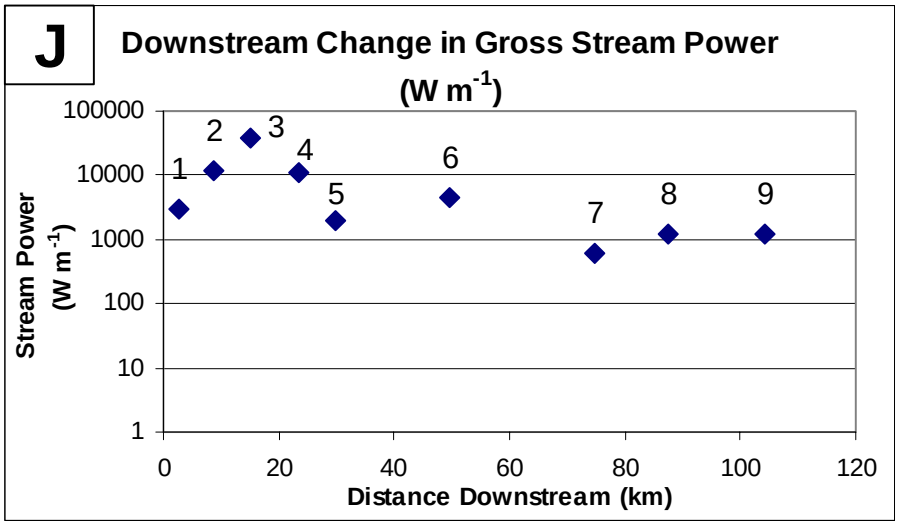

Figure 4.10 continued Downstream changes in monitoring site (**J**) gross stream powers.

SITE NAME	DISTANCE DOWN-STREAM (km)	CHANNEL WIDTH (m)	AVERAGE CHANNEL DEPTH (m)	WIDTH: DEPTH RATIO	CHANNEL SLOPE (m m^{-1})	CROSS-SECTIONAL AREA (m^2)
1. Beck Meetings	2.56	6.61	0.57	11.5	0.0280	3.8
2. Hoggarths	8.81	28.46	0.85	33.6	0.0146	24.1
3. Muker	15.24	40.64	1.39	29.2	0.0168	56.4
4.Low Row	23.39	52.12	1.52	34.36	0.0054	79.1
5. Reeth	29.94	90.73	0.81	112.1	0.0022	73.4
6. Easby	49.51	40.02	1.29	31.1	0.0045	51.4
7. Morton-on-Swale	74.66	51.95	1.49	35.0	0.0006	77.3
8. Greystone Farm	87.41	31.07	2.53	12.3	0.0006	78.5
9. Topcliffe	104.39	40.01	3.12	12.8	0.0005	124.8

SITE NO.	WETTED PERIMETER (m)	HYDRAULIC RADIUS (m)	BED SEDIMENT D_{84} (mm)	DARCY-WEISBACH FRICTION FACTOR (f)	ESTIMATED BANKFULL DISCHARGE (m^3 s^{-1})	GROSS STREAM POWER (W m^{-1})
1	7.5	0.5	86.0	0.138	11	2932
2	21.4	1.1	132.2	0.110	82	117.65
3	42.6	1.3	130	0.100	237	39081
4	53.6	1.5	124	0.091	207	11021
5	92.5	0.8	54.5	0.082	93	1969
6	41.7	1.2	141	0.108	103	4521
7	54.6	1.4	13.6	0.037	104	623
8	33.1	2.4	2.1	0.019	195	1186
9	42.5	2.9	12	0.028	253	1242

Table 4.6 Downstream changes in monitoring site: width, depth, width:depth ratio, slope, cross-sectional area, wetted perimeter, hydraulic radius, bed sediment D_{84}, Darcy-Weisbach fricton factor, estimated bankull discharge, and gross stream power.

4.4.5 Downstream Changes in Bank Vegetation

Very little vegetation was observed on the bank surfaces themselves at monitoring sites. This was probably due to the site selection technique (Section 3.4.2), which involved choosing steep unvegetated banks. There was also very limited instream vegetation at all the monitoring sites. The channel roughness produced by the vegetation was therefore minimised.

The herbaceous plants that were situated on the bank tops are listed in Table 4.6. Little data were available on the comparative rooting characteristics of these plants. It was therefore difficult to distinguish which of the plants were important in binding the soil mass with deep or wefted root systems. Information was available for rooting depths and erodibility of instream plants (Haslam, 1978), which describes *Ranunculus spp.* as shallow rooted (mostly in the upper 150 mm of the substrate). This is probably true for most of the other listed species (Table 4.6) found at the monitoring sites.

The number of species identified increased, from nine and seven upstream at Beck Meetings and Hoggarths (Sites 1 and 2), to a maximum of 19 species at Easby (Site 6). The number of species then decreased downstream. There is the potential for this change in species richness to be caused by differences in channel activity (Tabacchi *et al.*, 1996), with greater richness in more dynamic reaches with rapid changes in planform caused by meandering. The anthropogenic influence at most of the sites makes this hypothesis tenuous, however it may warrant more research.

HERBACEOUS SPECIES	UPSTREAM → DOWNSTREAM								
	Site 1	Site 2	Site 3	Site 4	Site 5	Site 6	Site 7	Site 8	Site 9
Achillea millefolium		■	■		■		■	■	■
Alliaria petiolata						■			
Anthriscus sylvestris						■			
Artemisia vulgaris							■		
Barbarea vulgaris							■		
Bellis perennis			■		■	■	■		
Centaurea nigra				■	■	■			
Centaurea scabiosa					■				
Chrysanthemum vulgare								■	
Cirsium plaustre			■						
Cirsium vulgare	■					■		■	■
Conopodium majus					■				
Cordunus aconthoides							■		
Crepis palludosa						■			
Epilobium hirsutum						■			
Euphrasia nemorosa				■	■				
Galium cruciata						■			
Galium saxatile	■	■	■						
Geranium robertianum						■			
Impatiens glandulifera							■		
Lapsana communis						■			
Leontodon hispidus			■	■					
Lotus corniculatus			■	■					
Matricaria matricarioides				■					
Montia sibirica		■							
Myosotis scorpioides								■	■
Myosoton aquaticum	■		■	■	■				■
Plantago lanceolata				■	■	■	■		
Plantago major	■		■						
Plantago media						■			
Prunella vulgaris	■		■	■	■				
Ranunculus repens	■	■	■	■	■	■	■	■	■
Rhinanthus minor				■	■				
Rorippa sylvestris							■	■	
Rubus fruticosus agg.						■			
Rumex acetosa	■	■		■	■				
Rumex obtusifolius		■				■	■	■	
Senecio jacobaea				■	■	■			
Taraxacum officinale agg.							■		
Trifolium dubium			■						
Trifolium pratense	■		■	■	■				
Trifolium repens	■	■		■	■	■	■	■	
Urtica dioica			■			■		■	■
Veronica chamaedrys							■		
Veronica officinalis			■						
Vicia sativa				■					
Veronica serpyilifolia						■			
TOTAL	9	7	14	15	13	19	13	9	6

Table 4.7 The distribution of herbaceous species throughout the catchment.

4.5 SUMMARY

1. The results from erosion pin and re-survey measurements indicated a mid-catchment increase in rates of erosion. The downstream trend of erosion rates could be modelled using polynomial regression equations.
2. The changes in river planform position from c.1854 – c.1980 were classified into seven categories of Channel Pattern Classification by Sedgwick (2000). The areas containing highly meandering reaches, and those that were stable, were in general agreement with the rates of change determined by this study.
3. Riverbank sediment was found to decrease in gravel and sand, and increase in silt and clay, from upstream to mid-catchment. Further downstream changes in sediment composition were more limited. Composite bank structures were found to be site specific and no downstream change of this variable was identified.
4. The organic content of the bank sediment was at a maximum at Beck Meetings (Site 1) but remained fairly stable at the rest of the sites with a loss of ignition of around 2.6-13.0 %.
5. The channel dimensions and bed-sediment b-axis D_{84} were used to predict the bankfull discharge at each monitoring site. The predicted discharges were then used to estimate the bankfull gross stream power. This indicated two peaks in stream power in the catchment, of 39081 W m^{-1} at Muker (Site 3) and 4521 W m^{-1} at Easby (Site 6).
6. Erosion rates have been found to follow a quadratic trend at a catchment scale. The timing of the erosion events may be used to identify any trends in erosional processes at the same scale; this will be the focus of Chapter 5.

CHAPTER 5

SEASONAL VARIABILITY IN BANK EROSION RATES

5.1 INTRODUCTION

The temporally lumped, or averaged, data that were considered in Chapter 4 revealed *spatial* (downstream) trends in bank erosion rates. Comparisons have been made between *spatial* changes in average rates of erosion and environmental variables, such as bed and bank sediment composition, throughout the catchment (Sections 4.3 and 4.4.3). A clearer model of the active processes of erosion that are controlling the catchment variability in erosion rates, however, may be drawn out from the *temporal* changes in erosion rates during the monitoring period.

Seasonal trends in erosion throughout the catchment may be co-incident with seasonal trends in environmental variables such as peak flow events (Thorne and Abt, 1993), the fluctuations around sub-zero temperatures (Lawler, 1993b), or bank moisture conditions (Grissinger, 1982). Determining the variable, or group of variables, that best statistically describe the seasonality in bank erosion rates may aid the identification of processes.

5.2 BANK EROSION SEASONALITY

Seasonal variations in erosion rates have been observed in other river systems (Wolman, 1959; Twidale, 1964; Leopold, 1973; Hooke, 1979; Lawler, 1986). This seasonality may be attributed to a change in efficacy of a particular process, or changes in the types of processes that were dominant.

The differing monitoring period lengths, and timing of erosion measurements, make direct statistical comparisons between rates of erosion at each of the monitoring sites difficult. Erosion seasonality at each site will be examined statistically using possible controlling variables later in the chapter (Section 5.4). The comparison of peaks and troughs in the erosion-monitoring period can highlight any obvious changes of erosion periodicity throughout the catchment. The time series of erosion rates for the nine study sites are shown in Figure 5.1 A - I.

The general trend at all sites was for a peak rate of erosion to occur during the winter months, at around January and February each year (Table 5.1). This was certainly true at Beck Meetings (Site 1) (Figure 5.1A) where the relatively low annual rates of erosion, of up to 1.4 mm day^{-1}, were concentrated in the months of January and February 1997 and 1998. From the period of January 1997 – March 1998; 78.7% of the erosion (Table 5.1) occurred during these periods, and the rest of the monitoring period was nearly devoid of erosion.

MONITORING SITE NUMBER	SITE NAME	PROPORTION OF EROSION IN THE PERIOD C. 01/97- 03/98 OCCURRING DURING JANUARY - FEBRUARY 1997 AND 1998 (%)
1	Beck Meetings	78.7
2	Hoggarths	80.6
3	Muker	63.9
4	Low Row	83.0
5	Reeth	33.2
6*	Easby	85.6
7	Morton-on-Swale	78.4
8	Greystone Farm	62.1
9	Topcliffe	75.6

Table 5.1 The proportion of erosion pin, * or surveyed, erosion from the period c. January 1997-March 1998 that occurred in the months of January and February.

At Hoggarths and Muker (Figures 5.1B and C) there was a similar pattern of erosion to that observed at Beck Meetings. The peak erosion values were higher, up to 4.9 mm day^{-1}, and the erosion season appeared to lengthen downstream. Erosion values of 0.6 mm day^{-1} occurred at Muker in August 1996 and August 1997, extending the period of active erosion.

The lower annual rate of erosion at Low Row (Figure 4.1) is reflected by much lower peak values of up to 1.4 mm day^{-1}. The length of the erosion season was shortened, with several values less than 0.1 mm day^{-1} during the summer months of April to July 1996, and April to September 1997 (Figure 5.1D).

The peak rates of erosion at Reeth appear to occur earlier in the winter season than at any of the sites upstream (Figure 5.1 E), reducing the proportion of erosion occurring during the January and February period (Table 5.1). High rates of erosion, of 2.4 mm day^{-1}, during the summer period from the 29/06/97 to 04/08/97 mark a return to a longer annual erosion season. This was also the case at Easby where the erosion was dominated by a large peak value of 74.4 mm

day^{-1} (Figure 5.1 F). The subsequent erosion events were much smaller in comparison to this peak value. They were, however, still high compared with rates of erosion at the other monitoring sites. During June 1997 the rate of erosion was 8.7 mm day^{-1}, which would suggest that erosion processes were still active during the summer months.

Almost all of the monitoring periods experienced some erosion at Morton-on-Swale (Figure 5.1 G). Summer rates were low, at around 0.1 mm day^{-1}, during the July periods. Higher rates of erosion during February 1996, 1997, and 1998 indicate the same winter peak as the other monitoring sites (Table 5.1).

The dominance of summer erosion increased at Greystone Farm (Figure 5.1 H). From the 03/07/97 to the 14/07/97 an average of 3.0 mm day^{-1} of erosion was recorded. This is around the same rate as experienced during the maximum winter peak from 05/01/97 to 07/03/97, resulting in only 62.1 % of the erosion occurring during the January and February period (Table 5.1)

At Topcliffe the rates of erosion decrease further from the mid basin peak at Easby (Figure 5.1 I). Despite this decrease in erosion rates the general trend of an elongated erosion period was maintained. This indicates that processes that were operating at this site were affected by summer events in either stream or meteorological variables. The erosion rates during the summer, however, were not as dominant as at Greystone Farm (Table 5.1). The maximum rates of erosion of 2.8 mm day^{-1} and 1.0 mm day^{-1} were experienced during the winter months of January to February 1997, and February to March 1998 respectively.

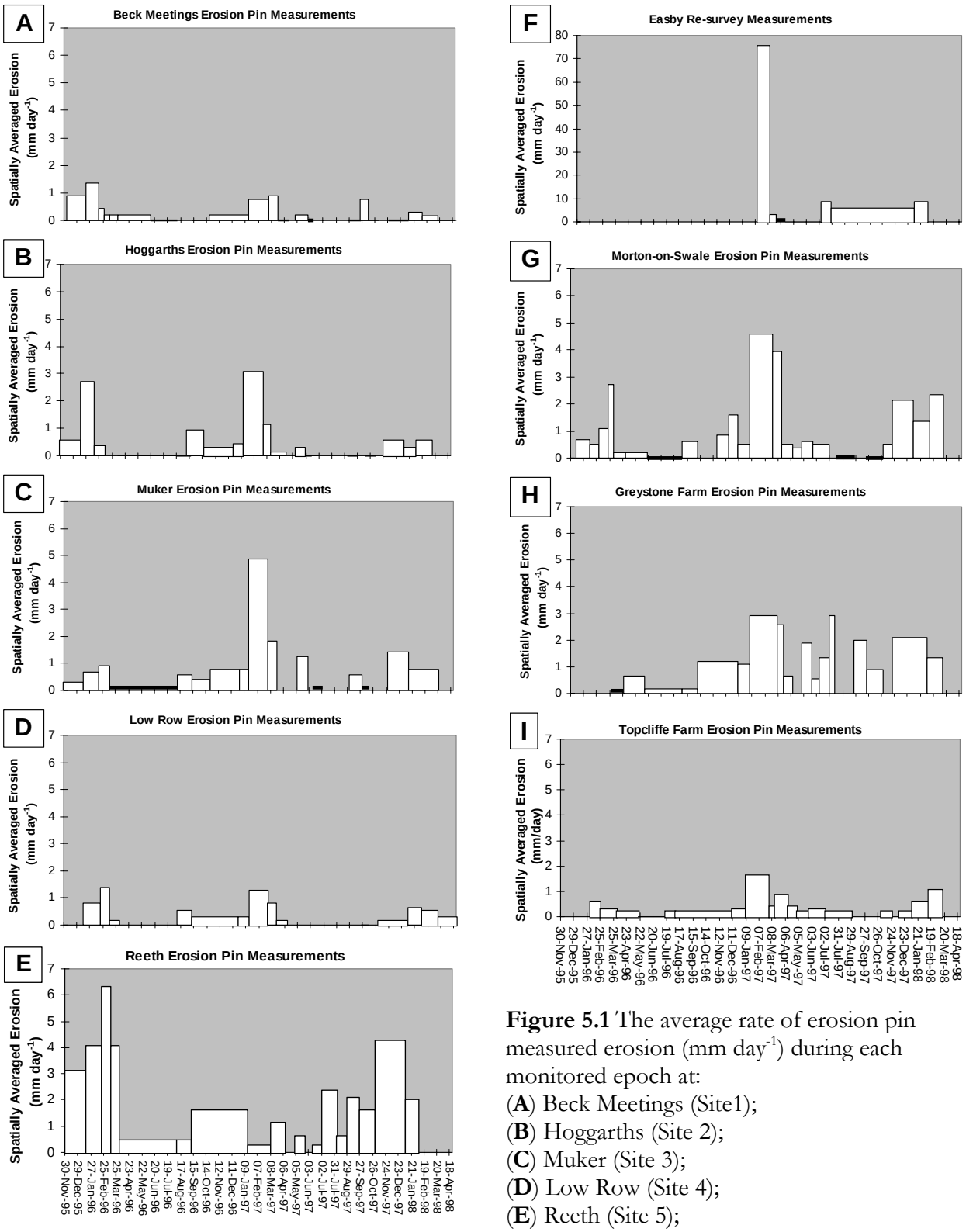

Figure 5.1 The average rate of erosion pin measured erosion (mm day^{-1}) during each monitored epoch at:
(**A**) Beck Meetings (Site1);
(**B**) Hoggarths (Site 2);
(**C**) Muker (Site 3);
(**D**) Low Row (Site 4);
(**E**) Reeth (Site 5);
(**F**) Easby (Site 6);
(**G**) Morton-on-Swale (Site 7);
(**H**) Greystone Farm (Site 8);
(**I**) Topcliffe Farm (Site 9).

5.3 REGRESSION TECHNIQUES AND SELECTION OF INDICES

5.3.1 Introduction

The seasonality in surrogate 'environmental' variables may be used to describe the temporal patterns in bank erosion rates. Further interpretation of the dominant variables allows processes to be inferred. Bivariate relationships between erosion rates and surrogate variables reveal the dominant controls on seasonal variations. The interaction of several explanatory variables can often be more important in defining active processes than the selection of those that are just highly correlated. Thus, a multivariate statistical technique was needed to enable the variation in erosion rates to be modelled by a set of seasonally varying environmental factors.

The statistical technique of Stepwise Linear Multiple Regression (Rawlings, 1988) selects, using varying procedures (Section 5.3.2), the 'best' subset of independent variables to explain the erosion rate. Another advantage of using this technique is that it allows comparisons with previous studies of bank erosion (Hooke, 1979; Lawler, 1986). The following sections introduce the Stepwise Linear Regression technique. The selection of independent environmental variables, and dependent erosion variables is also discussed.

5.3.2 Linear Stepwise Regression Methodology

The regression procedure selects a series of independent variables (or single variable) that are linearly related to the dependent variable of erosion.

The technique may select and remove independent variables in 3 different ways:

1. **Forward Selection**. No variables are initially entered in the model. The first variable to be selected is the one with the highest simple correlation with the dependent variable above a critical value of F. Each variable that is entered into the model is chosen so that it causes the largest reduction in the residual sum of squares (RSS) of the model. Entering variables that correlate most significantly with the residuals in the current model will produce the largest reductions in RSS. If no threshold criteria for entry is specified the selection will continue until all the variables are selected.

2. **Backward Selection**. All the independent variables are initially entered into the model. At each step the variable that causes the lowest increase in RSS will be removed. The variable causing the lowest increase in RSS will have the smallest partial sum of squares in the model. The elimination process will continue until only one variable is left in the model if no critical threshold value is specified.

3. **Stepwise Selection**. Selection commences as with Forward selection. After each addition of an independent variable to the model the partial sums of squares for all the variables is calculated. This procedure then allows variables that were previously significant in the model but became unimportant on the addition of other variables to be removed. The procedure switches to backward selection removing variables until all the variables meet the minimum threshold F value.

Stepwise selection is mathematically more complex, compared to a simple forward or backward selection, but produces a greater chance of finding the best subset models as more combinations are tested (Rawlings, 1988). This technique was compared against forward selection using the dependent variable ERRATE (Section 5.3.3) and the independent variables at 8 monitoring sites. Only once did a different variable enter into the model, and this was the variable with the lowest partial sum of squares.

It is common to set both selection and rejection F values the same; however, the exact value of F may vary with the number of independent variables (Seber, 1977). The larger the number of independent variables the higher, and therefore more rigorous, the F value that is needed to be exceeded. Efroymson (1960) used an F value of 2.5 whilst Draper and Smith (1966) used a value of 3.29 (in Seber, 1977). Three F values, 2.5, 3.29 and 4 were tested in both forward and stepwise selection using ERRATE as the dependent variable, and all the independent variables at eight of the monitoring sites. Slightly more variables were selected using the F value of 3.29 rather than 4, but there was almost no difference between the 3.29 and 2.5 levels. It was therefore decided to use 3.29 as the critical threshold in order to maximise the number of variables selected.

The stepwise selection process imposes certain constraints on the input data. There are three main problems encountered when trying to model a dependent variable using subsets of independent variables (Rawlings, 1988). These are:

1. Normality. Each of the variables should be normally distributed around its mean value to allow comparisons. For small data sets this is difficult to achieve even taking into account the possibility of transforming the original data. However this constraint need not be rigorously adhered to: " normality is needed only for tests of significance and construction of confidence interval estimates of the parameters" (Rawlings, 1998, p. 238)

2. Common Variance. Equal variances imply that every dependent variable observation contains the same amount of information. If the variance is heterogeneous, as it often is for non-normal distributions, then the transformation of the original data set may again be considered. An alternative is to use a weighted least squares selection procedure.

3. Correlated Errors. Time series measurements may incorporate errors within the measurements that will impact on the subsequent measurements. The residuals at each time step may become auto-correlated because of the associated errors. This problem can be overcome by the design of the experiment collecting the data or, in the case of this study, by the selection of surrogate variables.

Other problems that may be encountered are overly influential 'outlying' data points, and collinearity within the data. Transformation may again solve the problem of outliers. Collinearity, where variables are interconnected in the linear model due to their similar variability, may be checked using the correlations between variables (Ferguson, 1977). After the best sub-set was selected each of the independent variables was compared against the others that were selected. If the Pearson's correlation coefficient (r) was at, or above 0.8 (Hauser, 1974), then one of the indices was excluded (Hooke, 1979; Lawler, 1986). To rationalise the exclusions the variables that caused the highest occurrence of collinearity within all the other variables was the first to be removed.

5.3.3 Erosion Variable Selection

The erosion rates for each epoch at every monitoring site needed to be summarised into variables that could describe seasonal variations in the data. So that the study would be comparable with previous studies by Hooke (1979) and Lawler (1986) the same dependent variables of average erosion rates (ERRATE), the percentage of pins registering erosion (ERODE%), and the maximum amount of erosion for each epoch (ERMAX) were used (Table 5.2).

The high rates of erosion at some sites, where entire erosion pins were regularly removed, meant that the maximum amount of erosion during an epoch (ERMAX) would be constrained, in some circumstances, by the maximum pin length. The upper 'ceiling' of erosion measurements could mask the seasonal variation between epochs. To account for this problem, the 84th percentile of all the pins measured was calculated (Table 5.2). Similar to uses in other distributions, for example D_{84} in bed material measurements (Wolman, 1954), the 84th percentile describes where the upper range of erosion measurements is situated. The advantage is that in most cases there should be no 'topping out' of the erosion values.

DEPENDENT VARIABLE ABBREVIATION	VARIABLE DESCRIPTION	UNITS
ERRATE	The average rate of erosion registered at all measured erosion pins for each epoch	mm a^{-1}
ERMAX	The maximum amount of erosion registered on an erosion pin during an epoch	mm
ERODE84	The 84th percentile of erosion registered on erosion pins during an epoch	mm
ERODE%	The percentage of pins that registered erosion during an epoch	%

Table 5.2 A description of the dependent erosion variables used in the Stepwise Multiple Regression analysis.

5.3.4 Derivation and Selection of Independent Variables

The main aim of the independent environmental variable selection was to produce variables that would model the seasonal variations in erosion data, as an aid to process interpretation. To rationalise the number of exploratory variables used those identified as being influential in

previous U.K. studies (Hooke, 1979; Lawler, 1986) were chosen. The selection of variables was also limited by the availability of data from the study's fieldwork programme, as well as from external data sources such as gauging stations and meteorology stations. Due to the lack of background data during the beginning of the monitoring programme the length of the period being considered for regression was limited to less than the maximum period monitored using erosion pins (December 1996 – March 1998). The actual duration of erosion pin monitoring regressed was therefore fixed from mid January 1997 until late March 1998. This period includes two winters but only one summer which may bias the variables selected, resulting in the process inferred being mainly those that occur during the winter. As the majority of the erosion occurred during the winter (Table 5.1) this subjectivity is thought not to be a significant problem.

The initial aim of the stepwise regression was to describe the variations in bank erosion at the three main monitoring sites in the upper, middle and lower catchment (Beck Meetings (Site 1), Low Row (Site 4) and Greystone Farm (Site 8)). The data available from on site monitoring of air temperature, bank temperature, and stage (Section 3.3.5-3.3.6) allowed a more rigorous formulation of surrogate environmental variables than from offsite monitored data. Subsequently these data on independent variables have been extrapolated to include all the other sites, except for Easby, where the small sample size of erosion measurements (n = 10) invalidates many of the requirements for regression analysis (Section 5.3.2). Data from Beck Meetings (Site 1) were used to create the independent variables at Hoggarths (Site 2) and Muker (Site 3). Low Row (Site 4) data were used to model dependent variables at Reeth (Site 5), whilst Morton-on-Swale (Site 7) and Topcliffe (Site 9) used Greystone Farm (Site 8) data to create surrogate variables for each epoch. The variables have a selection of associated erosion processes that they could influence in both a univariate and multivariate manner. They can, in the main, be grouped into 4 categories (Hooke, 1979; Lawler, 1986): Temperature Indices; Streamflow Indices; Precipitation Indices and Antecedent Precipitation Indices, and the discussion below treats each group in turn. The definitions and units for each variable are provided in Table 5.3.

INDEPENDENT VARIABLE ABBREVIATION	VARIABLE DESCRIPTION	UNITS
Temperature Indices		
AIRFROST%	Number of days (0900-0900 GMT) of air temperatures ≤ 0.0 ^{O}C, as a percentage of the erosion epoch length	%
BANKFROST%	Number of days (0900-0900 GMT) of air temperatures ≤ 0.0 ^{O}C at the bank face, as a percentage of the erosion epoch length	%
FTCYC%	Number of episodes of temperatures ≤ 0.0 ^{O}C, as a percentage of the erosion epoch length	%
MAXRANGE	Maximum diurnal temperature range (0900-0900 GMT) within each epoch	$^{\circ}$C
Stream flow indices		
AMAXST	Absolute maximum stage recorded in each erosion epoch	m
MDSTAGE	Mean daily stage in each erosion epoch	m
MMAXST	Mean daily maximum stage in each erosion epoch	m
ST+90%	Percentage of epoch length when the bank face was inundated at or above 90% of its height	%
ST+60%	Percentage of epoch length when the bank face was inundated at or above 60% of its height	%
MAXDESC	Maximum rate of descent of stage, during the time in each erosion epoch when the bank face was inundated at or above 60% of its height	m min^{-1}
Precipitation indices		
GT5MM%	Number of days with >5.0 mm precipitation, as a percentage of the erosion epoch length	%
GT10MM%	Number of days with >10.0 mm precipitation, as a percentage of the erosion epoch length	%
MAXDP	Maximum daily precipitation in each erosion period	mm
Antecedent ground moisture indices		
API .94	Mean Antecedent Precipitation Index (API), with a decay constant (k) = 0.94, for each erosion epoch	mm
API.98	Mean Antecedent Precipitation Index (API), with a decay constant (k) = 0.98, for each erosion epoch	mm

Table 5.3 Independent environmental variables used in the Stepwise Multiple Regression analysis.

5.3.4.1 Temperature Indices

AIRFROST%

The number of days in each epoch that have air temperatures ≤ 0.0 °C gives an indication of the potential for frost action processes to occur. Needle ice formation and other freeze thaw processes may be active if the temperature is low enough, and if there is sufficient soil moisture present (Outcalt, 1971; Branson, 1992).

The number of days of air frost was determined using thermistor data at both Beck Meetings and Low Row (Figure 3.5). Greystone Farm AIRFROST% data were obtained from Leeming Meteorological Station (SE 4305 4891) minimum temperature data (Figure 3.1). The meteorological station daily measurements were recorded from 0900-0900 GMT. To allow comparisons throughout the data sets this daily interval was made the convention for all data.

Low Row did not have any air temperature measurements until 29/06/97, part way through the analysis period. Therefore, to fill this data gap, a common measurement period of air temperature at Beck Meetings and Low Row from 29/07/97-02/08/97 containing 324 data points, from 15 minute interval monitoring, was used to create a regression equation relating the two sites (Equation 5.1).

$$AIRTEMP_{LR} = 0.9477AIRTEMP_{BM} + 4.6019 \quad (5.1)$$

(R^2 = 87.0 %; n = 324; $p < 0.05$)

Where:

$AIRTEMP_{LR}$ = the air temperature at Low Row, from 29/07/97-02/08/97, (°C);
$AIRTEMP_{BM}$ = the air temperature at Beck Meetings, from 29/07/97-02/08/97, (°C).

The missing data at Low Row were estimated using the derived equation, allowing the percentage of days in each epoch with sub-zero temperatures to be calculated.

BANKFROST%

The actual surface temperature of the bank is a more specific measure of the bank thermal conditions than AIRFROST%. The effects of shading from vegetation and insulation from river water may be included in this variable, allowing a clearer picture of the likelihood of frost action processes occurring.

At all three main sites (Beck Meetings, Low Row and Greystone Farm) the temperature data provided by the Tinytalk thermistors (Section 3.3.6) were used for most of the analysis period. When the instruments were not accessible to download, due to flood inundation, air temperature was used to predict the bank face temperature. The regression equations and confidence limits for the relationships between air thermistor and Tinytalk data at each site are shown in Table 5.4.

SITE NO.	SITE NAME	LINEAR REGRESSION EQUATION	NUMBER OF PAIRS OF VARIABLES (n)	CO-EFFICIENT OF DETERMINATION (R^2) (%)	MALLOWS Cp (p)
1	Beck Meetings	$BANKTEMP_{BM} = 0.629AIRTEMP_{BM} + 3.107$	44680	42.2	<0.05
4	Low Row	$BANKTEMP_{LR} = 0.675\ AIRTEMP_{LR} + 0.745$	1703	92.0	<0.05
8	Greystone Farm	$BANKTEMP_{GS} = 1.164\ AIRTEMP_{GS} - 0.296$	7000	72.0	<0.05

Table 5.4 Regression equations relating Air Temperature to Bank Face Temperature at Beck Meetings (Site 1), Low Row (Site 4), and Greystone Farm (Site 8).

FTCYC%

The frequency of sub-zero temperature cyclicity during an erosion epoch may be important for predicting the effect of frost in the soil (Lawler, 1986). The number of times the air temperature fell to ≤ 0 °C may not necessarily be the same as the number of days of air frost. Several sub-zero fluctuations may occur in one night. These individual fluctuations have been linked to the multi-layered sediment bands that occur in needle ice due to re-freezing of water in the bank surface (Branson *et al.*, 1992; Lawler, 1993b). A single period of sub-zero temperatures may also extend over several days (Lawler, 1984).

The same air temperature data used to calculate AIRFROST% were used to determine FTCYC%, due to the greater availability of these data compared to BANKFROST%. The number of times the temperature was ≤ 0 °C during each 24-hour period was expressed as a percentage of the number of days in the epoch.

The air temperature data used to calculate the number of frost cycles was recorded at 15-minute intervals. This interval of measurement could potentially lead to an under-prediction of the number of frost cycles if the temperature was rapidly fluctuating.

MAXRANGE

Expansion and contraction of both the bank material and the air contained within the soil matrix can stress the bank surface. Extreme drying of the soil followed by wetting due to either rain or flood inundation could lead to slaking (Section 2.2.3) (Selby, 1982). During periods of low bank moisture the contraction of the soil may result in desiccation of the bank material, with soil flaking away from the bank surface (Duijsings, 1987). The highest daily range in each epoch indicates the most extreme temperature change during a 24-hour period, and therefore the potential for the highest stresses. It could also model the changes from frozen conditions to temperatures above 0 °C, representing the melting and either direct erosion or preparation of surface bank material.

At Beck Meetings and Low Row the daily maximum and minimum from the 15-minute interval air temperature data were used to determine MAXRANGE. At Greystone Farm the minimum and maximum daily temperatures at Leeming (Figure 3.1) were used.

5.3.4.2 Streamflow Indices

AMAXST

The dominant flood within each erosion epoch (AMAXST) was expected to vary seasonally due to the incidence of high flows during the winter - spring period, and low flows during the summer. This variable, however, allows the influence of low frequency and high intensity flow events, such as those caused by summer thunderstorms, to be accounted for. The height of the

dominant flood could lead to the prediction of a threshold level needed for certain processes to become active, such as entrainment or mass failure. The stage of the floodwater is therefore used to determine this variable, as opposed to discharge. The significance of 'catastrophic' events in causing the re-shaping of the channel by erosion could also be inferred from this measure.

Pressure transducer data from Beck Meetings and Low Row was used to calculate this index. Stage data from the I.H. gauging station at Crakehill (S.E. 4425 4734) (Figure 3.1) was used as an indicator for the water depth upstream at Greystone Farm. However, the left-hand tributary of Cod Beck enters the River Swale in between Greystone Farm and Crakehill (Figure 3.5). The actual stage and discharge will therefore differ between these monitoring sites; however the objective of using the AMAXST index was to reveal seasonal variations in stage. The timing of the maximum stage at these two downstream sites should be reasonably consistent.

The maximum stage events at Beck Meetings and Low Row were not recorded in all cases due to the removal of the pressure transducer support structure by floods, or blockages from trapped Coarse Woody Debris (CWD). Lack of upstream stage monitoring in Swaledale made it impossible to 'infill' the missing 5 % of the data with stages from the River Swale or any of its tributaries. Instead an upland gauging station at Moor Houses on Trout Beck (NY 758 335) (Figure 3.1) (Burt *et al.*, 1998) was used to estimate missing flow data. The common monitoring period from 14/01/97 – 06/01/98 at both Beck Meetings and Moor Houses, containing 2000 hourly data points, was used to perform a least squares linear regression analysis (Equation 5.2).

$$STAGE_{BM} = 0.724\ STAGE_{MH} + 0.0624 \qquad (5.2)$$

(R^2 = 46.2 %; n = 2000; $p < 0.001$)

Where:

$STAGE_{BM}$ = stage at Beck Meetings (m);
$STAGE_{MH}$ = stage at Moor Houses (m).

The same approach was used for the missing 20 % of the stage data at Low Row. A least squares linear regression was fitted to a common monitoring period from 16/12/97 – 06/01/98, which contained 2000 data points recorded at 15-minute intervals (Equation 5.3).

$$STAGE_{LR} = 13.75\ STAGE_{MH} + 3.70 \quad (5.3)$$

($R^2 = 36.7$ %; n = 2000; $p < 0.001$)

Where:

$STAGE_{LR}$ = stage at Low Row (m);
$STAGE_{MH}$ = stage at Moor Houses (m).

Equations 5.2 and 5.3 were then used to in fill all the data gaps at Beck Meetings and Low Row.

MDSTAGE

The mean daily stage in each epoch gives an indication of the average flow conditions in the channel. This reduces in significance the extreme events of high and low stage. The mean stage could model the height of most frequent saturation of the bank. If the mean stage in an epoch was high enough to encroach on the bank upper layers there could be a greater incidence of mass failure. A more probable lower average depth of stage could affect entrainment processes. Higher mean stages would result in greater shear stresses on the bank surface, resulting in increased levels of entrainment.

The same data sets used to calculate AMAXST were used determine the mean daily stages, which were then averaged for each epoch.

MMAXST

The index, produced by averaging the maximum daily stages in each erosion epoch, allowed the seasonal variations in the upper range of stage data to be highlighted. The index created values that were higher than MDSTAGE but lower than AMAXST. It was however the fluctuations of the index between epochs that were of importance. High values should occur when there were elevated stages either for a long single period or for several shorter time periods. It was not possible to differentiate between these two scenarios with this index. The higher the value of MMAXST the more likely the banks at that level, or just below, would become saturated, aiding mass failure processes. The lower the value the drier the banks and the greater chance that desiccation processes could have occurred.

ST+90%

Although the indices of AMAXST, MDSTAGE, and MMAXST all provide information on the level of inundation of the bank surface they do not describe the length of time that the bank was submerged. ST+90% was therefore devised as an index of the length of time that the stage was above 90 % of the bank height. The 90 % level was selected so that it included, at all sites, the upper 40 cm of the bank. This upper region was the most prone to cantilever block failures, prepared by previous entrainment undercutting the banktop (Thorne and Tovey, 1981). At Greystone Farm the bank height of 4 m resulted in the top 10 % of the bank being between 3.6 and 4 m. The longer cantilever blocks are inundated the greater the degree of saturation, and associated increase in weight. When the flood wave retreats the block may be too heavy to support its own weight, leading to collapse by surcharging (Abam, 1997). The high flows may also be associated with a higher potential for fluvial entrainment.

The lack of floods during the low flow periods could result in several zero values, thus limiting the use of the index to describe seasonal trends. However, if intermittent bank failures are the dominant source of erosion at a monitoring site then this index may be an effective model. There is also the problem of not being able to identify whether high stages are from one long single event or from several shorter events. Thus care must be taken in the interpretation of this variable.

ST+60%

This variable is similar to ST+90%. The ST+60% index records the amount of time that 60 % of the bank was inundated. The advantage of creating a larger zone than ST+90% was so that the likelihood of maintaining zero values could be reduced, and therefore seasonal variations in erosion better accounted for.

Processes of entrainment, slab failure, cantilever failure and rotational failure could all be favoured by having high values of ST+60%. Having a larger area of the bank inundated would also be expected to result in strong relationships with ERODE% as there is a greater potential for entrainment at the erosion pin sites.

MAXDESC

Hooke (1979) found problems in obtaining a consistent measure of hydrograph recession for an analysis of bank erosion rates. In an attempt to create a transferable variable between monitoring sites only the falling limbs that occurred whilst the bank was inundated at, or above, 60 % of its height were considered. The upper level of inundation includes floods potentially influential in causing mass failures on the receding limb on the hydrograph. The fastest fall in stage for each 15-minute interval was calculated for each flood over 60 % of the bank height. MAXDESC represents the maximum 15-minute recession rate for each epoch.

The rate of decline of stage has implications for the stability of the bank. If the water level drops rapidly then the bank may become unstable due to the increased weight and pore water pressures, from absorbed water (Darby *et al.*, 2000), being unsupported when the buttressing effect of the river water is removed (Abam, 1997).

Only the fastest rate of descent in each epoch was considered in this variable, so a bias was placed on the fact that single events in each epoch will dominate the erosion.

5.3.4.3 Precipitation Indices

GT5MM%

The percentage of days in each epoch with the relatively high rainfall rate of 5 mm day^{-1} was used to describe events that may be influential in explaining bank erosion. Hooke (1979) and Lawler (1986) used the percentage of days in each epoch in which precipitation had been recorded and therefore the variables should be comparable.

The rainfall data needed to calculate this variable was taken from Moor Houses (Figure 3.1) for Beck Meetings, Hoggarths and Muker; Richmond (NZ 172 016) (Figure 3.1) for Low Row and Reeth; and Leeming Meteorology Station (Figure 3.1) for Greystone Farm, Morton-on-Swale and Topcliffe. The suffixes (MH), (RM), and (LM) denote the different sets of data that were used to

create each index. Missing data at Moor Houses from December 1997-March 98 were directly replaced with data from Richmond from the same period, due to the lack of alternative data sources.

High rates of precipitation can affect the bank directly through rainsplash erosion (Duysing, 1986) removing weathered material as well as the non-subaerially prepared bank surface. There are also linkages between rainfall, river flow and soil moisture.

GT10MM%

Due to the upland nature of much of the Swale catchment high rates of rainfall occurred during the monitoring period. In order to characterise seasonality in the highest rates of rainfall a threshold of 10 mm day^{-1} was used as well as the 5 mm day^{-1} index.

MAXDP

The maximum precipitation event within an epoch may, as with AMAXST, model the influential 'catastrophic' events of bank erosion.

The same data used to determine GT5MM%, and GT10MM%, were used to calculate the maximum rainfall in each epoch. High rainfall rates could be associated with rainsplash erosion, or simply increase the stage and soil moisture.

5.3.4.4 Antecedent Precipitation Indices

API.94

The moisture content of the bank material can influence bank erosion processes, and in particular mass failures (Section 2.4). Directly measured soil moisture levels were not available for the erosion monitoring sites so surrogate variables of Antecedent Precipitation Indices (API), which describe catchment 'wetness', were used (Section 2.3.2). The method of calculation (Equation

2.2) was the same as that used by Gregory and Walling (1973). The past rainfall data at each site were multiplied by a decay factor (k) to model the drying of the site over time.

The decay constant may be varied to account for different rates of drainage, or drying, of the soil. Recommended values range from 0.85 to 0.98 (Gregory and Walling, 1973). Hooke (1979) and Lawler (1986) both used k = 0.94 for U.K. rivers, which is indicative of a slow drying/draining soil, so this constant was selected for comparability.

Rainfall data used to calculate API.94 for all the sites were from Moor Houses, Richmond, and Leeming, (Figure 3.1) the same as that used to determine GT5MM% and GT10MM%.

API.98

As part of the Environmental Change Network (ECN) (Burt *et al.*, 1998) moisture contents of the soil at Moor Houses (Figure 3.1) were monitored. Moor Houses (560 m OD) is a similar upland catchment to Beck Meetings (450 m OD), with both sites have a peaty soil classification. To test whether API.94 was the most effective variable for modelling moisture conditions at Beck Meetings a range of different APIs were created using varying decay coefficients (k). The moisture conditions were correlated against each API for the study period time series. The highest correlation coefficients were for the upper range of k values, those approaching unity. This represents a very poorly drained, or slow drying, system. A higher k value of 0.98 was therefore used to calculate an alternative API for wetter conditions. This allowed comparisons to be drawn on the effectiveness of each index in modelling variations in erosion.

For both API.98 and API.94 a single decay constant has been used to represent the loss of moisture from the catchment. In reality the changing climatic conditions throughout the year would alter the rates of evaporation with lower k values during the summer caused by high evaporation rates. Changing vegetation throughout the year could also alter the amount of evapotranspiration, with the summer increase in vegetation cover allowing a more rapid drainage, and drying of the soil. The degree of variation found between seasons and different monitoring sites was unknown and therefore for simplicity an annually constant k value was used.

5.4 CORRELATION AND REGRESSION RESULTS

5.4.1 Time Series of Independent Variables

The independent variables selected to be entered into the regression analyses needed to show a degree of seasonal variability so that they could describe variations in erosion. To be able to assess the trends in each of the independent variables the data have been presented as time series plots for the study period (Figures 5.2 - 5.4). Only the three main monitoring sites in the upper, middle and lower catchment (Beck Meetings (Site 1), Low Row (Site 4), and Greystone Farm (Site 8)) have been presented for ease of comparison.

5.4.1.1 Temperature Indices

The annual seasonality in AIRFROST%, BANKFROST% and FTCYC% was reasonably predictable, with a high frequency of frost during the winter months and lower frequency in the summer months (Figure 5.2A-C). The trend in a downstream direction is also fairly distinct, with a decline in the percentage of frosts due to altitudinal differences. Whilst AIRFROST% and BANKFROST% remained fairly similar during the year FTCYC% was more variable. The higher variations in frost indices were upstream at Beck Meetings (Site 1) (Figure 5.2A), whilst at Greystone Farm (Site 8) (Figure 5.2C) the variables were all closely grouped together at the low end of the range of frost frequencies.

The maximum diurnal temperature range (MAXRANGE) does not vary as systematically as the frost frequency variables (Figure 5.2A-C). A summer peak occurs at each of the sites, with the annual range of values decreasing downstream. At Beck Meetings (Figure 5.2A) and Low Row (Figure 5.2B) MAXRANGE remained elevated during most of 1997, until the month of November, then were consistently low until March 1998.

5.4.1.2 Streamflow Indices

Upstream at Beck Meetings (Figure 5.3 A) the streamflow indices remained comparatively low during the year. Moving downstream, the range of values increases, as does the frequency of

episodic peaks. The seasonality in the streamflow indices is less distinct downstream due to elevated periods of stage during the summer months.

Upstream MAXDESC has constant zero values over most of the year (Figure 5.3A), producing a clear distinction between the upper and lower catchment. The few periods that record a falling stage, above 60 % of the bank height, are comparatively high, reflecting the rapid nature of the flood waves passing through the upstream part of the catchment. Low Row (Figure 5.3B) had relatively low rates of descent, whilst the maximum values occurred at Greystone Farm with stage falling at up to 0.05 m s^{-1} (Figure 5.3C). The indices of MMAXST and MDSTAGE remain closely related in values, and seasonality, at all of the sites. This may be due to the flashy nature of the Swale, with flood events passing through the catchment rapidly. This would tend not to significantly alter the mean stage values due to the short periods of high flow. The increasing departure of AMAXST from the other two mean values further down the catchment probably resulted from a downstream increase in high, but infrequent, stage events.

5.4.1.3 Precipitation Indices

The expected peaks in rainfall during the winter months were not distinct at any of the monitoring sites (Figure 5.4A-C). All the rainfall indices, GT5MM%, GT10MM% and MAXDP fluctuated unsystematically throughout the year. In general the indices of rainfall decrease in magnitude downstream, as would be expected from normal altitudinal and longitudinal effects (e.g. Ferguson, 1977; Lawler, 1987a). A high summer peak in GT5MM% (LM) obscures this trend from 03/07/97-14/07/97 at Greystone Farm (Figure 5.4C). The peak maybe artificially elevated due to the short epoch length, thus increasing the importance of a few high rainfall events. These high intensity storms during the summer may be important in determining the length of the active erosion period at each site.

5.4.1.4 Antecedent Precipitation Indices

The seasonal trends in API indices are in effect smoothed versions of the rainfall indices of GT5MM% and GT10MM% (Figure 5.5A-C). At Beck Meetings (Figure 5.5A) the March 1997 peak values in API.94 (MH) and API.98 (MH) are followed by a gradual decline until August

1997. For the rest of the monitoring period both of the API indices remain fairly constant, at around 50 mm for API.94 (MH) and 200 mm for API.98 (MH).

At Low Row, API.98 (RM) and API.94 (RM) are both lower than the upstream values at Beck Meetings (Figure 5.5B). The initial peak in wetness was not present mid catchment and so the levels of the index are not so varied as upstream. Peaks occur from 28/02/97-19/03/97, 09/06/97-29/06/97 and 06/01/98-05/02/98 in both API.98 (RM) and API.94 (RM). This suggests a winter peak in catchment wetness as well as a summer peak.

Further down the catchment the start of the monitoring period remains very dry, until 08/06/97 (Figure 5.5C). Summer rainfall elevates API values up to 127.2 mm for API.98 (LM) and 56.4 mm for API.94 (LM). For the rest of the monitoring period the API indices remain fairly constant at around 100 mm for API.98 (LM) and 40 mm for API.94 (LM).

5.4.2 Correlation Analysis

The correlation coefficients, above a 95 % significance level, between each dependent variable and independent variables are shown for all the monitoring sites (except Easby) in Figures 5.6A-D. The downstream trends in significant linear bivariate relationships for each dependent variable may indicate a shift in the dominant erosion controlling variables.

ERRATE

Significant relationships between ERRATE and the independent variables appeared to show a downstream trend (Figure 5.6A). There was a shift from API, rainfall and temperature indices upstream to fluvial and temperature indices dominating downstream.

ERMAX

The maximum erosion in each epoch (ERMAX) (Figure 5.6B) appears to have a similar downstream trend to ERRATE. Upstream API dominates alongside temperature indices. From the middle to the lower catchment fluvial indices, alongside temperature indices, are significant in explaining the maximum erosion. The exception to this trend is at Greystone Farm (Site 8) where rainfall and API indices were significant rather than fluvial or temperature indices. This could be indicative of a different process, or suite of processes being active at this site.

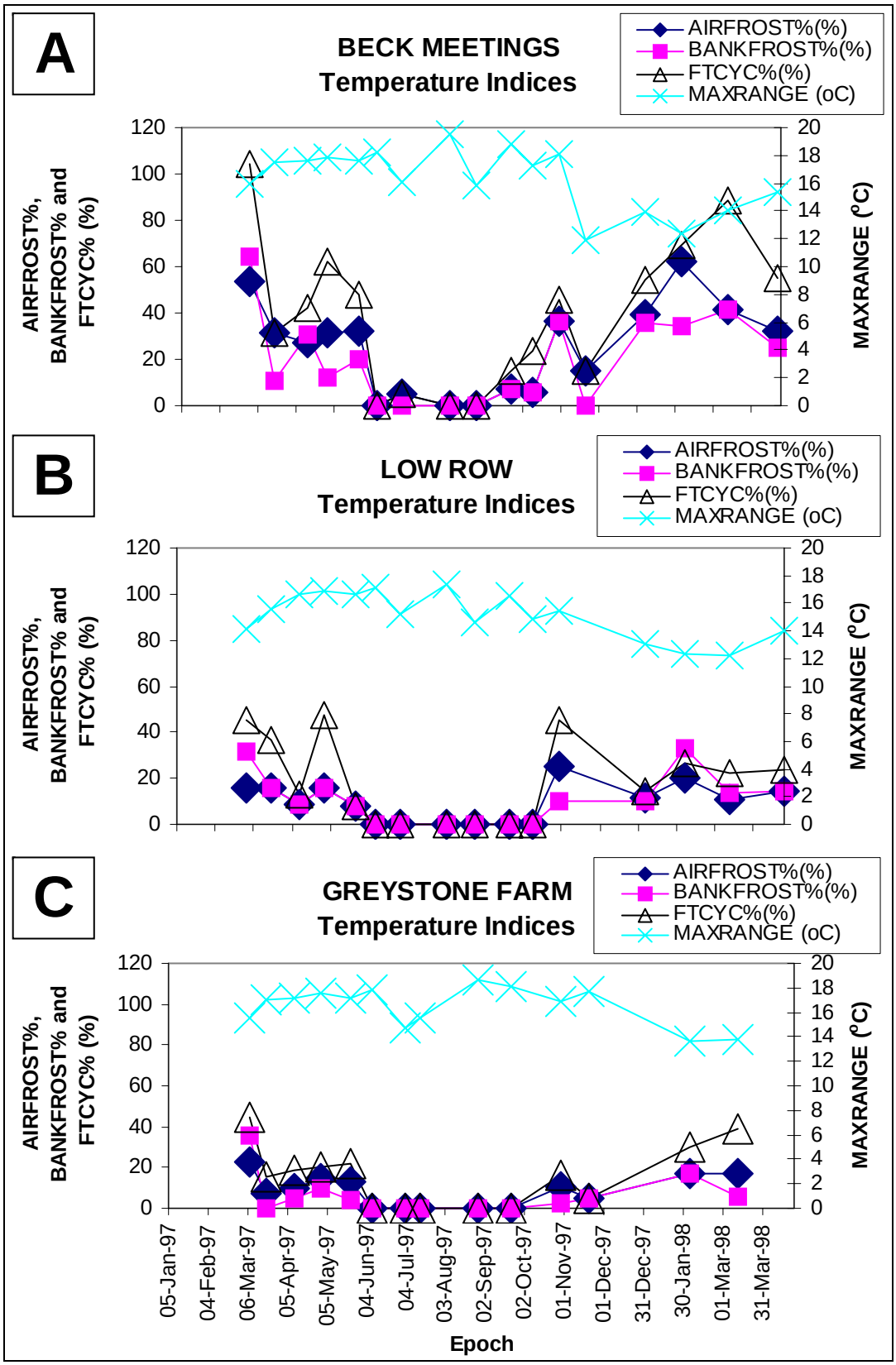

Figure 5.2 Time series of Temperature Indices from January 1997 to April 1998 at: (**A**) Beck Meetings (upstream); (**B**) Low Row (mid-catchment); (**C**) Greystone Farm (downstream).

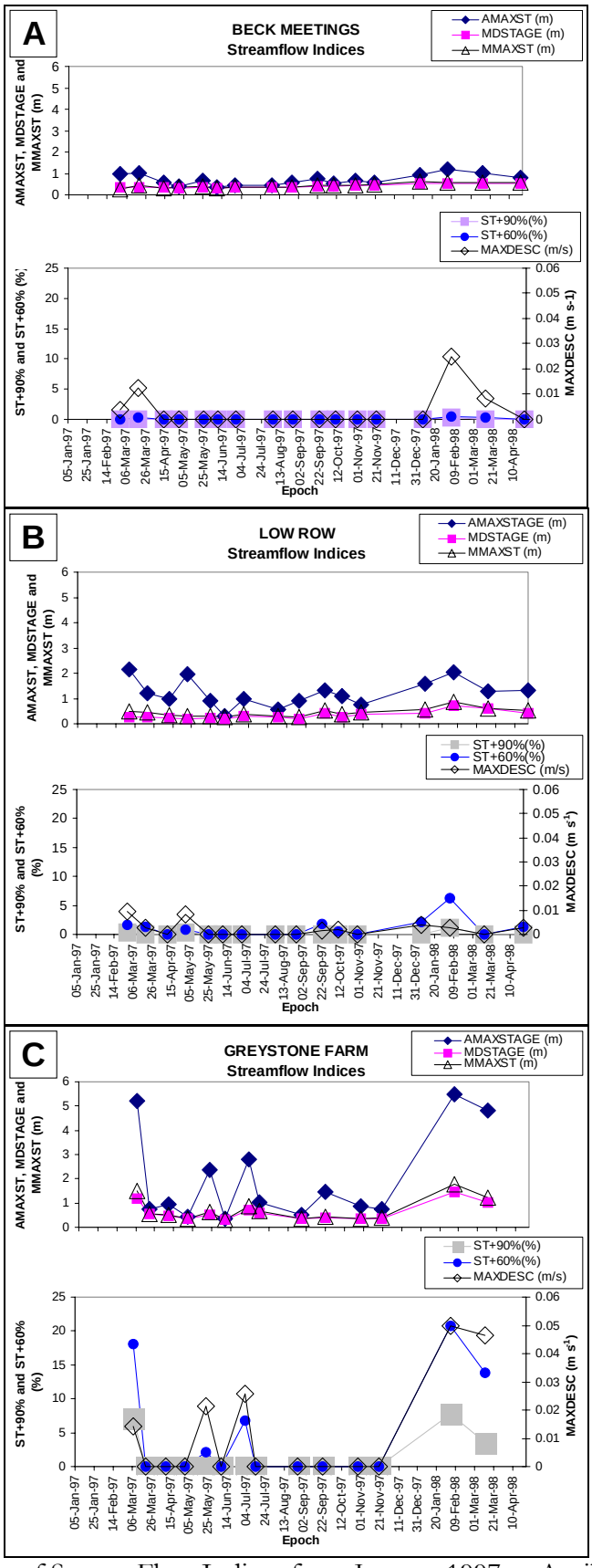

Figure 5.3 Time series of Stream Flow Indices from January 1997 to April 1998 at: (**A**) Beck Meetings (upstream); (**B**) Low Row (mid-catchment); (**C**) Greystone Farm (downstream).

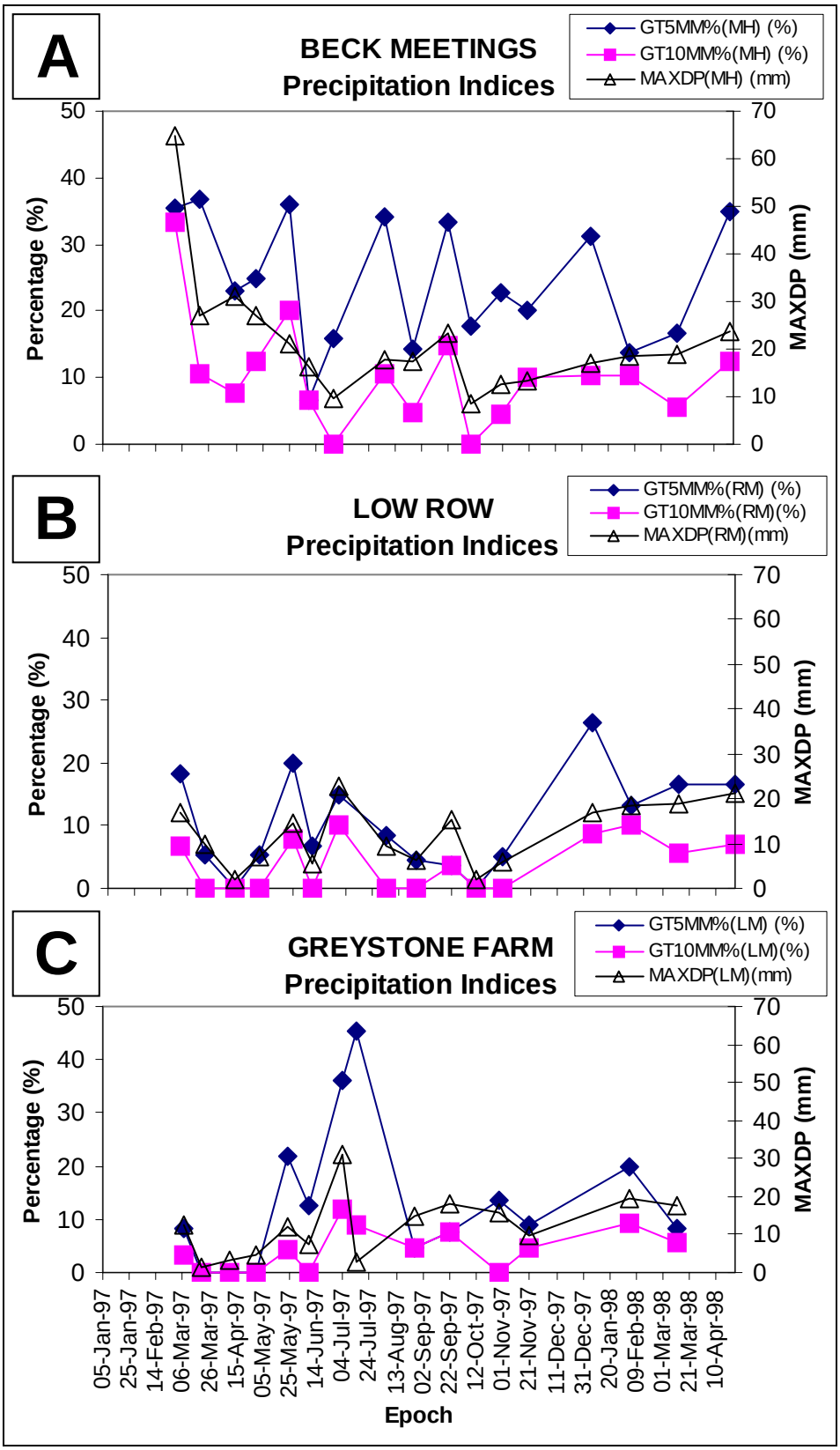

Figure 5.4 Time series of Rainfall Indices from January 1997 to April 1998 at: (**A**) Beck Meetings (upstream); (**B**) Low Row (mid-catchment); (**C**) Greystone Farm (downstream).

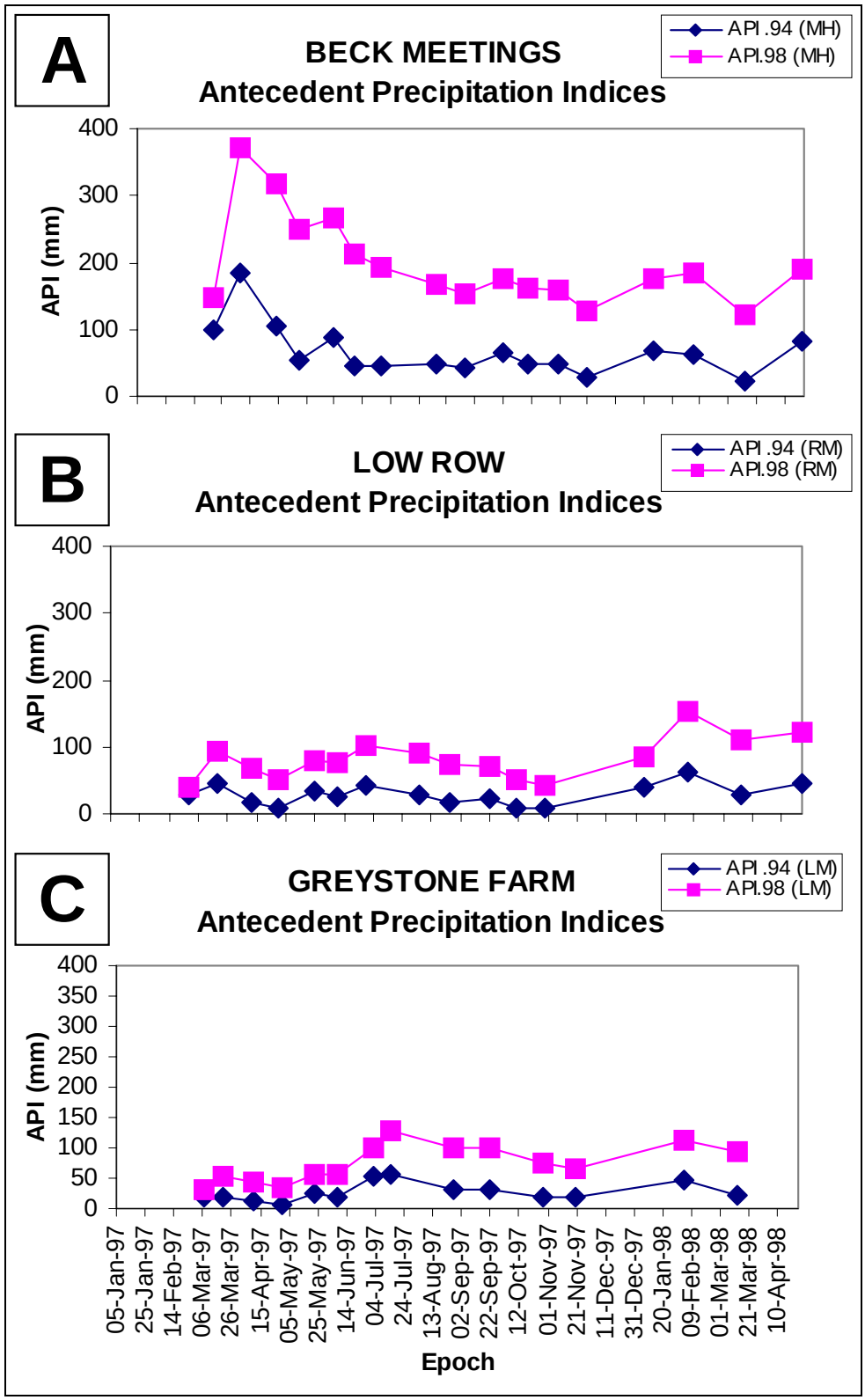

Figure 5.5 Time series of Antecedent Precipitation Indices from January 1997 to April 1998 at: (**A**) Beck Meetings (upstream); (**B**) Low Row (mid-catchment); (**C**) Greystone Farm (downstream).

ERODE84

The distinction between significant and non-significant bivariate relationships was greater for ERODE84 (Figure 5.6C); with most of the relationships being more than 99% significant. Rainfall and especially freezing indices produced the most significant relationships from Beck Meeting (Site 1) to Low Row (Site 4). The exception to this downstream trend was the fluvial index of AMAXST, which maintained a high level of significance for each these sites. The downstream sites of Morton-on-Swale (Site 7) and Greystone Farm (Site 8) also had strong correlation (above a 99% confidence level) between ERODE84 and AMAXST. From Morton-on-Swale downstream to Topcliffe (Site 9) temperature indices remained highly significant as well as stream flow indices.

ERODE%

The downstream trends in bivariate relationships for ERODE% were distinct for those above a 99% significance level (Figure 5.6D). The relationship is very similar to ERODE84 with AMAXST, rainfall and temperature indices dominating upstream, whilst downstream temperature and stream flow indices were most significant. Upstream stream flow indices were significant above a significant level of 95%. This may be due to the fact that although the rate of erosion was more strongly correlated with soil moisture and temperature indices, which may be preparing bank material for erosion, the actual spatial distribution of erosion during each epoch was also influenced by the stream flow indices.

The distribution of correlation coefficients for each dependent variable may vary significantly, with a sharp contrast between those independent variables that are or are not linearly related. The relationships between independent and dependent variables at three significance levels (95%, 97.5% and 99%) are shown for Beck Meetings (Figures 5.7A-D), Low Row (Figures 5.8A-D), and Greystone Farm (Figure 5.9A-D). If there is a rapid decrease in the correlation coefficients then the choice of variables in the stepwise regression is likely to be limited. If two 'borderline' variables are entered the result may be different 'subsets' selected by using alternative methods of stepwise regression (Section 5.3.2). A clear divide between significant and non-significant variables makes this change in subsets less likely to occur.

Upstream at Beck Meetings (Site 1) the soil moisture, stage, and precipitation variables were most significant in modelling the dependent variables of ERRATE and ERMAX (Figures 5.7A and B). The rainfall measured at Moor Houses created API.94 (MH) and API.98 (MH) values that were significant above a 99% confidence limit. The temperature variables were more significant in describing changes in ERODE84 and ERODE% (Figures 5.7C-D).

Mid-catchment at Low Row (Site 4) BANKFROST% and stream variables, especially AMAXST, were most strongly linearly correlated with all the dependent variables (Figures 5.8A-D). There was a sharp drop off in correlation coefficients between BANKFROST% and the other variables in ERRATE and ERODE% (Figures 5.8A and 5.8D).

At Greystone Farm ERRATE and ERMAX were not *strongly* correlated with any of the independent variables (Figures 5.9A and B). Only two independent variables in each case were correlated above a 97.5 % confidence level for both dependent variables. These were MMAXST and MDSTAGE for ERRATE, and GT5MM% and API.94 (LM) for ERMAX. The correlation between most of the stage and API indices were well above the 99% confidence limit for ERODE84 and ERODE%. BANKFROST% still remained significant, if less so, for both these dependent variables.

More detail on the bivariate relationships may be gained by examining the scatterplots of the original data. Due to the number of correlations possible only variables that were selected in the stepwise multiple regression (Sections 5.4.3 to 5.4.6) are presented (Figures 5.10 to 5.17). The correlation coefficients that were significant above a 95% confidence limit are shown with a linear least squares regression line. In general most of the bivariate relationships are linear in nature. There is the possibility that polynomial relationships may be more significant than linear ones. An investigation into these relationships is beyond the scope of this analysis.

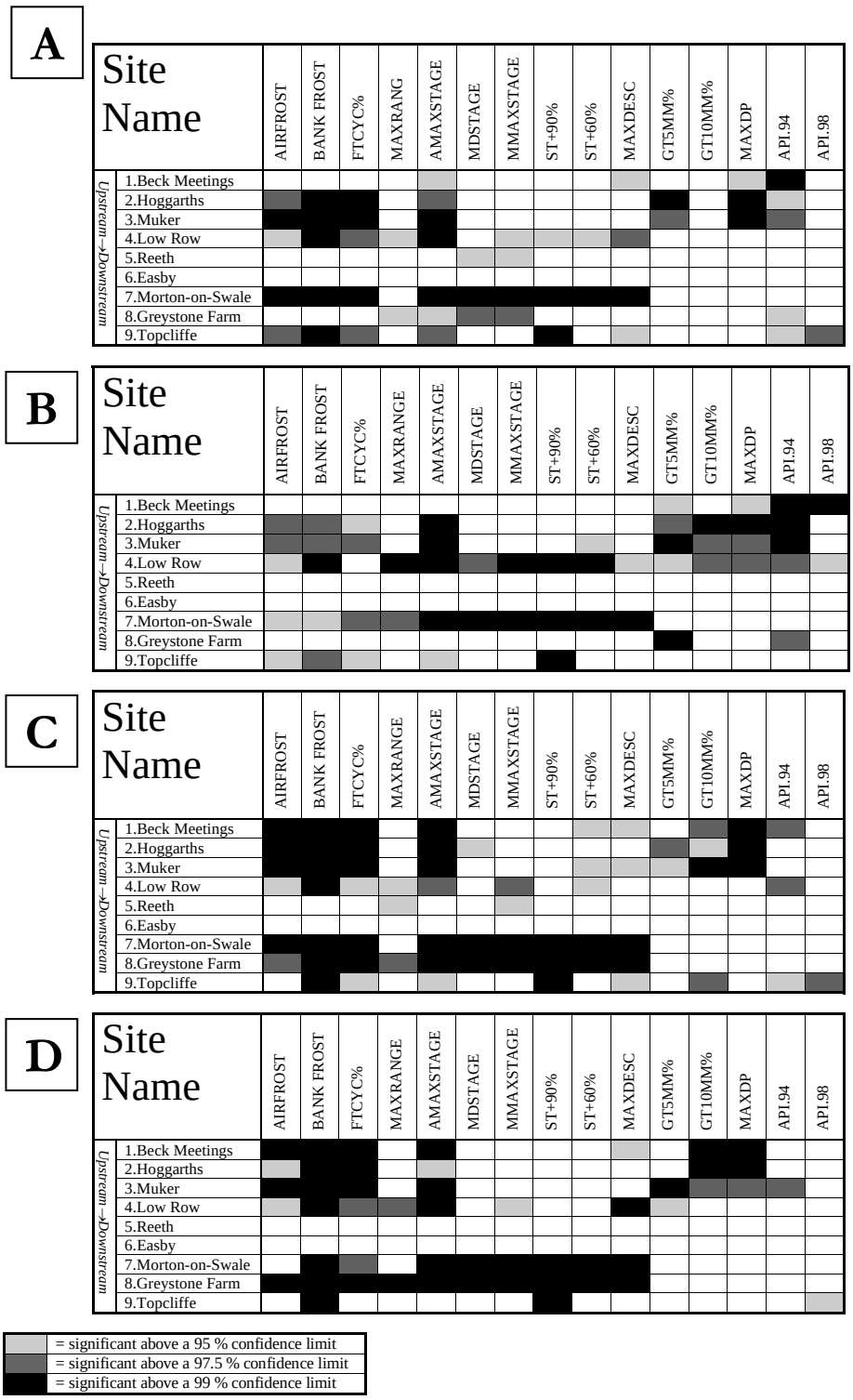

Figure 5.6 Significance levels of correlation coefficients between Environmental Independent Variables and (**A**) ERRATE, (**B**) ERMAX, (**C**) ERODE84, and (**D**) ERODE% above a 95 %, 97.5 % and 99 % confidence limit, for eight monitoring sites.

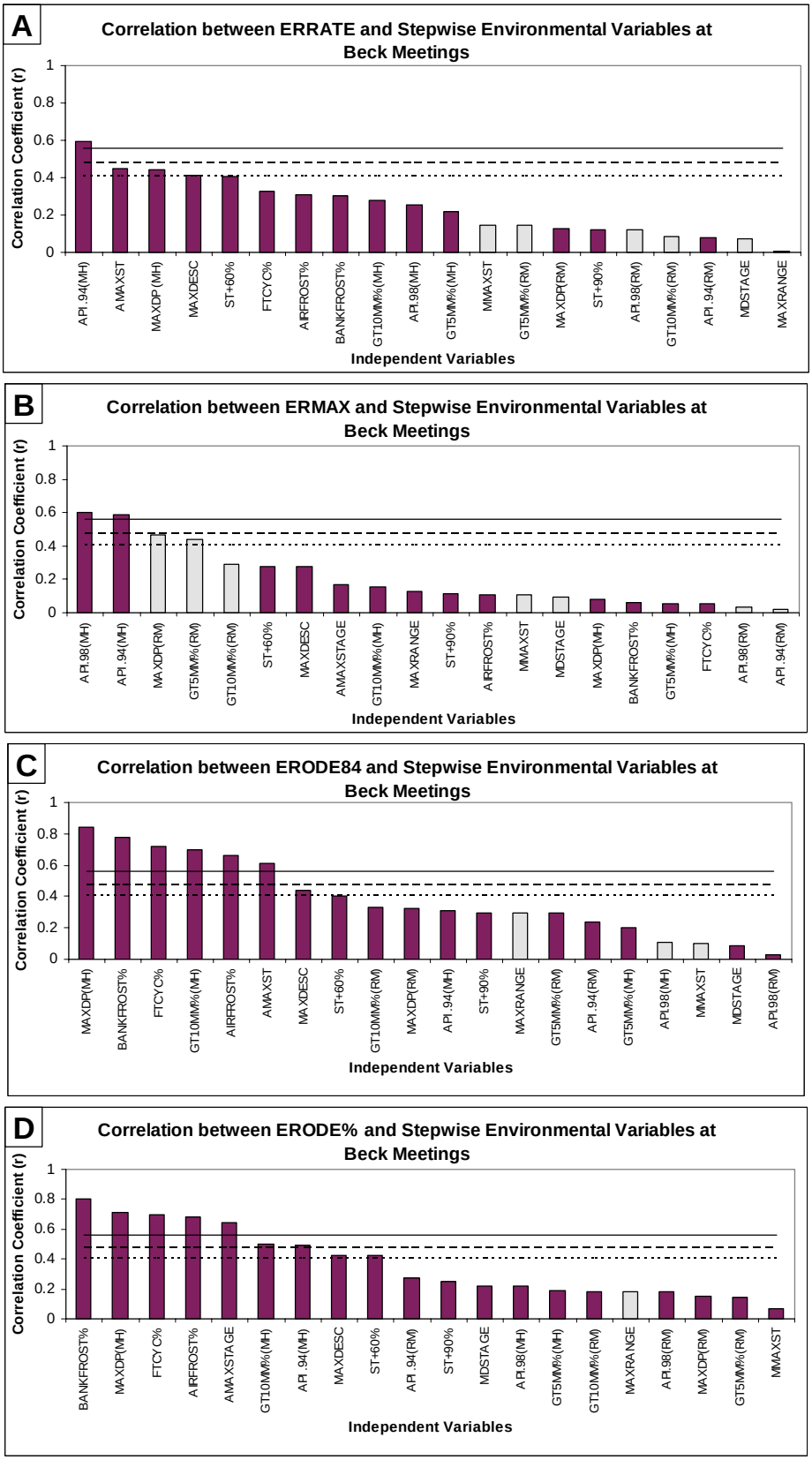

Figure 5.7 Correlation coefficients, at Beck Meetings, between independent variables and (**A**) ERRATE, (**B**) ERMAX, (**C**) ERODE84, (**D**) ERODE%. Significant levels at 99 % ——, 97.5 % – – – –, and 95 % ----- are plotted on each figure. Negative r-values are shown in light grey.

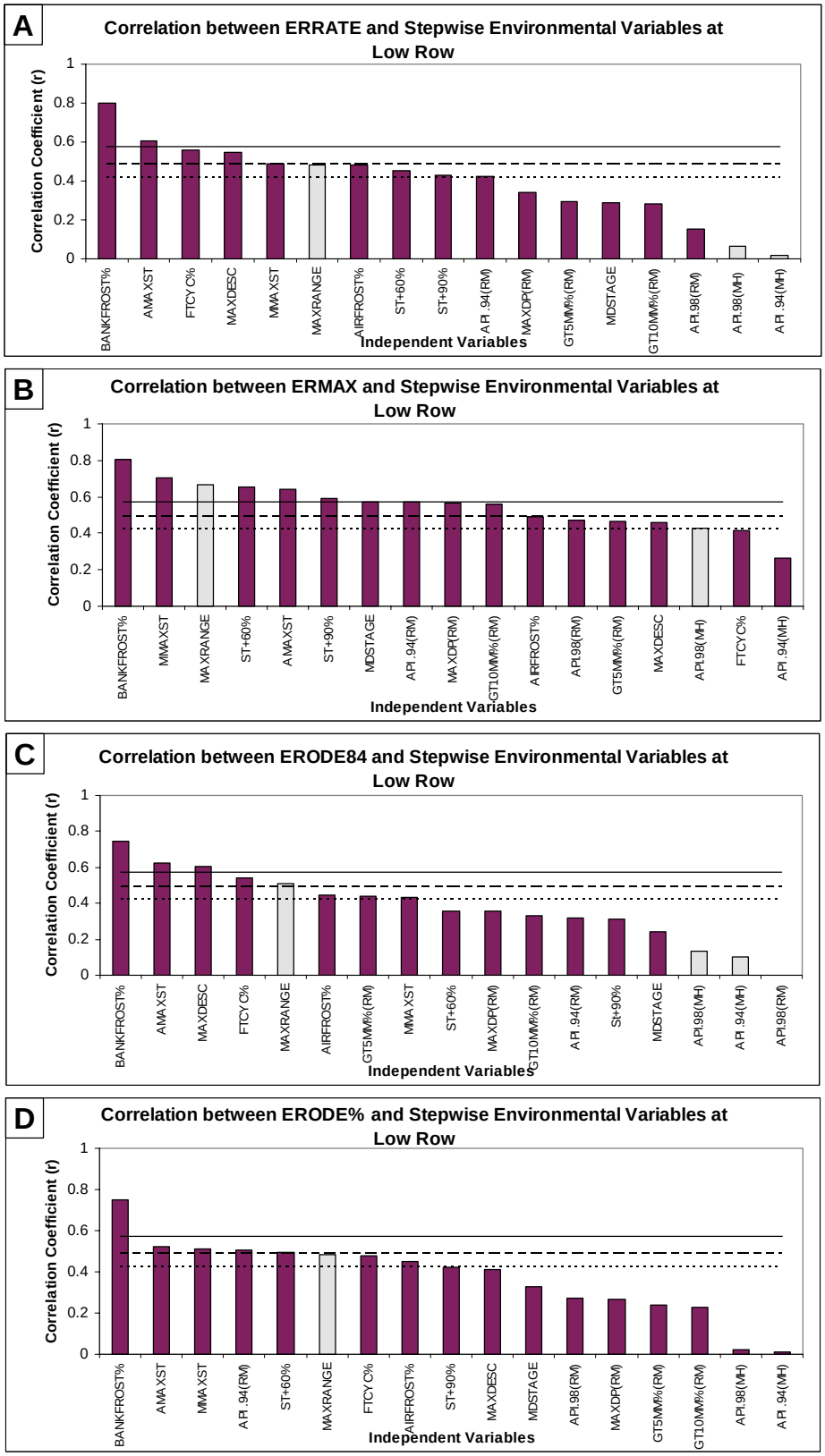

Figure 5.8 Correlation coefficients, at Low Row, between independent variables and (**A**) ERRATE, (**B**) ERMAX, (**C**) ERODE84, (**D**) ERODE%. Significant levels at 99 % ——, 97.5 % – – – –, and 95 % ----- are plotted on each figure. Negative r-values are shown in light grey.

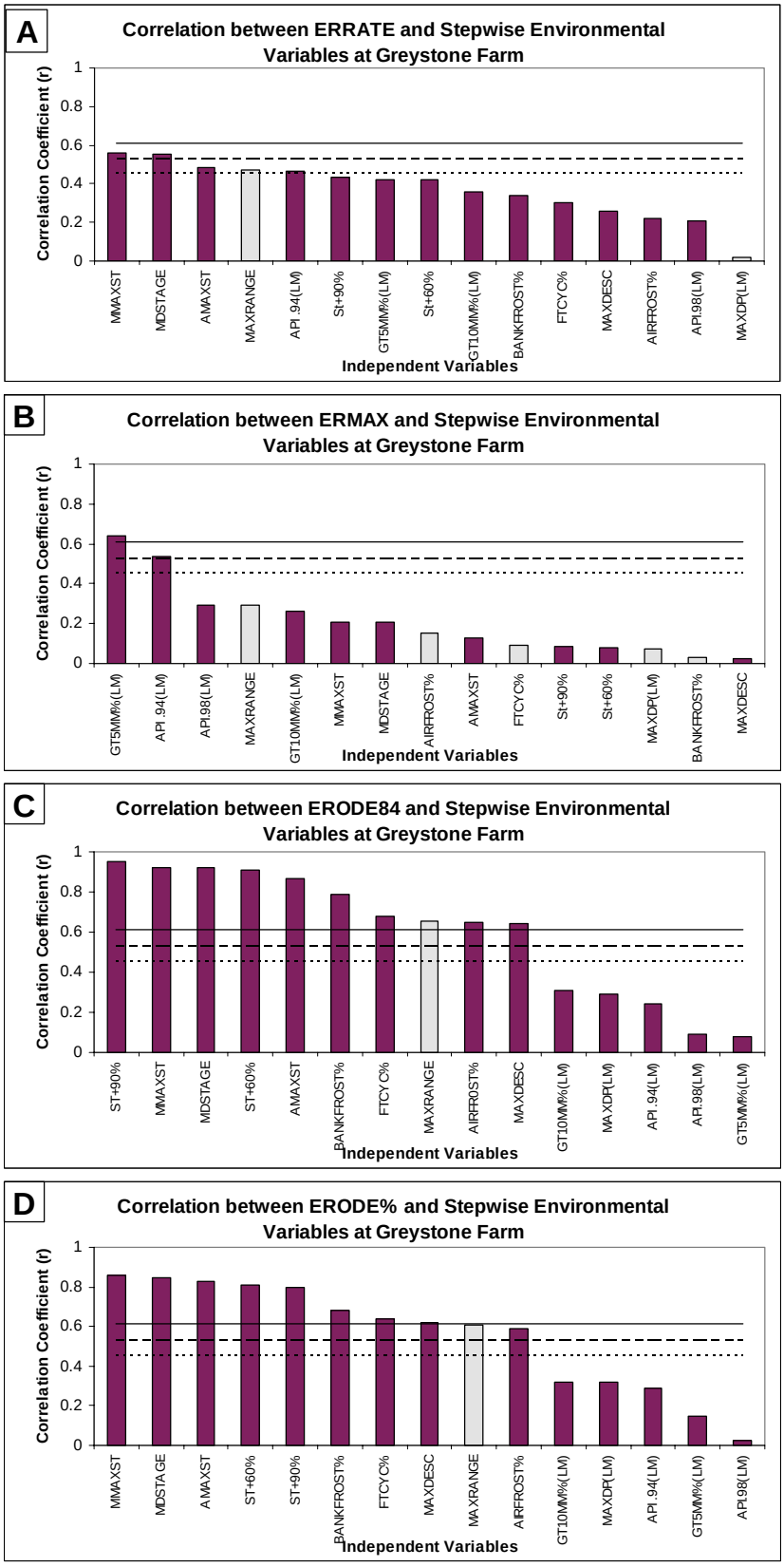

Figure 5.9 Correlation coefficients, at Greystone Farm, between independent variables and (**A**) ERRATE, (**B**) ERMAX, (**C**) ERODE84, (**D**) ERODE%. Significant levels at 99 % ——, 97.5 % – – – –, and 95 % ----- are plotted on each figure. Negative r-values are shown in light grey.

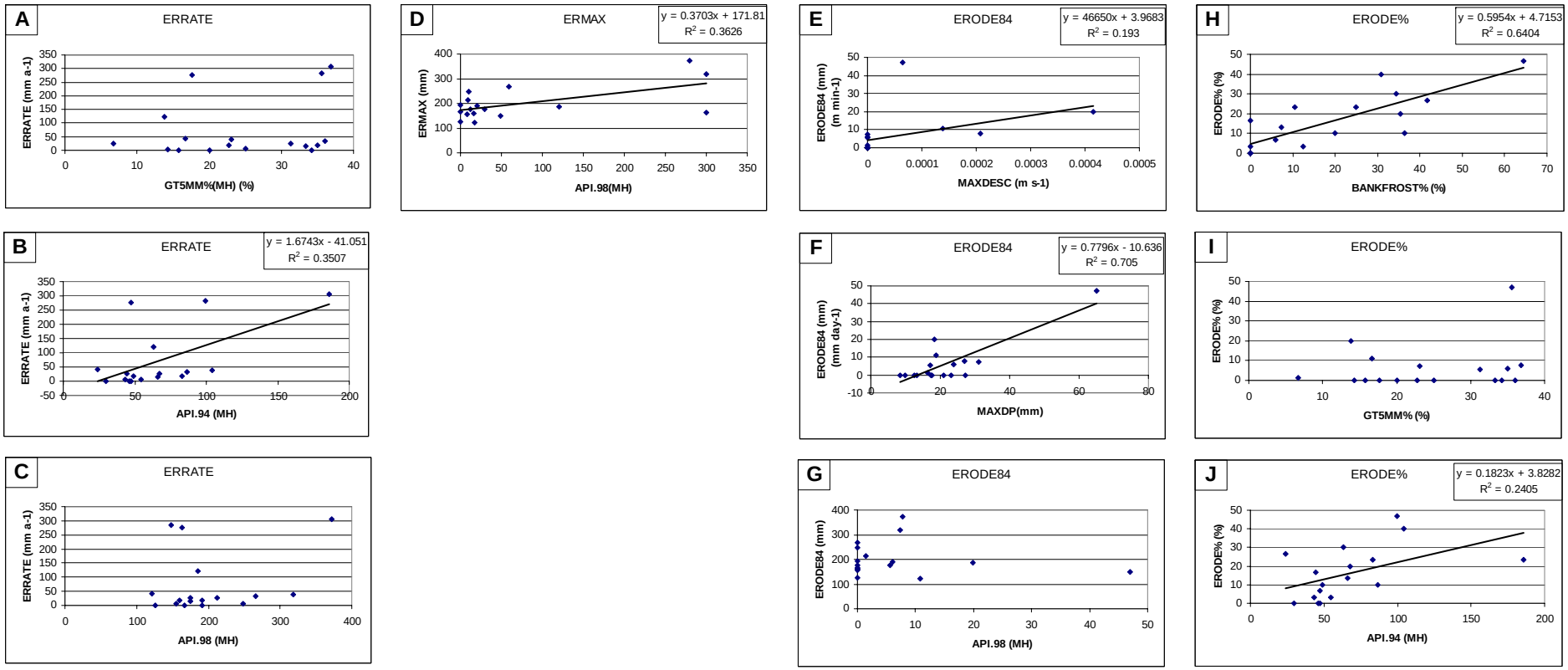

Figure 5.10 Scatterplots of bank erosion against surrogate environmental variables at Beck Meetings (Site 1):
(**A-C**): ERRATE vs. GT5MM%(MH), API.94(MH) and API.98(MH)
(**D**): ERMAX vs. API.98(MH)
(**E-F**): ERODE84 vs. MAXDESC, MAXDP, and API.98(MH)
(**H-J**): ERODE% vs. BANKFROST%, GT5MM%, and API.94(MH)
Relationships above 95 % significance are shown with a least squares regression line.

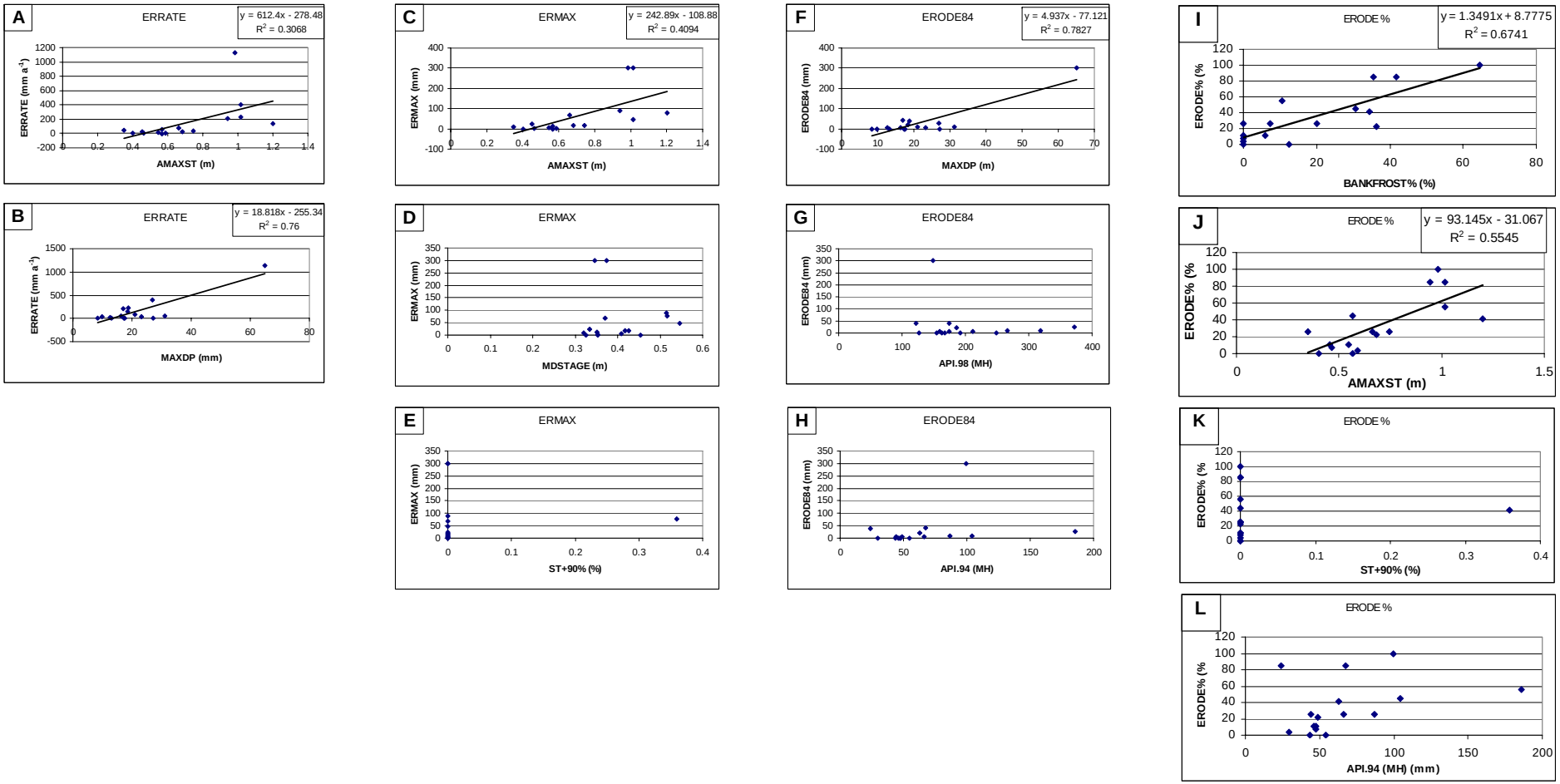

Figure 5.11 Scatterplots of bank erosion against surrogate environmental variables at Hoggarths (Site 2):

(**A-B**): ERRATE vs. AMAXST and MAXDP

(**C-E**): ERMAX vs. AMAXST, MDSTAGE, and ST+90%

(**F-H**): ERODE84 vs. MAXDP, API.98(MH) and API.94(MH)

(**I-L**): ERODE% vs. BANKFROST%, AMAXST, ST+90%, and API.94(MH)

Relationships above 95 % significance are shown with a least squares regression line.

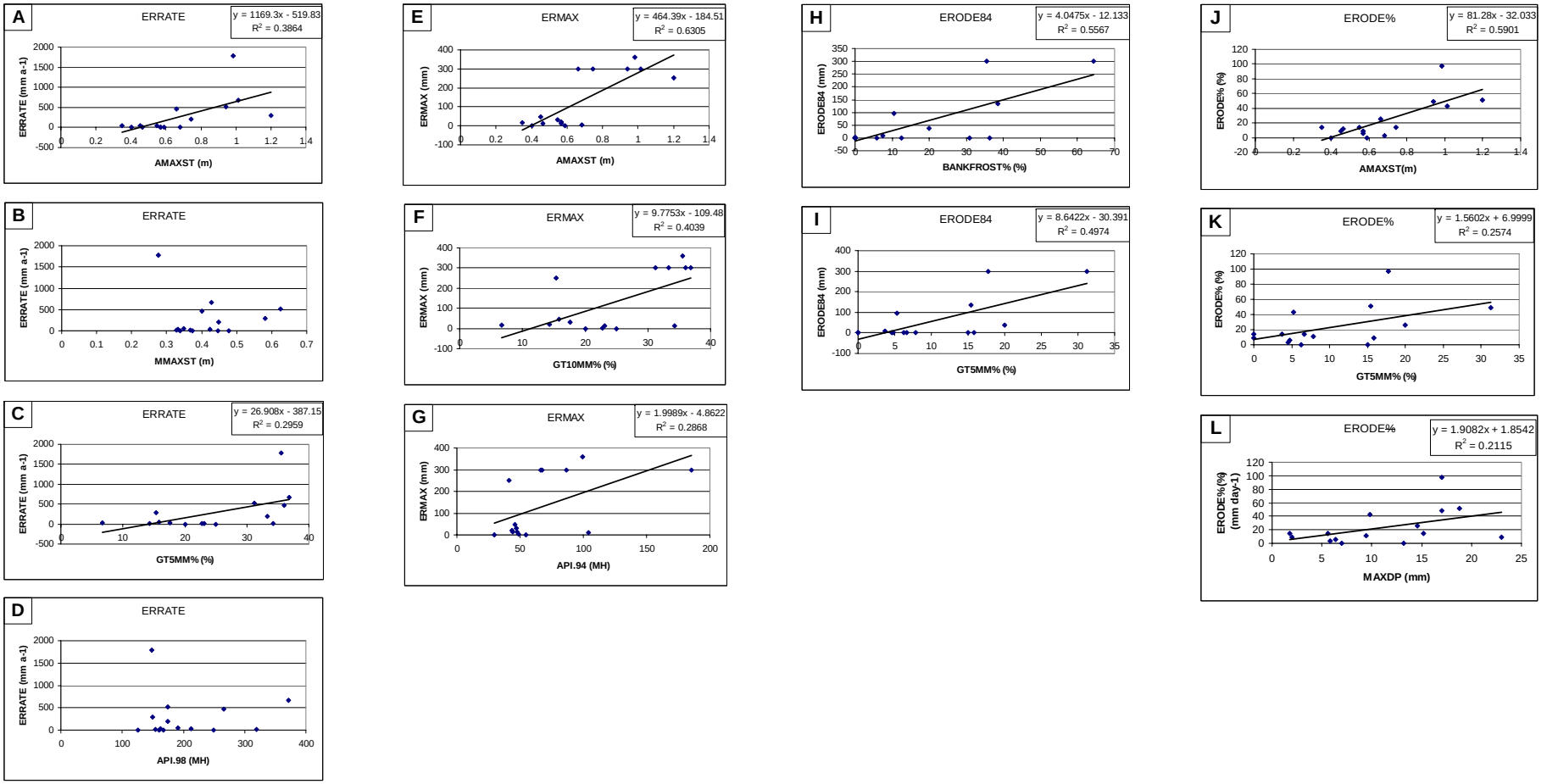

Figure 5.12 Scatterplots of bank erosion against surrogate environmental variables at Muker (Site 3):

(**A-D**): ERRATE vs. AMAXST, MMAXST, GT5MM% and API.98(MH)

(**E-G**): ERMAX vs. AMAXST, GT10MM% and API.94(MH)

(**H-I**): ERODE84 vs. BANKFROST% and GT5MM%

(**J-L**): ERODE% vs. AMAXST, GT5MM% and MAXDP

Relationships above 95 % significance are shown with a least squares regression line.

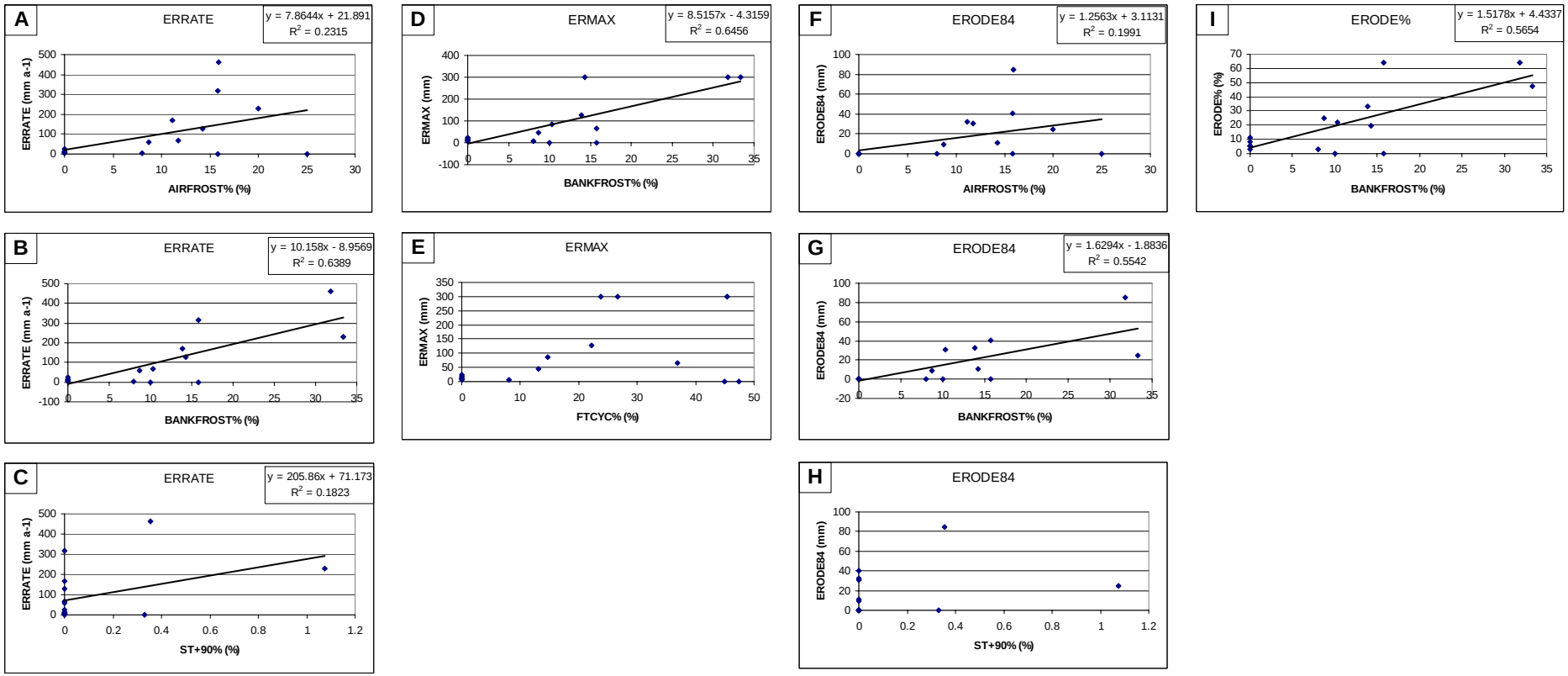

Figure 5.13 Scatterplots of bank erosion against surrogate environmental variables at Low Row (Site 4):

(**A-C**): ERRATE vs. AIRFROST%, BANKFROST% and ST+90%

(**D-E**): ERMAX vs. BANKFROST% and FTCYC%

(**F-H**): ERODE84 vs. AIRFROST%, BANKFROST% and ST+90%

(**I**): ERODE% vs. BANKFROST%

Relationships above 95 % significance are shown with a least squares regression line.

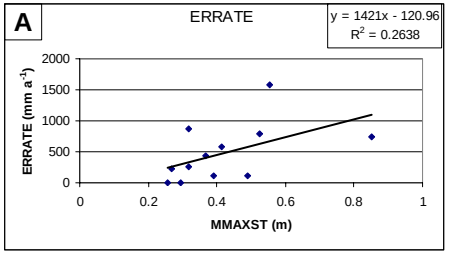

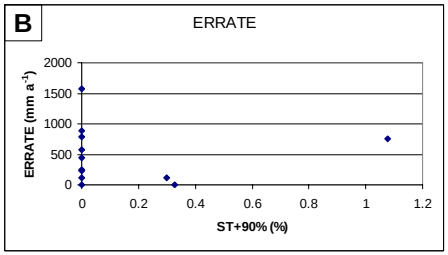

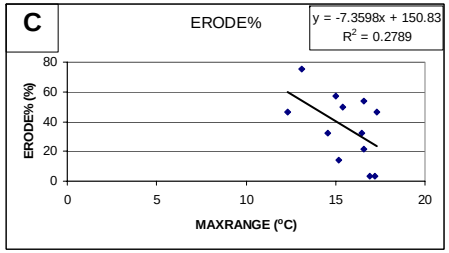

Figure 5.14 Scatterplots of bank erosion against surrogate environmental variables at Reeth (Site 5):
(**A-B**): ERRATE vs. MMAXST and ST+90%
(**C**): MAXRANGE
Relationships above 95 % significance are shown with a least squares regression line.

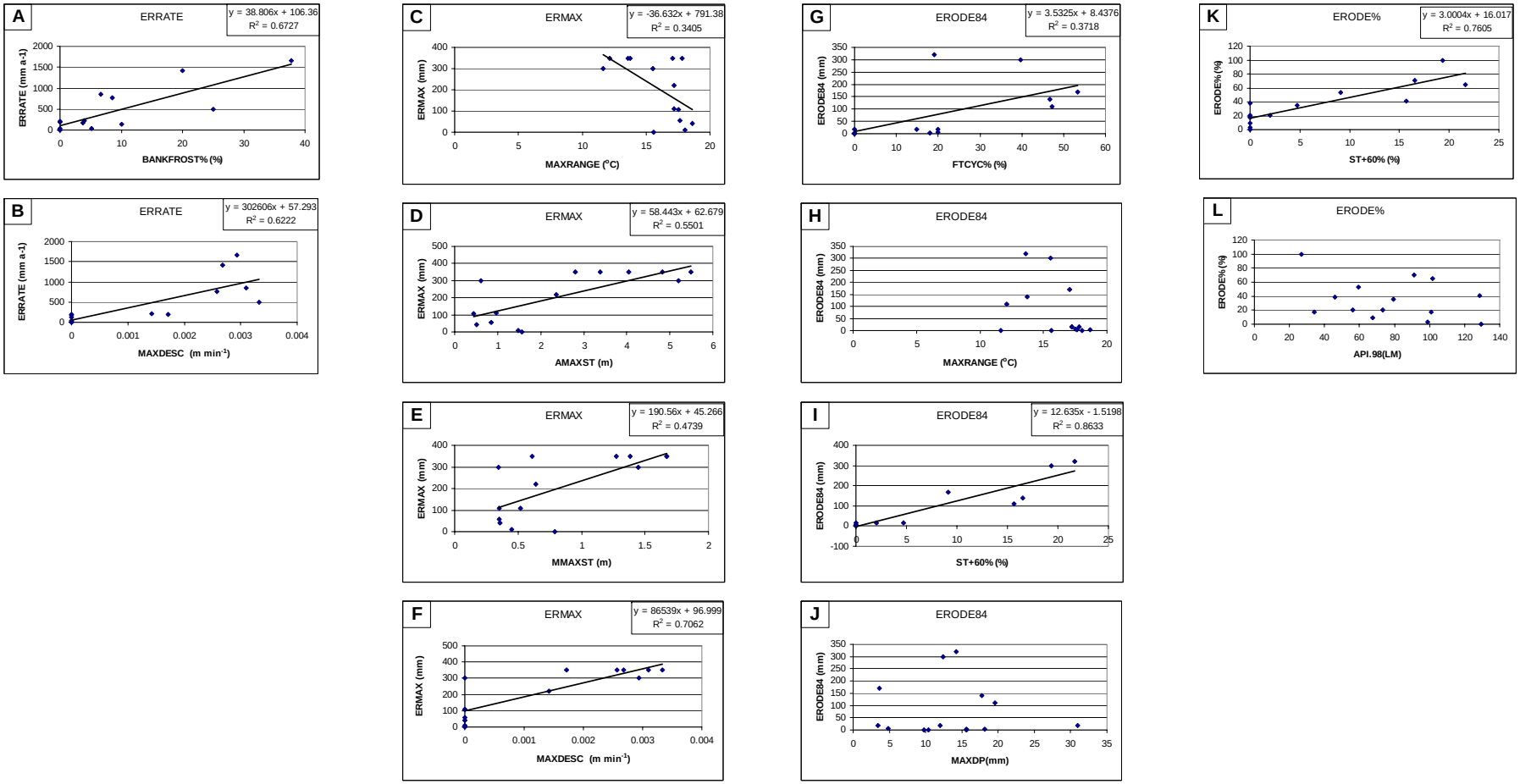

Figure 5.15 Scatterplots of bank erosion against surrogate environmental variables at Morton-on-Swale (Site 7):
(**A-B**): ERRATE vs. BANKFROST% and MAXDESC
(**D**): ERMAX vs. MAXRANGE, AMAXST, MMAXST and MAXDESC
(**E-F**): ERODE84 vs. FTCYC%, MAXRANGE, ST+60% and MAXDP
(**H-J**): ERODE% vs. ST+60% and API.98(LM)
Relationships above 95 % significance are shown with a least squares regression line.

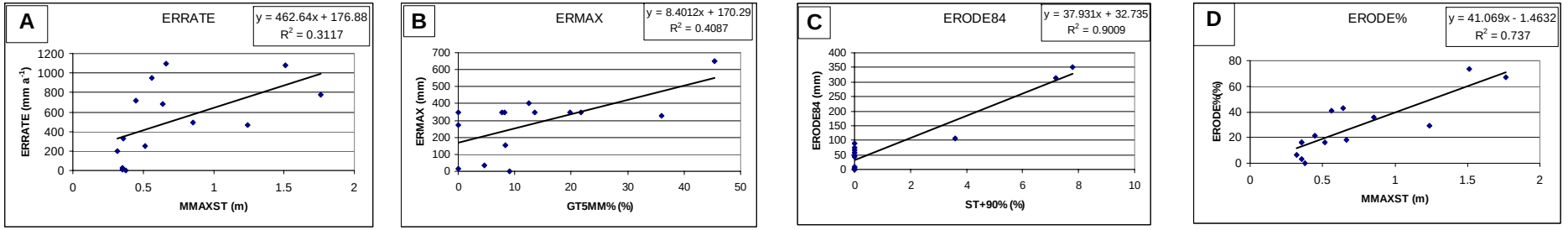

Figure 5.16 Scatterplots of bank erosion against surrogate environmental variables at Greystone Farm (Site 8):

(**A**): ERRATE vs. MMAXST

(**B**): ERMAX vs. GT5MM%

(**C**): ERODE84 vs. ST+90%

(**D**): ERODE% vs. MMAXST

Relationships above 95 % significance are shown with a least squares regression line.

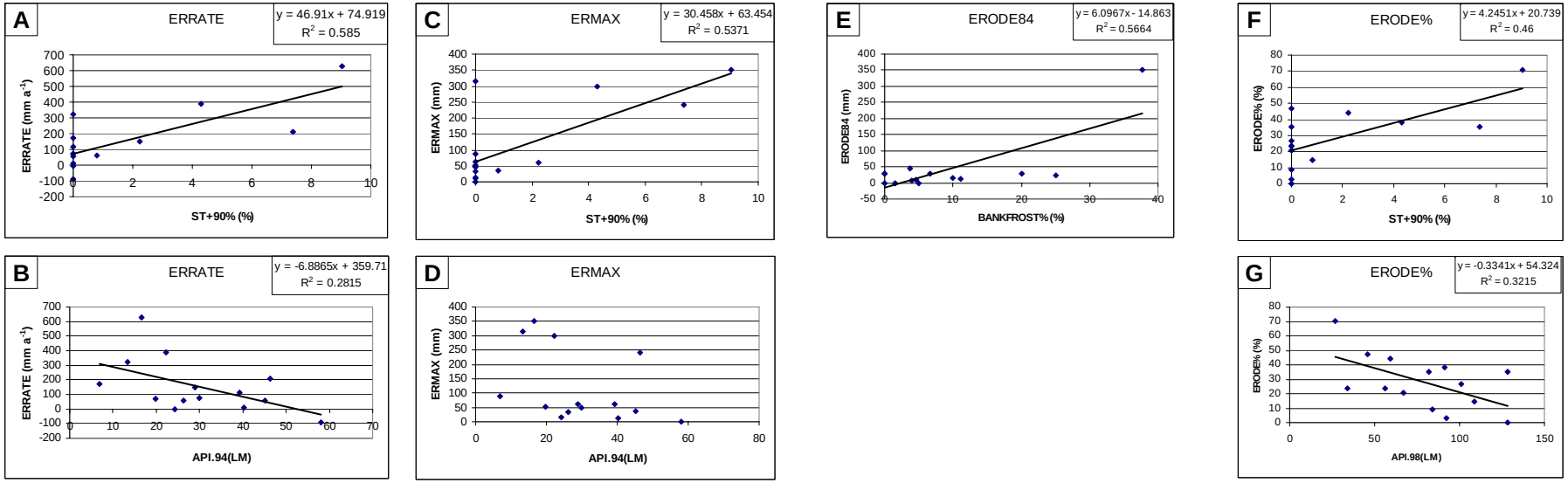

Figure 5.17 Scatterplots of bank erosion against surrogate environmental variables at Topcliffe (Site 9):

(**A-B**): ERRATE vs. ST+90% and API.94(LM)

(**C-D**): ERMAX vs. ST+90% and API.94(LM)

(**E**): ERODE84 vs. BANKFROST%

(**F-G**): ERODE% vs. ST+90% and API.98(LM)

Relationships above 95 % significance are shown with a least squares regression line.

5.4.3 Regression of Average Erosion Rates (ERRATE)

A significant finding is that the independent variables that best explain the average rate of erosion at each site change in strength of explanation and combination downstream (Figure 5.18) (Table 5.5). Broadly; rainfall and the related antecedent precipitation indices, describing soil moisture, dominate upstream. The significance of river flow indices increases downstream, however, in the mid-catchment the temperature indices were the main explanatory variables (Figure 5.18).

Table 5.5 shows that API.94 (MH), API.98 (MH) and GT5MM% (MH) describe the seasonal variability in the erosion rates at Beck Meetings (Site 1). The API values were significantly different from zero ($p < 0.05$), however GT5MM% (MH) and the equation constant for Beck Meetings were not (Table 5.5). The combination of all three variables produced an R^2 value of 60.4%, of which 35.1% was explained by using API.94 (MH) (Table 5.5). The moisture content of the bank material was indicated as being an influential variable in explaining the seasonal erosion patterns, with both positive (API.94) and negative coefficients (API.98) indicating that as the soil moisture increased erosion rates increased and decreased. This may be through cantilever failures under saturated conditions, and increased entrainment under dry conditions. The peaty banks at the site are likely to store absorbed water efficiently, and can thus increase the weight of the bank material considerably from a drier state. No large-scale mass failures of the bank caused by saturation were observed but cantilever failures did occur during the monitoring period. These comparatively large erosion events would increase the mean value of erosion for the epoch considerably when compared to the low background rates of erosion.

The negative coefficients for API.98 (MH) and GT5MM% (MH) possibly indicate erosion during periods of bank drying. This may be due to the desiccation of the bank material during the summer; however, little bank erosion was measured during the summer months. The cantilever failures may have been active after the main wet events in the catchment, as the bank drained. So the failures would not have coincided with the highest values of API.98 (MH) or GT5MM% (MH) but on their declining limbs.

At Hoggarths (Site 2) the two variables MAXDP (MH) and AMAXST were both significantly different from zero ($p < 0.05$) (Table 5.5). MAXDP (MH) explained 76% of the variance in the

data, whilst both variables explained a total of 83.8 % of the sample variance. The combination of these two variables tentatively suggests that bank material was saturated, destabilised, and then removed during the highest flows. No evidence of large-scale mass failures was found during the monitoring period, but cantilever failures were again observed at this site (Plate 5.1).

At Muker (Table 5.5) four independent variables GT5MM% (RM), AMAXST, MMAXST and API.98 (RM) explained the variability in ERRATE. GT5MM% (RM) and AMAXST could be explaining the same type of processes as further upstream. Blocks of material may be removed by fluvial entrainment after having been prepared over a period of time by other subaerial processes such as frost action. The negative coefficients for MMAXST and API.98 (RM) suggest that low stages and bank moisture are significant in causing bank erosion. This may be indicative of drying of the bank surface, exposed by the low flow, during the summer. As with Beck Meetings little erosion was measured during the summer. Again the negative values of MMAXST and API.98 (RM) could be modelling periods of cantilever failure, when the banks were unsupported by lateral river water pressure but the bank material was saturated.

Moving downstream temperature variables became significant in the regression models explaining the average rates of erosion at Low Row (Site 4). Both BANKFROST% and AIRFROST% were selected, as well as ST+90%. The effects of frost action would be expected to be more severe further upstream, with longer periods of sub-zero temperatures. One possible explanation for this dichotomy may be that the low temperatures upstream were below the threshold for effective frost action whereas the temperatures downstream fluctuate more closely around 0 ^{o}C. This would leave the bank 'stressed' for longer periods (Branson *et al.*, 1992), increasing the opportunities for material was being removal from the bank surface. This hypothesis is not borne out by an increase in FTCYC% between upstream and mid-catchment sites (Figure 5.2 A and B). There may however be a longer period of temperatures just beneath the 0 $^{\circ}$C cut off value. An alternative explanation would be that the bank material is more susceptible to frost action. The inclusion of a negative coefficient for ST+90% could be representing the direct removal of frost heaved material during periods of low flows, whilst the negative coefficient for AIRFROST could be describing the entrainment of sediment during periods when material had been subaerially prepared but there was no frost. Occasional quick, rising and subsiding, floods would give smaller ST+90% values. These flood types could be influential in eroding prepared bank material after winter frost action.

Flow variables dominate at Reeth (Site 5), MMAXST and ST+90% together describe 57.9% of the variability in ERRATE values. Large pop out failures occurred all along this site (Plate 5.2) so it was expected that the variable MAXDESC would be influential in describing this process of erosion. MMAXST could be modelling pop out failures more effectively, describing all the flow events that are competent enough to trigger this mode of erosion. The negative coefficient for ST+90% could be representing the competence of flashier floods in producing failures, as described for the Low Row (Site 4).

At Morton-on-Swale (Site 7) 67.3% of the variance in ERRATE was explained by BANKFROST% ($p < 0.05$). It was unexpected that frosts should apparently have such a dominant effect on erosion rates so far down the catchment because of the comparatively low incidence of air and bank frosts. The bank material at this site may be particularly susceptible to frost action (Figures 4.6 - 4.8), the silt-clay content is not the optimum value for frost action of 20-30 % (Branson, 1992), but closer to 44%. The bank material at Low Row (Site 4) is very similar to that at Morton-on-Swale so perhaps both are more susceptible to frost heaving than the rest of the catchment. It may also be that the variability in BANKFROST% is similar to another influential variable not included in the analysis.

The other explanatory independent variable selected was MAXDESC. Both cantilever failures and sapping were evident at the site (Plates 5.4 and 5.5), which could be in part described by MAXDESC.

Greystone Farm (Site 8) was only modelled by a single independent variable, MMAXST, which explained a relatively low 31.2% ($p < 0.05$) of the variability in ERRATE (Table 5.4). The mean maximum stage could influence several processes, such as fluid entrainment, mass failure, piping, and sapping. Mass failures and cantilever failures were evident at the site (Plate 5.5).

The site furthest downstream, Topcliffe (Site 9), was modelled by a combination of ST+90% and API.94 (LM) (Table 5.4). High flows, and falling moisture contents, which are inferred from the selected indices, could be indicating the episodic mass failures of material observed during monitoring.

Site Name	1st Variable Selected	2nd Variable Selected	3rd Variable Selected	4th Variable Selected	Constant
1. Beck Meetings	***API.94 (MH)***	***API.98 (MH)***	***GT5MM% (MH)***		
Coefficient	4.39	-1.37	-5.1		174.0
P-value	0.001	0.018	0.074		0.059
Partial R^2	35.1	48.9	60.4		
2. Hoggarths	***MAXDP (MH)***	***AMAXST***			
Coefficient	16.7	328			-438.8
P-value	<0.001	0.026			<0.001
Partial R^2	76.0	83.8			
3. Muker	***GT5MM% (RM)***	***AMAXST***	***MMAXST***	***API.98 (RM)***	
Coefficient	25.3	1713	-3784	-4.7	708.1
P-value	<0.001	<0.001	<0.001	0.026	0.004
Partial R^2	38.6	71.9	88.1	92.9	
4. Low Row	***BANKFROST%***	***ST+90%***	***AIRFROST%***		
Coefficient	22.6	-306	-10.4		-6.9
P-value	<0.001	0.005	0.007		0.770
Partial R^2	63.9	71.6	84.8		
5. Reeth	***MMAXST***	***ST+90%***			
Coefficient	3203	-1249			-692.2
P-value	0.007	0.029			0.078
Partial R^2	26.4	57.9			
7. Morton-on-Swale	***BANKFROST%***	***MAXDESC***			
Coefficient	24.9	163530			18.68
P-value	0.023	0.056			0.861
Partial R^2	67.3	76.8			
8. Greystone Farm	***MMAXST***				
Coefficient	463				176.9
P-value	0.038				0.310
Partial R^2	31.2				
9. Topcliffe	***ST+90%***	***API.94 (LM)***			
Coefficient	45.8	-6.5			271.81
P-value	<0.001	0.002			<0.001
Partial R^2	58.5	83.9			

Table 5.5 ERRATE Stepwise Regression Equations for all the Monitoring Sites (except Easby), including R^2 and p-values. P-values shaded in grey are not significant at or above 95 % confidence level.

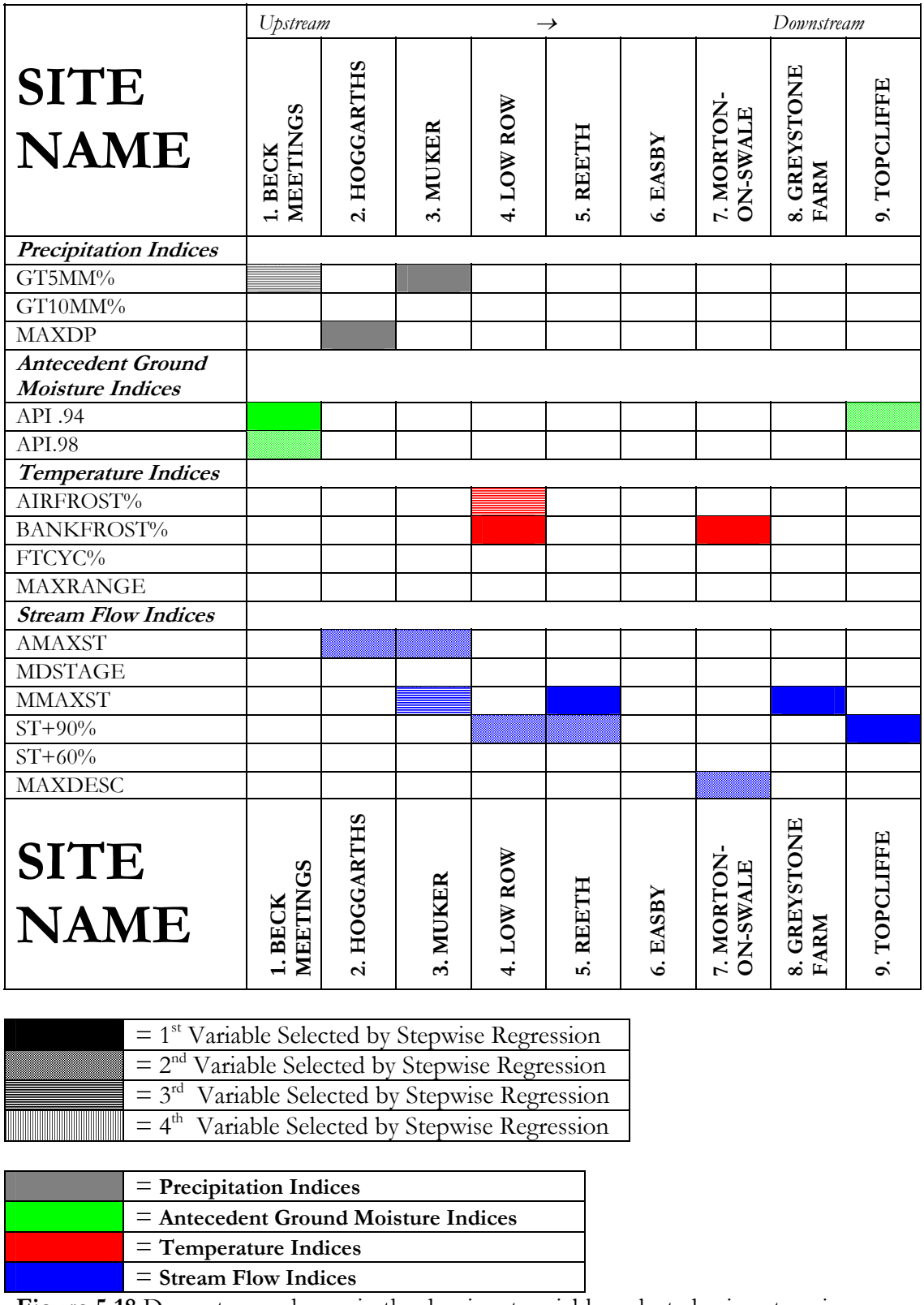

Figure 5.18 Downstream change in the dominant variables selected using stepwise regression to model ERRATE.

5.4.4 Regression of Maximum Erosion Rates (ERMAX)

The maximum erosion at each site (ERMAX) generally follows the same downstream trend as the environmental variables selected for the average rate of erosion (ERRATE) (Figure 5.19). Antecedent moisture conditions dominate upstream, temperature indices mid-catchment, and stream flow explains the most variance both upstream (Sites 2 and 3) and downstream (Sites 7 and 9).

At Beck Meetings (Site 1) 90.3 % ($p < 0.05$) of the variance in ERMAX was explained by the single independent variable API.98 (MH) (Table 5.6). This would seem to confirm the inferences made from the ERRATE modelling that the high values of erosion are occurring during wet periods, and possibly causing destabilisation of the upper bank material by cantilever failures.

The highest erosion values at Hoggarths (Site 2) were modelled using the best subset of AMAXST, MDSTAGE, and ST+90% (Table 5.6). The combination of variables described 89.1 % of the variability in ERMAX, with all the coefficients being significant at $p < 0.05$. High stage events are therefore indicated as being responsible for describing the periodicity in maximum erosion events. This could mean that material was directly entrained, prepared material removed or mass failures triggered. The largest erosion events were usually related to the failure of cantilever blocks, suggesting that these are failing around the time of high stage events. The negative coefficients of MDSTAGE and ST+90% could suggest that periods of low flow allowed more subaerial entrainment, as a larger area of the bankface was exposed.

A combination of stage and ground moisture indices (Table 5.6) explained the maximum erosion values at Muker (Site 3). The high flow events (AMAXST) combined with wet bank conditions (GT10MM% (RM) and API.94 (RM)) were probably responsible for the removal of cantilever blocks in the upper bank region.

BANKFROST% was the most significant independent variable at Low Row (Site 4) (Table 5.6). The two variables BANKFROST% and negative coefficient of FTCYC% explain 74.4 % ($p < 0.05$) of the variance in the ERMAX time series. If the process of frost action best modelled the maximum erosion during an epoch then it may the case that fluvial entrainment and mass failure are less prevalent at the site. The bank material may need to be prepared before it becomes

available for removal, which would explain why reducing the number of frost cycles during the spring flood events would increase the amount of erosion.

No variables were above the regression selection criteria for Reeth (Site 5). This could indicate that the combination of processes active at the monitoring site was too complex to be modelled by the independent variables available. The amount of erosion at the site resulted in entire erosion pins often being removed, causing a ceiling on the maximum erosion values. This 'topping out' of erosion values was also a possible cause for the poor relationship between maximum erosion and the independent variables.

MAXDESC describes 70.6 % ($p < 0.05$) of the variance in the ERMAX time series at Morton-on-Swale (Site 7) (Table 5.6). This independent variable is intended to describe the rapid descent of high flows that could be responsible for mass failures of the bank material. The negative coefficients of the variables also selected AMAXST and MMAXST, would appear to indicate the influence of lower events in causing the maximum amounts of erosion. This could be due to the bank being desiccated during periods of low flow. As MAXRANGE also has a negative coefficient the summer period with maximum temperatures ranges and greatest potential for desiccation does not implicate this process in producing maximum erosion values. The declining MAXRANGE values during the winter-spring period (Figure 5.2C), at the same time as AMAXST and MMAXST decreased (Table 5.3C), indicates that this is the period of maximum erosion values that these variables were describing.

The univariate model at Greystone Farm uses GT5MM% (LM) to describe the maximum erosion during each epoch. The value of R^2 was 40.9 %, describing less of the variance than most of the other monitoring site subsets (Table 5.6). The amount of erosion at Greystone Farm could have had the same effect as at Reeth, where erosion reached a ceiling value constrained by the maximum pin length, resulting in little distinction between maximum erosion values for epochs. The lengths of the erosion epochs were also relatively long due to the periods of inundation at Greystone Farm. The combination of these two factors would tend to mask individual process 'signatures', decreasing the ability of a regression model to identify consistent variations.

Topcliffe has the same independent variables of ST+90% ($p < 0.05$) and API.94 (LM) ($p < 0.05$) as used to model ERRATE. The similarity between timings of maximum erosion and mean

erosion could indicate the dominance of a few events within the monitoring period, with lesser rates of erosion not pulling down the mean values. Large-scale episodic events, such as mass failure, could be modelled using the high stage and falling soil moisture indices.

Site Name	1st Variable Selected	2nd Variable Selected	3rd Variable Selected	4Th Variable Selected	Constant
1. Beck Meetings	***API.98 (RM)***				
Coefficient	0.98				-122.1
P-value	0.011				0.102
Partial R^2	90.3				
2. Hoggarths	***AMAXST***	***MDSTAGE***	***ST+90%***		
Coefficient	525	-1123	-348		151.71
P-value	<0.001	<0.001	0.015		0.020
Partial R^2	40.94	81.77	89.13		
3. Muker	***AMAXST***	***GT10MM%***	***API.94 (RM)***		
Coefficient	262	8.2	3.4		-220.4
P-value	0.011	0.004	0.036		0.001
Partial R^2	63.05	77.66	85.30		
4. Low Row	***BANKFROST%***	***FTCYC%***			
Coefficient	12.5	-3.1			9.936
P-value	<0.001	0.043			0.666
Partial R^2	64.56	74.44			
5. Reeth					
Coefficient					
P-value					
Partial R^2					
7. Morton-on-Swale	***MAXDESC***	***AMAXST***	***MAXRANGE***	***MMAXST***	
Coefficient	227693	-83	-27.3	-167	698.01
P-value	<0.001	0.040	0.005	0.070	0.001
Partial R^2	70.62	78.98	88.24	92	
8. Greystone Farm	***GT5MM%***				
Coefficient	8.4				170.3
P-value	0.014				0.009
Partial R^2	40.87				
9. Topcliffe	***ST+90%***	***API.94 (LM)***			
Coefficient	29.9	-3.4			165.21
P-value	0.001	0.044			0.008
Partial R^2	53.71	68.49			

Table 5.6 ERMAX Stepwise Regression Equations for all the Monitoring Sites (except Easby), including R^2 and p-values. P-values shaded in grey are not significant at or above 95 % confidence level.

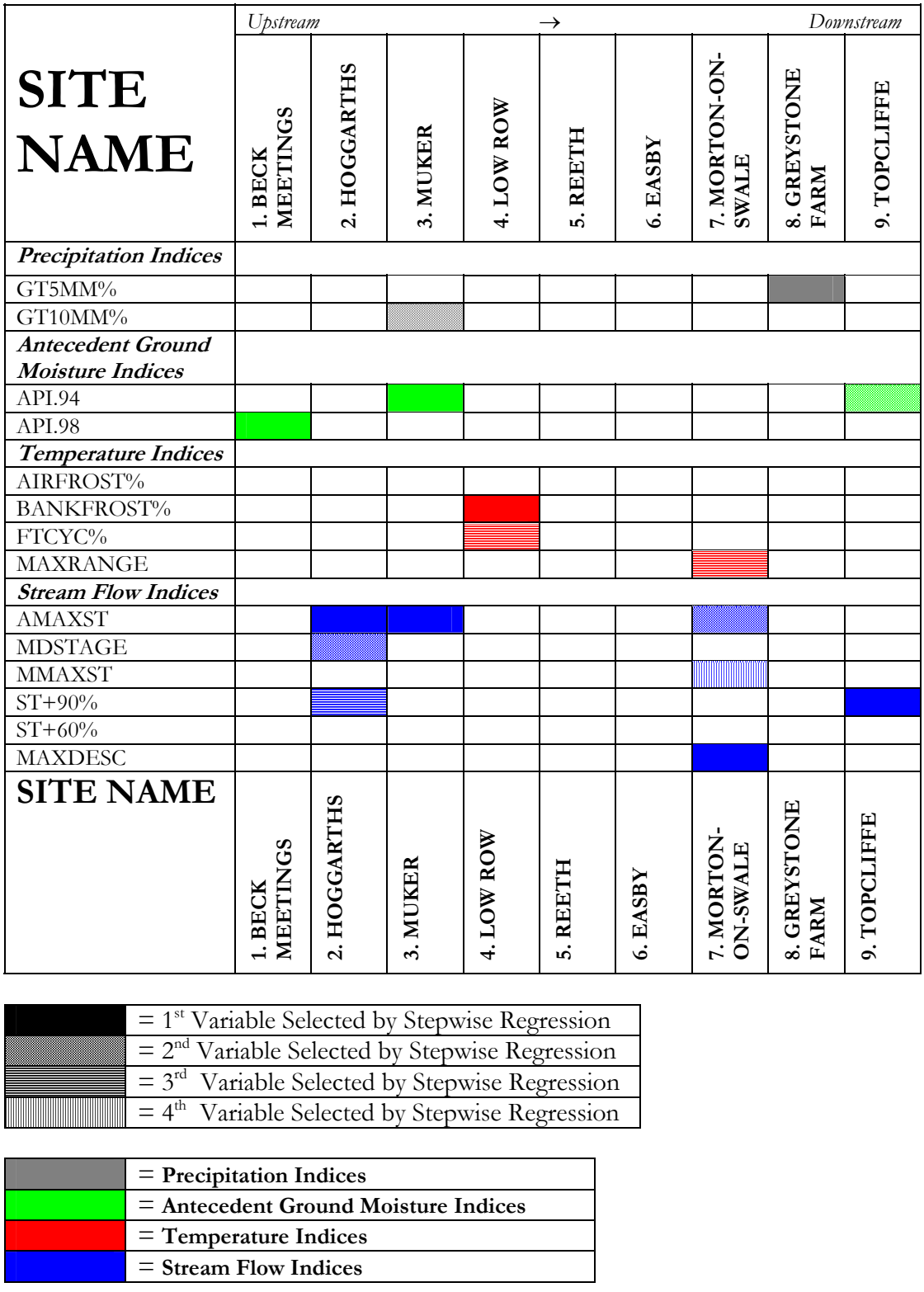

	= 1st Variable Selected by Stepwise Regression
	= 2nd Variable Selected by Stepwise Regression
	= 3rd Variable Selected by Stepwise Regression
	= 4th Variable Selected by Stepwise Regression

	= **Precipitation Indices**
	= **Antecedent Ground Moisture Indices**
	= **Temperature Indices**
	= **Stream Flow Indices**

Figure 5.19 Downstream change in the dominant variables selected using stepwise regression to model ERMAX.

5.4.5 Regression of the 84th Percentile of Erosion Rates (ERODE84)

The 84th percentile of the erosion measured on the erosion pins at each site during an epoch was intended to avoid the problems encountered using ERMAX, whereby whole erosion pins were eroded out on successive epochs. As the index was a measure of the upper rates of erosion it was expected that the results of the stepwise regression would be of a similar nature to the ERMAX results. This was in fact not the case (Figure 5.20). The upstream sites appear to be dominated by rainfall and soil moisture indices to a greater extent than for ERMAX. Temperature indices were most important mid-catchment and largely persisted in significance until Topcliffe (Site 9). The flow variables best explained the variance in the data downstream at Morton-on-Swale (Site 7) and Greystone Farm (Site 8).

Beck Meetings (Site 1) was described by a combination of MAXDP (MH), MAXDESC and API.98 (MH), which explained 92.2 % of the variation in the 84th percentile values of erosion (Table 5.7). The maximum daily precipitation (MAXDP (MH)) and antecedent precipitation (API.98 (MH)) again confirm the influence of ground moisture on upland erosion. The inclusion in this subset of MAXDESC would appear to agree with the assumption that the wetting up of bank material followed by collapse of unstable upper bank material during rapidly receding flow affects the highest rates of erosion. The negative coefficient of API.98 (MH) suggests that erosion occurred after the main periods of soil saturation as the bank was draining.

At Hoggarths MAXDP (MH) was, as with ERRATE, the dominant independent variable (R^2 = 78.3 %, $p < 0.05$) (Table 5.7). The other two descriptive independent variables, API.98 (MH) and API.94 (MH), were indicative of soil moisture conditions influencing the 84th percentile of pin erosion during each epoch. This is unlike the regression model for the maximum erosion during each epoch (ERMAX) which consists entirely of stage/flow related variables. This difference may be explained by the fact that only extreme flow events produce comparably extreme amounts of erosion. The rest of the 'high', 84th percentile, erosion events were more controlled by the moisture levels in the bank material, possibly regulating the degree of preparation of bank material. Both positive and negative coefficients for API variables suggest that the rising, and falling, catchment moisture were important.

At Muker (Site 3) the dominant independent variable was BANKFROST (R^2 = 55.4 %, $p < 0.05$) (Table 5.7). The number of days with rainfall over 5 mm day^{-1} (GT5MM% (RM)) was included in the regression model. This was the main variable used to model ERRATE, and the similar rainfall variable GT10MM% (RM) was included in the equation to describe ERMAX. The preparation of the bank material by frost action could explain the influence of BANKFROST% on the level of erosion. High rates of erosion occurred during wet (both in terms of rainfall and bank moisture) periods, which are also associated with the timing of high stage events.

ERODE84 at Low Row (Site 4) was modelled using BANKFROST%, ST+90% and AIRFROST% (R^2 = 85.5 %, $p < 0.05$) (Table 5.7). This was the same combination of independent variables as used to model ERRATE at the same site. The influence of frost in explaining ERRATE, ERMAX, and ERODE84, and the small variation in explanatory independent indices selected for each of the dependent variables, suggests that extreme erosion events such as block failure were limited. Frost action probably dominated in eroding and preparing bank material for subsequent removal by rapidly peaking floods.

At Reeth (Site 5) no explanatory independent variables could be extracted in the analysis of ERODE84. The use of ERODE84, instead of ERMAX, in limiting the effects of complete removal of erosion pins on several occasions was negated for this example. It may be that none of the independent variables, or combination of variables, was adequate when explaining the processes operating at the site.

At Morton-on-Swale (Site 7) the combination of stage, rainfall, and temperature indices that were used indicated a complex interaction of processes. The independent variables explain 96.7 % of the variance in ERODE84, with ST+60% alone explaining 86.3 % of the variance ($p < 0.05$) (Table 5.7). The dominance of periods of inundation above 60 % of the bank height in producing relatively high erosion values suggests a mechanism of erosion related to bank saturation, or entrainment. The lowering of the number of frost cycles producing more erosion may be due to the entrainment of frost prepared material.

At Greystone Farm (Site 8) periods with stages above 90 % of the bank height explained 90.1% ($p < 0.05$) of the variance in ERODE84 (Table 5.7). Long periods of inundation can lead to bank saturation, and then to mass failure with the retreat of stage. The longer contact time of the

bank with the river water also allows a greater potential for entrainment. Mass failures did occur at Greystone Farm during the monitoring period, and cantilever failures were also frequently observed. The high values of erosion produced by these comparatively large events must be reasonably episodic to correlate so well with ST+90%. This would reinforce the importance of floods in eroding material at the lower end of the catchment.

At Topcliffe ERODE84 was modelled using the single independent variable BANKFROST% (Site 9) (Table 5.7). Unlike ERRATE and ERMAX where ST+90%, API.94 (LM) and API.98 (LM) indicated that bank moisture and mass failures affected the erosion, BANKFROST% suggests that frost action was occurring, or that the colder periods were associated with higher rates of erosion. Frost heaved material was observed at the site (Plate 5.6), and due to the inefficiency of other processes in causing erosion at this site, it may be that this was responsible for the upper values of erosion rates.

Site Name	1st Variable Selected	2nd Variable Selected	3rd Variable Selected	4Th Variable Selected	Constant
1. Beck Meetings	***MAXDP (MH)***	***MAXDESC***	***API.98 (MH)***		
Coefficient	0.789	42425	-0.053		-2.369
P-value	<0.001	<0.001	0.002		0.454
Partial R^2	70.49	83.49	92.19		
2. Hoggarths	***MAXDP (MH)***	***API.98 (MH)***	***API.94 (MH)***		
Coefficient	4.42	-0.67	0.76		16.56
P-value	<0.001	0.002	0.039		0.494
Partial R^2	78.27	88.71	92.18		
3. Muker	***BANKFROST%***	***GT5MM% (RM)***			
Coefficient	3.05	6.1			-57.3
P-value	0.003	0.006			0.032
Partial R^2	55.67	76.95			
4. Low Row	***BANKFROST%***	***ST+90%***	***AIRFROST%***		
Coefficient	4.16	-68	-1.91		-2.549
P-value	<0.001	0.001	0.004		0.524
Partial R^2	55.42	70.27	85.49		
5. Reeth					
Coefficient					
T-value					
Partial R^2					
7. Morton-on-Swale	***ST+60%***	***MAXDP (LM)***	***MAXRANGE***	***FTCYC%***	
Coefficient	17.7	-5.3	10.8	-1.6	-102.96
P-value	<0.001	0.001	0.016	0.017	0.126
Partial R^2	86.33	91.15	93.53	96.67	
8. Greystone Farm	***ST+90%***				
Coefficient	37.9				32.74
P-value	<0.001				0.011
Partial R^2	90.09				
9. Topcliffe	***BANKFROST%***				
Coefficient	6.1				-14.86
P-value	0.002				0.508
Partial R^2	56.64				

Table 5.7 ERODE84 Stepwise Regression Equations for all the Monitoring Sites (except Easby), including R^2 and p-values. P-values shaded in grey are not significant at or above 95 % confidence level.

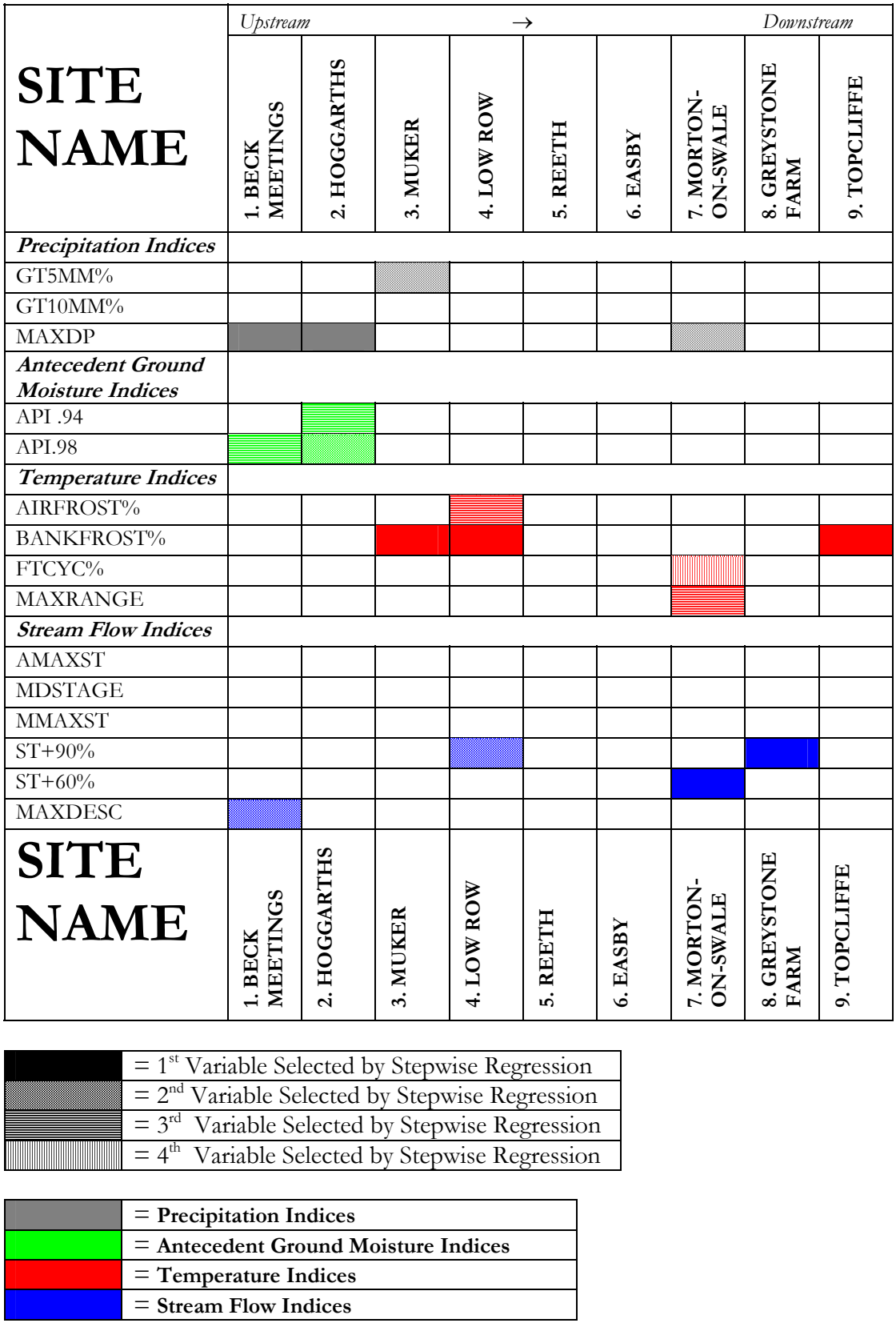

Figure 5.20 Downstream change in the dominant variables selected, using stepwise regression, to model ERODE84.

5.4.6 Regression of the Spatial Extent of Erosion (ERODE%)

The spatial extent of erosion during each epoch can be modelled using ERODE%. High values indicate that a large percentage of the pins over the bank surface experienced some erosion. The general trend (Figure 5.21) was for temperature indices, especially BANKFROST% to dominate upstream. Downstream the stream flow indices were the primary explanatory variables. Rainfall and API were of secondary significance throughout the catchment.

BANKFROST% (R^2 = 64.0 %, $p < 0.05$) dominated at Beck Meetings (Site 1) (Table 5.8), this suggests that although most of the pins were registering erosion, probably due to frost action, this was not the process that caused the maximum amounts of erosion (ERMAX). The antecedent moisture index (API.94 (MH)) and the negative coefficient number of days with rainfall over 5 mm day^{-1} (GT5MM% (MH)) were also included in the regression equation. These variables could be explaining periods without bankfrost conditions, where to facilitate a high spatial extent of erosion the bank needed to be saturated, after periods of higher rainfall.

BANKFROST% again dominated at Hoggarths (Site 2) (R^2 = 67.4 %, $p < 0.05$), producing a large spatial coverage of erosion. Frost may have been effective during periods of lower flows represented by the negative coefficient of ST+90%. The other independent variables of API.94 (RM) and AMAXST were responsible for describing flood events and wet bank conditions (Table 5.8). It may be that the periods devoid of bank frost were most affected by erosion taking place during high flow conditions, or that the combination of frosts and flow describes the removal of prepared material.

At Muker (Site 3) the maximum stage in each epoch (AMAXST) suggests that periods of high flow were responsible for the greatest number pins eroding during each epoch (Table 5.8). Together with MAXDP and GT5MM% 86.6 % of the variance in ERODE% was accounted for. The combination of all three variables was not significant with $p > 0.05$, however, if only AMAXST and MAXDP are used there is only a small decrease in the variance explained (R^2 = 81.0%) with $p < 0.05$. No direct rainsplash erosion was noted at Muker and so the rainfall variables are though not to be modelling this process. It may be that the high rainfall values were associated with the high flows, although stream flow indices were not strongly correlated.

The single independent variable of BANKFROST (R^2 = 56.6 %, $p < 0.05$) was selected to describe ERODE% at Low Row (Site 4) (Table 5.8). This again confirms the influence of frost processes in the mid-catchment region.

A single independent variable was selected for Reeth (Site 5) (Table 5.8). The MAXRANGE index describes the maximum diurnal temperature range within an epoch. The coefficient of –7.4 ($p = 0.078$) for MAXRANGE means that, combined with an intercept of 150.8 ($p = 0.028$), the lower the maximum diurnal temperature range the higher the percentage of pins eroding. The expected relationship would be that the increasing maximum range would lead to greater desiccation of the bank surface due to greater stresses on the bank surface. At Reeth the low values of MAXRANGE occurred during the winter months. The negative relationship could therefore be interpreted as signalling periods of either cold temperature with associated frost action, or periods of high flows and associated entrainment or mass failure. The low R^2 value of 27.9 % ($p > 0.05$) means that little of the variance within the data was explained by this variable.

At Morton-on-Swale stages over 60 % of the bank height (ST+60%) combined with the negative coefficient of high antecedent precipitation values (API.98 (LM)) were responsible for describing 91.5 % ($p < 0.05$) of the variance in ERODE% (Table 5.8). Prolonged periods of inundation and falling moisture contents in the bank are indicative of mass failure processes being important in causing the highest spatial extent of erosion at Morton-on-Swale (Site 7).

The mean maximum stage in an epoch (MMAXST) explains 73.7 % ($p < 0.05$) of the variance in ERODE% at Greystone Farm (Site 8) (Table 5.8). The high stages could indicate either mass failure processes, or entrainment, produced the highest spatial coverage of erosion at the monitoring site.

At Topcliffe (Site 9) the period of inundation above 90 % of the bank height (ST+90%), and the negative coefficient of the antecedent precipitation index (API.98 (LM)) were selected to describe the percentage of pins that experienced erosion during each epoch. The period of inundation being selected rather than just the peak flow (AMAXST) suggests that the wetting up of the bank was significant in producing the widest coverage of erosion at Topcliffe. The episodic nature of ST+90%, with several zero values, could indicate a sporadic process limited to the winter months

with high flows. The negative coefficient of API.98 (LM) may be representing the removal of summer desiccated material during the late summer.

Whilst the epoch time interval measurements allow processes of erosion to be inferred increasing the temporal resolution of the bank erosion monitoring could allow a more accurate picture of the processes operating. Comparing erosion rates with environmental variables recorded at a flood event interval would allow the contribution of sub-aerial preparation, fluvial entrainment, and mass failures to be defined. The following chapter will seek to identify individual processes; confirming or disproving the process inferences made from the erosion pin data.

Site Name	1st Variable Selected	2nd Variable Selected	3rd Variable Selected	4Th Variable Selected	Constant
1. Beck Meetings	***BANKFROST%***	***API.94 (MH)***	***GT5MM% (MH)***		
Coefficient	0.58	0.197	-0.49		3.84
P-value	<0.001	0.003	0.044		0.420
Partial R^2	64.0	75.1	82.0		
2. Hoggarths	***BANKFROST%***	***API.94 (RM)***	***ST+90%***	***AMAXST***	
Coefficient	1.02	0.72	-168	45	-32.51
P-value	0.001	0.030	0.003	0.079	0.015
Partial R^2	67.4	74.6	85.6	89.2	
3. Muker	***AMAXST***	***MAXDP***	***GT5MM%***		
Coefficient	49	1.01	0.80		-40.65
P-value	0.004	0.001	0.056		0.001
Partial R^2	59.0	81.0	86.6		
4. Low Row	***BANKFROST%***				
Coefficient	1.52				4.434
P-value	0.001				0.404
Partial R^2	56.5				
5. Reeth	***MAXRANGE***				
Coefficient	-7.4				150.8
P-value	0.078				0.028
Partial R^2	27.9				
7. Morton-on-Swale	***ST+60%***	***API.98 (LM)***			
Coefficient	3.13	-0.352			42.65
P-value	<0.001	0.001			0.000
Partial R^2	76.1	91.5			
8. Greystone Farm	***MMAXST***				
Coefficient	41.1				-1.463
P-value	<0.001				0.810
Partial R^2	73.7				
9. Topcliffe	***ST+90%***	***API.98 (LM)***			
Coefficient	4.05	-0.312			45.7
P-value	0.001	0.006			0.000
Partial R^2	46.0	73.9			

Table 5.8 ERODE% Stepwise Regression Equations for all the Monitoring Sites (except Easby), including R^2 and p-values. P-values shaded in grey are not significant at or above 95 % confidence level.

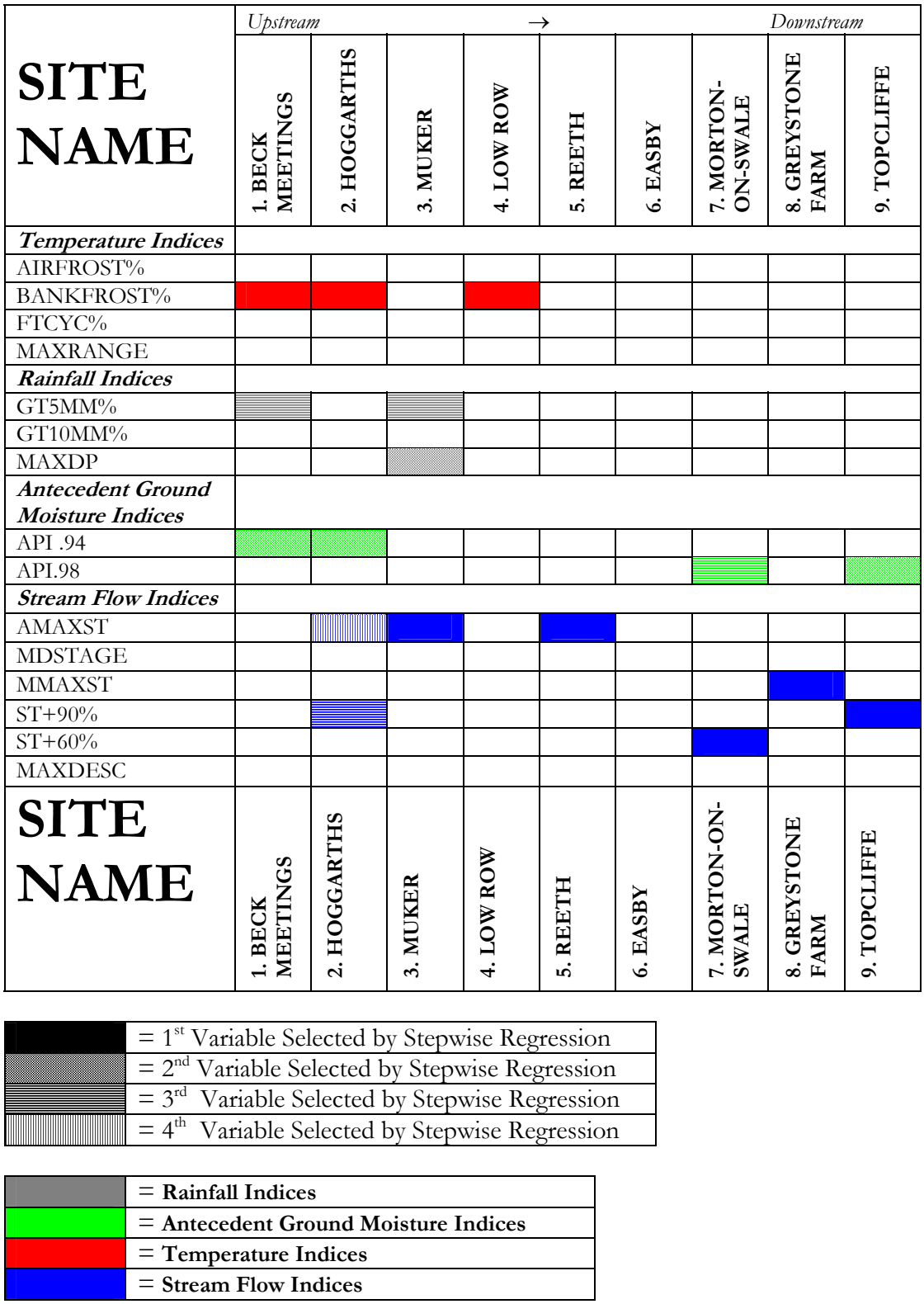

	= 1st Variable Selected by Stepwise Regression
	= 2nd Variable Selected by Stepwise Regression
	= 3rd Variable Selected by Stepwise Regression
	= 4th Variable Selected by Stepwise Regression

	= **Rainfall Indices**
	= **Antecedent Ground Moisture Indices**
	= **Temperature Indices**
	= **Stream Flow Indices**

Figure 5.21 Downstream change in the dominant variables selected, using stepwise regression, to model ERODE%.

5.4 SUMMARY

1. Seasonality in the rates of erosion was evident at all nine of the monitoring sites on the River Swale. Peak rates of erosion occurred during the winter months of January, February (Table 5.1).

2. A downstream trend in the annual seasonality was observed throughout the catchment. The length of the active erosion period appears to increase in a downstream direction (Lawler *et al.*, 1999). This may indicate an increasing number of processes being active at the downstream sites, or an increase in process efficacy further down the catchment.

3. Independent variables based on temperature, stream flow, rainfall and soil ground moisture (API) were plotted as time series in order to identify seasonality in the data. Frost frequency decreased downstream alongside rainfall and catchment wetness, whilst the range of stream flow indices increased down the catchment. The number of high flows during the summer months also increased downstream, creating a more episodic seasonal time series.

4. Dependent variables based on rates, or spatial coverage, of erosion were compared against surrogate environmental indices. Bivariate analysis revealed that upstream indices of API, temperature, and rainfall were the most significant. In the middle and lower reaches of the Swale temperature and stream flow indices best explained erosion rates and spatial extent of erosion.

5. Stepwise regression was used to indicate the best multivariate model able to describe the seasonal variation in bank erosion variables. The best subset may be indicative of specific processes, or a suite of processes that were active at the site during monitoring. Using field observations to aid interpretation of the results the following conclusions may be drawn:

    A. Upstream, frost action and cantilever failures were dominant, best explained by high API and rainfall.

    B. Mid catchment, frost action and fluvial processes were most significant.

    C. Downstream, API and stream flow indices model intermittent bank failures.

Plate 5.1 A beam cantilever failure at Hoggarths (Site 2) (18/02/96). An A4 black notebook is shown mid-frame for scale. Flow is into the page.

Plate 5.2 A pop-out failure at Reeth (Site 5) with a failed block remaining *'in situ'*, rather than being entrained (23/10/96). The bank height is approximately 2 m. Flow is from left to right of the frame.

Plate 5.3 Cantilever failures at Morton-on-Swale (Site 7), possibly preceded by a pop-out failure. The white 1 m long ruler is shown for scale. Flow is out of the page.

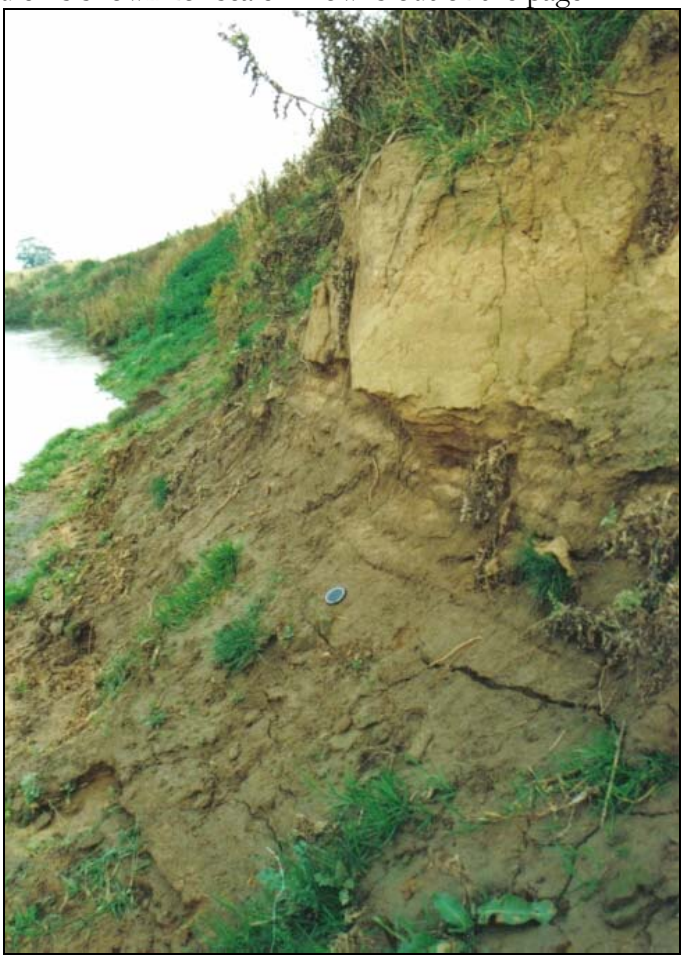

Plate 5.4 Sapping at Morton-on-Swale (Site 7) (22/10/96), shown by the distinct notch mid-frame. Some tension cracking is evident on the upper bank. The lens cap shown for scale is 50 mm in diameter. Flow is out of the page.

Plate 5.5 Cantilever failures at Greystone Farm (Site 8) (03/07/97), a shear failure block in the mid-frame and a beam failure in the foreground. Flow is out of the page.

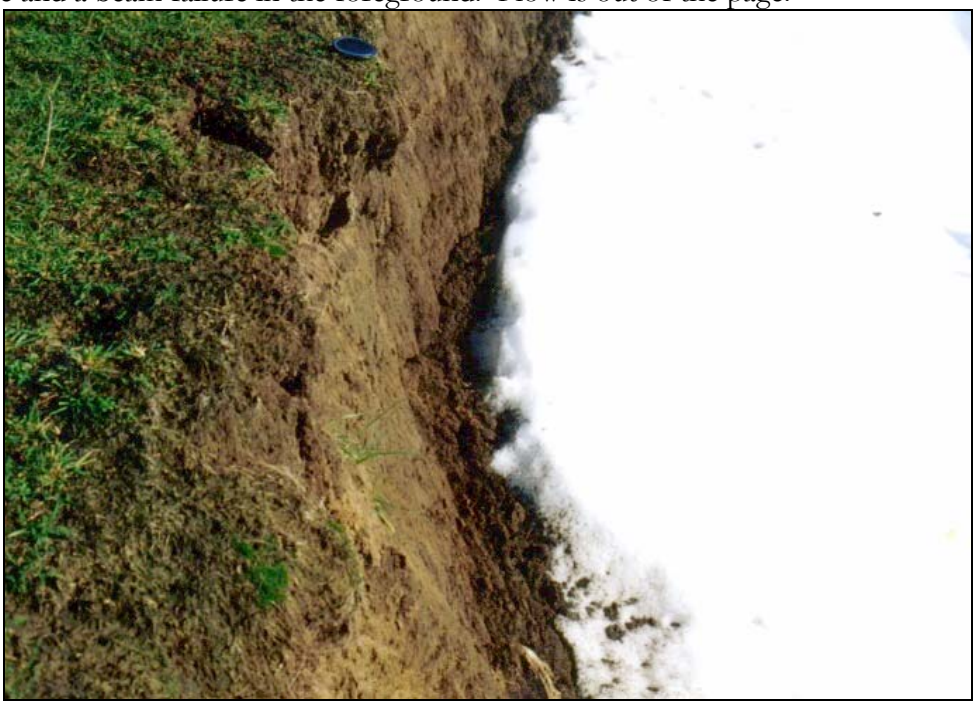

Plate 5.6 Frost heaved debris between the base of the bank and a snow-patch at Topcliffe (Site 9) (04/02/96). The photograph is taken from the banktop looking down towards the base of a vertical section of the bankface. A lens cap 50 cm in diameter is shown for scale.

CHAPTER 6

THE DISTRIBUTION OF EROSION PROCESSES IN SPACE AND TIME

6.1 INTRODUCTION

Chapters 4 and 5 dealt with the variations in the environmental composition of each of the monitoring sites in terms of variables such as bank material, channel morphology, and flood discharges. The erosion that took place between each of the fortnightly site visits was also investigated. The temporal variability of the data has not allowed an accurate determination of the erosion processes that were active at each of the sites. Using the Photo-Electronic Erosion Pin (PEEP) sensors (Section 3.3.4) the temporal variability in the bank surface elevation may be compared more accurately with other environmental indicators, such as temperature, stage, and precipitation. The 15-minute monitoring interval allowed the environmental conditions before, during and after each event to be observed with much greater confidence than with the fortnightly erosion pin data. This should permit a more accurate assessment of the erosion and deposition processes that were active at each of the PEEP monitored sites.

Seasonal variations of daily PEEP measurements provide a simplified time-series that can be used to estimate the dominant environmental variables responsible for erosion during monitoring. This can then be compared against the actual erosion measurements at a 15-minute interval, and the observations made manually in the field, to give an indication of the identifiable process(es) that were active.

6.2 COMPARISONS BETWEEN PEEP AND EROSION PIN MEASUREMENTS

Eleven PEEP sensors were placed at 3 sites in the upper, middle and lower catchment (Table 3.7). Whilst the PEEPs were automatically recording the bank surface elevations they could also be measured as conventional erosion pins. The length of the PEEP exposed was measured in the same way as the erosion pins (Section 3.4.3) at each downloading session. The rate of erosion manually measured on each PEEP, during an epoch, was compared against the mean rate

of pin erosion measured at each site during the same epoch (Table 6.1). This allowed a comparison between the average conditions at each site and the intensively monitored sections.

Only one out of the eleven PEEPs was significantly related to the average pin erosion above a 95% confidence level, PEEP 7 (Table 6.1). There could be two alternative explanations why the PEEPs were not representative of the average Erosion Pin measurements.

1. The PEEPs only registered processes that occurred intermittently at different areas of the bank surface due to the high spatial variability of erosion (Table 4.1) similar to that found by Hooke (1980) Lawler (1989), Lawler *et al.* (1997), and Laubel *et al.* (1999). Thus the recorded erosion may be representative of only a small area of the bank surface around the sensors. Care must therefore be taken in extrapolating the point-value results to the whole site as other parts of the bank may be at different stages of erosion process evolution, or subject to different shear stresses due to the flow structures in the channel. An example of this may be cantilever collapse, which may occur on a 50 cm length of the upper bank and may register on one sensor during an epoch. The rest of the bank may stay stable but be in the processes of undercutting to produce a failure.

2. The PEEPs were recording in different environmental conditions compared to those recorded by the erosion pins. This may be due to the vertical auger holes aiding the creation of a failure plane within the bank. This may not occur during the initial stages of insertion, but after the bank has retreated over time, the hole will become closer to the bank face, and influence the structure of slab or cantilever failures. The horizontal auger holes may aid failure planes development at the base of cantilever and slab failures. The larger diameter of the protruding PEEP sensor may create more resistance to flow than the erosion pins. This could result in higher velocities around the sensor, increasing entrainment, and lower flow velocities in the lee of the sensor.

SITE NAME	PEEP NUMBER	NUMBER OF MEASUREMENTS (n)	CORRELATION COEFFICIENT OF EACH PEEP AND THE SITE AVERAGE PIN EROSION (r)	CRITICAL 95 % CORRELATION COEFFICIENT (r)
1. Beck Meetings	**1** (Upper)	18	0.290	0.468
	2 (Middle)	18	0.145	0.468
	3 (Lower)	15	0.267	0.514
4. Low Row	**5** (Downstream Lower)	11	0.406	0.602
	7 (Upstream Lower)	14	0.605	0.532
	11 (Downstream Upper)	16	0.202	0.497
	6 (Upstream Upper)	9	0.659	0.666
8. Greystone Farm	**4** (Downstream Lower)	11	0.356	0.602
	9 (Upstream Lower)	9	0.177	0.666
	8 (Downstream Upper)	8	0.294	0.707
	10 (Upstream Upper)	10	0.203	0.632

Table 6.1 Correlation coefficients of PEEP manually measured erosion compared against mean erosion pin erosion at 3 monitoring sites: (**1**) Beck Meetings (Upper Catchment); (**2**) Low Row (Mid Catchment) and (**3**) Greystone Farm (Lower Catchment).

To investigate this further; the PEEPs were correlated with the single nearest erosion pin measurements during each epoch (Table 6.2). Only three of the PEEPs, numbers 1,2, and 7 were correlated, above a 95 % confidence limit, with measurements at the nearest erosion pin in a horizontal direction to the sensor. The lack of consistency between measurements could be caused by the small-scale heterogeneity of the bank material and erosion processes, or the differing way in which the pins and PEEPs affect their surrounding material. PEEPs present a larger surface area to flow events potentially causing elevated levels of scouring, whilst pins more efficiently conduct heat, cooling or heating the surrounding bank material.

The average of the three columns of erosion pins nearest to the PEEPs was also correlated with the amount of erosion recorded around each PEEP sensor (Table 6.3). This allowed the relationship between the PEEPs and the surrounding bank region, rather than the whole bank surface or another single point erosion value, to be assessed. Only three of the PEEPs, numbers 5,7, and 10 correlated above a 95 % confidence interval with the average erosion over the surrounding bank surface.

This indicates that the individual PEEPs were generally not representative of the average rates of bank erosion, measured by the erosion pins. This may be due to the heterogeneous nature of bank erosion at each site. Erosional and depositional processes may only be operating on a small

scale spatially on the bank surface rather than uniformly, with PEEPs only registering processes intermittently. Alternatively the PEEPs may not have been representative because they were not affected by the processes active on other sections of the bank surface. To determine if this was the case the processes of erosion registered on the PEEPs will be compared with field observations and spatial patterns of pin erosion at each monitoring site.

SITE NAME	PEEP NUMBER	NUMBER OF MEASUREMENTS (n)	CORRELATION COEFFICIENT OF EACH PEEP AND ITS NEAREST EROSION PIN (r)	CRITICAL 95 % CORRELATION COEFFICIENT (r)
1. Beck Meetings	**1** (Upper)	18	0.536	0.468
	2 (Middle)	18	0.629	0.468
	3 (Lower)	15	-0.115	0.514
4. Low Row	**5** (Downstream Lower)	11	-0.357	0.602
	7 (Upstream Lower)	14	0.742	0.532
	11 (Downstream Upper)	16	0.345	0.497
	6 (Upstream Upper)	9	0.555	0.666
8. Greystone Farm	**4** (Downstream Lower)	10	0.023	0.602
	9 (Upstream Lower)	9	-0.365	0.666
	8 (Downstream Upper)	8	0.544	0.707
	10 (Upstream Upper)	10	-0.060	0.632

Table 6.2 Correlation Coefficients of PEEP manually measured erosion compared against the nearest single erosion pin monitoring sites: **(1)** Beck Meetings (Upper Catchment); **(2)** Low Row (Mid Catchment) and **(3)** Greystone Farm (Lower Catchment).

SITE NAME	PEEP NUMBER	NUMBER OF MEASUREMENTS (n)	CORRELATION COEFFICIENT OF EACH PEEP AND AVERAGE EROSION FROM THE 3 NEAREST EROSION PIN COLUMNS (r)	CRITICAL 95 % CORRELATION COEFFICIENT (r)
1. Beck Meetings	**1** (Upper)	18	0.143	0.468
	2 (Middle)	18	-0.183	0.468
	3 (Lower)	15	0.509	0.514
4. Low Row	**5** (Downstream Lower)	11	0.602	0.602
	7 (Upstream Lower)	14	0.621	0.532
	11 (Downstream Upper)	16	0.0003	0.497
	6 (Upstream Upper)	9	0.009	0.666
8. Greystone Farm	**4** (Downstream Lower)	10	0.341	0.602
	9 (Upstream Lower)	10	-0.308	0.666
	8 (Downstream Upper)	11	0.547	0.707
	10 (Upstream Upper)	11	-0.749	0.632

Table 6.3 Correlation Coefficients of the PEEP sensor epoch erosion values and the in an epoch compared against the single erosion pins next to PEEP sensors: (**1**) Beck Meetings (Upper Catchment); (**2**) Low Row (Mid Catchment) and (**3**) Greystone Farm (Lower Catchment).

6.3 RATES OF EROSION

6.3.1 PEEP Data Reduction Methodology

Initial screening of the PEEP data to determine when processes were active, and the annual distribution of rates of erosion, may be undertaken on a daily timescale. Although many of the environmental variables had been monitored at a 15-minute interval, rainfall close to the sites and the associated Antecedent Precipitation Index were only available at a daily resolution. Thus to be able to compare all the environmental variables with the rates of erosion initially a daily interval was desirable.

Ideally the ratio of the reference cell to the cell series should be almost constant for the entire period of daylight during monitoring, in the absence of erosion or deposition (Figure 6.1). This situation was most likely to occur during overcast weather conditions where light levels remained almost constant during the entire length of the day. In clear conditions the light levels may vary between reference cell and cell series during the dawn and dusk period, creating photovoltaic ratios (Lawler, 1989) that may not be representative of the length of PEEP exposed. The data that were recorded in the dawn and dusk periods was therefore often unreliable.

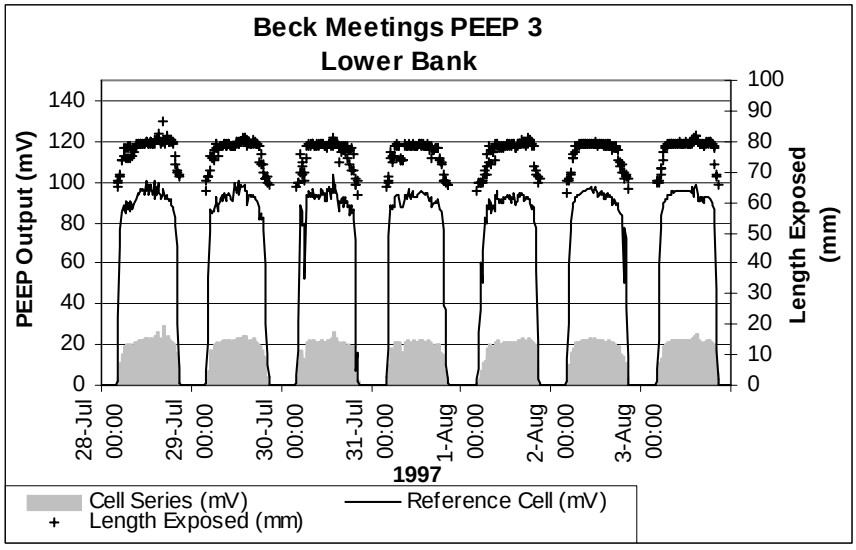

Figure 6.1 An example of a relatively consistent output of Cell Series (mV), Reference Cell (mV) and Length of Exposure (mm) from PEEP 3 situated in the Lower Bank at Beck Meetings. The start of each day is indicated by the date and time on the x-axis.

During direct sunlight conditions the orientation of the PEEP may allow sunlight to shine directly through the sensor, over all the photovoltaic cells. The 'light-piping' effect (Lawler, 1992b) allows sunlight to strongly illuminate the cell series. Usually the sun is low against the horizon to maximise this effect; so winter periods and dusk/dawn are particularly affected. This phenomenon may result in a sudden elevation in the output from the cell series (Figure 6.2). The same increase in solar radiation is not registered at the already exposed reference cell. The ratio of cell series to reference cell, the photovoltaic ratio, is therefore similar to that experienced during an erosion event. If the same signal is recorded the following day, a reduced 'normal' output followed by a rapid set of peak values, then this 'shouldering' effect may be suspected. A reduction back to normal values the following day may also lead to the same conclusion.

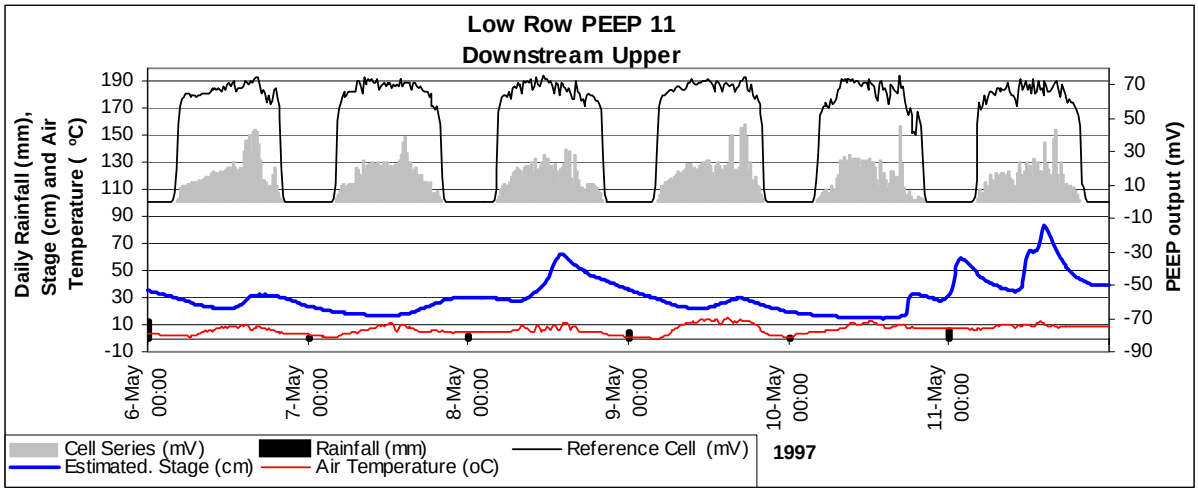

Figure 6.2 An example of a disproportional increase in cell series, compared to the reference cell, during the afternoon at PEEP 11 (Low Row). The sensor is facing in a N direction and may be coming out of the shade in the afternoon, allowing direct sunlight to radiate into the sensor.

The photovoltaic ratio may also be distorted during flood conditions. When the PEEP is immersed the signal may be lost altogether or significantly reduced (Lawler, 1992a). During the reduction of the PEEP output the voltage from the reference cell may be nearly as low as the combined cell series. If only the photovoltaic ratio and associated calibration equations are used to predict the amount of erosion then a false picture may be gained. A decrease in both cell series and reference cell output alongside an increase in stage indicates a period of inundation.

To overcome the problems of irregularities in the daily signals several different time periods were used to create a daily time series. The selected method was to use the photovoltaic ratio from each PEEP at midday. The advantages of this method were:

1. Simplicity, reducing the amount of data processing needed;
2. Dusk and dawn values were avoided;
3. Shouldering at low solar azimuths were avoided.

Although this method only effectively uses one measurement a day it compares well with an averaged value of measurements around the midday period, and avoids the likelihood of erosion taking place between measurements used to create an average value. The disadvantage of using a single value is that there may be a time delay of a day before the erosion is noted. This may cause problems in identifying processes that are consistently occurring during a particular time of the day, such as melting of frost heaved material in the mid-morning. The initial analysis on a daily time scale is intended to aid the identification of seasonal trends in erosion during the monitoring period, however more detailed information will be needed to analyse specific erosion processes (Sections 6.4.2-6.4.4).

6.3.2 Seasonal Trends in Manual and Automatically Monitored Erosion

The upstream site of Beck Meetings (Site 1) (Figure 3.5) was monitored at 3 levels on the bank surface, upper, middle and lower. The sensors were in a diagonal pattern over the bankface, approximately 0.3 m apart horizontally and 1.0 m apart vertically. PEEP 1, 0.2 cm from the bank top (Figure 6.3A) confirmed the seasonal trend already identified (Section 5.2) that the winter periods dominated the seasonal pattern of erosion. The total cumulative erosion measured manually over the monitoring period for each PEEP is shown in Table 6.4. The correlation coefficients of the erosion measured manually for each epoch and the automatically recorded epoch erosion values, calculated using the photovoltaic ratio and sensor calibration (Section 3.3.4), are also presented in Table 6.4.

PEEP NUMBER (*Bank Position*)	MANUALLY MEASURED LENGTH EXPOSED (mm) *(Time Period)*	CORRELATION COEFFICIENT BETWEEN MANUAL AND AUTOMATIC MEASUREMENTS (r)	NUMBER OF MEASUREMENTS	CRITICAL 95 % CONFIDENCE COEFFICIENT (r)
1. Beck Meetings				
PEEP 1 (*Upper Bank*)	**32** *(14/01/97-22/04/98)*	0.813	17	0.482
PEEP 2 (*Mid Bank*)	**22** *(14/01/97-22/04/98)*	-0.558	16	0.497
PEEP 3 (*Lower Bank*)	**44** *(13/02/97-22/04/98)*	0.784	14	0.532
2. Low Row				
PEEP 5 (*Downstream Lower*)	**31** *(15/01/97-02/02/98)*	-0.098	11	0.602
PEEP 7 (*Upstream Lower*)	**95** *(15/01/97-13/03/98)*	0.723	14	0.532
PEEP 11 (*Downstream Upper*)	**140** *(15/01/97-13/03/98)*	0.908	16	0.497
PEEP 6 (*Upstream Upper*)	**99** *(15/01/97-30/10/97)*	0.855	9	0.666
3. Greystone Farm				
PEEP 4 (*Downstream Lower*)	**356** *(05/01/97-04/02/98)*	0.667	7	0.755
PEEP 9 (*Upstream Lower*)	**205** *(05/01/97-04/02/98)*	0.061	4	0.950
PEEP 8 (*Downstream Upper*)	**44** *(05/01/97-04/02/98)*	-0.609	5	0.878
PEEP 10 (*Upstream Upper*)	**791** *(05/01/97-04/02/98)*	0.900	4	0.950

Table 6.4 The cumulative length of erosion measured manually on the PEEPs during each erosion epoch correlated against the automatically recorded amount of erosion during the same period.

The distribution of erosion over the bank profile shows a decline mid bank, with 22 mm of erosion from 14/01/97 to 22/04/98 (Table 6.4) (Figure 6.3B). Most erosion appears to have occurred on the lower bank, despite the shorter measurement period, with 44 mm of erosion being recorded manually on the sensors (Table 6.4) (Figure 6.3C). Correlating the measurements taken manually during each pin reading epoch with the sum of automatically registered daily erosion series for the same epoch (Table 6.4) revealed that all sensors were significantly related above a 95% confidence level at Beck Meetings (Site 1). This indicates that the automatically measured readings were closely linked to the manual readings. The relationship does not indicate that the actual automatic and manual values were the same, only that the variations of the two variables are similar, thus indicating that erosion/deposition events had taken place during equivalent periods on both data series.

Four PEEPs were installed mid-catchment at Low Row (Site 4) (Table 3.7) in two columns, 9.1 m apart. The upper bank PEEPs were approximately 0.2 m beneath the bank top, whilst the lower PEEPs were 0.8 m beneath the bank-top surface. The amount of erosion measured on each of the PEEPs shows a wide range of values. The maximum erosion of 140 mm occurred on the downstream upper PEEP (PEEP 11), whilst the downstream lower PEEP (PEEP 5) only registered 31 mm of erosion for approximately the same period (Table 6.4). Both the lower bank PEEPs (PEEPs 5 and 7) had less erosion than the upper bank PEEPs at the same upstream/downstream position (Table 6.4). This may be because of a different set of processes were dominating on the lower bank compared to the upper bank. It may also be a product of the variations in the sediment composition of the bank restricting the same process in the lower bank. This could cause processes to operate at different intensities in the upper and lower bank. The processes responsible for the erosion events at each PEEP will be investigated further in Section 6.4.

All of the PEEP manual measurements at Low Row correlated above a 95% confidence level with the variations in the automatic readings, apart from PEEP 5 (Downstream Lower) (Table 6.4). The plot of the manual and automatic measurements for PEEP 5 (Figure 6.4A) showed that the two data series are numerically close to each other; however the poor correlation coefficient was probably a result of the asynchronous variability of the two variables. The low

levels of erosion activity may have resulted in the two series varying within their error bands resulting in low correlation coefficients.

At Greystone Farm up to 791 mm of erosion was registered during the monitoring period (Table 6.4), complementing the downstream trend of increasing rates of erosion at the PEEP installed sites. One of the PEEPs was considerably less eroded than the rest, PEEP 8, with only 44 mm of erosion (Table 6.4) (Figure 6.5B). Only the manual measurements on PEEP 10, upstream upper, correlated at a 95 % level with the automatic measurements. The small number of samples where both manual and automatic measurements were available meant that the site might not be very representative of the entire monitoring period, reducing the correlation coefficients. The discontinuous nature of the automatic measurements taken at Greystone Farm, caused by removal of the PEEP sensors from the bank in large erosion events and faults in the datalogger, make the time-series of data appear stepped (Figure 6.5A-D). The infrequent large erosion events portrayed by the time series is probably a reasonable representation of the 'catastrophic' erosion at the site.

In terms of erosion seasonality for each of the sensors in the upper catchment, at Beck Meetings (Site 1), they all had a distinctively stable summer period and active winter period (Figures 6.3A-C). Mid catchment at Low Row there was more variability in the daily erosion time series for the monitoring period (Figures 6.4A-D). This may be because of the scour holes that developed on the bank surface around the sensors possibly due to:

1. Preferential drainage through the horizontally augured PEEP insertion holes;
2. A weakening of the soil structure due to the disturbance caused by auguring;
3. Increased flood velocities around the PEEPs during inundation caused by the sensor altering the flow structure, thus increasing the rate of entrainment.

These holes may have made a measurable difference between the cell series and reference cell ratio during overcast and direct sunlight conditions.

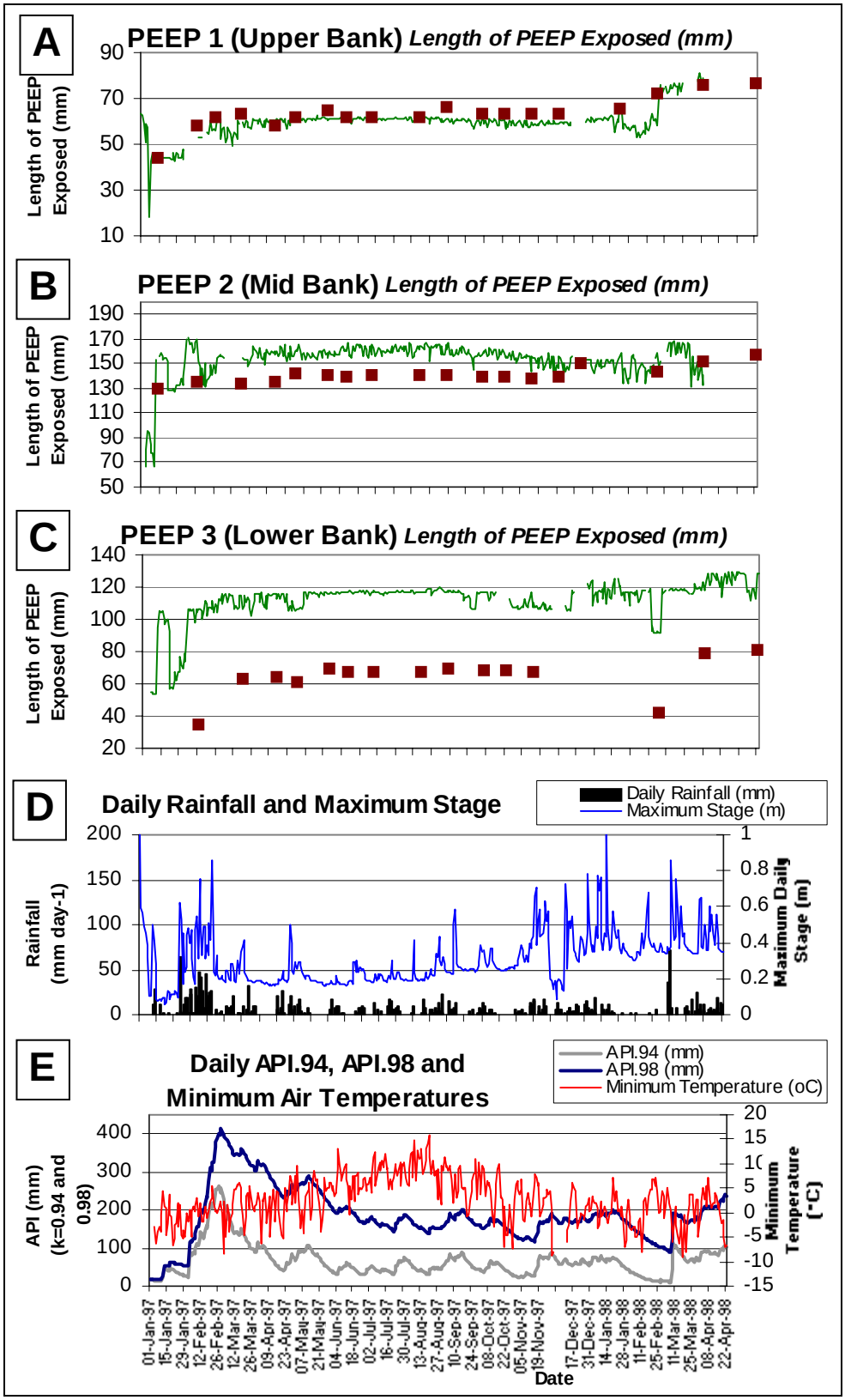

Figure 6.3 The length of PEEP exposure measured manually ▮ and automatically ——— at Beck Meetings (Site 1) on: (**A**) the upper bank PEEP 1; (**B**) the mid-bank PEEP 2; (**C**) the lower bank PEEP 3; compared against: (**D**) daily rainfall and maximum stage; (**E**) daily API.98, API.94 and minimum temperature.

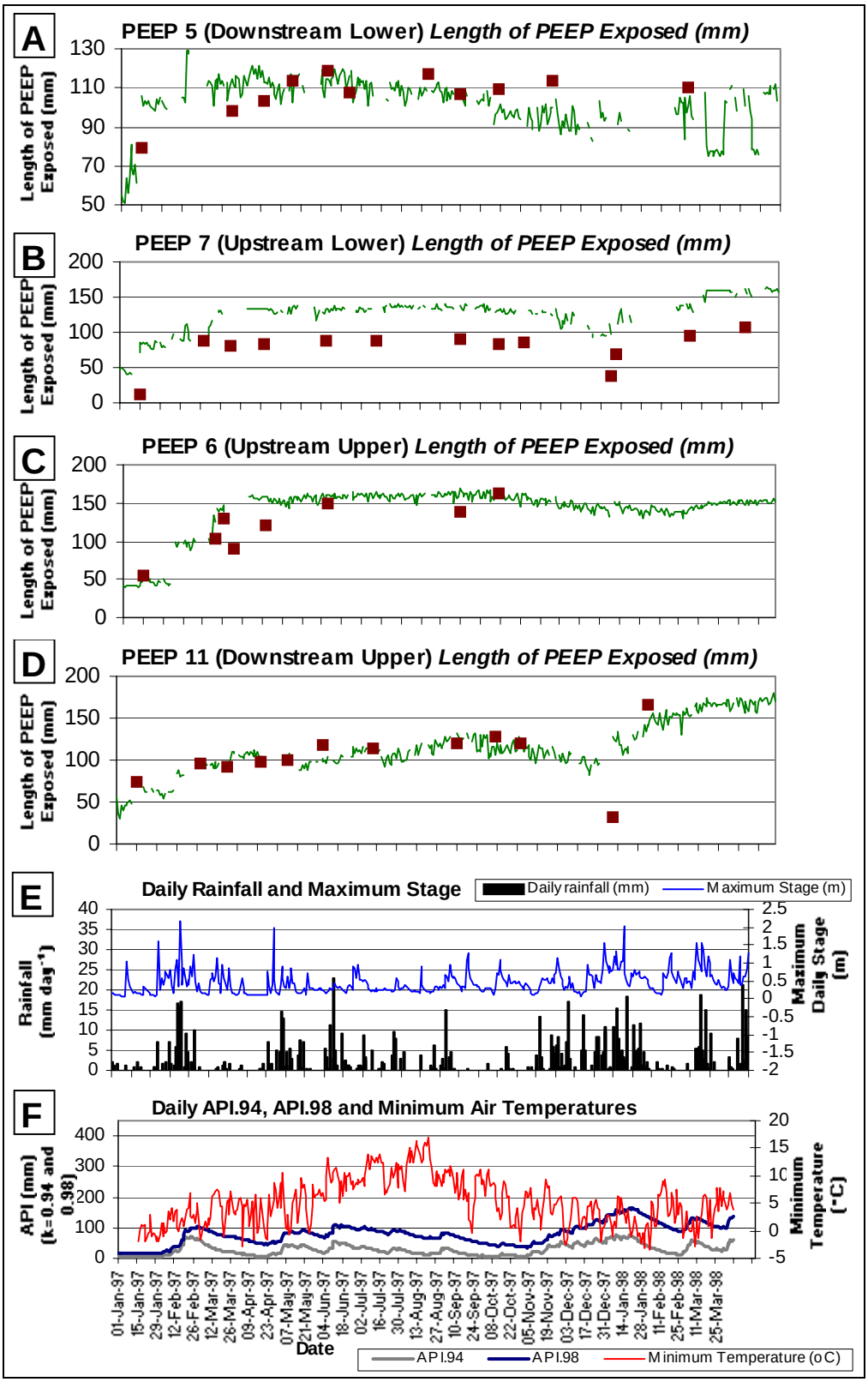

Figure 6.4 The length of PEEP exposure measured manually ■ and automatically — at Low Row (Site 4) on: (**A**) the downstream lower PEEP 5; (**B**) the upstream lower PEEP 7; (**C**) the upstream upper PEEP 6; (**D**) downstream upper PEEP 11; plotted alongside: (**E**) daily rainfall and maximum stage; (**F**) daily API.98, API.94 and minimum temperature.

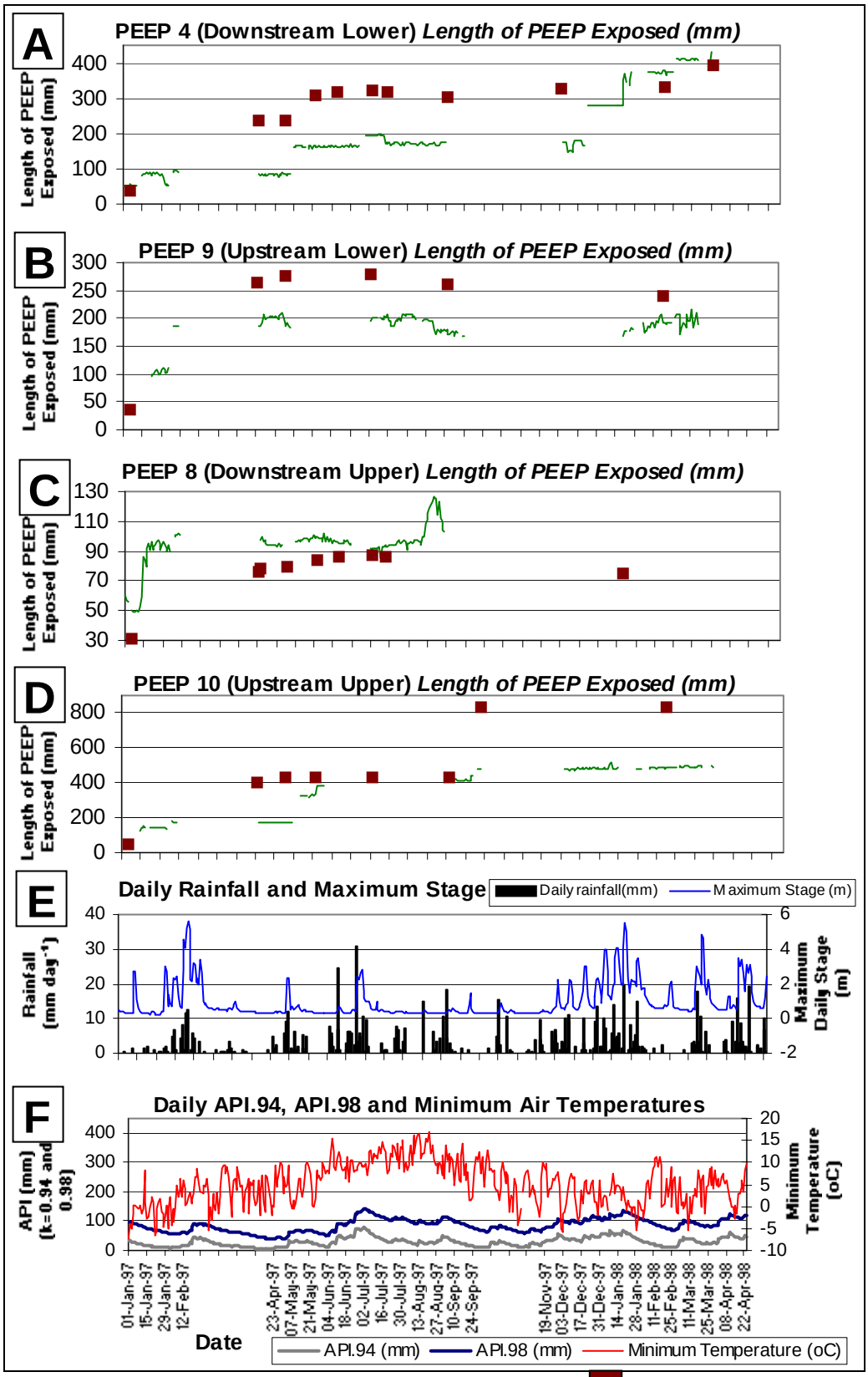

Figure 6.5 The length of PEEP exposure measured manually and automatically at Greystone Farm (Site 8) on: (**A**) the downstream lower PEEP 4; (**B**) the upstream lower PEEP 9; (**C**) the downstream upper PEEP 8; (**D**) upstream upper PEEP 10; plotted alongside: (**E**) daily rainfall and maximum stage; (**F**) daily API.98, API.94 and minimum temperature.

6.4 EROSION PROCESS IDENTIFICATION USING PEEP DATA AND ENVIRONMENTAL VARIABLES

6.4.1 Introduction

The discontinuous nature of the PEEP data series due to datalogger failures, inundation, and removal from the bank during mass failure processes meant that erosion events could not regressed against other environmental variables, as with the pin data (Chapter 5), to investigate the annual distribution of erosion events. Regressing the data at each site would not allow the downstream change in erosion processes to be inferred because of the inherent bias produced by the disparate periods that the sensors were operational over. To overcome this problem the individual erosion events will be examined for each sensor, and then the manual observations and pin measurements will be used to place these erosion events in context against the annual distribution of erosion events/processes.

6.4.2 A Flow Diagram for Process Inference

The confidence in determining certain types of process that had been occurring at each of the monitoring sites was dependent on the type of sensory equipment installed. With the PEEP sensors comparisons could be made between the timing of an erosion episode and stage, temperature and rainfall data. At sites without PEEPs, pin data could be used to describe the rates and distribution of erosion over the bank surface. As well as these data the manual observations of the bank at each fortnightly visit could provide substantial data on the type of process by describing the bank morphology.

The author provides a flow diagram (Figure 6.6) so that the structure of process identification is transferable, aiding other PEEP users and general observers of erosion processes. The diagram presented is intended as a guide to the user, aiding the inference of processes due to the general principles of bank erosion presented in the literature. The complex interactions between sedimentology, climate, and hydrology resulting in each erosion processes (e.g. needle ice formation in Lawler (1993b) was not presented to avoid complexity, and allow comprehension by a general readership.

The system takes the user through the selection of five monitored environmental indicators to aid process identification. The environmental indicators used are Rainfall, Antecedent Precipitation Index, Bank/Air Temperature, Stage, and Bank Profile. These variables were chosen as they could be determined for the monitoring sites in this study, provide differing evidence for the processes that were observed, and also be available to other end-users. At each indicator box a decision must be made which will either lead the user in to the inference of a particular process, or on to the next decision.

For most of the decision boxes the knowledge of the conditions that were active at or after the event are important. For some decisions, especially for mass failure, the conditions that were present before the failure took place are important, and influence the type of erosion that occurred. The system is not site specific and could be used as a scoping exercise for erosion process identification on any basin. Evidence confirming the type of process indicated by the system would be desirable before a firm conclusion was reached.

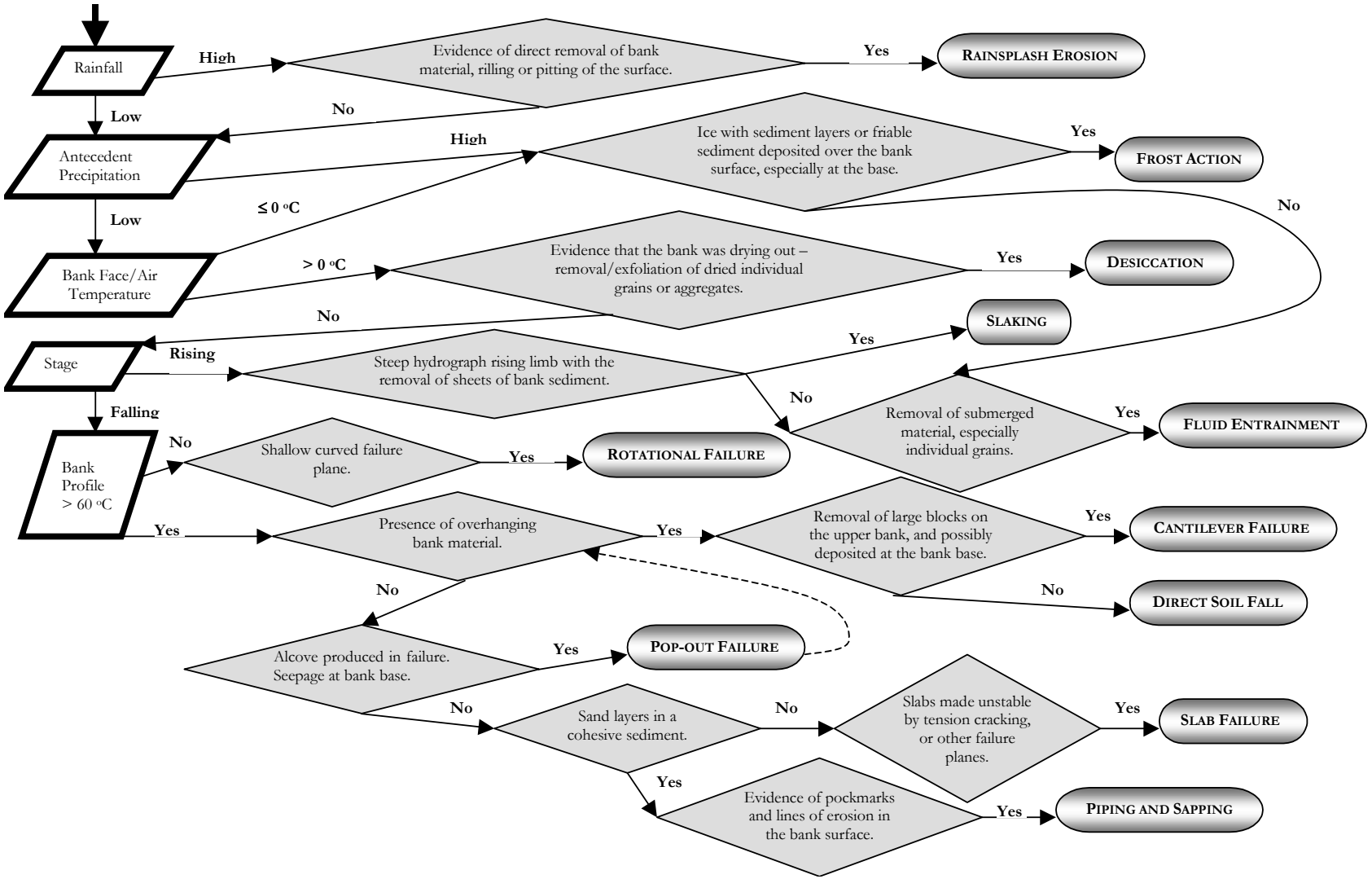

Figure 6.6 A flow diagram of erosion process determination using environmental variable of rainfall, API, bankface/air temperature, stage and the cross-sectional shape of the bank profile.

6.4.3 Inferences and Observations of Upstream Erosion Processes

PEEP Monitored Processes of Erosion and Deposition

Applying the flow diagram of erosion process identification (Figure 6.6) to the monitoring sites allows the distribution of erosion events during the maximum period that the PEEPs were monitored, from 01/01/97 to 22/04/98, to be surmised. Combining manual observations with a detailed examination of the automated erosion time-series meant that significant processes could be evaluated.

PEEP NUMBER (EVENT)	DATE	DESCRIPTION OF EROSION OR DEPOSITION	AMOUNT OF EROSION OR DEPOSITION (mm)		
			Deposition	Erosion	Net Erosion
1a	03/02/97-04/02/97	A preceding period of frost action causing deposition, followed by entrainment of the prepared material.	2.8	9.5	6.7 ± *8.4*
1b	05/02/98-06/02/98	Direct soil fall of frost prepared material.	0	16.3	16.3 ± *8.4*
2a	11/01/97-12/01/97	A preceding period of frost action causing deposition, followed by entrainment of the prepared material.	27.0	86.0	59.0 ± *5.6*
2b	03/02/97-04/02/97	A preceding period of frost action causing deposition, followed by entrainment of the prepared material.	0.5	13.0	12.5 ± *5.6*
2c	19/02/97-01/03/97	Disruption of PEEP signal by rainsplash erosion.	0	0	0 ± *5.6*
2d	08/01/98-09/01/98	Spalling of PEEP after a flood event.	15	0	+15 ± *5.6*
2e	11/02/98-13/02/98	A preceding period of frost action causing deposition, followed by entrainment of the prepared material.	Variable	15	15 ± *5.6*
3a	11/01/97-12/01/97	A preceding period of frost action causing deposition, followed by entrainment of the prepared material.	1	40	39 ± *5.4*
3b	29/01/97	Slide of saturated sediment after ice melt.	0	10	10 ± *5.4*
3c	03/02/97-04/03/97	Entrainment of frost prepared material.	0	17	17 ± *5.4*
3d	29/01/98-07/02/98	Spalling of PEEP by frost shattered bank sediment, followed by flood entrainment.	25	25	0 ± *5.4*

Table 6.5 A description of the erosion and deposition events that occurred at Beck Meetings: (**1**) PEEP 1 upper bank; (**2**) PEEP 2 mid-bank; (**3**) PEEP 3 lower bank. Net erosion errors are based on a 95 % confidence interval of the calibration regression standard error (Table 3.8).

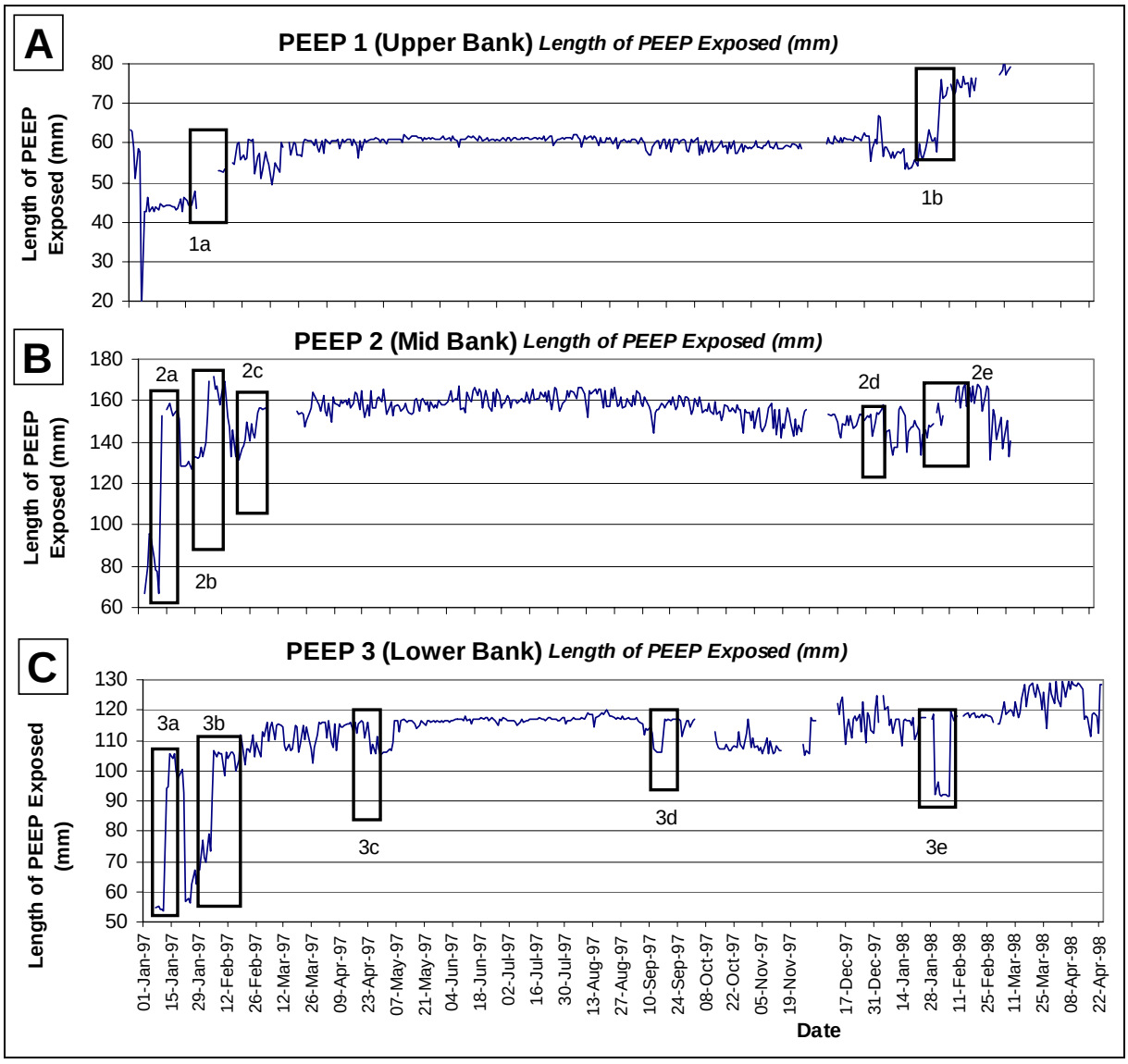

Figure 6.7 A time-series of erosion/deposition events (highlighted in boxes) described in Table 6.5 for Beck Meetings (Site 1): (**A**) PEEP 1 upper bank; (**B**) PEEP 2 mid-bank; (**C**) PEEP 3 lower bank.

At Beck Meetings (Site 1) six of the ten erosion events were preceded by a period of sub-zero temperatures, which led to deposition on the sensor (Table 6.5) (Figure 6.7). These depositional periods could be caused by:

1. Ice forming on, or in, the bank causing it to heave over the cell series or reference cell. If the ice were to grow on the bank surface then needle ice may form (Lawler, 1987b). This would result in the PEEP being covered by either pure ice or an amalgamation of ice and bank material (Figure 6.8B). The alternative would be for ice to be contained within the bank itself, as a lens of material, pushing the soil out over the PEEP (Figure 6.8C). In both these cases the length of time and severity of sub-zero temperatures would influence the amount of ice-growth.
2. The deposition of bank material on to the sensor decreasing the PEEP signals. Direct soil fall or the release of upper bank sediment eroded by interstitial ice could lead to deposition on to the PEEP surface (Figure 6.8D).
3. Snowfall over the bank surface, acting like deposited sediment on the PEEP output. However snow would be more likely to disrupt incoming solar radiation during sub-zero temperatures, whereas sediment would be more likely to be deposited during over zero temperatures when ice has melted.

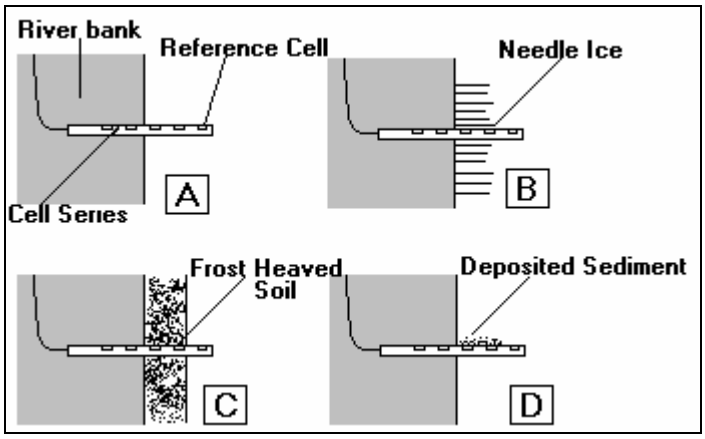

Figure 6.8 A diagrammatic representation of 3 different types of deposition over the PEEP surface: (**A**) normal PEEP position; (**B**) needle ice growth covering the sensor; (**C**) frost heaved material covering the sensor; (**D**) deposited sediment lying on the sensor surface. (The PEEP is shown with 4 cells in series, rather than the usual 10, for simplicity)

An example of a depositional period during a period with sub-zero temperatures is shown in Figure 6.9, and the procedure for process inference from the flow diagram in Figure 6.10.

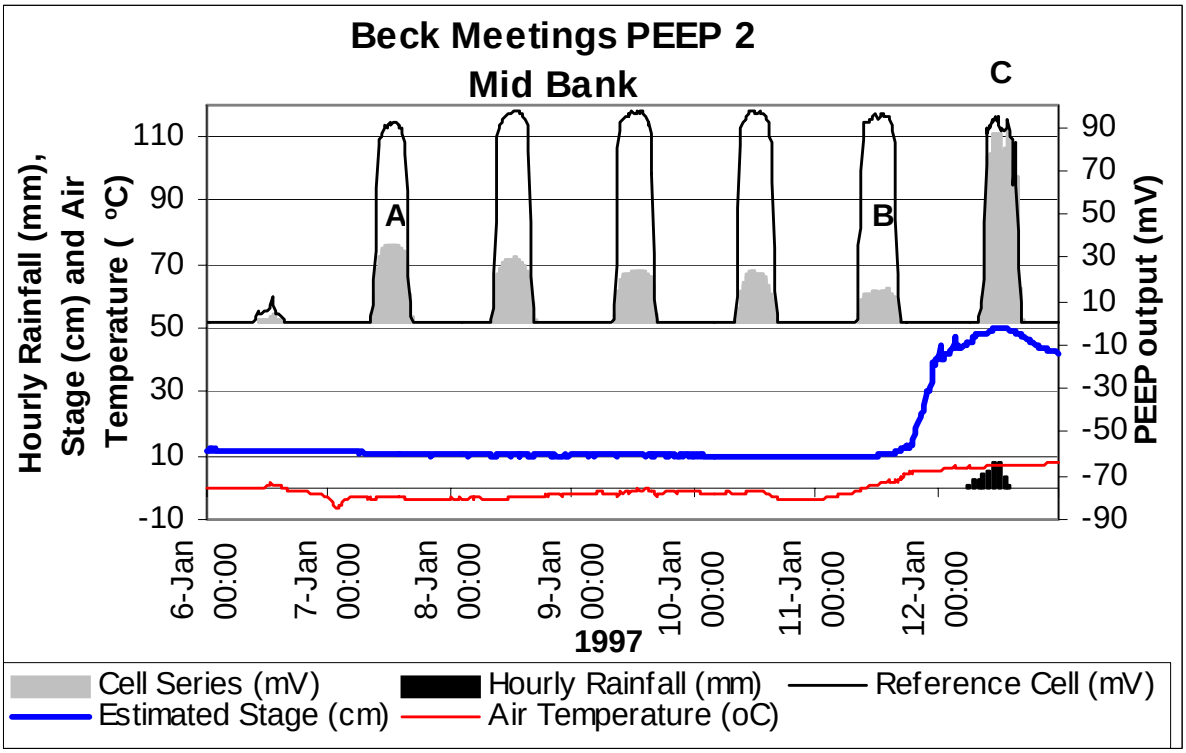

Figure 6.9 An example of a period of sub-zero temperatures followed by entrainment during a flood event. PEEP 2, in the middle of the bank at Beck Meetings, 06/01/97-12/01/97. From points (**A**) to (**B**) there is a decrease in the cell series output due to frost shattered bank debris falling on the sensor, or needle ice growth around the sensor.

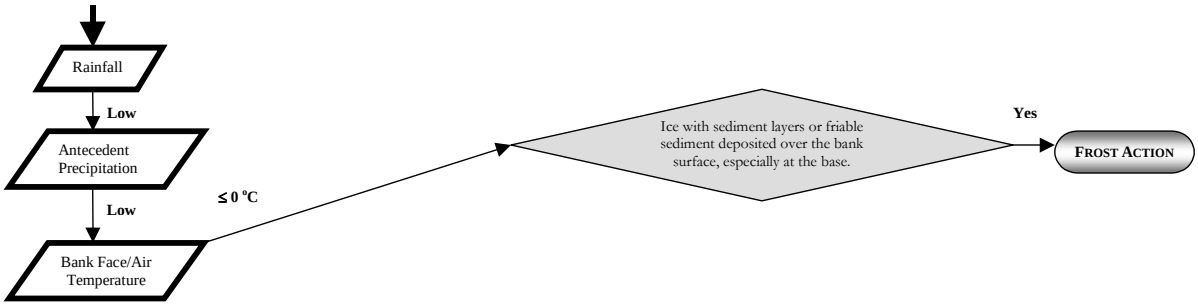

Figure 6.10 The flow diagram procedure for the inference of frost subaerial preparation for the depositional/erosional event in Figure 6.9.

The rainfall during the example was low (Figure 6.9), as was the antecedent precipitation index. The bankface temperature was below 0°C (Figure 6.9) until the flood event on the 12/01/97. There was no site visit before the flood event; however on the 14/01/97 small amounts of frost shattered material were observed. Previous manual observations at the site have revealed episodes of needle ice (Plate 6.1) releasing sediment on melting to the basal region of the bank (Plate 6.2).

Another indication that either ice growth or snow cover was affecting the PEEP output is the rapid rise of the cell series voltage during the day, in combination with a rise in air temperature. Figure 6.11 shows the entrainment event that occurred on 04/02/97 (Table 6.5 *3b* and *3c*). On the 29/01/97 a period of sub-zero temperatures resulted in a low cell series output in the morning. As the temperature rose to nearly 10°C at midday the cell series output also rapidly rose. The reference cell voltage did not rise in a similar fashion, indicating melt out and 10 mm of erosion. This may have been needle ice melting and falling down the bank combined with frost heaved material (Lawler, 1987b).

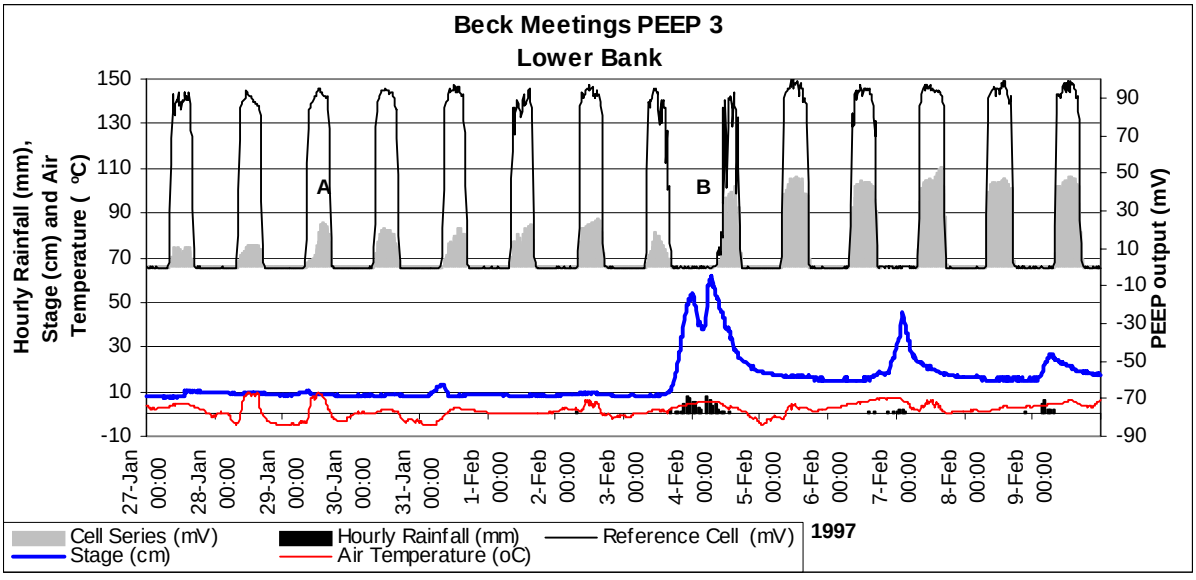

Figure 6.11 An example of a period of sub-zero temperatures with growth of ice around the sensor, the melting of the ice as the temperature goes above 0 °C is shown by point (**A**). The entrainment of frost action prepared sediment is shown at point (**B**). PEEP 3 in the lower bank at Beck Meetings (Site 1), 27/01/97-09/02/97.

The extended period of rainfall combined with flood events disrupted the reference cell and cell series output in the middle of the bank from 17/02/97-02/03/97 (Figure 6.12) (Table 6.5 *2c*).

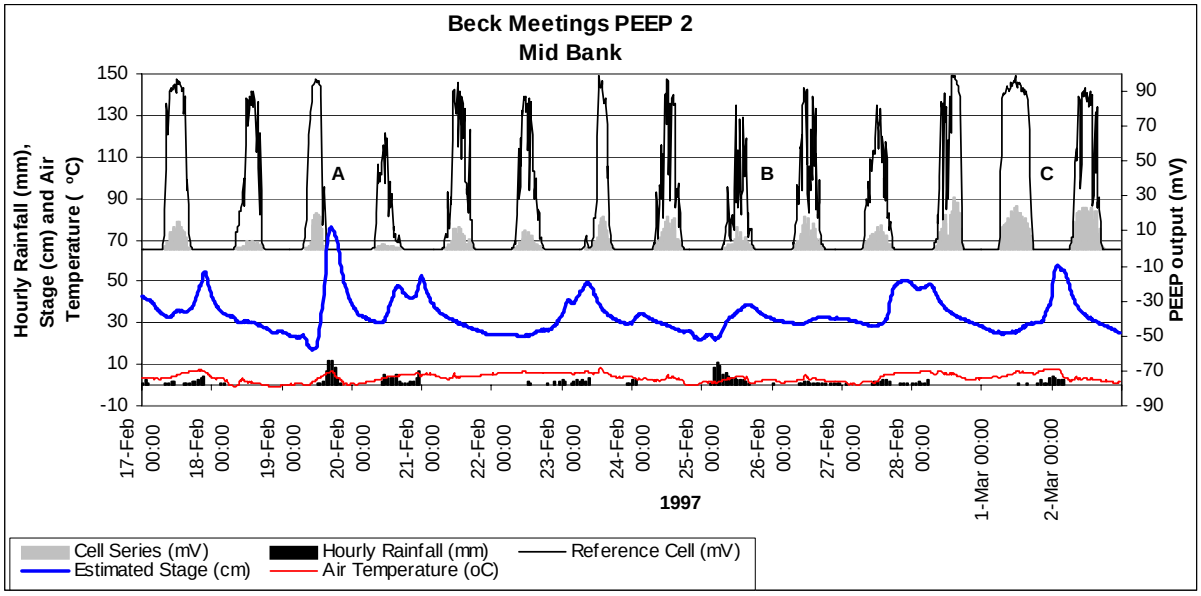

Figure 6.12 An example of a period of rainfall and flooding disturbing the PEEP output. The reduced PEEP signal is shown after the flood event at (**A**). The disrupted PEEP output from either rainfall or floodwater deposited sediment is highlighted at (**B**)**,** whilst at (**C**) the sediment has been removed. PEEP 2, in the middle of the bank at Beck Meetings, 05/01/98-11/01/98.

There appears to be no overall erosion or deposition from the sensor, however material appears to be deposited and eroded during the inundation and rainfall events. This may reflect a surface film of sediment being deposited during one flood event and removed during the next. The alternative is that rainfall deposited small amounts of sediment on to the surface of the PEEP from the upper bank, which was subsequently removed. As the peak stage events are nearly coincident with the rainfall events, distinguishing between the different processes is impossible without manual observations.

Deposition on the sensors also occurred due to waterborne vegetation, and other waterborne debris, becoming entangled around the sensor. Figure 6.13 is an example of this process. The flood event that occurred overnight on the 08/01/98-09/01/98 was at a stage high enough to inundate PEEP 2, in the middle of the bank face, depositing debris around it as the stage fell. An example of this type of deposition can be seen in Plate 6.3, where debris had become attached to the pressure transducer housing.

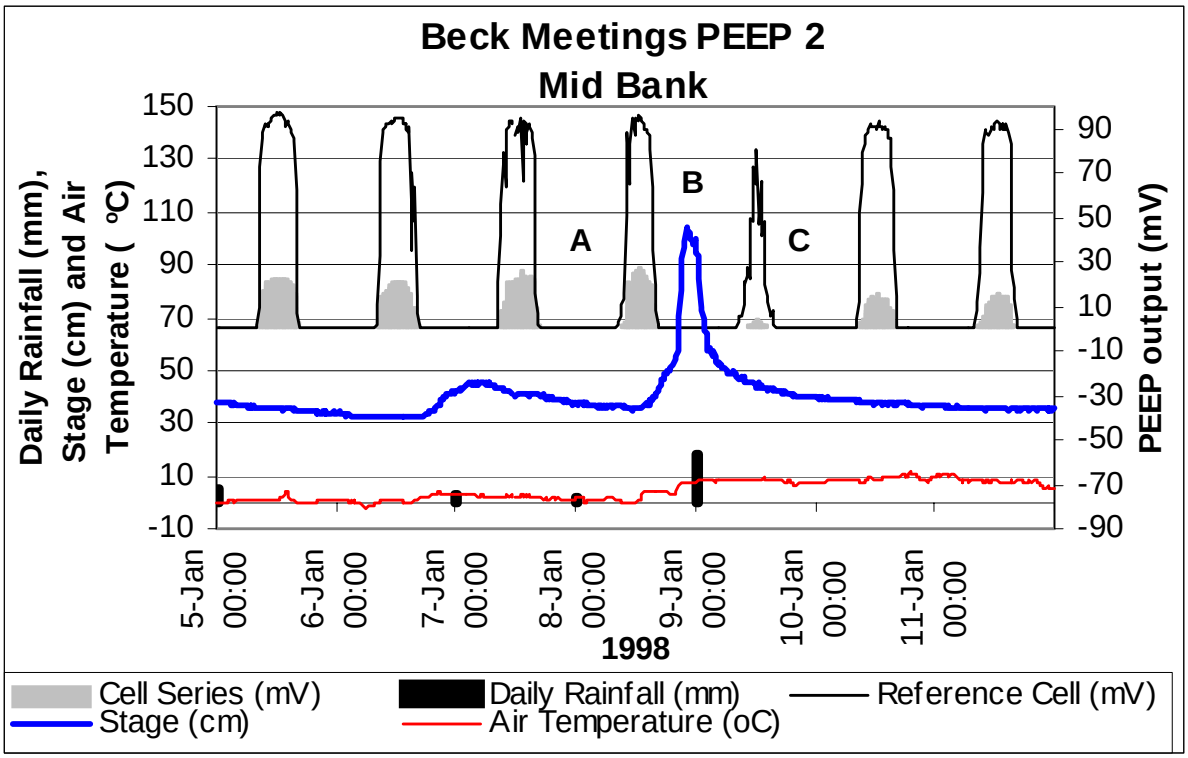

Figure 6.13 An example of overnight flood inundation, reducing the PEEP output from the level at (**A**), to a reduced level at (**C**), due to flood deposition of material from the flood event at (**B**). PEEP 2, in the middle of the bank at Beck Meetings, 05/01/98-11/01/98.

Manually Observed Processes of Erosion and Deposition

Other than Beck Meetings, two other monitoring sites were considered to be in the upper catchment, Hoggarths (Site 2) and Muker (Site 3) (Figure 3.5). The rates of erosion that occurred at these three sites from the erosion pin data (Figure 5.1), and the processes of erosion that affected the PEEPs sensors at Beck Meetings, all aid the identification of any downstream trends in erosion processes. The manual observations that were made during site visits also provided important data that may either have not been registered on the monitoring devices, or used to assist the explanation of the erosion events that were recorded.

Frost action, like that observed at Beck Meetings, was also evident at Hoggarths and Muker. Although it is difficult to ascertain any difference in frost severity between the three sites, more frost shattered debris was noted at Beck Meetings when compared to the other sites.

All the sites were also affected by cantilever failures (Thorne and Tovey, 1981). Muker was more active in terms of the number of failure blocks and the size of the failures (Plate 6.4). Beck

Meetings (Site 1) and Hoggarths (Site 2) were more likely to produce grassroot matts rather than cantilever blocks, perhaps as a result of the rooting depth compared to the bank height (Plate 6.5). The peaty consistency of bank sediment at Beck Meetings meant that the drying of the bank surface during the summer months was a prominent feature (Plate 6.6). No similar effects were noted at the other two upstream sites and no production of desiccated material was observed, even at Beck Meetings.

6.4.4 Inferences and Observations of Mid-Catchment Erosion Processes

PEEP Monitored Processes of Erosion and Deposition

In a downstream direction the next set of PEEPs was installed at Low Row (Site 4). The majority of the erosion events at Low Row appeared to be caused by high flows entraining bank material (Figure 6.14A-D) (Table 6.6). In most cases the erosion was preceded by a period of sub-zero temperatures. The erosional events differ from those experienced at Beck Meetings (Site 1) as the sub-zero temperatures did not appear to cause deposition on the PEEPs (e.g. Figure 6.15 (Table 6.6 *6a*)). The banks may have tended to be better drained with a higher silt-clay content than the peaty bank material upstream at Beck Meetings, thus restricting the water available for frost heave/needle ice. The length of time that the bank was below 0^{o}C was also shorter at Low Row than upstream. This may restrict the growth of ice crystals, which is required to push the bank sediment off the bank surface. Scour holes, or holes from piping were evident around the PEEPs. These could be responsible for restricting the sensitivity of the sensors to growth or contraction of the bank surface. A flood wave with a similar stage on the 15/09/97 inundated PEEP 5: this event did not cause any erosion and was not preceded by any frost action. This would seem to indicate the importance of frost in preparing the bank for entrainment.

PEEP NUMBER (EVENT)	DATE	DESCRIPTION OF EROSION OR DEPOSITION	AMOUNT OF EROSION OR DEPOSITION (mm)		
			Deposition	Erosion	Net Erosion
5a	11/01/97 - 12/01/97	Direct entrainment of bank material preceded by sub-zero temperatures.	0	40.6	40.6 ± *8.4*
5b	05/02/97 - 06/02/97	Direct entrainment	0	0	6 ± *8.4*
7a	11/01/97 - 12/01/97	Direct entrainment of bank material preceded by sub-zero temperatures.	0	11	11 ± *8.0*
7b	05/02/97 - 06/02/97	Delayed failure after flood event, possibly piping or sapping.	0	25	25 ± *8.0*
7c	05/12/97 - 11/12/97	Two fluvial entrainment episodes, the first preceded by sub-zero temperatures.	0	69 + 13	81 ± *8.0*
7d	14/02/98 - 15/02/98	Delayed erosion after flood event, possibly piping or sapping.	0	16	16 ± *8.0*
6a	11/01/97 - 12/01/97	Direct entrainment of bank material preceded by sub-zero temperatures.	0	44	44 ± *6.6*
6b	03/02/97 - 04/02/97	Direct entrainment of bank material preceded by sub-zero temperatures.	0	59	59 ± *6.6*
6c	03/03/97 - 07/03/97	Frost action causing erosion followed by a depositional event, and then another erosional event.	9	38 + 19	48 ± *6.6*
11a	11/01/97 - 12/01/97	Direct entrainment of bank material preceded by sub-zero temperatures.	0	17	17 ± *2.5*
11b	10/02/97	No bank removal after large flood event followed by the main erosional event during a subsidiary flood.	0	23	23 ± *2.5*
11c	18/03/97 - 19/03/97	Direct entrainment.	0	6	6 ± *2.5*
11d	04/12/97 - 11/12/97	Entrainment during a flood event preceded by frost events.	38	68	30 ± *2.5*

Table 6.6 A description of the erosion and deposition events that occurred at Low Row (Site 4): (**5**) PEEP 5 Downstream Lower; (**7**) PEEP 7 Upstream Lower; (**6**) PEEP 6 Upstream Upper; **(11)** PEEP 11 Downstream Upper. Net erosion errors are based on a 95 % confidence interval of the calibration regression standard error (Table 3.8).

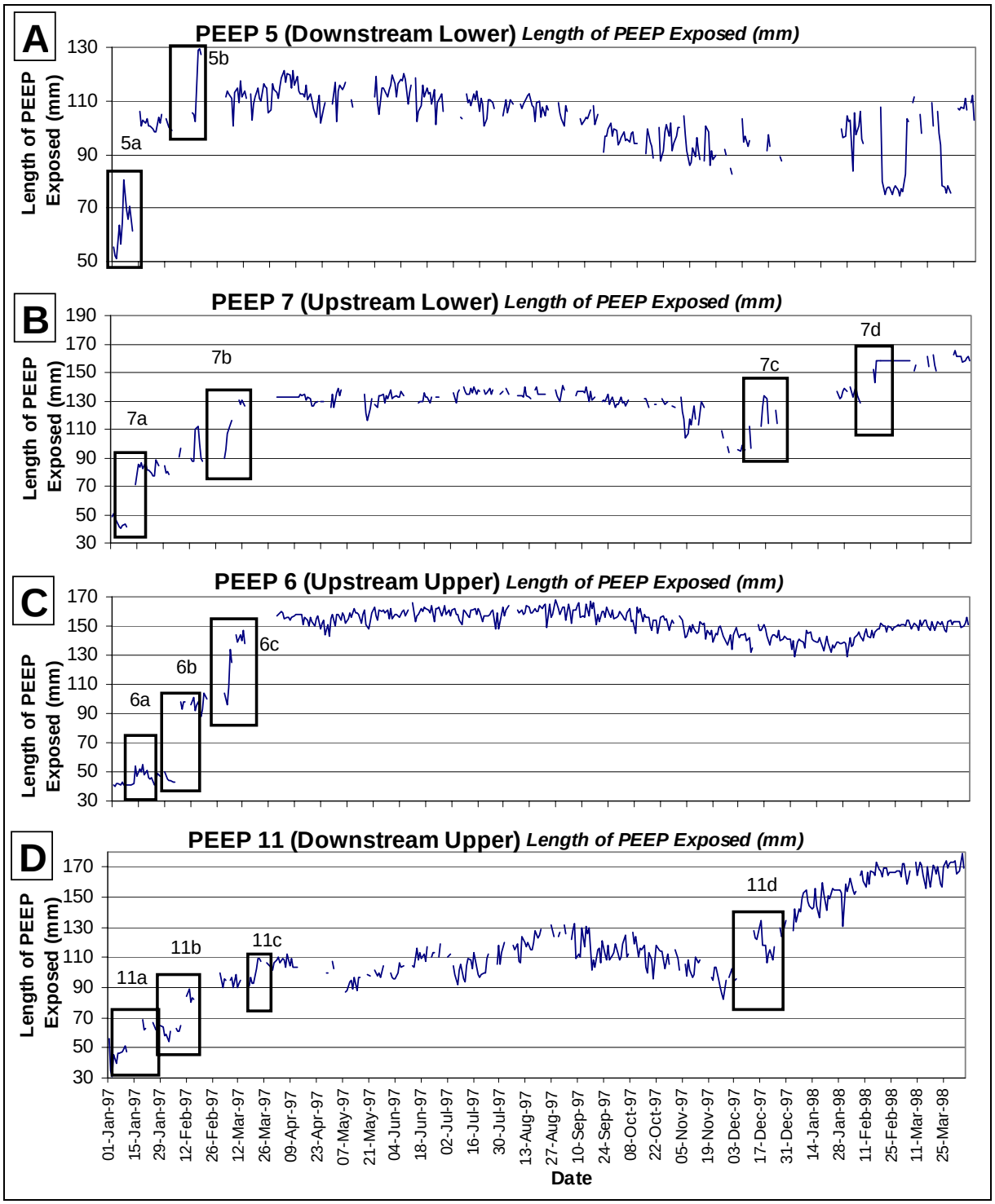

Figure 6.14 A time-series of erosion/deposition events (highlighted in boxes) described in Table 6.6 for Low Row (Site 4): (**A**) PEEP 5 Downstream Lower; (**B**) PEEP 7 Upstream Lower; (**C**) PEEP 6 Upstream Upper; (**D**) PEEP 11 Downstream Upper.

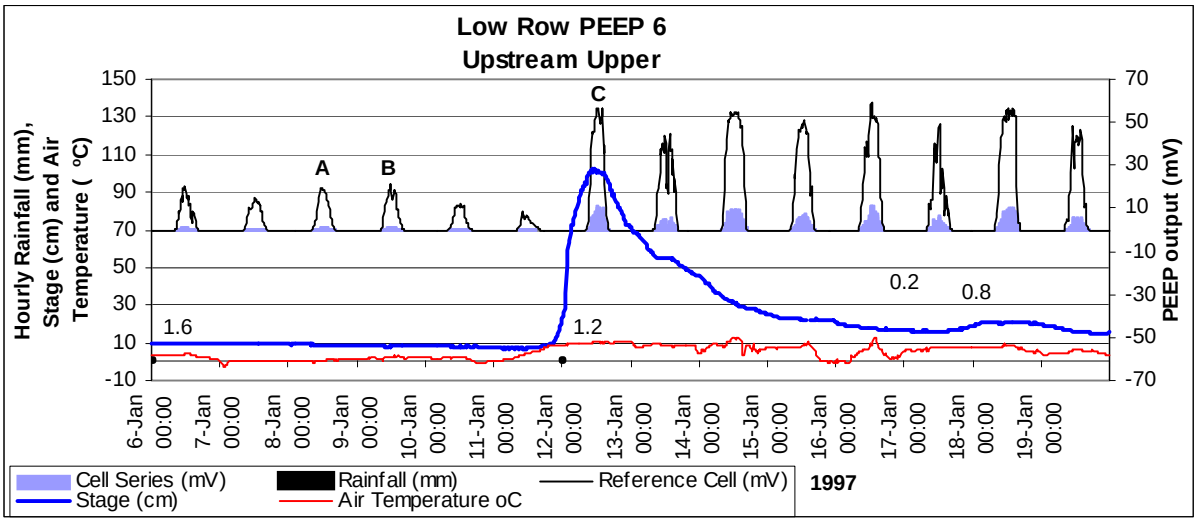

Figure 6.15 An example of a flood entraining bank sediment, with a proceeding period of sub-zero temperatures. The rise in the temperature from below to above 0 °C does not appear to cause any erosion of frost prepared sediment between points (**A**) and (**B**), whilst the bank was eroded during a the flood event at (**C**). The low daily values of rainfall are highlighted by labelling them with their values in mm day^{-1}.

The upstream upper and lower PEEPs, numbers 6 and 7 respectively, produced an unusual erosion-deposition-erosion sequence from 03/03/97-07/03/97 (Figures 6.16 and 6.17). The upper bank (PEEP 6) was exposed by 38 mm (Figure 6.16) on the day after a sub-zero event, 04/03/97, whereas the lower PEEP (7) was not eroded until the following day (Figure 6.17). This may be due to frost shattered material collapsing at different times as it dries out on the bank surface. The deposition that occurred after the flood event may either be:

1. Smearing of the sensor by suspended sediment;
2. Woody debris entangled around the sensor;
3. Sediment destabilised by the retreating floodwater, falling on to the sensor;
4. Snowfall covering the sensor.

As the deposited material was then removed the most likely explanation is snowfall, however debris tangled round the sensor may have fallen, or a rainfall event not registered in Richmond may have cleaned the sensor of deposited or smeared sediment.

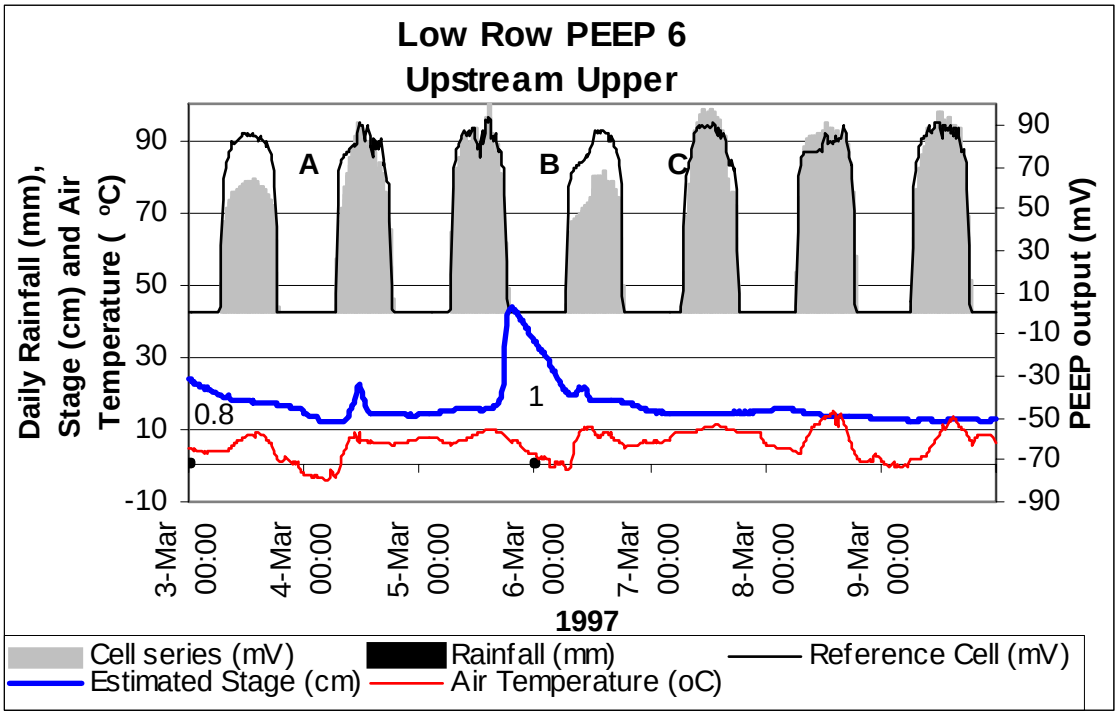

Figure 6.16 An example of frost action at (**A**), followed by a flood event depositing material (**B**) and then further erosion (**C**). PEEP 6 in the upstream upper section of the bank at Low Row, 03/03/97-07/03/97. The low daily values of rainfall are highlighted by labelling them with their values in mm day^{-1}.

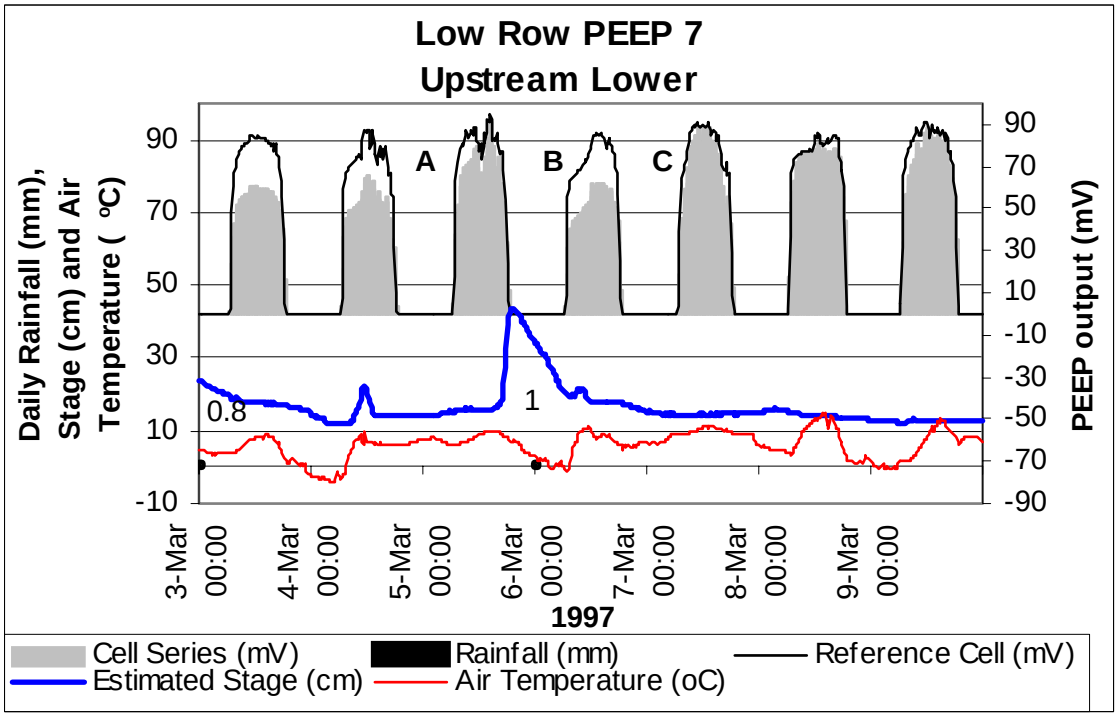

Figure 6.17 An example of frost action at (**A**), followed by a flood event depositing material (**B**) and then further erosion (**C**). PEEP 7 in the upstream lower section of the bank at Low Row, 03/03/97-07/03/97. The low daily values of rainfall are highlighted by labelling them with their values in mm day^{-1}.

The flood event on the 07/02/98 (Figure 6.18) (Table 6.6 *7d*) did not appear to entrain any material on re-exposure of upstream lower PEEP (PEEP 7) the following day. This was a period when the pressure transducer was inoperable at the site, the decrease in PEEP output and flood event monitored on the same day upstream indicate that a flood event did occur. A prolonged period of overcast conditions and submergence followed until the 14/02/98. This again resulted in no marked erosion. However on the 15/02/98 16 mm of erosion had occurred. The delay in erosion would indicate a small mass failure (Figure 6.6); this was however not observed in the field and the amount of material that failed was not typical of the other cantilever failures observed at the site. An alternative explanation could be the removal of sediment around the PEEP by piping or sapping, the falling stage allowing the infiltrated water in the bank profile to drain out of the sandier layers, removing material around the sensor (Hagerty, 1991a). The elongated hollows possibly associated with sapping were evident during field observations (Plate 6.7). With low rainfall, high API, no frost action, and no removal of submerged material, piping and sapping are indicated by the selection procedure outlined in Figure 6.6.

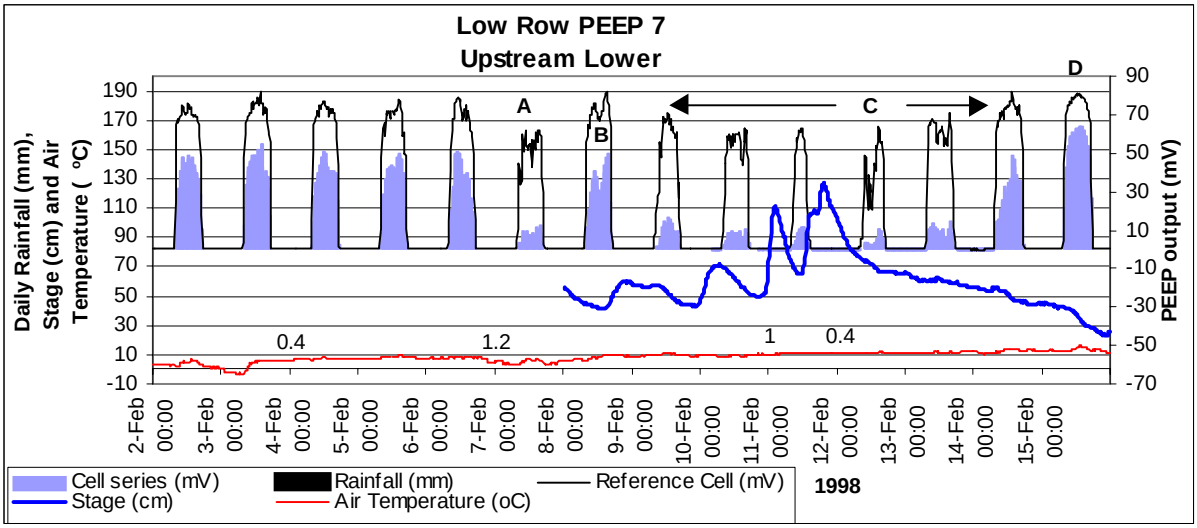

Figure 6.18 An example of a delay in erosion (**D**) after a flood event (**A**) caused no erosion (**B**), and a further sequence of rainfall and a flood peak (**C**) only disrupted the PEEP output. PEEP 7 in the upstream lower section of the bank at Low Row, 02/02/98-15/02/98. The low daily values of rainfall are highlighted by labelling them with their values in mm day^{-1}.

The flood event on the 04/02/97 caused 6 mm of erosion on PEEP 5 (downstream lower) (Table 6.6 *5b*). The downstream upper bank sensor (PEEP 11) did not show erosion during the same period (Figure 6.19) (Table 6.6 *11b*). A subsidiary flood peak on the 10/02/97, though substantially lower than the flood event on the 04/02/97, was associated with 23 mm of erosion. The erosion was preceded by a disruption in the amount of light reaching the sensor; this may be

caused by the submergence of the PEEP in turbid water. The rapid increase in photovoltaic output could be due to the retreat of the floodwater revealing the amount of erosion that occurred due to entrainment. The wetting up of the bank by precipitation could have made the upper bank more prone to erosion than the preliminary flood.

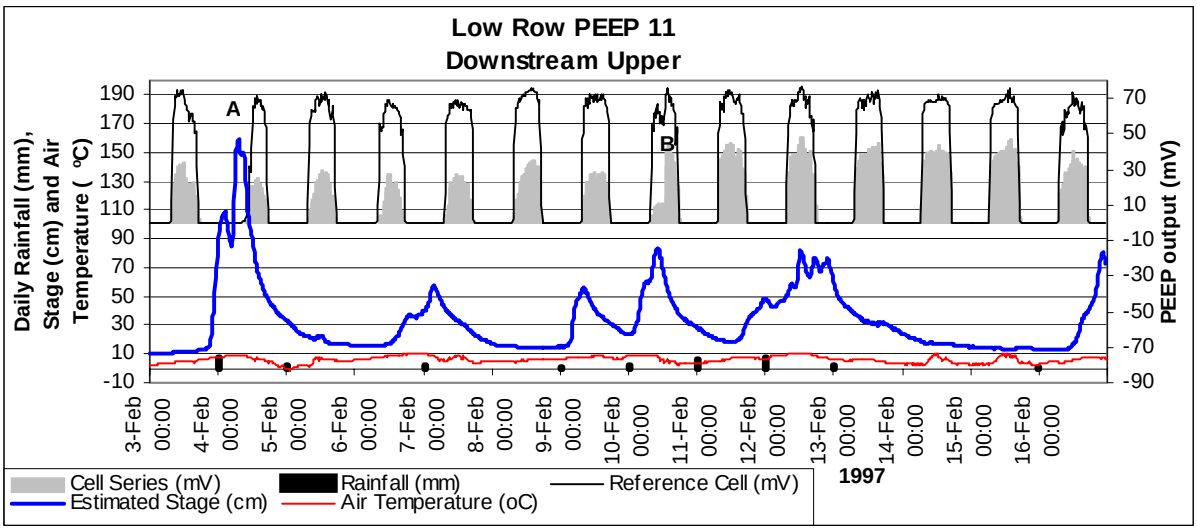

Figure 6.19 An example of an erosion event during a smaller subsidiary flood (**B**), after there was no erosion following the main flood peak (**A**). PEEP 11 in the downstream upper section of the bank at Low Row, 03/02/97-16/02/97.

Manually Observed Processes of Erosion and Deposition

Reeth (Site 5) and Easby (Site 6) as well as Low Row (Site 4) were all considered to be situated within the middle reaches of the River Swale (Figure 3.5). Low Row was limited in the processes that were observed during the monitoring period. As with the upper catchment, cantilever failures were evident at all of mid-catchment sites. The most evidently active site in terms of cantilevers was Reeth (Plate 6.8).

At Reeth a suite of erosive processes were active. Arched structures at the base of the bank (Plate 5.2) that indicate pop-out failures (Simon, 1989; Thorne, 1993) were observed regularly. These would then provide ideal conditions for cantilever failures, as they left the upper bank material unsupported. Slab failures (Selby, 1982) were another common failure mechanism at Reeth (Plate 6.9). Some of the slab failures were able to remove whole columns of 370 mm long erosion pins in a single event. Depending on the size of the failure and the competence of the flood wave that triggered the failure, the basal material from the collapse material may either remain *in situ* or be entrained. The removal of the basal debris, which often occurred, meant that the bank was left unprotected during the following floods (Thorne and Osman, 1988). Drying of

the bank sediment lead to the formation of sheets of desiccated material at Reeth (Plate 6.10). The exfoliated sheets appeared to stay in place throughout the summer months; however the rapidly rising flood events could probably entrain the sub-aerially prepared material.

Easby failed in a more catastrophic manner than the other 2 sites. The length of root exposure (Plate 6.11) indicated the speed of material removal. There has been little evidence of failure after flood events that appear to have aided the removal of the sediment. The floods have entrained most of the failed material immediately, leaving the bank unprotected for the next event.

6.4.5 Inferences and Observations of Lower Catchment Erosion Processes

PEEP Monitored Processes of Erosion and Deposition

The erosion events at Greystone Farm (Site 8) were distributed throughout the annual cycle (Table 6.7) (Figure 6.20) rather than being concentrated during the winter as they were in the upper and middle catchment (Figures 6.7 and 6.14). The magnitude of the failures meant that the PEEPs were often completely eroded out of the bank leaving gaps in the data series (Figure 6.20).

The deposition of lower bank material at Greystone Farm (Site 8) on the 14/07/97 (Figure 6.21) (Table 6.7 *4e*) could be due to desiccation of the bank surface during the summer months. The flood events that had passed through the monitoring site since the previous erosion event on the 01/07/97 had failed to reach the same height as PEEP 4, thus keeping the bank relatively dry. Alternatively the sheep that grazed on the bank top also had access to the bank surface during dry conditions. Bite marks were found on the PEEP sensor casings, indicating that the sheep had accessed the bank. Sheep rubbing against the bank could deposit sediment on to the lower PEEPs, giving the same voltage response.

PEEP NUMBER (EVENT)	DATE	DESCRIPTION OF EROSION OR DEPOSITION	AMOUNT OF EROSION OR DEPOSITION (mm)		
			Deposition	Erosion	Net Erosion
4a	10/01/97-14/01/97	Direct entrainment of bank material preceded by deposition from frost events.	23	56	33 ± *9.2*
4b	04/02/97 - 06/02/97	Entrainment during flood event proceeded by deposition from frost action. No erosion during following subsidiary flood peak.	32	39	7 ± *9.2*
4c	05/05/97-06/05/97	Fluvial entrainment or a slab failure.	0	81	81 ± *9.2*
4d	26/06/97-30/06/97	No erosion during first flood peak, erosion occurs during secondary higher flood.	0	31	31 ± *9.2*
4e	14/07/97	Desiccation or sheep disturbance depositing material on to the sensor.	17	0	-17 ± *9.2*
4f	19/08/97-20/08/97	Desiccation or rainsplash erosion depositing material on to the sensor.	10	0	-10 ± *9.2*
4g	08/12/97 - 12/12/97	Complete exposure of PEEP in one flood event. Most likely mass failure due to the amount of erosion, could however be a large entrainment event.	0	> 116	>116 ± *4.6*
4h	11/02/98-13/02/98	Direct entrainment	0	37	37 ± *9.2*
4i	01/03/98 - 11/03/98	Entrainment during first flood event, followed deposition/smearing after the second flood, and further entrainment after the third flood.	30	23 + 32	25 ± *9.2*
9a	04/02/97 - 06/02/97	Complete exposure of PEEP during a flood proceeded by frost events. The erosion could be a mass failure with no time delay on the flood receding limb.	0	> 79	> 79 ± *4.4*
9b	28/04/97-05/05/97	Direct soil fall followed by PEEP burial by a collapse on the upper bank.	20 + 67	0	-87 ± *8.9*
9c	30/06/97-03/07/97	Re-exposure of buried sensor by entrainment and wet flow.	0	85	85 ± *8.9*
8a	12/01/97 - 14/01/97	Direct entrainment of bank material preceded by frost events followed by more frost action. Then further erosion due to direct soil fall or rainsplash erosion.	0	36 + 5	41 ± *14.0*
8b	04/02/97-06/02/97	Entrainment during flood. No erosion during following subsidiary flood peak flow.	0	10	10 ± *14.0*
8c	11/08/97-17/08/97	Rainsplash erosion of previously desiccated bank material.	0	23	23 ± *14.0*
8d	27/08/97	Cantilever failure during dry conditions	0	> 100	>100 ± *7.0*
10a	03/02/97-06/02/97	Fluvial entrainment proceeded by frost events.	0	74	74 ± *5.7*
10b	28/04/97-07/05/97	Cantilever or slab failure completely exposing the sensor after the flood has receded. Burying the lower bank PEEP, number 9	0	> 155	>155 ± *2.8*

Table 6.7 A description of the erosion and deposition events that occurred at Greystone Farm: (**4**) PEEP 4 Downstream Lower; (**9**) PEEP 9 Upstream Lower; (**8**) PEEP 8 Downstream Upper; (**10**) PEEP 10 Downstream Upper. Net erosion errors are based on a 95 % confidence interval of the calibration regression standard error (Table 3.8).

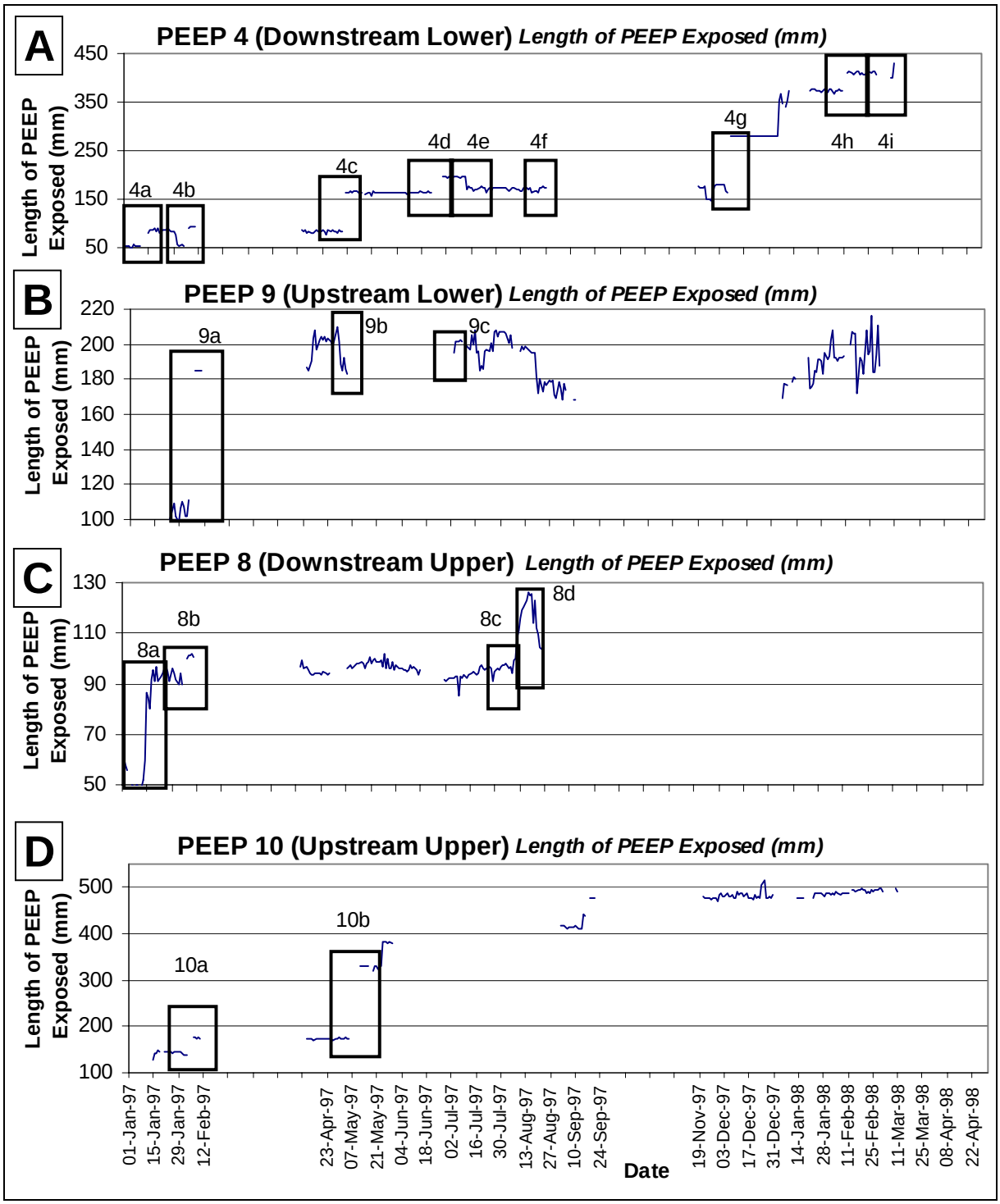

Figure 6.20 A time-series of erosion/deposition events (highlighted in boxes) described in Table 6.7 for Greystone Farm (Site 8): (**A**) PEEP 4 Downstream Lower; (**B**) PEEP 9 Upstream Lower; (**C**) PEEP 8 Downstream Upper; (**D**) PEEP 10 Upstream Upper.

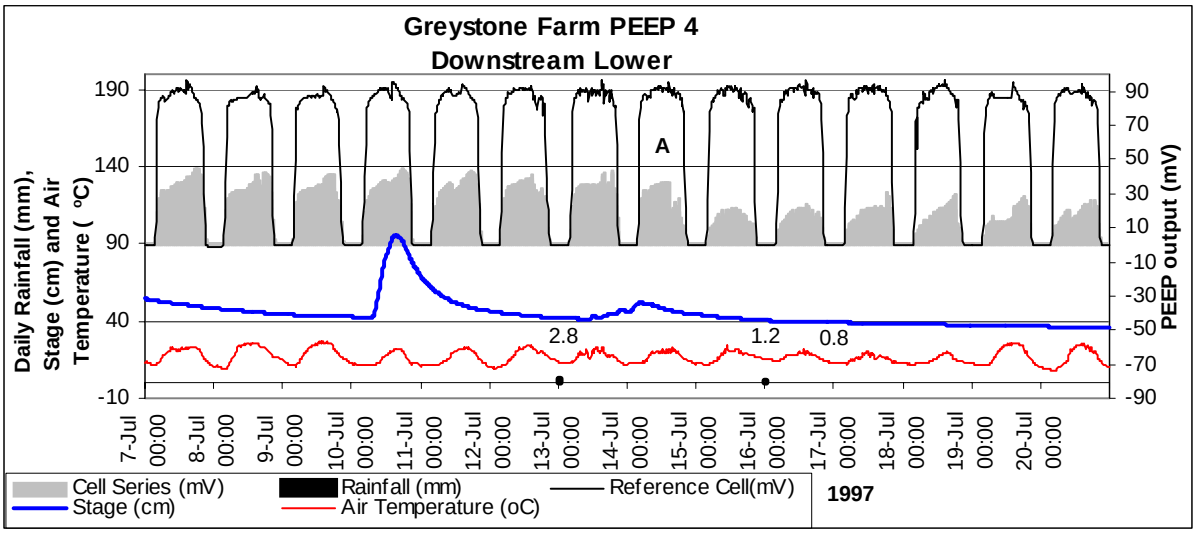

Figure 6.21 Desiccation or animal disturbance depositing sediment on to, or around the sensor at (**A**). PEEP 4 in the downstream lower section of the bank at Greystone Farm, 07/07/97-20/07/97. The low daily values of rainfall are highlighted by labelling them with their values in mm day^{-1}.

It was unlikely that desiccation alone caused the erosion on the downstream upper PEEP (PEEP 8) (Figure 6.22) (Table 6.7 *8c*). The gradual increase in PEEP output could be due to desiccation at first on the 12/08/97. The rainfall event on the 13/08/00 would have been expected to remove sediment on the bank that was loosened by desiccation. It did not, however, appear to produce a sudden increase in voltage output expected if rainsplash erosion was taking place. Just over a week after the desiccation event on PEEP 8 the entire PEEP was exposed (Plate 6.12) (Figure 6.23) (Table 6.7 *8e*). This may have been due to the drying of the interface between a cantilever block and the main bank. The enlargement of any crack between the two surfaces would decrease the shear strength, and if the cantilever block remained fairly moist with only surface drying it would have produced a relatively high shear stress.

The flood on the 06/05/97 affected both the upstream PEEPs, numbers 9 and 10 (Figures 6.24 and 6.25) (Table 6.7 *9b* and *10b*), as well as the downstream lower PEEP (PEEP 4) (Table 6.7 *4c*). High daily rainfall rates of up to 12 mm day^{-1} occurred during the three days preceding the flood event. This would have the effect of wetting up the bank, which a flood peak of short duration would be unlikely to do effectively. The upper bank (PEEP 10) did not erode until the flood wave had passed (Figure 6.25): the sensor was left completely exposed after > 155 mm of erosion at least 24 hours after the flood peak. This was indicative of a mass failure, or delayed cantilever failure (Lawler and Leeks, 1992). Using the expert system (Figure 6.6) the presence of overhanging bank material before the event would lead to the conclusion that a cantilever failure

took place. The much lower output produced by the reference cell and exposed cell series on complete exposure, could either be the effect of moisture entering the PEEP, or the sensor falling against the bank surface because of the lack of supporting bank material.

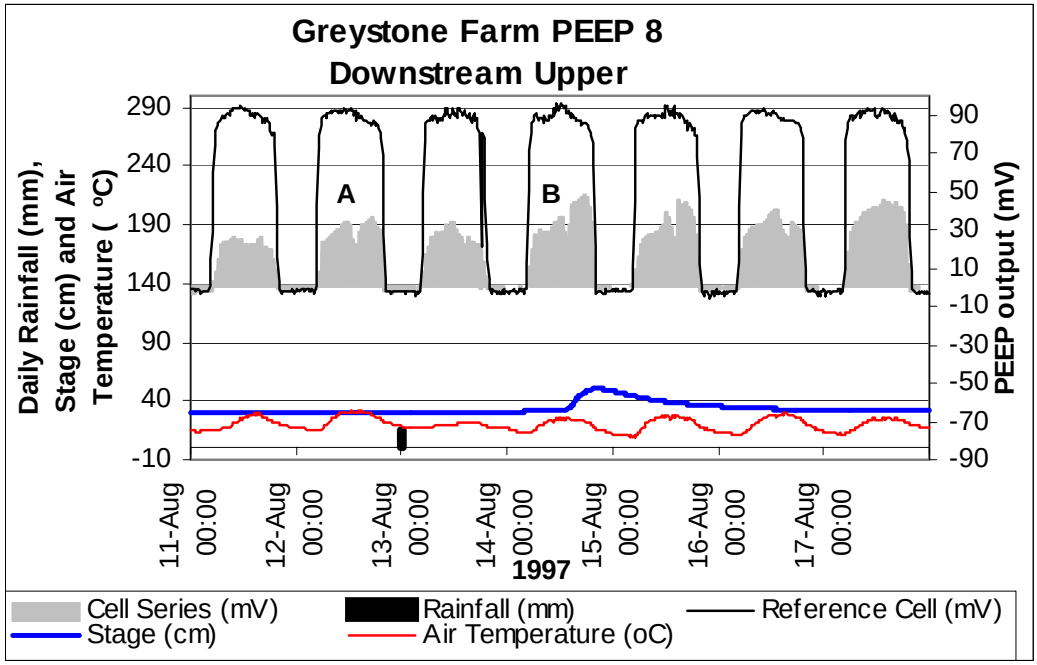

Figure 6.22 Erosion of desiccated material (**A** and **B**), possibly influenced by the rainfall event on 13/08/97. PEEP 8 in the downstream upper section of the bank at Greystone Farm, 11/08/97-17/08/97.

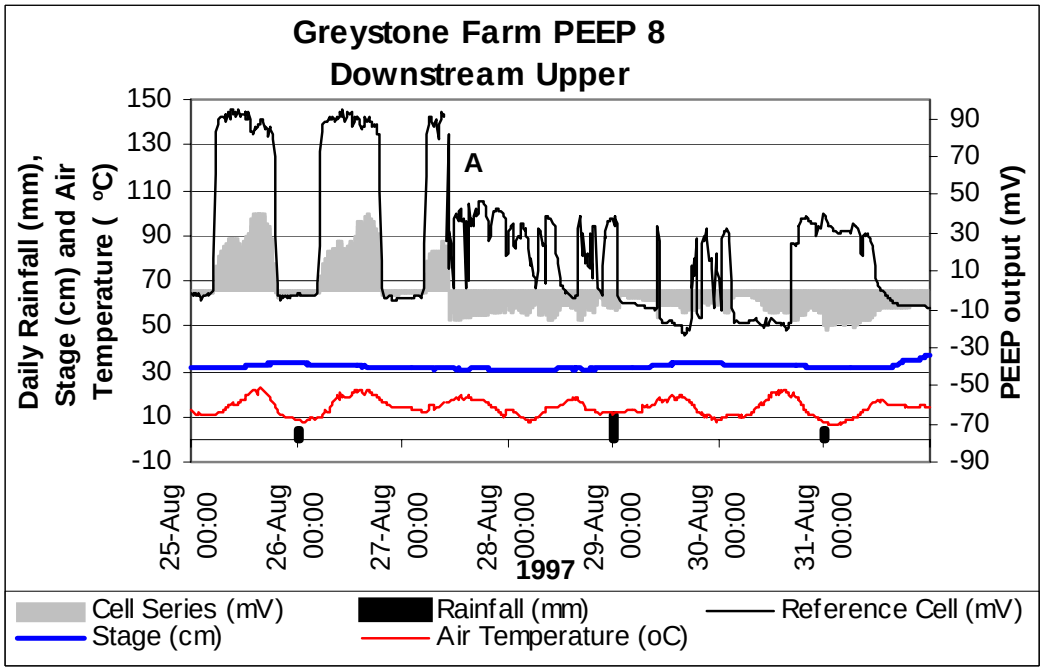

Figure 6.23 Complete exposure of the sensor (**A**) caused by a cantilever collapse of surrounding material. The failure was observed at the following downloading session. PEEP 8 in the downstream upper section of the bank at Greystone Farm, 25/08/97-31/08/97.

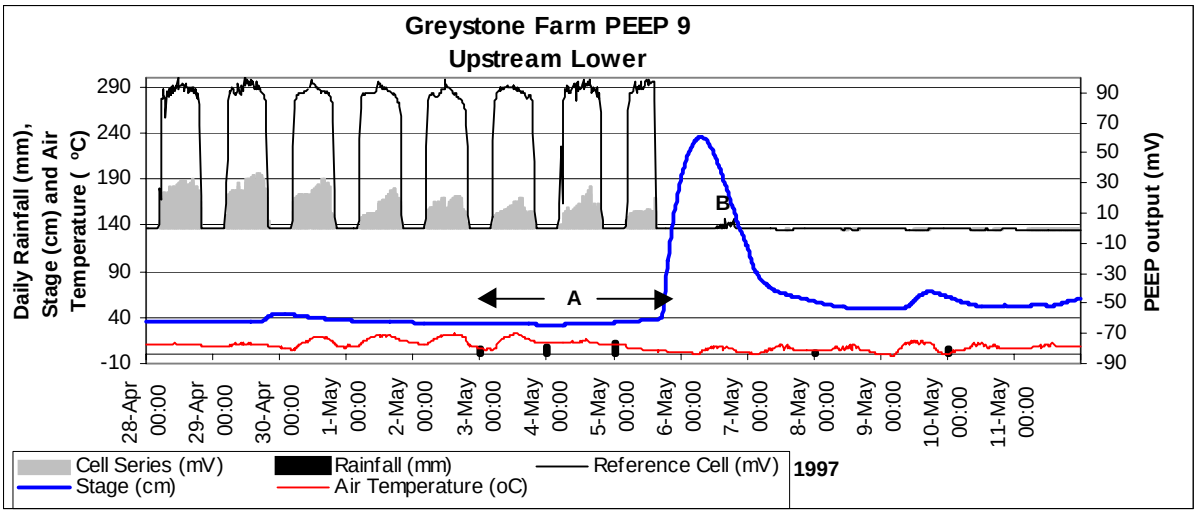

Figure 6.24 Complete burial of PEEP 9 during an upper bank cantilever collapse (**B**), that was preceeded by rainfall events from the 03/05/97-05/05/97 (**A**). PEEP 9 in the upstream lower section of the bank at Greystone Farm, 28/04/97-11/05/97.

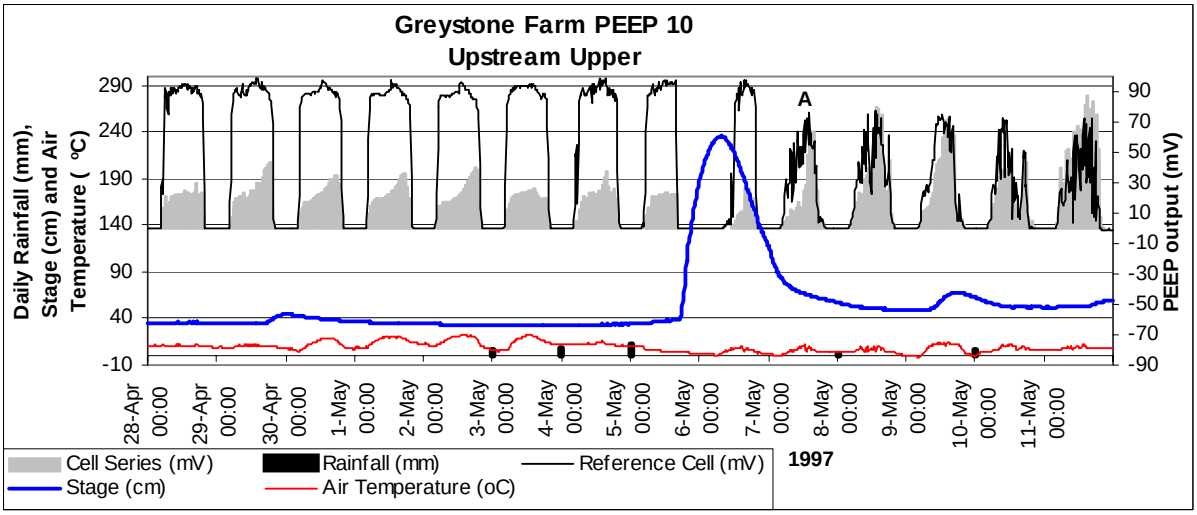

Figure 6.25 A cantilever collapse (**A**) eroding PEEP 10 in the upper bank at Greystone Farm, 28/04/97-11/05/97.

The lower bank PEEP (PEEP 9) (Figure 6.24) ended up completely buried by the upper bank sediment. It is difficult to determine whether the deposition occurred at the same time as the erosion around the upper PEEP. The small signal from the reference cell on the 06/05/97 could be from partial burial of PEEP 9 from overlying bank material or it could be that the sensor was still partially covered by the floodwater. For the following days a signal of around 0 mV was observable from both the cell series and the reference cell, indicating complete burial by the upper bank collapse.

During the two flood peaks that passed through Greystone Farm from the 26/06/97 to 01/07/97 both of the lower bank PEEPs (4 and 9) were eroded (Table 6.7 *4d* and *9c*). The upstream PEEP (PEEP 9) that was buried almost two months previously was re-exposed by the twin peaked flood event (Figure 6.26). Partial exposure of the sensor occurred after the second flood peak had passed through the monitoring site, however re-burial then took place. This may have been by the flood entraining the lower bank material thus making the overlying sediment unstable which then collapsed burying the PEEP again. The actual sustained exposure of the PEEP took place on the 03/07/97, leaving the sensor exposed by 20.1 mm (Figure 6.26).

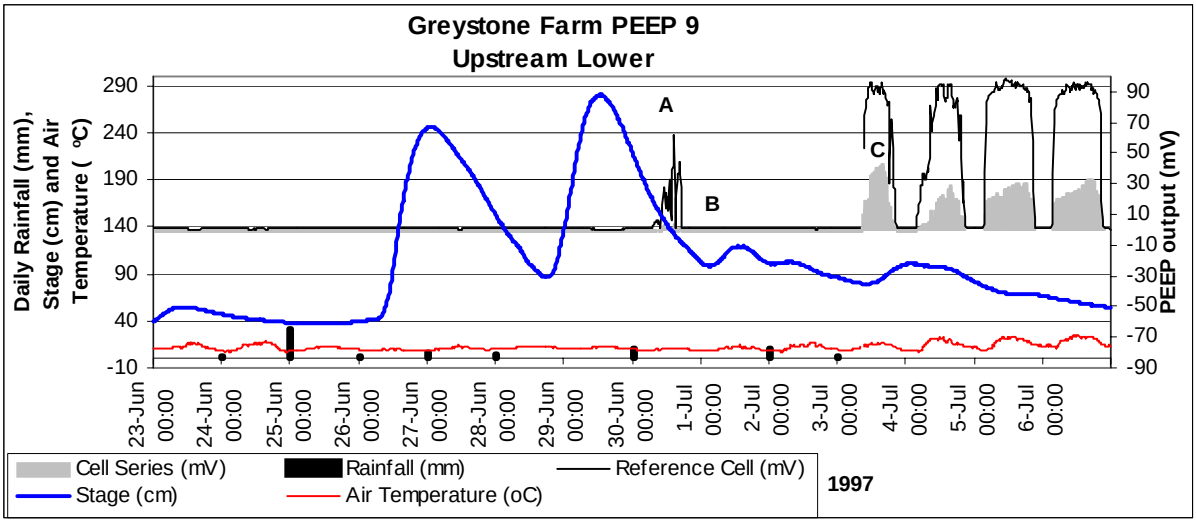

Figure 6.26 The re-exposure of the previously buried upstream lower PEEP (**C**). The PEEP was partially exposed at (**A**) then re-buried at (**B**). PEEP 9 in the upstream lower section of the bank at Greystone Farm, 23/06/97-06/07/97.

The upstream lower PEEP (PEEP 4) (Figure 6.27) (Table 6.7 *4d*) was above the river water level on the 29/06/97 between both peak flows. This period of re-exposure showed that no erosion had taken place during the first peak flow. On the second slightly higher flood peak, with a stage of 2.79 m, 32.2 mm of erosion occurred. The period of inundation on the first flood event could have aided the erosion by increasing the soil moisture content. With the decrease in support from the floodwater the bank may have collapsed immediately in the form of a small mass failure, or the increase in pore water pressure may have aided entrainment.

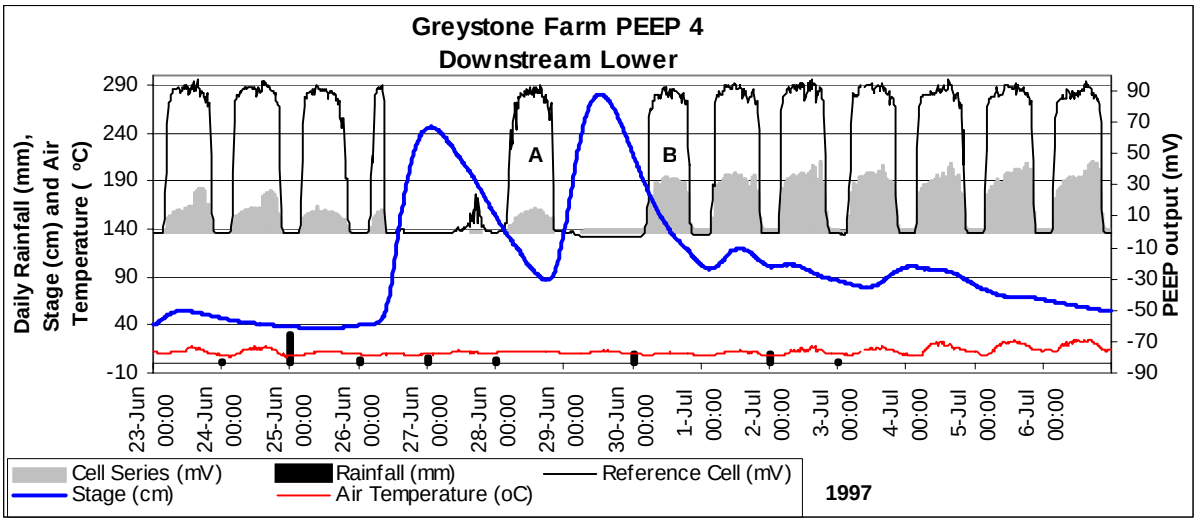

Figure 6.27 The delayed erosion of the lower bank until after the second flood peak had passed through the catchment (**B**), shown by the lack of erosion when the sensor was revealed after the first flood event (**A**). PEEP 4 in the downstream lower section of the bank at Greystone Farm, 23/06/97-06/07/97.

Manually Observed Processes of Erosion and Deposition

Larger scale failures were evident at Morton-on-Swale (Site 7), Greystone Farm (Site 8), and Topcliffe (Site 9). All three of the lower-basin sites were, as with all the other monitoring sites, subject to cantilever failures. The long toe slope as Morton-on-Swale allowed cantilever failed blocks to 'decompose' above the low water level (Plate 6.13). At the other two sites the failed blocks often ended up in the river channel, leading to a faster rate of removal. At Greystone Farm beam failures were often observed as well as other forms of cantilever failure (Thorne and Tovey, 1981) (Plate 5.5). Tension cracking occurred in previously beam failed structures at Topcliffe, increasing the rate of infiltration, and thus pore pressures, behind the slope (Darby and Thorne, 1994) (Plate 6.14).

All three of the monitoring sites were influenced by different modes of biogenic activity, one of which was through the burrowing of sand martins during the summer months. The shallower toe area, compared to the banks upstream, provided more access for sheep and horses (Trimble, 1994; Trimble and Mendel, 1995; Sansom, 1996). It is difficult to quantify the effects of the disturbance caused by trampling and burrowing within the bank. However the amount of disturbance was greater than that observed at the upstream sites.

Mass failures were only observed at the mid catchment and downstream sites. These failures tended to be spatially widespread but temporally intermittent. At Topcliffe, failure of the entire slope may be due to removal of basal material by entrainment, creating conditions for a translational failure plane (Plate 6.15). Undercutting of basal material may also be responsible for the creation of slab failures at Topcliffe (Plate 6.16).

Using the downstream trends in erosion processes identified in this and the preceding chapters the model suggested by Lawler (1992a; 1995) can be evaluated in the next chapter. This will be alongside putting the monitored erosion sites in context globally and within the U.K.

6.5 SUMMARY

1. Although the PEEPs have been able to monitor erosion and deposition events effectively throughout the catchment they did not correlate well with erosion pin measurements at an erosion epoch timescale. The spatial extrapolation of the high temporal resolution data, provided by the small number of PEEPs, to the whole bank must be undertaken with care and using other supporting data i.e. field observations and erosion pin readings.

2. Photovoltaic ratios taken from the midday region of the daily time-series data provide the reliable data on which to estimate daily lengths of exposure of the sensors. This in turn enables a long time series of data to be examined to identify critical erosion and deposition periods.

3. Observing the PEEP data in more detail revealed the importance of frost events upstream at Beck Meetings (Site 1) in preparing material for entrainment. Mid-catchment, at Low Row (Site 4), frost was also important in preparing the bank material for entrainment; however deposition of frost heaved material was not as common as upstream at Beck Meetings. Piping and sapping were also thought to be responsible for the erosion around the PEEPs at Low Row. At Greystone Farm larger failures were monitored by the PEEPs, with cantilever failures and slab failures thought to be responsible for leaving the sensors completely exposed after flood events. Desiccation and animal disturbance was also noted downstream.

Plate 6.1 An example of needle ice growth at Beck Meetings (Site 1) (28/02/96). The top yellow erosion pin tip is 30 mm in length, and mid-bank another erosion pin is only just visible because of surrounding ice growth. Stream flow is out of the picture.

Plate 6.2 The accumulation of frost heaved sediment deposited in the basal region at Beck Meetings (Site 1) after the ice has melted (28/02/97). The tripod on the right of the frame was 1.2 m in height. Stream flow is out of the picture.

Plate 6.3 The accumulation of vegetative debris around the pressure transducer housing on the left-hand side of the frame at Beck Meetings (Site 1) (28/02/97). Flow is out of the picture.

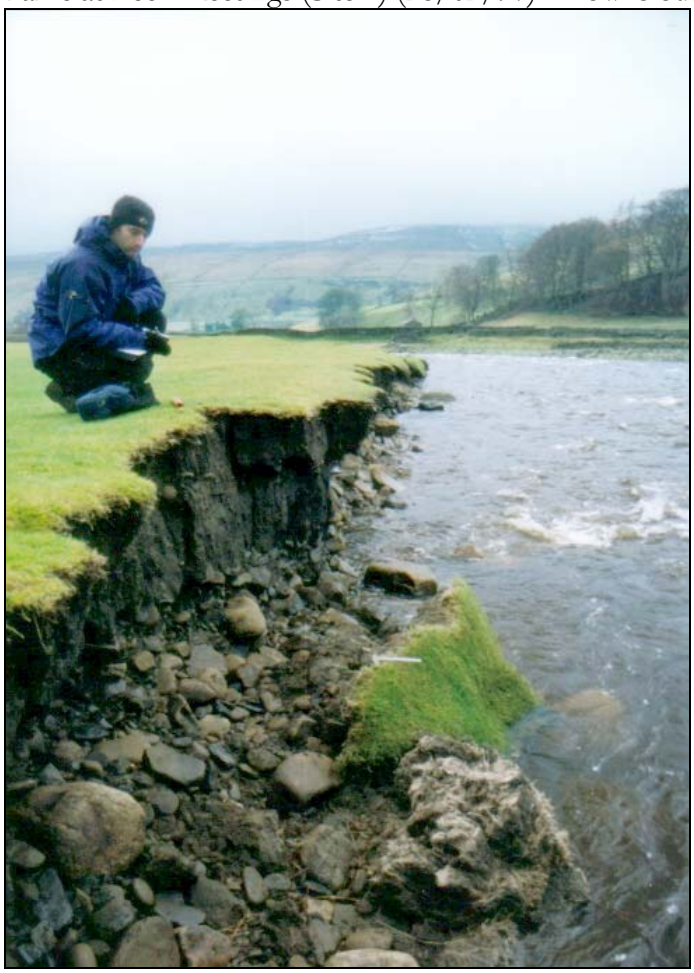

Plate 6.4 Two toppled cantilever failures at Muker (Site 3) (07/01/98). The callipers on the failed block are 120 mm in length. River flow is into the picture.

Plate 6.5 An overhanging grassmatt on the right of the frame, at Hoggarths (Site 2) (18/02/96). The callipers on the A4 file are 120 mm in length. The ends of the two erosion pins in the grassmatt are exposed by 30 mm. Flow is into the picture.

Plate 6.6 An example of the desiccated structure of the peat surface at Beck Meetings (Site 1) (20/10/96). The cracks in the dried surface are creating a flow path in the centre of the frame. The bank height is approximately 1.2 m. Stream flow is from left to right of the picture.

Plate 6.7 Hollows created along the bank profile at Low Row (Site 4) from piping and sapping (09/06/97). Two 30 mm diameter yellow erosion pins are visible in the foreground. The grass on the bank toe is the remains of previously failed cantilever blocks. Flow is out of the picture.

Plate 6.8 An example of overhanging upper bank material along the reach at Reeth (Site 5) (23/10/96), with some failed cantilever blocks resting on the bank toe. River flow is from left to right of the picture.

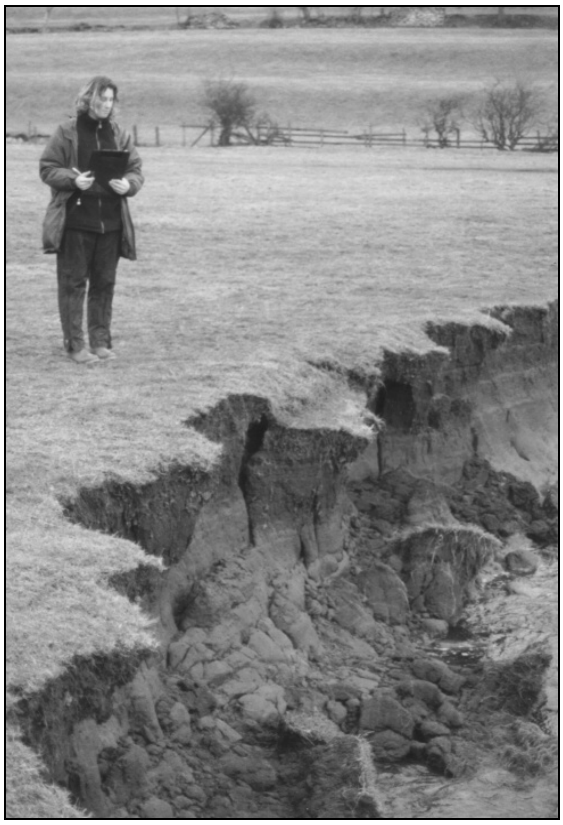

Plate 6.9 A series of failed, or failing, slab failures at Reeth (Site 5) (15/01/97). River flow is from left to right of the picture.

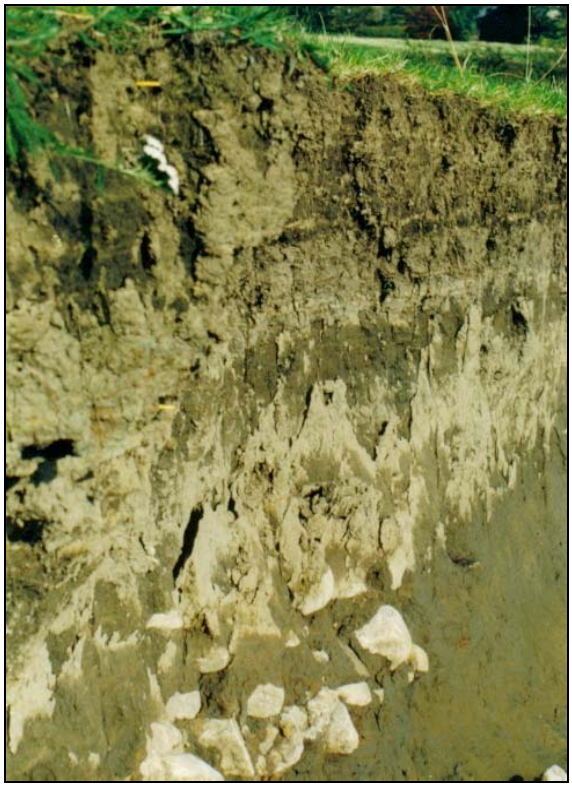

Plate 6.10 Sheets of desiccated material at Reeth (Site 5) (23/10/96). The ends of the two yellow erosion pins exposed are 30 mm are visible in the foreground. Flow is from left to right of the picture.

Plate 6.11 Exposed roots cause by rapid erosion at Easby (Site 6) (09/06/97). The bank height is approximately 2.5 m. River flow is out of the picture.

Plate 6.12 A PEEP 8 monitored cantilever failure at Greystone Farm (Site 8) (27/08/97) (Table 6.10 *8d*). The exposed sensor hanging in the centre of the picture is 450 mm in length. Flow is out of the picture.

Plate 6.13 Grass covered cantilever failed blocks lying on the bank toe at Morton-on-Swale (Site 7) (25/05/97). The height of the bank shown is approximately 4 m. River flow is into the picture.

Plate 6.14 A tension crack running along the back of a previously beam failed block, in the centre of the frame. The picture was taken on 27/02/97 at Topcliffe Farm (Site 9). The black book resting on the block is A4 in size. River flow is into the picture.

Plate 6.15 A translational failure observed at Topcliffe Farm (Site 9) (27/02/97). The failure plane surface can be observed on the left-hand side of the failure. The top of the failure led to undercutting of the bank, and then a cantilever failure. The black book lying in centre frame is A4 in size. River flow is from left to right of the picture.

Plate 6.16 An example of a slab failure at Topcliffe (Site 9) (27/02/97). The block probably became unstable because of undercutting of basal material by fluvial entrainment, as well as an increase in pore water pressure and material weight on saturation. The bank height is approximately 2 m, and river flow is out of the picture.

CHAPTER 7

AN EMPIRICAL MODEL OF BANK EROSION PROCESS EFFICACY THROUGHOUT A CATCHMENT

7.1 INTRODUCTION

Catchment scale, and annual, variations in erosion rates have been monitored within the River Swale system (Chapter 4). The data provided by pin measurements have allowed erosion processes to be inferred using multivariate analysis (Chapter 5). Data of finer temporal resolution, provided by the PEEPs (Chapter 6), has allowed processes, and process sequences, to be identified at an event time-scale. These combinations of data mean that the spatial distribution of erosion processes can be determined throughout the catchment.

This chapter seeks to test the model proposed by Lawler (1992a; 1995) (Figure 1.1) by synthesising the data on rates and processes into a model describing downstream change of erosion process efficacy for the Swale catchment. The change in the temporal distribution of rates and processes at an annual time interval will also be examined for the upper, middle, and lower catchment.

So that this work may be placed in a global context it will be compared against other studies of erosion rates at differing drainage basin scales. The downstream change in catchment characteristics and processes will also be contrasted against previous catchment scale models in both temporal and spatial dimensions.

7.2 MODELS OF BANK EROSION PROCESS EFFICACY AT A CATCHMENT SCALE

7.2.1 An Empirical Model for the River Swale

Combining and summarising the findings from Chapters 4 - 6 allows the testing of the downstream change in processes model suggested by Lawler (1992a; 1995) (Figure 1.1). The downstream changes in efficacy of the four main process categories (Frost Action, Desiccation, Fluid Entrainment, and Mass Failure) are presented for the River Swale during the study (Figure 7.1), and for a catchment of idealised hydro-geomorphological characteristics (Figure 7.2). The distributions of the four main process groups are outlined in Table 7.1 and Figure 7.1 for the monitored sites on the River Swale (Figure 3.5).

CATCHMENT SEGMENT	PROCESS	DOWNSTREAM PROCESS TRENDS
UPSTREAM *(Sites 1-3)*	Frost Action	The maximum rates occurred in the upper catchment, with a decreasing influence downstream as: 1. The water availability on the bank lowered as the bank becomes less peaty. 2. The length of the frost season decreased.
	Desiccation	This was observed when peaty sediment dried in the summer at Site 1; however no sediment erosion was recorded.
	Fluid Entrainment	Entrainment was limited by the amount of frost preparation. There was sufficient energy to remove all the prepared material at the sites, so the efficiency is on a par with frost action at Site 1. The energy was not sufficient to remove all the failed cantilever blocks from the basal region; however, the energy available to do this increased downstream. The stream power may be 'artifically' increased at Site 3 due to a bedrock reach upstream.
	Mass Failure	Only observed in the form of cantilever failures, which increased in efficacy downstream because of the trend in fluid entrainment, causing undercutting.
MID-CATCHMENT *(Sites 4-6)*	Frost Action	Due to the limitations of the bank sedimentology on fluid entrainment, at Site 4, the efficacy of frost action increased compared to Site 3. The efficacy declined at Sites 5 and 6 for the same reasons as at the upstream sites, and as other processes became more efficient.
	Desiccation	There was no PEEP or pin evidence that material was eroded through desiccation, although surface sheets of sediment were heaved from the bank at Site 6, perhaps preparing the bank surface.
	Fluid Entrainment	Limited entrainment at Site 4 but increasing in efficacy, to a catchment peak, as the second stream power peak at Site 6 was reached. Almost all the basal failed debris at Sites 5 and 6 was removed leaving the bank unsupported.
	Mass Failure	Slab and Pop-out failures were observed at Site 5, the first monitoring site experiencing mass failures (excluding cantilever failures). No mass failures were observed *in situ* at Site 6, however this does not mean that they did not occur. The root mass left exposed by erosion indicates that wet flows would be the principle mechanism of failure if mass failures had occurred.
DOWNSTREAM *(Sites 7-9)*	Frost Action	The influence of frost action increased at Site 7 (Section 5.4), this may be due to the bank sedimentology, or flow structure, being restrictive for other erosional processes. There was a slight rise in efficacy downstream, at Sites 8 and 9, as the amount of erosion from other processes decreased but frost heaving only slightly declined in efficacy.
	Desiccation	Desiccation was thought to be effective at influencing erosion at Site 7, resulting in a more attenuated annual erosion pattern, including the summer months (Figure 5.1). The influence of desiccation increased downstream as the climate changed to drier conditions.
	Fluid Entrainment	As the stream power decreased downstream so did the ability of the flow to entrain failed basal debris. The more cohesive nature of the bank sediment also restricted the amount of direct entrainment of surficial material.
	Mass Failure	As mass failure events decreased in frequency their efficacy also decreased in a downstream direction (Section 7.2.5). The magnitude of the failures increases downstream with a higher potential for translational, and rotational failures.

Table 7.1 The upper, middle and lower catchment distribution of erosion process efficacy. The processes under consideration are frost action, desiccation, fluid entrainment, and mass failure.

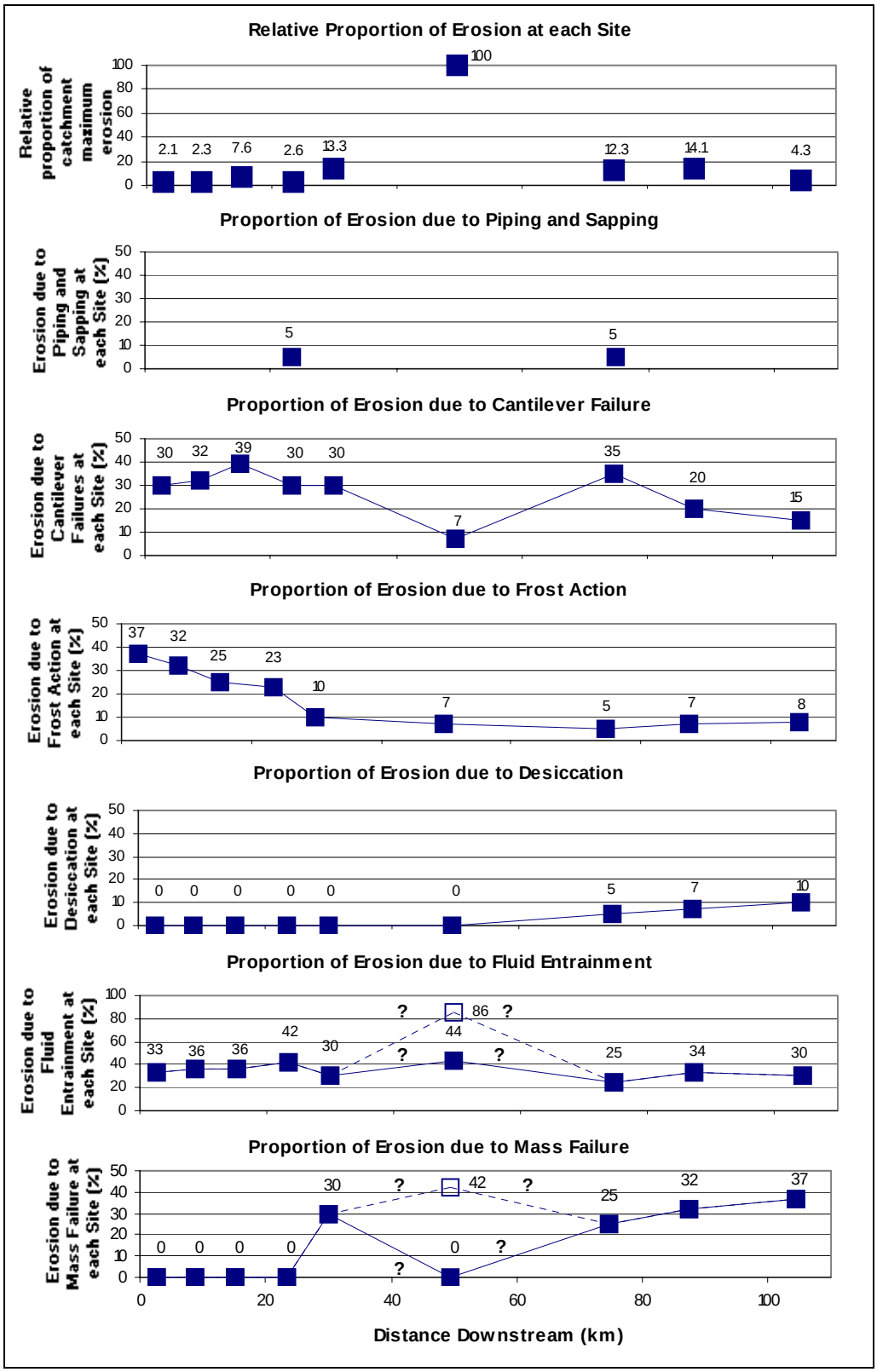

Figure 7.1 Relative erosion dominance at each site throughout the River Swale, in terms of frost action, desiccation, fluid entrainment, and mass failure. The probability of sapping erosion and cantilever failures is included on separate plots because of their greater spatial variance. The relative proportion of maximum catchment erosion allows the efficacies of each process to be compared throughout the catchment.

In the River Swale study (Figure 7.1) there appeared to be an identifiable downstream change in sub-aerial processes, fluvial entrainment and mass failures. The sedimentology of the bank, however, made the spatial prediction of cantilever failures, piping, sapping and pop-out failures awkward. The location of composite banks is crucial to the degree of undercutting, and hence to the distribution of cantilever failures (Thorne and Tovey, 1981; Rinaldi and Casagali, 1999). A peak in stream power mid-basin may increase the potential for entrainment of noncohesive basal material, resulting in cantilever failures being the dominant form of erosion. This may account for the selection by Harris (1996) of a region of cantilever failures in the mid-basin region. The formation of a composite bank with large clasts in the basal region is more likely to occur upstream, due to the downstream fining of bed material (Ferguson, 1981). There was in the Swale system, however, the potential for the river to erode into an area of glacial moraines, supplying large clasts to the channel which may be deposited as on the river bed, potentially forming channel bars. These bars could over time lead to the formation of a composite bank structure, disturbing the theorised downstream fining trend. Tributaries may also alter the degree of bed and bank material grain size fining.

The position of bedrock sections within the downstream profile may alter the downstream trend in stream power (Ahnert, 1994). The increase in velocities through bedrock reaches may result in a specific change in erosion processes. For example downstream of the bedrock reaches entrainment should be higher compared to the other sites in the region e.g. Muker (Site 3) and Easby (Site 6).

The occurrence of sandy horizons within the bank profile increases the likelihood of piping and sapping (Jones, 1981), as well as pop-out failures. The potential for sand deposition is enhanced in the middle reaches of the basin (Figures 4.6 – 4.8). The rapid draining of the bank is needed to produce the high pressures that destabilise the bank material. The flood hydrograph needs to be prolonged enough to saturate the bank material, which should ideally be of a consistency that will allow a reasonably rapid ingress of floodwater but not drain instantly, i.e. silty material (Hagerty, 1991a). The longest periods of inundation would occur downstream; however the cohesive bank material in this region would limit the infiltration of the water. The falling limb on the hydrograph should also be reasonably quick in order to create a rapid outflow from the bank. Rapid stage fluctuations occurred at the upstream sites; however, it is thought that the coarser

bank material did not allow the creation of high-energy preferential flow paths. Thus the mid-catchment reaches have the highest potential for piping, sapping and pop-out failures (Figure 7.1) as they contain the optimum situation of bank sedimentology (Figures 4.6 – 4.8) and flood hydrograph shape (Figures 6.15 – 6.19).

The conceptual model presented by Lawler (1992a; 1995) was correct in its assumptions of decreasing frost frequency downstream coupled with increasing amounts of desiccation, when tested on the River Swale. In terms of erosion efficacy in subaerial processes the decline in efficacy of other processes downstream results in subaerial preparation, and erosion, becoming more influential in the downstream reaches, which was not predicted (Lawler, 1992a; 1995).

The potential fluvial entrainment, which in this study considers the ability of the river to entrain prepared, failed, and *in situ* bank material, was theoretically meant to be maximised mid-catchment due to the increase in stream power in this region. Two peaks in stream power were thought to exist in the Swale catchment, possibly formed as a result of bedrock reaches immediately upstream of the monitoring sites lowering the channel boundary resistance. The bimodal distribution results in distortion of the predicted efficacy of fluid entrainment; however, a mid-basin peak was still thought to have existed in this process on the Swale.

Mass failures, not including cantilever failures, were observed at the monitoring sites from Reeth downstream. The bank heights at the monitoring sites did not increase downstream, so the prediction that a critical bank height should be reached before mass failures occurred was not validated on the Swale. The combination of bank height, bank sediment size, and efficacy of basal entrainment are probably a more comprehensive combination of predictive variables. The efficacy of mass failures was not thought to increase downstream, instead larger failures were proposed to occur less frequently.

These findings will be explored in more detail in Sections 7.3-7.5.

7.2.2 A Model of Erosion Process Efficacy in an Idealised Catchment

The concepts of process distribution produced from the Swale catchment may be transferred to a more general case (Figure 7.2). This allowed the variability associated with the specific

morphology of the Swale to be removed whilst retaining all the process distribution concepts, making the model more generally applicable.

An ideal catchment would, in terms of the downstream change in bank erosion predictions, contain:

1. A decreasing frequency of frosts downstream;
2. Increasing summer temperatures downstream;
3. A decreasing annual rainfall downstream;
4. One stream power peak in the middle of the catchment;
5. A decreasing bank sediment size downstream;
6. Increasing bank height downstream;
7. Composite banks with large uncohesive basal clasts in the upstream reaches;
8. Sand pipes within silty-sand sediment in the middle or upper middle catchment region.

The downstream trend of erosion processes (Figure 7.2) would be similar to that in the Swale (Figure 7.1). Frost action would decrease in efficacy downstream until the mid-catchment, alongside decreasing frost frequencies, but would increase as other processes decline in efficacy downstream. Desiccation would not be influential upstream, and would increase in efficacy downstream. Entrainment would increase in efficacy to a maximum mid-catchment, decreasing again downstream. Mass failures, excluding cantilever failures, would be at maximum efficacy once the bank height, sedimentology and basal entrainment had reached a point at which failures could occur. They would then decrease in significance downstream.

Lawler (1992a; 1995) proposed that the processes of subaerial preparation, fluid entrainment, and mass failure should systematically vary with distance downstream (Section 1.1.2). The variable of distance from river source is probably a poor predictive tool in terms of stream power; with different catchment shapes, longitudinal slope profiles and drainage densities all affecting the distribution of both slope and discharge. Knighton (1999) found that the large increase in mid-basin discharge associated with a series of large, closely spaced tributaries, moved the stream power peak far downstream on the River Trent. Ideally an index that could effectively be used in models of the eight variables listed above would be used instead of distance downstream; however, currently distance downstream is the most comprehensive variable available.

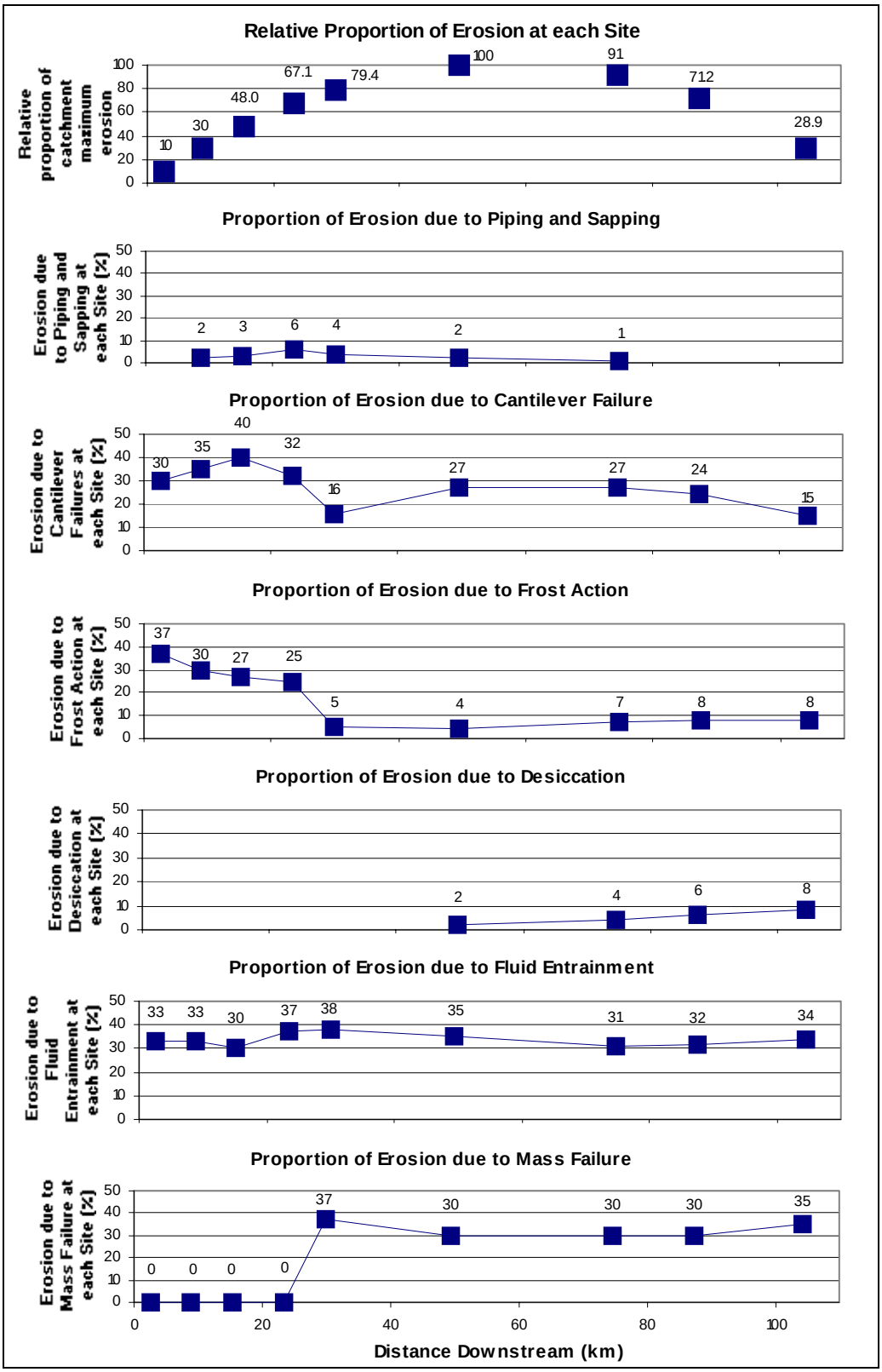

Figure 7.2 A general model of erosion process efficacy throughout an 'ideal' catchment. The probabilities of sapping erosion and cantilever failures are included on separate plots due to their greater spatial variation. The relative proportion of maximum catchment erosion, calculated from Equation 4.2, allow the efficacies of each process to be compared throughout the catchment.

7.2.3 The Catchment Scale Distribution of Preparation Processes

In the model by Lawler (1995) a distinction was made between freeze-thaw and desiccation efficacy downstream (Figure 1.1). Freeze-thaw activity decreased in relation to the reduction in frost frequencies downstream (Lawler, 1988b). Desiccation processes were predicted to increase in a downstream direction alongside decreasing rainfall, increasing summer air temperatures, and higher evapotranspiration rates.

In theory, the influence of frost action should decline downstream in the erosion pin multivariate models of erosion (Section 5.4), as should the amount of erosion identified during PEEP measured events (Section 6.4). The incidence of BANKFROST% and AIRFROST% (Table 5.3) only appeared to dominate in multivariate models at Low Row (Site 4), and for some erosion variables at Morton-on-Swale (Tables 5.5 - 5.8). The PEEP data from Beck Meetings (Site 1) indicated the influence of sub-zero events in preparing the bank surface for entrainment (Table 6.5). The seasonality in bank erosion rates, from Beck Meetings (Sites 1) to Hoggarths (Site 3), also indicated the influence of sub-zero temperatures in causing erosion or preparing the bank material for entrainment, because of the greater erosion during the winter periods (Figures 5.1A - C).

The inclusion of periods of frost within the erosion pin time-series model at Low Row (Site 4) (Table 5.5 - 5.8) indicated that the frost events at this site are able to prepare and erode the bank material during an erosion epoch. The 15-minute data from the periods before, during, and after erosion events at Low Row (Section 6.4.3) do not produce the same deposition-erosion sequence experienced upstream at Beck Meetings (Section 6.4.2). The action of frost on the bank may not be the same at different sites. The growth of needle ice pushing sediment and ice out over the PEEPs at Beck Meetings was not registered as often at Low Row (Table 6.6). The bank material structure/cohesion may be weakened by ice growth in sediment voids (Harry, 1986) but the sediment may not be eroded by ice heaving, simply remaining *in situ* in its lowered shear strength state. The scour/piping hollows around the PEEPs at this site may desensitise the sensors to small changes in bank elevation, so that the growth of ice and sediment heaving may not actually be observed during frost events. The flood events that did cause entrainment were mostly those

that were preceded by frost (Table 6.6), which indicated that sub-zero temperatures were causing a weakening of the bank structure and preparing the sediment for erosion.

The lower catchment did experience depositional events during sub-zero temperatures preceding flood events that entrained bank material (Table 6.7), indicating both erosion and preparation of the bank from frost action. Frost frequencies were lower at Greystone Farm (Site 8) with the period that material was heaved from the bank being shorter than at both Beck Meetings and Low Row (Figure 6.10). At the downstream sites, the distribution of frost action may also be more dependent on the degree of shading on the bank surface, reducing the amount of insolation.

Periods of desiccation were evident at Greystone Farm (Site 8), contributing a small amount of erosion to the annual budget (Table 6.7). This is unlike the desiccation of peat at Beck Meetings (Site 1), which did not appear to become destabilised. The desiccation at Greystone Farm (Site 8) occurred during periods of low flow. During these periods there were also high intensity rainfall events, which probably aided the removal of the dried material (Table 6.7 *4f* and *8c*). Desiccation was also observed in the field at both Morton-on-Swale (Site 7) and Topcliffe (Site 9).

The erosion pin data may be used to assess the relative significance of desiccation and frost action at each of the sites. The correlation coefficients (r) between ERRATE (Section 5.3.3) and independent variables thought to be associated with each process are compared throughout the catchment in Figure 7.3. The regions of greater process efficacy should be associated with more significant r-values. Care must be used in interpretation of the correlation results, as the direction of the relationship will be dependent on whether the r-value is positive or negative. Using individual variables will also be more subjective than multivariate techniques. They do, however, allow comprehensive comparison of the relationship strengths between sites throughout the catchment.

AIRFROST%, BANKFROST% and FTCYC% (Table 5.3) were selected to model the distribution of frost action processes (Figure 7.3 A).

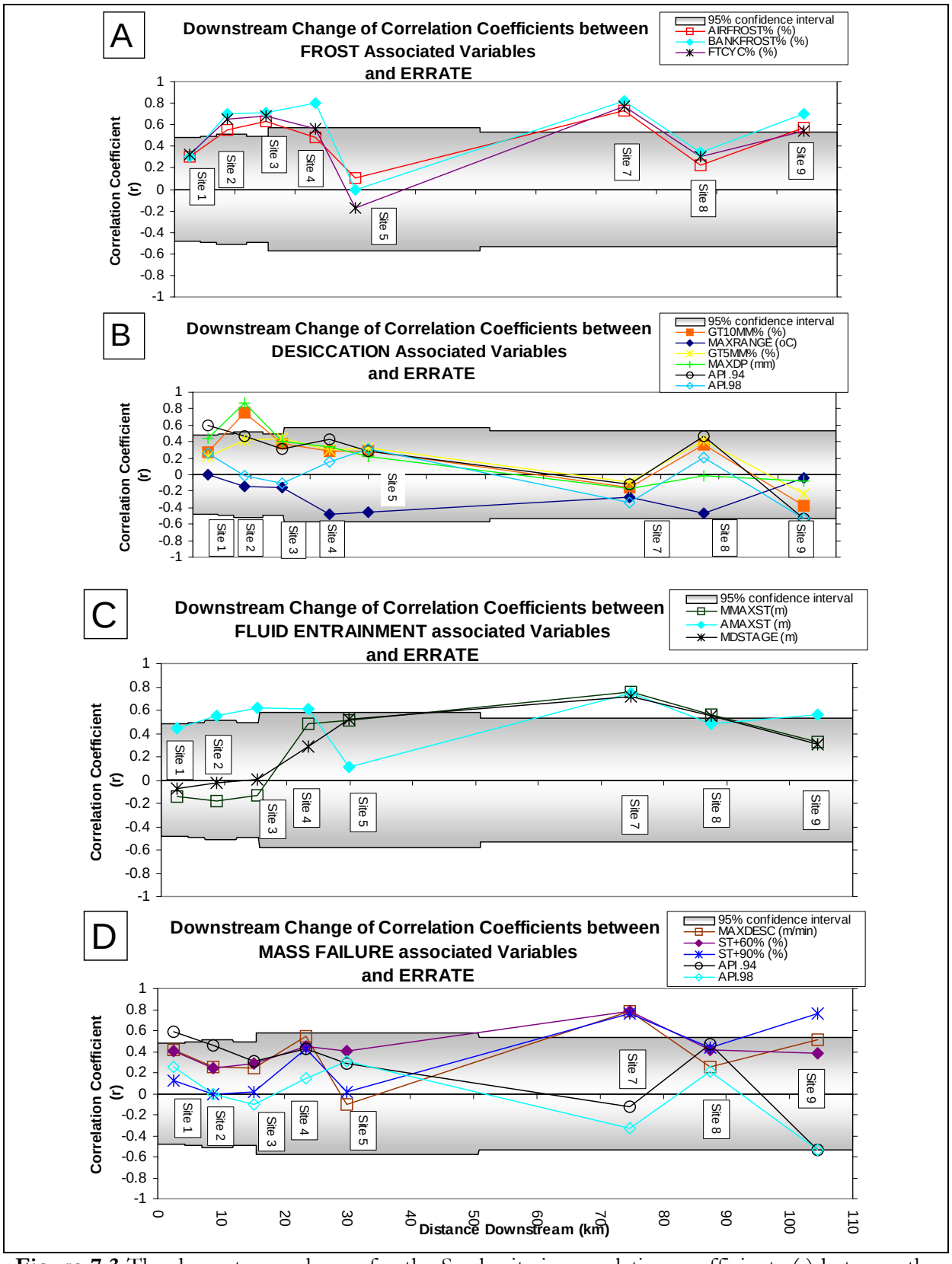

Figure 7.3 The downstream change for the Swale site in correlation coefficients (r) between the average epoch pin erosion (ERRATE) and independent variables used to represent: (**A**) Frost Action; (**B**) Desiccation; (**C**) Fluid Entrainment; (**D**) Mass Failures. Correlation r-values are significant at a 95 % significance level if they fall outside the shaded region.

Beck Meetings (Site 1) had a low correlation coefficient for ERRATE and frost related variables, perhaps because a stronger relationship existed between bank moisture and cantilever failures (Section 5.4.3). Frost variables at Hoggarths (Site 2) and Muker (Site 3) all correlated with ERRATE above a 95 % confidence level. BANKFROST% remained significant at Low Row (Site 4) however there was a decrease in the r-values of the other variables at this site. This may be due to the temperature buffering effect from the river (Lawler, 1993b), meaning the air frosts are no longer sufficient to cause ice to form on/in the bank. High r-values at Morton-on-Swale (Site 7) were unexpected, as frost was not observed to be significant in the field. The dominant erosion processes, for example entrainment, may simply be coincident with frost at this site. It may, however, be that the north-westerly aspect of the site or silt-sand bank sediment (Figures 4.6 – 4.8) are particularly prone to frost action.

Periods of low bank moisture content (Bello *et al.*, 1978), and high daily temperature fluctuations, should encourage the desiccation of bank sediment. The variables GT5MM%, MAXDP, API.94, and API.98 would all be expected to show strong negative correlation coefficients, with ERRATE, if low moisture conditions in the bank were significant. MAXRANGE, on the other hand, would be expected to have positive r-values during periods of intensified contraction and expansion (Section 5.3.4.1).

The strongest negative coefficients, not including MAXRANGE, were for Topcliffe (Site 9), whilst the variables were also negative to a lesser extent at Morton-on-Swale (Site 7) (Figure 7.3 B). These sites were expected to be affected by the drying of the bank due to warmer/drier environmental conditions. The downstream trend in desiccation efficacy (Lawler, 1995) was disrupted by the relationship at Greystone Farm (Site 8) (Figure 7.3 B). This may be caused by more vegetation shading at the site decreasing the summer temperatures (Abernethy and Rutherfurd, 1998); the more confined channel morphology meaning that the bank remained wetter for longer; or the increased influence of other forms of erosion, such as slab and cantilever failures were active during periods that the proposed desiccation variables were dominant.

7.2.4 The Catchment Scale Distribution of Fluid Entrainment

A mid basin peak in stream power should increase the efficacy of fluid entrainment in this region (Lawler 1992a; 1995). In a test of the hydraulics component of Lawler's model, Knighton (1999) found that the peak in stream power was 142-153 km downstream from the source on the River Trent, U.K. 20 km downstream on the River Derwent, U.K. and 4.8 km downstream on the River Noe, U.K. Lecce (1997) stated that values of gross stream power achieved maximum values at drainage areas between 10 and 100 km^2 on the 208 km^2 Blue River catchment in the U.S.A. The longitudinal stream power peak distribution was investigated on the River Swale (Section 4.4.4) using estimated bankfull discharges at each of the monitoring sites. Two peaks were identified within the basin, at Muker (Sites 3) and Easby (Site 6) (Figure 3.5), with gross stream powers of 39081 W m^{-1} and 4521 W m^{-1} respectively (Figure 4.10J). The peak at Muker was 15.2 km downstream (DBA 83 km^2) and at Easby the peak was 49.5 km downstream, (DBA 399 km^2). These sites have bedrock reaches upstream, which should increase flow velocities (Huang and Nanson, 1997), and an uncohesive sedimentology at the base of the bank. The clasts from the lower bank region may be supplying a larger clast size than is transportable by the current flow velocities. This may have resulted in an overestimation of the stream power due to the technique used to gauge the downstream bankfull discharges (Limerinos, 1970; McEwen, 1994) (Section 4.4.4). It would, however, still be expected that the reaches containing the stream power peaks also had high stream powers compared to the other sites.

At Beck Meetings (Site 1), entrainment was responsible for the removal of subaerially prepared material. In most cases the amount of erosion that occurred was greater than the amount of deposition from frost action that preceded the entrainment (Table 6.5). This could mean that, as well as removing the frost heaved material, the flood events also directly entrained undisturbed bank material. It is difficult to validate this hypothesis, as the sub-zero temperatures will have probably have caused some ice nucleation beneath the surface skin of needle ice heaved material. It may be that only material weakened by frost action has the potential to be entrained.

At Hoggarths (Site 2) and Muker (Site 3) maximum stage (AMAXST) emerged as the strongest correlating variable with ERRATE (Table 5.5). This may be owing to the increasing influence of entrainment as the stream power increased to a peak at Muker (Site 3). It may also reflect the increased importance of cantilever failures, which were eroded during the high flow conditions.

At Low Row (Site 4) none of the regression equations for the erosion pin dependent variables (ERRATE, ERODE%, ERODE84 and ERMAX) show any influence of the high flow events. These events should have the highest stream power, and entrain the most sediment (Tables 5.5 – 5.8). The PEEP events indicate that entrainment was occurring (Table 6.6); however, other variables must have been more influential in the stepwise regression selection procedure. This may be because the presence of prepared material creates a negative feedback hysteresis loop so there is no clear linear trend between stage and the amount of material entrained, as floods will not be as effective after the prepared material has been removed. This is exemplified by the low level of erosion during the second peak of a double peaked flood hydrograph (Table 6.6 *7c*). The basal material at Low Row may also be more cohesive than the surrounding sites because of the higher organic content (Section 4.3.5) (Haynes and Swift, 1990), which could also reduce the influence of entrainment.

The next site downstream, Reeth (Site 5), was influenced by high flow events, shown by the inclusion of MMAXST and ST+90% in the multivariate pin erosion models for ERRATE (Table 5.5). The high stage events did not necessarily entrain material directly from the bank but were responsible for creating higher pore water pressures and seepage patterns, which influenced slab, pop-out and cantilever failures. The high stages may have also been more efficient than at upstream sites for removing deposits from previous failures, allowing the creation of an unstable basal area. This would be a changeover area between sites of *impeded* and *unimpeded removal* to sites of *excess basal capacity,* in Thorne's (1982) model of basal endpoint control (Section 2.3.4).

The second catchment peak in stream power, at Easby (Site 5) (Figure 4.10), was associated with a rapid rate of erosion (Table 4.1) that could perhaps indicate an optimum erosion situation, where shear stresses are maximised and shear strengths are minimised. The decreased shear strengths could be related to the sediment composition. The composite nature of the bank, with a non-cohesive boulder sized lower component and silty-sand upper bank, could lead to the failure of the lower material into the flow by overcoming its angle of internal friction under saturation. The upper bank material would then be left unsupported, fail, and subsequently be entrained (Rinaldi and Casagali, 1999; Thorne and Tovey, 1981). The organic content of the upstream sample was also very low in the middle and upper bank (Table 4.8), perhaps reducing the soil aggregate stability (Haynes and Swift, 1990), and therefore the effectiveness of floods.

High flow events, represented by ST+90%, ST+60%, and AMAXST, were all included in models of pin erosion at Morton-on-Swale, Greystone Farm, and Topcliffe (Tables 5.4-5.7). All these variables could be modelling the fluvial entrainment of bank material during competent high flows. The API indices also included may be indicating that elevated pore pressures within the bank, during wet periods, increase entrainment susceptibility. They could also be implicating the increased potential for mass failures due to surcharging.

At Greystone Farm (Site 8) the amount of entrainment was difficult to determine due to lack of distinction between mass failure processes and entrainment (Section 6.4.4). Mass failures should theoretically predominate on the falling limb of the flood hydrograph because of increased pore water pressures and surcharging of bank material, which is no longer supported laterally by the flood water (Twidale, 1964; Thorne, 1982; Ashbridge, 1995; Lawler *et al.*, 1997). Failures that were observable at Greystone Farm, and which could be pin pointed to a particular event on the PEEP time-series, often occurred rapidly as the flood was receding (Figures 6.25) perhaps as a result of a loss of suction during saturation. This meant that entrainment and mass failures were difficult to distinguish between because of the lack of lag time before a mass failure occurred after a flood peak. Process differentiation was, therefore, based around observations made during the site visits following the erosion events, and the amounts of erosion that occurred. Mass failures were likely to have occurred if large blocks of sediment had been eroded, rather than a more spatially even erosion surface caused by entrainment.

The correlation coefficients between ERRATE and the independent variables MMAXST, AMAXST, and MDSTAGE with ERRATE were used to represent the differing efficacy of entrainment throughout the catchment (Figure 7.3 C). High stage events were considered to be the most influential in producing conditions for entrainment as they acted over a larger surface area, and had higher stream powers. The low significance of MMAXST and MDSTAGE upstream could be the result of the supply limitations of sediment by frost action, whilst the inclusion of AMAXST was possibly caused by cantilever failures.

At Low Row and Reeth MMAXST becomes more significant, alongside MDSTAGE (Figure 7.3 C), perhaps indicating the increasing influence of lower magnitude flows in eroding bank material. This erosion may be through the entrainment of basal material, or the increasing likelihood of sapping, piping and pop-out failures due to the drainage conditions of the bank. A

peak of all the entrainment variables was experienced at Morton-on-Swale (Site 7). All the variables then decreased, in r-values, downstream to Topcliffe (Site 9) with AMAXST staying nearer the 95 % confidence level. Thus the probability of entrainment may be increased at these sites, but there may also be an increased probability of saturation of the bank, leading to mass failure, during the high stage events.

7.2.5 The Catchment Scale Distribution of Mass Failures

An optimal point within a catchment was predicted by Lawler (1992a; 1995) where increasing bank heights downstream become higher than the critical height for a slab/wedge failure, using the Culman formula (cited in Selby, 1982, p.138) (Section 2.4.3). In the Swale study the number of mass failures occurring upstream was limited. Cantilever failures occurred at Beck Meetings (Site 1), Hoggarths (Site 2) and Muker (Site 3). This was, however, the only form of mass failure observed in the field. The steep slopes of the catchment meant that direct colluvial sediment inputs might be a relatively common occurrences, caused by the oversteepening of the slopes through preparation processes (Anhert, 1994). In the Swale catchment a peat slide (Carling, 1986; Wilson and Hegarty, 1993) was observed just downstream from Beck Meetings during February 1997. This had the effect of completely moving the river channel to the opposite site of the floodplain and causing a new channel to be incised into the floodplain.

The number of cantilever failures observed was highest at Muker (Site 3) when compared to the two sites upstream (Section 6.4.2). This may well be caused by the sedimentology of the reach. The composite bank structure had a greater potential for leaving the upper alluvial material unstable because of the collapse/removal of the unconsolidated lower bank sediment (Huang and Nanson, 1997; Thorne, 1998). The sedimentology of the bank is probably caused by the meandering nature of the reach (Figure 4.4). Past river bars have become buried by alluvial deposition, as the bar has become more peripheral to the main channel (Hemphill and Bramley, 1989). The changing river pattern means that incision occurs into the relic flood plain. In terms of a downstream trend in bank erosion, it is difficult to predict where in longitudinal profile of the river composite banks may occur. Theoretically, bars of unconsolidated course material are more likely to occur in the upstream reaches of a river system, due to downstream fining of bed and bank material (Knighton, 1998; Ashworth and Ferguson, 1986). Harris (1996) found the

opposite to be the case on the River Severn, U.K., where the proportion of basal coarse material increased downstream when he surveyed the upper reaches. In either of these scenarios, the input from tributaries, and the palaeo-migration history of the channel will lead to uncertainty in the sediment distribution downstream. The field identification of composite bank regions (Thorne, 1993; 1998) will be important in determining the areas most prone to cantilever failures.

At Low Row (Site 4) cantilever failures were again the only form of mass movement to be observed, and these were on a much smaller and less frequent scale than at Muker. Reeth (Site 5) was much more active in terms of mass failure processes. Pop-out, slab, and cantilever failures (Section 2.4) were all observed during the monitoring period. This site must be considered the threshold point within the catchment, from the sites monitored, for the banks to be suitable for mass failures (cantilever failures excluded). Upstream of this site bank heights were as high or higher (Figure 4.10A), vertical in cross-sectional profile, and devoid of vegetation. This may mean that silty-sand sedimentology in this reach (Figure 4.5), combined with low organic contents in the basal bank region (Figure 4.9), and sandy layers could all have contributed to the decreasing mass failure stability in terms of aggregate stability and drainage.

The dependent variables used to represent the erosion pin time series (Table 5.2) were not well explained by the independent variables selected in the multivariate regression models (Tables 5.5 – 5.8). This may be caused by an inadequate independent variable selection for the erosion processes at the site. The greatest level of explanation for the average erosion rate resulted from a combination of the independent variables MMAXST and ST+90% (Table 5.4). This suggested that the high stage events were influential in the processes of erosion. This would certainly be true in the case of pop-out failures, which would be dependent on the rapidity of the hydrograph recession limb and sediment composition.

At Easby, the differentiation between entrainment and mass failure, or whether there is a combination of both types of processes, was indistinct (as mentioned earlier in this Section). The erosion of the bank by slab, pop-out and cantilever failures followed by the rapid entrainment of the failed material, possibly during the same flood, would leave no specific evidence of mass failures. The shape of the failure surface may provide some evidence of the type of erosion; however, the planform retreat of cuspate forms does not allow a firm conclusion of either erosion mechanism. If the failed blocks were of a coherent form as they failed, such as a

slab/wedge failure (Plate 6.9), then the large extruded roots (Plate 6.11) would very probably have been severed by the force of the block falling. If, however, the failure was of a more liquid nature, such as a wet flow (Selby, 1982), the roots may have stayed intact.

The rapid rate of erosion at Easby (Site 6) probably relates to high flood velocities in a bedrock-confined channel, bank composition, and historical land-use. Local knowledge suggests that historically there was a weir structure in the channel, just upstream of the monitoring site, built to supply water to the abbey nearby through a small conduit. This may have disturbed the flow structures and weakened the bank sediment. The bank material is generally sandier here with a reduced silt content (Figures 4.6-4.8) than adjacent sites, and lower organic content in the middle-upper sediment of the upstream section (Figure 4.9). This may make the sediment less cohesive. There may also be an effect of surcharging of the upper bank by the isolated mature trees (Thorne, 1990), which were brought to the bank edge by the erosion. However anthropogenic disturbance does not explain the rapid erosion upstream of this site on exposed morainic material, which was subject to erosion that removed a public footpath and erosion warning signs.

At Morton-on-Swale MAXDESC, AMAXST, MMAXST and ST+60% emerged as the dependent variables best explaining variations in erosion rates (Tables 5.5 – 5.8). Mass failures were observed at the site with occasional pop-out failures and slab failures; however, cantilever blocks were predominantly observed on the bank toe (Plate 6.13). A rapidly falling hydrograph, modelled by MAXDESC (Table 5.3), which was often associated with high stage events, could be responsible for the surcharging of the overhanging cantilever blocks. The lowering stage removing lateral support whilst the bank remained saturated/poorly drained. It is unclear as to why the sediment is prone to the formation of cantilever failure. It may be that the increase in sand sized sediment mid-bank (Figures 4.6 – 4.8) is enough to facilitate undercutting. The bank top vegetation was grassland, which was similar to many of the other monitoring sites (Section 4.4.5). It is unlikely that the vegetation re-enforces the upper bank, increasing the shear strength so that only the lower unvegetated material is entrained during floods, as this is not the case at the other monitoring sites. It may be that:

1. The site is prone to high basal flow velocities during floods. This would result in enhanced entrainment on the lower bank compared to the rest of the slope;

2. The stage reaches the bank toe height more frequently, increasing the potential for entrainment;
3. Seepage through the bank through a preferential flow pathway destabilises the lower bank material as a form of sub-aerial preparation (Section 5.4.3) (Plate 5.4). Thus allowing the rapid entrainment of basal material in following floods;
4. The sediment is more susceptible to sub-aerial preparation by other means, such as frost action, weakening the lower bank shear strength. This would explain the inclusion of BANKFROST% in the multivariate model of ERRATE (Table 5.5). However, frost preparation of surface material was not frequently observed.

The erosion pin data at Greystone Farm (Site 8) was modelled using MMAXST, GT5MM%, and ST+90% implicating high rainfall and high river flow conditions in causing erosion (Figures 5.5 - 5.8). Cantilever failures, wet flows and slab failures were all observed, or inferred from the PEEP data (Table 6.7). The difference between mass failures and fluvial entrainment was difficult to determine; however, the dynamic equilibrium between mass failures and subsequent removal of debris was monitored and observed in the field e.g. Figures 6.24 and 6.26. The collapse of upper bank material on the 05/05/97, with subsequent removal of the debris on the 03/07/97, reveals the speed at which basal material can be remobilized. This emphasises the potential of the PEEP system to monitor bank collapse in relation to suspended sediment dynamics (Bull, 1996).

The furthest site downstream, Topcliffe (Site 9), was again subject to mass failures. These tended to be larger, probably because of the more cohesive sediment (Figures 4.4 – 4.8) and higher banks. Translational failures occurred during the monitoring period (Plate 6.15), triggered by the entrainment of basal sediment in the path of the failure plane. Cantilever and slab failures were also observed at the site. The independent variable ST+90%, and high API indices, included in the regression model of pin erosion (Table 5.5) support the importance of high flows and a wet catchment in triggering mass failures. They are also indicative of the importance of mass failures in describing the seasonal erosion variability at the site.

From field observations it appeared that although mass failures occurred at Sites 5 –9 the frequency of the failures decreased downstream, although the magnitude of the failures increased. Without detailed comparative survey data it is difficult to justify this observation. The declining rates of erosion downstream (Figures 4.1 and 4.2) and reduced channel change since 1854 (Figure

4.4) suggests; however, that the river becomes more stable in the lower reaches. The maximum erosion pin reading for each epoch (ERMAX) may be indicative of the frequency of mass failure events. The frequency of complete pin removal occurred, almost always, in a mass failure event. ERMAX decreased downstream, apart from at Greystone Farm (Site 8), with maximum values/complete pin removal occurring in 66.7 % of epochs at Reeth (Site 5) and 21.4 % of erosion epochs at Topcliffe (Site 9) from 05/01/97-13/03/98.

As the sediment increases in cohesion, due to higher clay contents downstream (Figure 4.5), the fluvial entrainment efficacy declines; however, this also increases the bank stability. The higher banks and lower hydraulic conductivies may mean that the factor of safety of the bank sediment is less frequently lower than unity, as it would take longer for saturation or pore water to reduce the shear strength. The higher banks would only occasionally be inundated to their maximum height and the length of time the bank was inundated would need to lengthened for the sediment to reach saturation, or increase pore water pressures.

The efficacy of mass failures was investigated using independent variables related to rapidly falling stage (MAXDESC), high flow events (ST+60% and ST+90%), and high catchment moisture (API.94 and API.98). The correlation coefficients with ERRATE did not distinguish the commencement of mass failures as opposed to cantilever failures (Figure 7.3 D). A peak in all but the API variables occurred at Morton-on-Swale (Site 7), whilst more failures were observed at Greystone Farm (Site 8) than at Morton-on-Swale and Topcliffe (Site 9).

The complex interaction of pre-conditioning factors for mass failure may be too difficult to replicate using the variables selected in this study. MMAXST or MDSTAGE (Figure 7.3 C) appeared reasonable indicators of mass failures. The r-values were, however, higher than they should be at Morton-on-Swale, and no failures occurred at Low Row.

7.3 THE DOWNSTREAM CHANGE IN THE MAGNITUDE AND FREQUENCY OF BANK EROSION

7.3.1 Introduction

The downstream change in bank erosion process efficacy, and process combinations, means that the timing of the erosion 'season' may also change throughout the catchment (Lawler *et al.*, 1999). The magnitude and frequency of differing processes will also affect the dominance, and timing, of the peak erosion period during an annual cycle.

To characterise the annual dynamics of erosion at each of the monitoring sites schematic changes in bank profiles are outlined in Figures 7.4 -7.6. The bank profile progression from winter to winter represents the extreme case of an instability being triggered. The entire bank profile may not be at the same stage of development; some segments being relatively stable others approaching failure. The timings of the extreme failures are important in terms of the rapid fluxes of suspended sediment and morphological changes. The critical preparation processes that are needed to create the major failures are also influential.

7.3.2 Upper Catchment Seasonal Erosion Variability

During both the monitored winters frost heave and needle ice were seen to be active from Beck Meetings (Plate 6.1) to Low Row. The resultant melting of the bank and its associated sediment laden ice creates a layer of basal debris (Figure 7.4 *2A-3A*) that is then removed by competent flow events (Figure 7.4 *4A*). This is not always associated with elevated basal pin erosion as the bottom pins are often buried then subsequently re-exposed creating a lower average amount of erosion during an epoch.

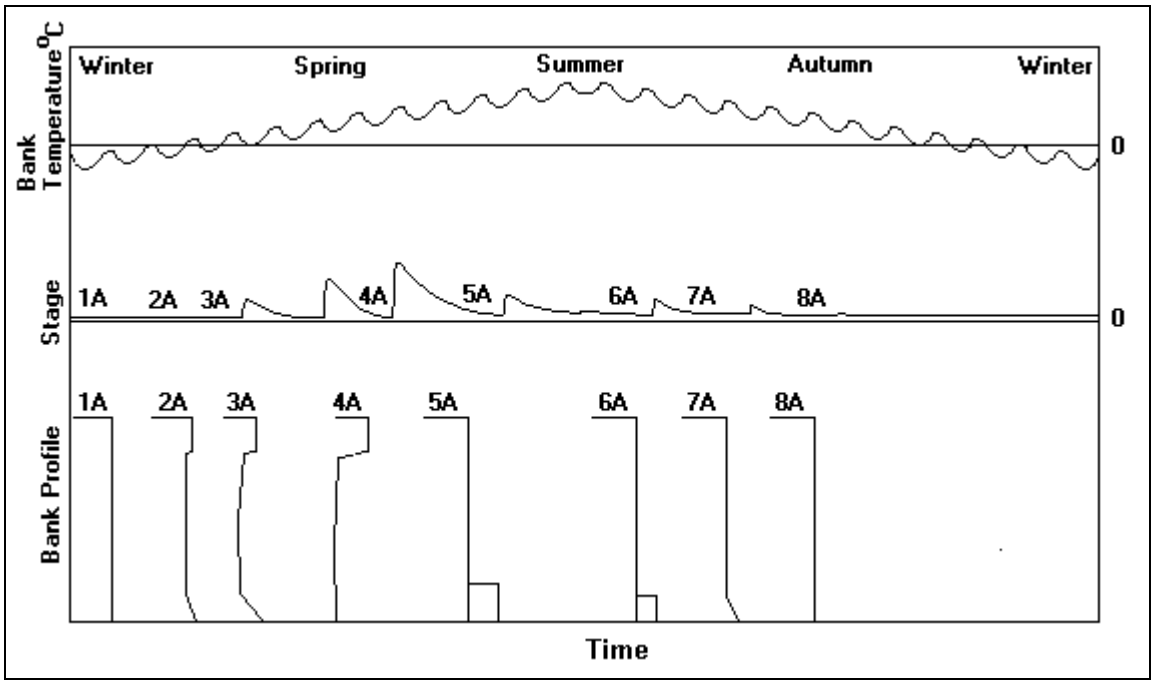

Figure 7.4 The annual change in bank morphology at an upstream site, in relation to a typical cycle of temperature and stage changes.

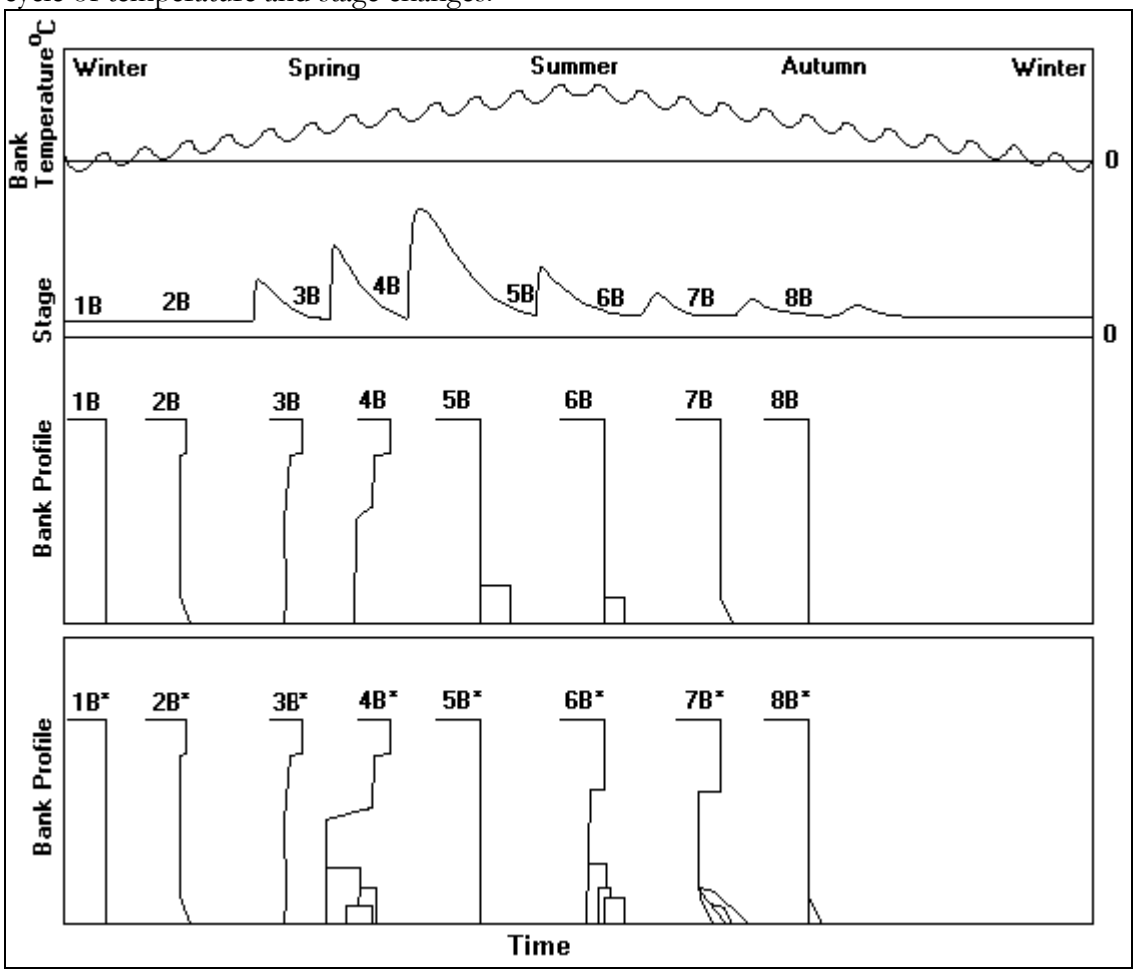

Figure 7.5 The annual change in bank morphology at a mid-catchment site, in relation to a typical cycle of temperature and stage changes.

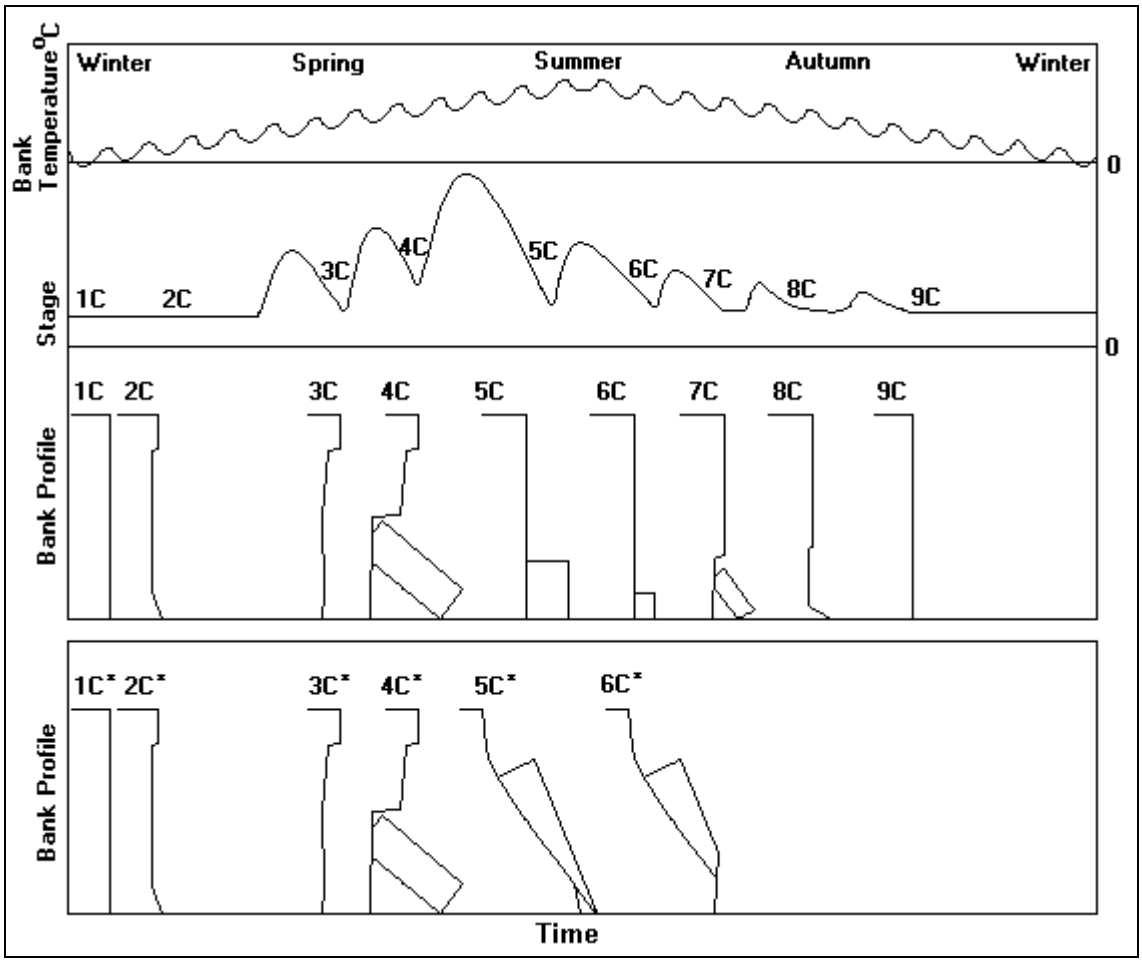

Figure 7.6 The annual change in bank morphology at a lower catchment site, in relation to a typical cycle of temperature and stage changes.

The extreme case is that the bank has become undercut enough to create a relatively unstable overhang of material (Figure 7.4 *4A*). Where this occurred, the saturation during peak flow events, followed by a drop in river level, leaving a more unstable block of material because of surcharging. The result is that cantilever failures (Figure 7.4 *5A*) can be seen at the base of banks after flood events (Thorne and Tovey, 1981). In some cases the block may be entrained during following flood events. It may also stay *in situ*, subject to sub-aerial erosion such as desiccation (Bello *et al.*, 1978), but protecting the bank behind it (Figure 7.4 *6A-7A*), until removed by a competent flow (Figure 7.4 *8A*). A bankfull flood after an intense period of frost action will remove prepared material and trigger all the upper bank cantilever failures leaving a state of relative stability. In the case of Beck Meetings the river was frozen during some winter periods. The flood stages that were associated with the period of 'defrosting' were high, caused by snowmelt, and resulted in high rates of erosion compared to the rest of the year (Figure 7.7). During the summer months the drying of the bank did not lead to a significant amount of

erosion (Figures 5.1 A-C), but may be responsible for enlarging any tension cracks (Darby and Thorne, 1994), preparing the cantilever blocks for the following winter floods.

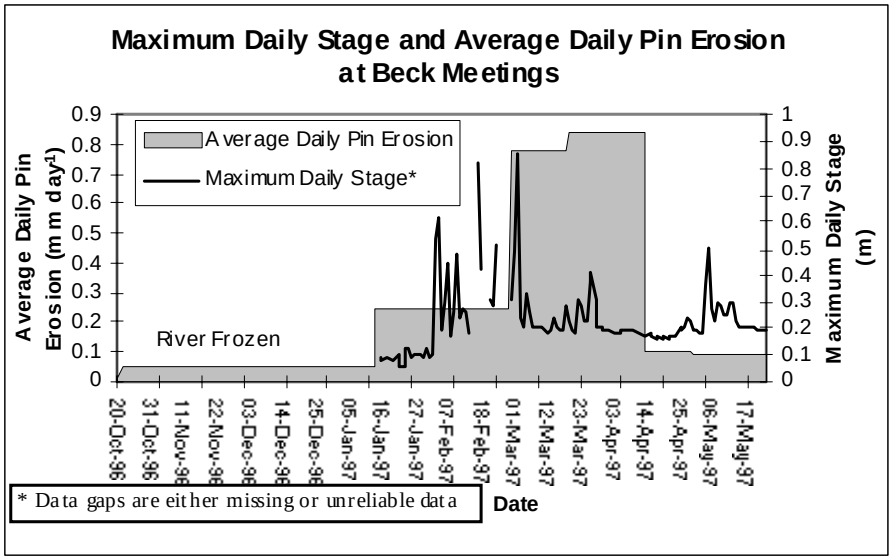

Figure 7.7 The effect of the melting of the river and bank ice on the amount of erosion measured at Beck Meetings during the winter of 1996-1997. The erosion rate is calculated by averaging the erosion at all the pins during an epoch, then dividing by the number days in the epoch.

The processes that were active at the upper catchment sites were basically restricted to the winter periods. The preparation of the bank sediment by frost action was responsible for a steady 'relatively' low rate of erosion during the periods of sub-zero temperature followed by flood events. The other main erosion process cantilever failure provided an episodic supply of larger blocks of sediment. The cantilevers mainly failed during winter/spring periods when they were saturated by flood events. This seasonal concentration of erosion during the winter/spring has implications for the release of any contaminants, such as heavy metals, within the bank material (Grove and Sedgwick, 1998).

In the upper reaches the rise in average annual erosion downstream (Figures 4.1 and 4.2) may be caused by an increase in the frequency of cantilever failures due to a rise in stream power which would increase the potential for basal undercutting, and the removal of subaerially prepared material. The potential for overhangs to be brought to failure by animal trampling during grazing (Trimble and Mendel, 1995) remains throughout the year: it was, however, not experienced during this study.

7.3.3 Mid-Catchment Seasonal Erosion Variability

Freezing of the bank surface during the winter months was still evident in the mid-catchment but to a lesser degree than at the upstream sites (Figure 7.5 *2B*). A smaller basal layer of frost heaved debris accumulated but is rapidly removed (Figure 7.5 *2B-3B*). The development of overhanging material was also aided by entrainment. Once the basal layer had been removed the bank is undercut by direct removal of bank material (Figure 7.5 *4B*). On the PEEP data at a mid-catchment site, Low Row (Site 4) (Table 6.6), there was a change in the erosion events over the year. The winter periods were preceded by frost preparation and then followed by direct entrainment during subsequent flood events. It is suggested that as with the upstream sites the bankfull floods triggered cantilever failures by saturating the upper bank. This, it is thought, increased the cantilever block weight and increased pore pressures, leading to block collapse after the flood peak passed (Figure 7.5 *5B*).

Piping and sapping erosion (Jones, 1981; Hagerty, 1991a; 1991b) was more likely to occur where the sediment size had decreased to a silty-sand with sand layers. This process increased in efficacy in the reaches where there was an attenuated flood peak (Gregory and Walling, 1973) which maintained a steep falling limb on the hydrograph. These processes may occur along with pop-out failures (Simon, 1989) (Figure 7.5 *4B** and *6B**) as the bank reaches a sufficient height for mass failure. This process change would occur as the sediment hydraulic conductivity allowed a rapid ingress of water as the flood wave passed. The rapidly falling stage would then lead to drainage of stored water through preferential drainage routes such as sand lenses. This would result in either a blow out of the lower bank material as a pop-out failure (Figure 7.5 *4B** and *6B**), or the formation of hollows due to piping and sapping. The timing of these failures is not dependent on freeze-thaw preparation of the bank sediment, but more on the flood hydrograph. This shift away from seasonally varying frost frequencies causing erosion could contribute to the lengthening of the erosion season in the mid-catchment, compared to upstream (Figure 5.1).

The removal of failed basal material, especially at Reeth and Easby, was rapid in the middle reaches. This may be the result of the proximity of the stream power peaks and/or the flow structure at the sites leading to strong basal velocities. The removal of the basally deposited material (Figure 7.5 *7B-8B* and *5B**) resulted in less protection for the lower bank, creating either

a vertical or an undercut bank face much more rapidly than sites upstream. This means that, although the failed blocks may be small, as the bank height is only just high enough for a failure to occur, the speed at which the failed blocks are removed and a new failure occurs creates a rapid cycle of erosion (Figure 7.5 *4B*-6B**). This may be the cause of the mid-basin peak in erosion (Figures 4.1 and 4.2). The process of *in situ* degradation of failed material (Figure 7.5 *6B*-8B**) may still occur by subaerial processes (Section 2.2) if the blocks are too large to be entrained.

7.3.4 Lower Catchment Seasonal Erosion Variability

Higher winter temperatures downstream, e.g. Figure 6.5F compared against Figures 6.3E and 6.4F, restricted the influence of frost action during the winter months at the downstream sites (Figure 7.6 *1C-2C*). There was evidence of heaving of material with fallen debris clearly visible on snow patches at Greystone Farm (Plate 5.6). Early in the spring flood season, flood events removed the basal material and wetted up the bank (Figure 7.6 *3C*). The lower hydraulic conductivity of the finer cohesive bank sediments meant that the drainage of the bank was slow, creating a waterlogged bank for a longer period than upstream. Basal slumping of material (Plate 6.16) follows the initial lower flood sequences (Figure 7.6 *4C*) (Hooke, 1979). The removal of the lower bank sediments results in sections of the bank being left with overhanging material which in following floods may be removed or collapse as the bank dries out and tension cracks are enlarged (Figure 7.6 *5C*) (Plate 6.12) (Thorne and Tovey, 1981; Abam, 1997).

The other scenario that may result from the complete submergence of the bank during a flood event is the complete mass failure of the bank (Figure 7.6 *5C**). The removal of basal support either by preceding floods, or by the rising limb of the flood hydrograph, will facilitate the failure especially if the failure plane passed through the removed material. This may be through slab failure or rotational failure (Thorne and Osman, 1988), or, as at Topcliffe (Site 9), a translational failure (Plate 6.15). Slab failures were occurred from Reeth (Plate 6.9) down to Topcliffe (Plate 6.16), however none of the study sites were shallow and high enough for rotational failures to occur. The larger mass failures downstream appeared to take several annual erosion cycles for the bank profile to recover back to its original state. Undercutting of the failure (Figure 7.6 *6C**) and further basal failures gradually returning the bank to its initial profile form.

Drying out of the bank during the summer may also create differing layers within the sediment even if the sediment is nearly homogenous (Abam, 1997). This may aid the failure of banks by creating a weaker failure plane, meaning that flashy summer rainfall or summer floods became more effective (Table 6.7 *4f* and *8c*). The potential remains for many forms of mass failure to occur during less frequent summer floods, such as cantilevers, lengthening the annual erosion season (Figure 5.1).

The growth of vegetation could lead to an increase in the weight of the potential failure block, with the root zone being shorter than the depth to the failure plane. The higher banks with more gentle gradients in the downstream part of the catchment were able to support larger forms of vegetation such as shrubs and trees on their slopes, rather than just on the banktop (Plates 3.1-3.9). This increased weight may be countered by a more efficient drainage network from the root system creating macropore flow (Thorne, 1990). This would remove the surcharging caused by rain or floodwater.

7.4 COMPARATIVE STUDIES OF BANK EROSION RATES AND PROCESSES

7.4.1 A Global Bibliography of Bank Erosion Rates

In order to put the rates of erosion measured at each of the River Swale monitoring sites in context with other river systems a bibliography erosion studies has been compiled. The compilation is largely based on the work by Hooke (1980), Lawler (1993a), Harris (1996), and Stott (1999). So that the changing rates of erosion against catchment size could be investigated a common scale reference was needed. Drainage Basin Area (DBA) was more frequently quoted than distance from river source and so this was the scale adopted. The varying scale of erosion studies has resulted in different techniques being used to monitor erosion. Larger study areas were often measured using periodic re-mapping techniques (Lawler, 1993a). This means that the annual rate of erosion may be an average of erosion that had occurred over decades or centuries. Some of the other studies may have had a monitoring period of less than a year, meaning that the average rates of erosion would have to be extrapolated to an annual rate. The differing margins

of error are unknown, and so not quoted, so caution must therefore be taken in the interpretation of the data.

Where the author(s) quoted ranges of drainage basin areas, and/or ranges of erosion rates, the highest number in each case was selected. This was based on the assumption that as DBA increased so should erosion rates. Whilst this may not always be the case (Lawler *et al.*, 1999) it does avoid small catchments being attributed too large an erosion rate. Using the highest erosion rates also allowed a reasonable comparison with the River Swale monitoring sites. This is because the Swale sites were selected to be actively eroding sites (Section 3.4.2) that would be expected to lie in the upper range of erosion values for the drainage basin area.

For this Swale study the erosion pin data was collected at each of the monitoring sites, except Easby, for a longer period than the PEEP data. This was therefore considered the best data to compare against annual rates of erosion quoted by other authors, Table 7.2 presents the drainage basin area and average annual erosion for each of the River Swale sites. The erosion process indices also presented will be discussed in Section 7.4.2.

SITE NAME	DRAINAGE BASIN AREA (km^2)	AVERAGE ANNUAL PIN EROSION ($m\ a^{-1}$)*	EROSION PROCESSES IDENTIFIED	EROSION PROCESS INDEX S	SP	F	FM	M
1. Beck Meetings	4.2	0.07	Frost Action, Fluvial Entrainment, Cantilever Failures					
2. Hoggarths	52.4	0.14	Frost Action, Fluvial Entrainment, Cantilever Failures					
3. Muker	82.6	0.26	Frost Action, Fluvial Entrainment, Cantilever Failures					
4. Low Row	141	0.09	Frost Action, Fluvial Entrainment, Piping, Cantilever Failures					
5. Reeth	183	0.62	Frost Action, Fluvial Entrainment, Slab Failures, Cantilever Failures, Pop-out Failures					
6. Easby *	399	3.58	Fluvial Entrainment, Cantilever Failures, (possibly Wet Flow)					
7. Morton-on-Swale	593	0.35	Frost Action, Fluvial Entrainment, Piping, Slab Failures, Cantilever Failures, Pop-out Failures					
8. Greystone Farm	748	0.41	Frost Action, Desiccation, Fluvial Entrainment, Slab Failures, Cantilever Failures, Wet Flow					
9. Topcliffe	1282	0.13	Frost Action, Desiccation, Fluvial Entrainment, Slab Failures, Cantilever Failures, Translational Failures					

Table 7.2 Drainage basin areas, average annual erosion pin measurements from 29/02/96-13/03/98, and erosion process indices at each of the monitoring sites. The dominant erosion process indices refer to Table 7.5, where: **S** = Subaerial Erosion; **SP** = Subaerial Preparation; **F** = Fluvial Entrainment; **FM** = Fluvial Entrainment/Mass Failure; **M** = Mass Failure. * Easby was monitored using bank-top re-survey from 16/01/97-13/03/98, not erosion pins.

	Dominant erosion processes
	Subsidiary erosion processes

AUTHOR	RIVER	AREA	DRAINAGE BASIN AREA (km^2)	EROSION RATE ($m\ a^{-1}$)	EROSION PROCESS				
					S	SP	F	FM	M
Andrews (1982) ***	East Fork River	Wyoming, U.S.A.	502	0.1-0.2				■	
Ashbridge (1995) ****	River Culm	Devon, U.K.	276	0.23-0.33		▒		■	
Bluck (1971) *	River Endrick	Scotland, U.K.	97.7	0.5					
Bray (1987) ***	North Nashwaaksis	New Brunswick, Canada	26.9	>3			■		
Brice (1973) *	White River	Indiana, U.S.A.	6042	0.67					
Brunsden and Kesel (1973) ***	Mississippi River	Port Hudson, U.S.A.	1000000	0-20				▒	■
Bull (1996)	River Severn	Wales, U.K.	3.5	0.0129		■	■		
			4	0.0488		■	■		
			4	0.0156		■	■		`
			8	0.0591		■	■		
			3.5	0.0648		■	■		
			170	0.2341	▒	▒	▒	■	
			380	0.4603	▒	▒	▒	■	
Church and Slaymaker (1989) ****	Liard and Peach River	Sikanni Chief, British Columbia, Canada	10530	2.9					
		Fontas, B.C., Canada	8110	2.9					
		Muskwa, B.C., Canada	1510	2.7					
		Prophet, B.C., Canada	6765	2.3					
		Fort Nelson, B.C., Canada	47815	4.4					
	River Beatton	Beatton, BC, Canada	4070	0.5					
	Upper Fraser River	Upper Eagle, B.C., Canada	150	1.3					
		Lower Eagle	1385	0.7					
Coleman (1969) *	River Brahmaputra	India	934990	6-275					■
	River Brahmaputra	India	934990	15-792					■
Cummins and Potter (1972) ***	Bradgate Brook	Leicestershire, U.K.	33	0.03	▒		■		
Davis and Gregory (1994) ***	Highland Water	Hampshire, U.K.	11.4	0.066	■	▒	▒		
Duysings (1986) ***	Schrondweilerbaach	Luxembourg	0.61	0.02-0.035	■	▒	■		▒
Gardiner (1983) ***	River Lagan	N. Ireland, U.K.	85	0.076-0.138	▒	▒	■	▒	
Hagerty et al. (1981) ***	Ohio River	Pittsburgh, U.S.A.	10000	5.0-15.0			▒	▒	■
Hey and Thorne (1984)	River Severn	Wales, U.K.	375	0.6				■	
Hickin and Nanson (1975) *	River Beatton	British Columbia, Canada	16000	0.48			■		■
Hill (1973) ***	Crawfordsburn River	N. Ireland, U.K.	3	0.005-0.05	▒	▒	■		
	Clady River		4	0.04-0.064	▒	▒	■		
Hooke (1979) ***	Rivers Exe, Creedy and Culm	Devon, U.K.	235-620	0.62-1.18		▒	■		
	Rivers Axe, Yarty, Coly, and Hookmoor Brook		9.6-288	0.15-0.46		▒	■		
Hooke (1987) ***	River Dane	Cheshire, U.K.	152	3			■		
Hooke (1995)	River Bollin	Cheshire, U.K.	~55	1.25-2.11			■		
			~55	1.88-2.19			■		
Hughes (1977) ***	River Cound	Shropshire, U.K.	100	0.64			■	■	
Kesel and Baumann (1981) ***	Mississippi River	Port Hudson, U.S.A.	>1000000	6.8-18.9	▒		▒	▒	■
Kesel et al. (1974) ***	Mississippi River	Port Hudson, U.S.A.	>1000000	14.9	▒				■
Klimek (1974) ***	River Wisloka	Carpathians, S. Poland	4245	1.0-11.0	▒			▒	■
Knighton (1973) *	River Bollin-Dean	Cheshire, U.K.	120	0.01-0.09		▒	■	■	▒
Kondolf and Curry (1986) ***	Lower Carmel River	Monterey County, U.S.A	660	0-1.2			■		

Table 7.3 cont. on following page Process categories: (**S**) Subaerial Erosion;(**SP**) Subaerial Preparation;(**F**) Fluvial Entrainment;(**FM**) Fluvial Entrainment/Mass failure;(**M**) Mass Failure (Table 7.5).

■	Dominant erosion process index
▒	Subsidiary erosion process index
▒	No erosion process indicated

AUTHOR	RIVER	AREA	DRAINAGE BASIN AREA (km^2)	EROSION RATE ($m\ a^{-1}$)	EROSION PROCESS				
					S	SP	F	FM	M
Laczay (1977) *	River Hernad	Czechosloviakia	5400	5-10					
Lawler (1984) ***	River Ilston	Gower, U.K.	6.75	0.006					
			13.18	0.012					
Lawler (1986) **	River Ilston	Gower, U.K.	6.75-13	0.04-0.31					
Lawler (1987b) **	River Ilston	Gower, U.K.	6.75	0.067					
Lawler (1994) ***	River Arrow	Warwickshire, U.K.	98	0.034					
Leeks et al. (1988) **	River Trannon	Wales, U.K.	72	0.03-0.96					
Leopold et al. (1964) **	Watts Branch	Maryland, U.S.A.	9.6	~0.5					
Leopold et al. (1966) **	Slopewash Tributary	New Mexico, U.S.A.	0.13	0.006					
Lewin (1972) *	River Rheidol	Wales, U.K.	179	1.75					
	River Tyfi	Wales, U.K.	633	2.65					
Lewin et al.(1974) **	Maesnant	Wales, U.K.	0.54	0.03					
McGreal and Gardiner (1977) **	Lagan	County Down, Northern Ireland	85	0.08-0.14					
Mosley (1975) *	River Bollin-Dean	Wales, U.K.	114	0.16					
Murgatroyd and Ternan (1983) ***	Narrator Brook	Dartmoor, U.K.	4.75	0.03					
Nanson and Beach (1977) **	Beatton	British Columbia, Canada	<~4000	0.3-0.7					
Nanson and Hean (1985) **	Illawarra	N.S. Wales, Australia	1.6-37.8	0-32.7					
Odgaard (1987) ***	East Nishnabotna River	Iowa, U.S.A.	1129	2.1					
			2314	3.2					
	Des Moines River	Iowa, U.S.A.	32320	2.4					
			34640	3.7					
			36360	3.2					
Scott (1982) ***	Kenai River	Alaska, U.S.A.	5700	0.3					
Stanley et al. (1966) ***	Mississippi River	Fort Jackson, U.S.A.	100000	4.6					
Stott (1997)	Ballquhidder	Monachyle, Scotland	7.7	0.059					
		Kirkton, Scotland	6.85	0.047					
Stott (1999)	(River Seven) Tanllwyth	Wales, U.K.	0.89	0.035					
	Tanllwyth (clearfelled)		0.89	0.095					
	Cyff (upland grassland)		3.1	0.031-0.065					
Stott et al. (1986) **	Kirkton Glen	Balquhidder, U.K.	<7.7	0.016-0.076					
Sundborg (1956) *	River Klaralven	Sweden	5420-11820	1.6					
			5420-11820	0.23					
			5420-11820	0.32					
Thorne (1982) ***	River Severn	Wales, U.K.	375	0.02-0.2					
Thorne and Lewin (1979) ***	River Severn	Wales, U.K.	375	0.015-0.025					
			375	0.03-0.35					
Twidale (1964) ***	Torrens River	nr. Adelaide, Australia	77.7	0.58					
Walker et al. (1987) **	Colville	Alaska, U.S.A.	53000	4.0					
Williams et al. (1979) **	Ottawa	Canada	148000	0.35					
Wolman (1959) ***	Watts Branch Creek	Maryland, U.S.A.	9.6	0.46-0.61					
Wolman and Leopold (1957)**	Watts Branch Creek	Maryland, U.S.A.	9.6	0.075					

Table 7.3 cont. Published bank erosion rates and process indices for catchments with a known drainage basin area. The rates of erosion and processes were quoted by the following: *= Hooke (1980); **= Lawler (1993a); ***= Harris (1996); ****= Stott (1999). Process categories (Table 7.5): (**S**) Subaerial Erosion; (**SP**) Subaerial Preparation; (**F**) Fluvial Entrainment; (**FM**) Fluvial Entrainment/Mass failure; (**M**) Mass Failure, defined largely by Harris (1996), extended for more recent studies by the author.

	Dominant erosion process index
	Subsidiary erosion process index
	No erosion process indicated

The cited research (Table 7.3) incorporates a wide range of drainage basin areas and erosion rates (Figure 7.1). Studies above a drainage basin area of 1000 km^2 were infrequent, with 30 % of the 92 study sites above this size (Table 7.3). Due to the large outlying values, with high erosion at large DBA values, the median values rather than means are thought to better represent the 'average' study size and erosion rates (Table 7.4). The world-wide range of studies includes a much larger range of drainage basin areas than studies in the U.K. To put this study in context the research undertaken in the U.K. has been selected and analysed separately (Table 7.4) (Figure 7.9). The range of DBA values and erosion rates are much smaller than those measured world-wide, and may be more confidently compared with Swale data.

	WORLD-WIDE DISTRIBUTION OF BANK EROSION STUDY DRAINAGE BASIN AREAS (km^2)	U.K. DISTRIBUTION OF BANK EROSION STUDY DRAINAGE BASIN AREAS (km^2)	WORLD-WIDE DISTRIBUTION OF BANK EROSION STUDY EROSION RATES ($m\ a^{-1}$)	U.K. DISTRIBUTION OF BANK EROSION STUDY EROSION RATES ($m\ a^{-1}$)
Minimum	0.13	0.54	0.006	0.006
Maximum	1000000	1281.8	792	3.58
Average	56240.31	161.970	13.154	0.505
Median	170	63.5	0.4603	0.139

Table 7.4 The range, and average, erosion rates measured within the U.K. and world-wide.

The average annual erosion rates determined from the Swale study are within the range of other world-wide studies (Figure 7.8). This is a useful indication that the study sites were not 'extraordinary' in terms of the rates of erosion monitored. The other UK studies show the same trend, with the smaller DBA sites of a similar erosion rate to those of this study (Figure 7.9). The Swale study apparently has the largest DBA of any bank erosion study within the UK adding a new dimension to previous research. As similar 'large scale' DBA studies have not been undertaken in the UK no comparative data are available. This highlights the need for more large-scale studies within the UK.

The world-wide and UK distribution of erosion rates (Figures 7.8-7.9) both show a generally increasing trend of erosion rates with drainage basin area; however there is a lot of scatter within the data. The erosion rates may be modelled against DBA using linear regression equations (Equation 7.1 and 7.2).

$$WWER = 0.002DBA + 0.8972 \quad (7.1)$$

(n = 83, R^2 = 30.9 %, R^2 95 % significance level = 4.4 %, R^2 90 % significance level = 3.3 %)

Where:

WWER = World-wide erosion rates (m a^{-1});

DBA = Drainage Basin Area (km^2).

$$UKER = 0.0018DBA + 0.2526 \quad (7.2)$$

(n = 43, R^2 = 15.7 %, R^2 95 % significance level = 9.2 %, R^2 90 % significance level = 6.6 %)

Where:

UKER = UK erosion rates (m a^{-1}).

$$ER9698 = -3x10^{-06}DBA^2 + 0.004DBA + 0.0792 \quad (7.3)$$

(n = 9, R^2 = 22 %, R^2 95 % significance level = 44.3 %, R^2 90 % significance level = 33.9 %)

The Swale catchment had maintained a quadratic trend of erosion rates throughout the catchment (Equation 7.3); however, this trend was not as significant as Equations 4.1 - 4.3 which regressed distance downstream against erosion rates. Neither the global or U.K. distribution of erosion rates showed a strong quadratic trend when compared against DBAs (Figures 7.8 and 7.9). This was probably due to the varying temporal and spatial scales used to determine erosion rates in the different studies, rather than the more coherent/consistent sampling strategy used in this study.

The change in erosion rates with catchment area may be due to:

1. Variations in measurement techniques (Lawler, 1993a);
2. A change in the efficacy of a singular erosion process;
3. The dominance of different erosion processes.

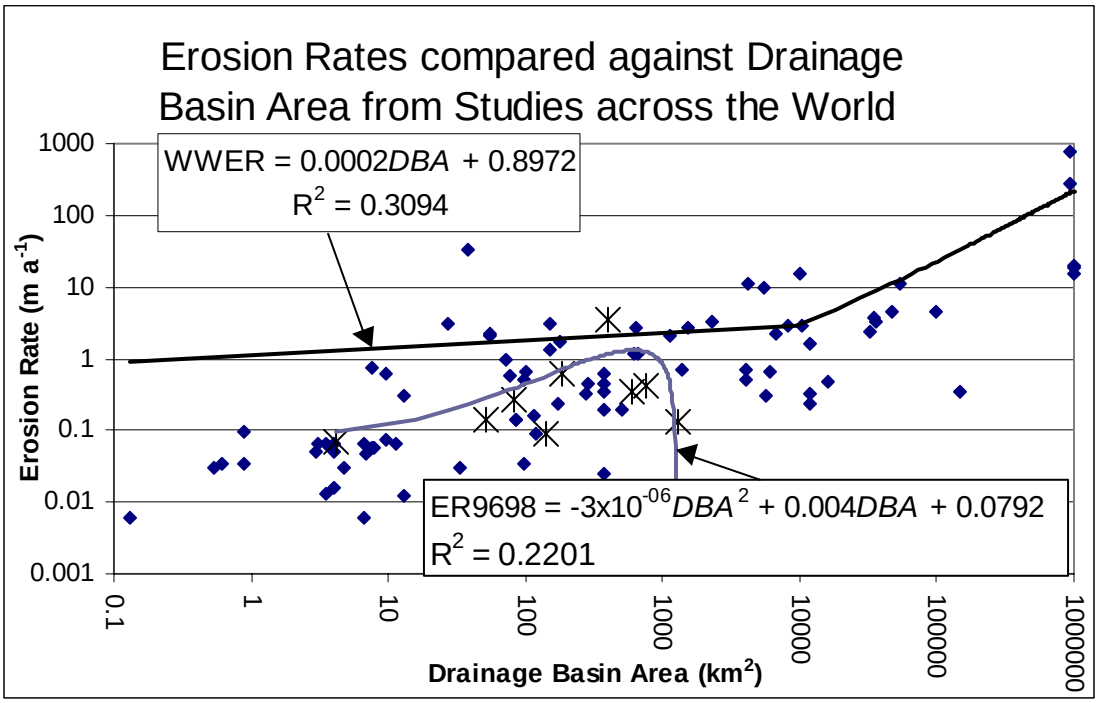

Figure 7.8 Average annual bank erosion rates for the Swale compared with world-wide rates. * = rates of erosion from the Swale study. The data are mainly compiled from Hooke (1980); Lawler (1993a); Harris (1996); and Stott (1999).

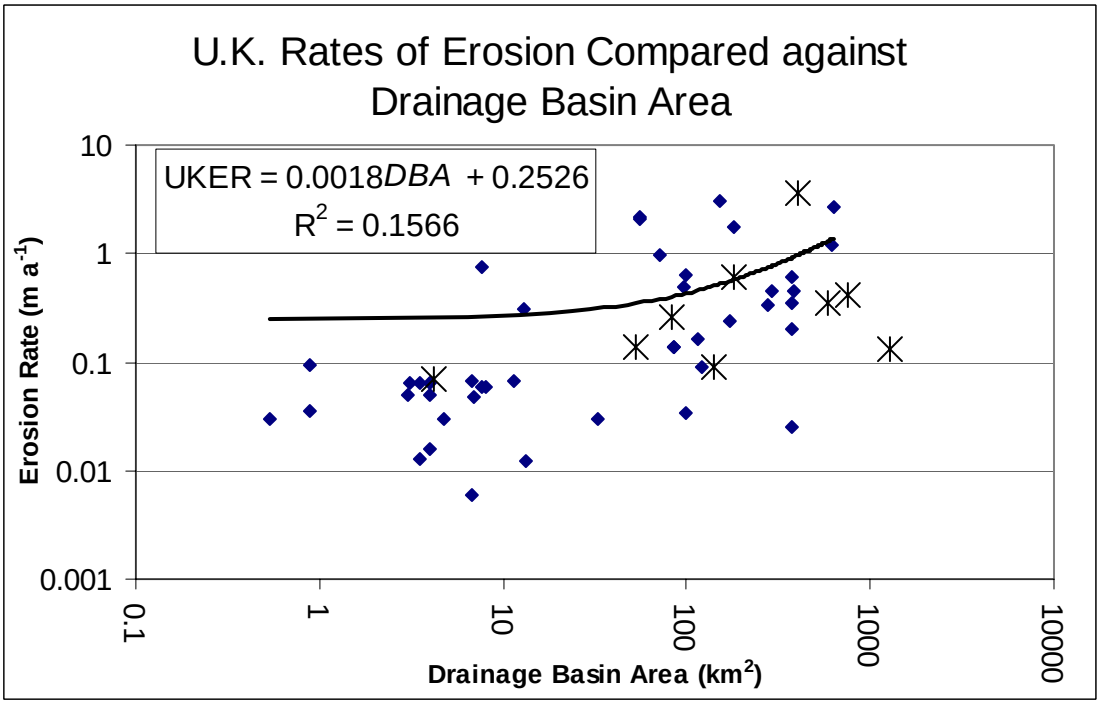

Figure 7.9 Average annual bank erosion rates for the Swale compared with other UK rates. * = rates of erosion from the Swale study. The data are mainly compiled from Hooke (1980); Lawler (1993a); Harris (1996); and Stott (1999).

7.4.2 A Global Bibliography of Bank Erosion Processes

It was possible to test the idea that DBA was influential as a predictor for dominant erosion processes, as Lawler (1992a; 1995) envisaged. As there are numerous types of erosion processes (Chapter 2), and combinations of processes, five indices of erosion were selected to encompass most of the common erosion processes, which were suggested by Harris (1996) (Table 7.5). This meant that the bibliographic research by Harris (1996) could be extended to include recent publications, as well as the data from this study (Table 7.2). Where processes are not specifically categorised by the original author(s) some subjectivity may enter the classification.

EROSION PROCESS CATEGORY	A DESCRIPTION OF PROCESS TYPES INCLUDED IN EACH CATEGORY
Subaerial Erosion	Where processes such as frost action (Outcalt, 1971; Lawler, 1986; Branson *et al.*, 1996), desiccation (Bello *et al.*, 1978), sapping (Jones, 1981; Hagerty, 1991a; 1991b), piping (Jones, 1981; Hagerty, 1991a; 1991b), and rainsplash erosion (Duysings, 1986) directly remove sediment from the bank surface.
Subaerial Preparation	The same processes that cause subaerial erosion instead of, or alongside, directly removing bank material also weaken the bank structure reducing the sediment shear strength (Lawler, 1993b). Subsequent erosion processes that follow a period of preparation may require less energy to displace the weakened sediment.
Fluvial Entrainment	The removal of the bank sediment by the detachment of individual grains, or aggregates, by a river flow which has a shearing stress competent enough to overcome the shear strength of the particles in contact with the river (Thorne, 1978). Bank material is incorporated into the suspended load, and/or the bed load, of the river.
Fluvial/Mass Failure	The failure of a block of material due to preceding fluvial entrainment. In this study cantilever failures (Thorne and Tovey, 1981; Casagli *et al.*, 1999) are thought to be the main erosion process within this category. These occur due to the undercutting of the bank, leaving an unstable elevated block of material.
Mass Failure	Mass failures involve the development of a failure plane through the bank surface, which may fail as the shear stresses exceed the shear strength of the sediment. A mass of material is released from the bank, this may occur in many different forms from shallow slab failures (Abernethy and Rutherfurd, 1998) up to large rotational failures (Selby, 1982).

Table 7.5 A description of the indices used to classify erosion processes identified in bank erosion literature. The different classification criteria are adapted from Harris (1996), in this study Fluvial Entrainment/Mass Failure is predominantly considered as the processes of cantilever failure.

There appeared to be no discrete change downstream from one process index to another (Figures 7.10 and 7.11). This is probably because processes act in combination with each other, such as fluvial undercutting and mass failure (Thorne, 1982), or preparation processes followed by fluvial entrainment (Lawler, 1987b; Stott *et al.*, 1986). In many of the references, more than one of the process indices was understood to be dominant, despite the simplification from individual types of erosion processes (Table 7.3). The scales of drainage basin area that each of the process indices was active over, and the rates of erosion associated with each of the indices, are shown in Table 7.6. The trends apparent from the classification are:

1. Increasing median erosion rates as the processes changes from Subaerial Erosion(**S**)-Subaerial Preparation(**SP**)-Fluvial Entrainment(**F**)-Fluvial Entrainment/Mass Failure(**FM**)-Mass Failure(**M**);
2. The ranges of erosion values follow a similar trend, although **FM** has a smaller range of values than **F** and **M**;
3. The median DBA for each process category increases in the order **S**-**SP**-**F**-**FM**-**M**;
4. Subaerial erosion occurred at a smallest range of DBA sizes;
5. Subaerial preparation occurred at a wider range of DBA values than both **F** and **FM**;
6. Mass failures occurred over the widest range of DBA values.

EROSION INDEX	RANGE OF EROSION VALUES MIN-MAX (m a^{-1})	MEDIAN RATE OF EROSION (m a^{-1})	RANGE OF DRAINAGE BASIN AREAS MIN-MAX (km^2)	MEDIAN DRAINAGE BASIN AREA (km^2)
S (Sub-aerial Erosion)	0.035 – 0.066	0.051	0.6 – 11.4	6
SP (Sub-aerial Preparation)	0.006 – 4	0.066	0.5 – 53000	7.85
F (Fluvial Entrainment)	0.013 – 3.7	0.14	0.5 – 36360	55
FM (Fluvial Entrainment/Mass Failure)	0.025 – 0.7	0.32	4.8 – 5700	375
M (Mass Failure)	0.09 - 792	4	114 - 1000000	16000

Table 7.6 The range and average rate of erosion, and drainage basin area, for each of the erosion process indices on a global scale.

Plotting the results from the Swale study against other erosion indices identified in the U.K. indicates that subaerial preparation and fluvial entrainment dominated the smaller catchment studies - those less than 100 km^2 (Figure 7.11). Fluvial/Mass Failure erosion and Fluvial Entrainment were influential in the 100-1000 km^2 drainage basin range, with rates of erosion of

around 0.1-1 m a^{-1} (Table 7.6). The largest drainage basins were dominated by mass failures; however, unlike the erosion examples from world-wide studies (Figure 7.10), the rates of erosion for the mass failure examples were not the highest. Fluvial erosion was attributed as the erosion index that produced the highest rates of erosion in the UK.

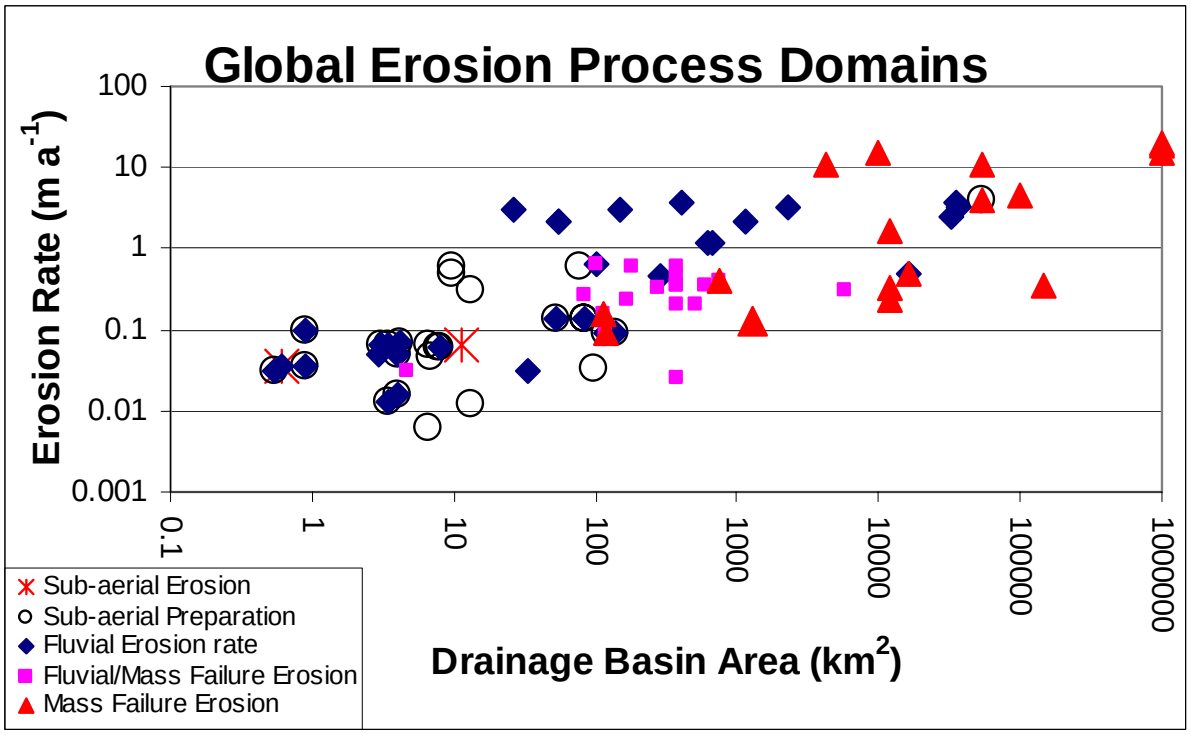

Figure 7.10 Erosion rates and processes plotted against drainage basin area for a world-wide bibliographic database of bank erosion literature sourced, and updated, mainly from Hooke (1980); Lawler (1993a); Harris (1996); and Stott (1999). Process categories defined largely by Harris (1996), extended for recent studies by the author.

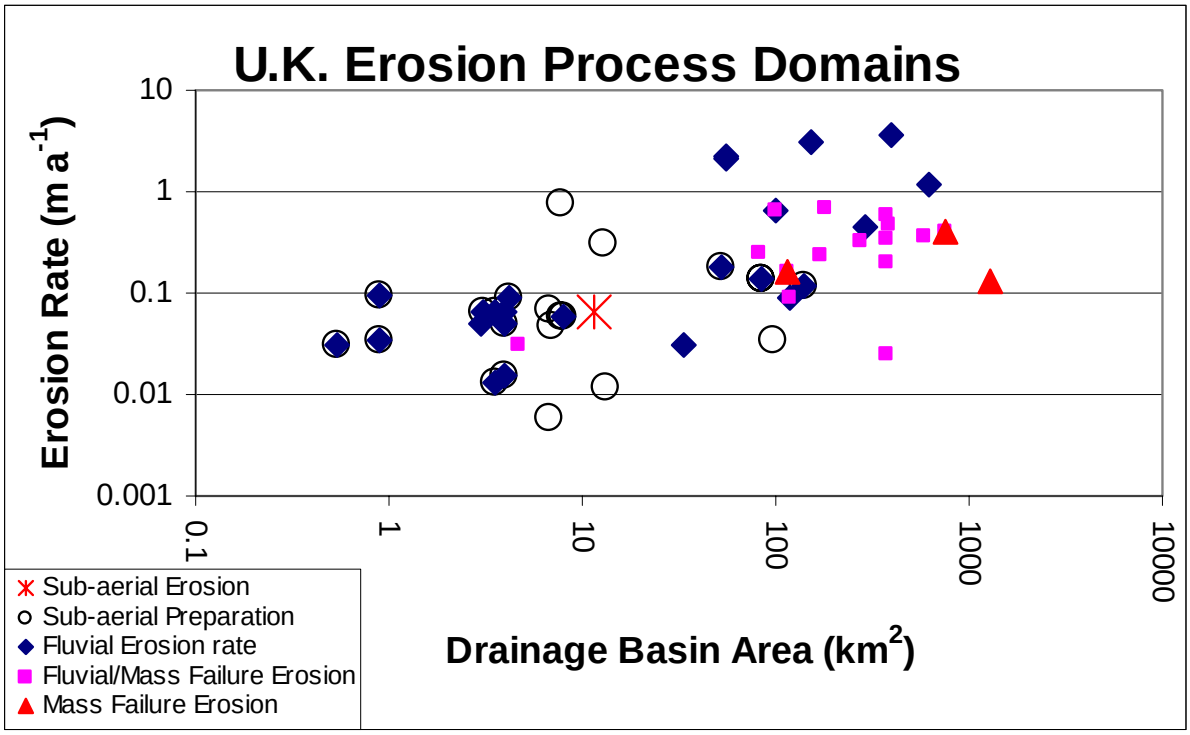

Figure 7.11 Erosion rates and processes plotted against drainage basin area for a world-wide bibliographic database of bank erosion literature sourced, and updated, mainly from Hooke (1980); Lawler (1993a); Harris (1996); and Stott (1999). Process categories defined largely by Harris (1996), extended for recent studies by the author.

7.5 Comparative Studies of Bank Erosion Process Efficacy at a Catchment Scale

The bibliography of rates and processes of erosion at different catchment scales (Section 7.4) indicated that the monitoring sites in this study were not unusual when compared to other published work. The fact still remains that actively eroding sites were selected for the Swale study (Section 3.4.2). This selection has the potential to bias the results by perhaps choosing sites that had particular flow structures i.e. impinging flow, sedimentary or vegetational characteristics not representative of the rest of the catchment.

Previous work on the River Swale (Dunnet, 1994; Longfield, 1994; Newson and Padmore, 1995; Walling *et al.*, 1999) has identified bank erosion as a significant process. However, erosion has either been a secondary aim of the study (Longfield, 1994; Newson and Padmore, 1995), or the methodology used has not been designed to distinguish between different process types (Dunnet, 1994; Walling *et al.*, 1999). This means that although they confirm the importance of bank erosion rates on land-use and suspended sediment fluctuations they cannot be compared with the changing processes identified in this study. Other studies have examined the downstream change

in erosion rates and processes (Harris, 1996; Brierley and Murn, 1997; Abernethy and Rutherfurd, 1998; Petkovic *et al.*, 1998): these allow a comparison with the model of changing erosion process domains (Figures 7.1 and 7.2).

A mapping evaluation of the change in channel alignment from 1961 to 1994 on the Juzna Morava River, Yugoslavia, gives an indication of the spatial distribution of erosion rates in another catchment (Petkovic *et al.*, 1998). The river has a DBA of 15000 km^2, total length of around 250 km, and an estimated annual amount of bank erosion of about 10^5 m^3 a^{-1}. The distribution of annual rates of fluvial erosion along the river channel produces a bell shaped distribution (Figure 7.12), with a mid-catchment peak of erosion of ~ 0.25 x 10^6 m^3 a^{-1} at approximately 150 km from the source, and 100 km from its mouth.

"….the total annual sediment transport of the river (about 2.10^6 m^3) is close to the annual input from bank erosion." "Consequently, it can be concluded that the bank erosion plays a very important role in the processes of sediment transport and channel changes" (Petkovic *et al.*, 1998, p. 363).

The mid-catchment peak in erosion rates may well coincide with a peak in stream power, as with the River Swale, however no information on stream power was provided. As the study is based on re-mapping, the differing processes throughout the catchment cannot be compared.

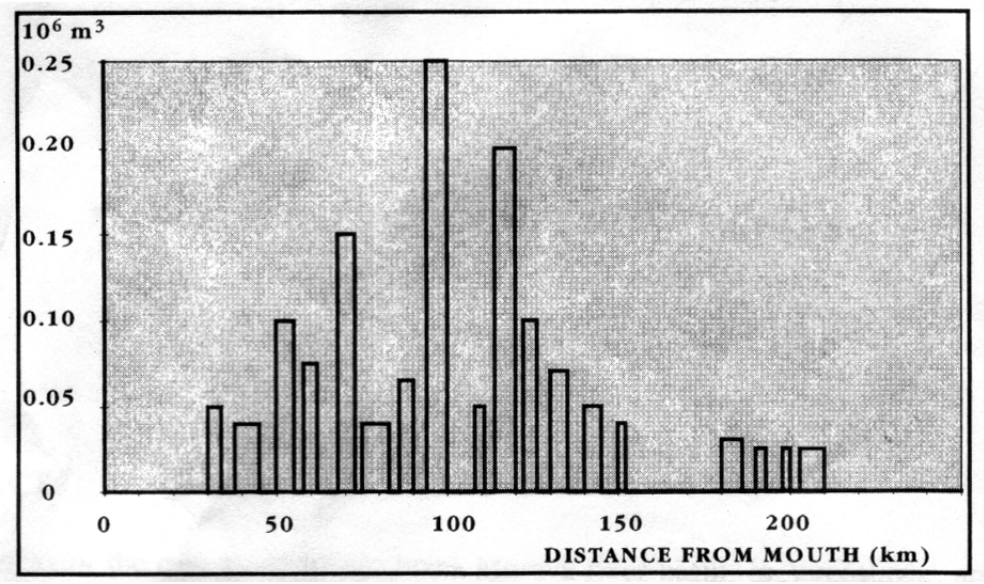

Figure 7.12 Distribution of mean annual rates of fluvial erosion along the Juzna Morava River, Yugoslavia (Petkovic *et al.*, 1998).

At a catchment scale, Abernethy and Rutherfurd (1998) examined the potential of vegetation for stabilising the riverbank against failures, on 230 km of the Latrobe River, Victoria, Australia. In order to achieve this aim they reviewed the differing bank erosion processes active throughout the system. They divided the river into seven different reaches (Figure 7.13) with different geomorphological characteristics. The model of different types of erosion they developed was subdivided into three main process categories:

1. Subaerial;
2. Fluvial Entrainment;
3. Mass failure.

The first category was found to dominate in the upper catchment, reach 1, with windthrow and Large Woody Debris (LWD) flow deflection producing most of the eroded sediment. They reasoned that other processes of erosion must dominate in the rest of the catchment as the low levels of erosion provided by subaerial processes do not explain the much higher levels of instability downstream.

Stream power was reasoned to dominate 60 km downstream in Reach 3, "as channel slope and catchment area combine to produce peak values of flow-erosivity" (Abernethy and Rutherfurd, 1998, p. 68). The effect of this was for fluvial entrainment to dominate 30 –90 km downstream in Reaches 2-4 (Figure 7.13), where vegetation was predicted to be the most influential in reducing erosion.

Field measured bank heights and slope angles were compared with estimated values derived from an adapted version of a log-spiral toe-failure analysis (Chen, 1975). The number of failures observed in the field was then contrasted with the estimated potential for failure to occur. The outcome of the analysis was that the greatest potential for mass failure was 160 – 200 km downstream in Reaches 5 and 6, as they contained high steep banks with suitable bank material. The bank height decreased in Reach 7 decreasing the likelihood of mass failures; however some were observed. Bank heights did not decrease downstream in the Swale, and therefore the models (Figure 7.1 and 7.2) do not account for this.

The basic process domains identified for the Swale study are in agreement with the model of Abernethy and Rutherfurd (1998), with an upstream, mid-catchment and downstream divide. The lack of monitoring especially of preparation processes, which may not be immediately assessable by visual means, does not allow for an accurate assessment of downstream efficacy changes.

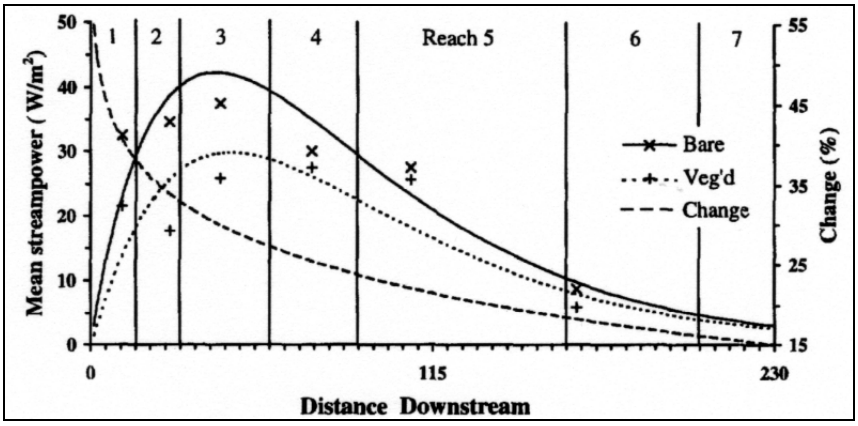

Figure 7.13 Mean streampower (ω) as a function of distance downstream for the cases of fully vegetated and bare banks on the Latrobe River. The percentage change between the two plots is shown (Abernethy and Rutherfurd, 1998).

- Reach 1, 0-15 km downstream with a catchment area of 65 km^2, is dominated by subaerial processes;
- Reach 2, 15-30 km downstream with a catchment area of 375 km^2, is dominated by subaerial and fluvial processes;
- Reach 3, 30-60 km downstream with a catchment area of 525 km^2, is dominated by fluvial processes;
- Reach 4, 60-90 km downstream with a catchment area of 1895 km^2, is dominated by slumping and fluvial processes;
- Reach 5, 90-160 km downstream with a catchment area of 3880 km^2, is dominated by slumping and fluvial processes;
- Reach 6, 160-200 km downstream with a catchment area of 4425 km^2, is dominated by slumping and fluvial processes;
- Reach 7, 200-230 km downstream with a catchment area of 4670 km^2, is dominated by fluvial processes.

Harris (1996) compiled a database of bank erosion literature, classifying different studies by their dominant processes and categories (Table 7.5) of erosion. From the database a model of process distribution downstream was constructed for: subaerial, fluvial, cantilever, and mass failure processes (Figure 7.14). Using the data collected Harris (1996) was able to determine the distances from river source that each process would dominate. Subaerial processes were proposed to dominate in the upper 4 km of the catchment, fluvial processes from 4 – 20 km downstream, and mass failures 20 km from the river source to its estuary. Using field

measurements from the River Severn, UK, the model was adapted with two transition zones being added: subaerial preparation between subaerial erosion and fluvial erosion dominance zones, and fluvial/ mass failure erosion between fluvial erosion and mass failure erosion dominance zones (Figure 7.15).

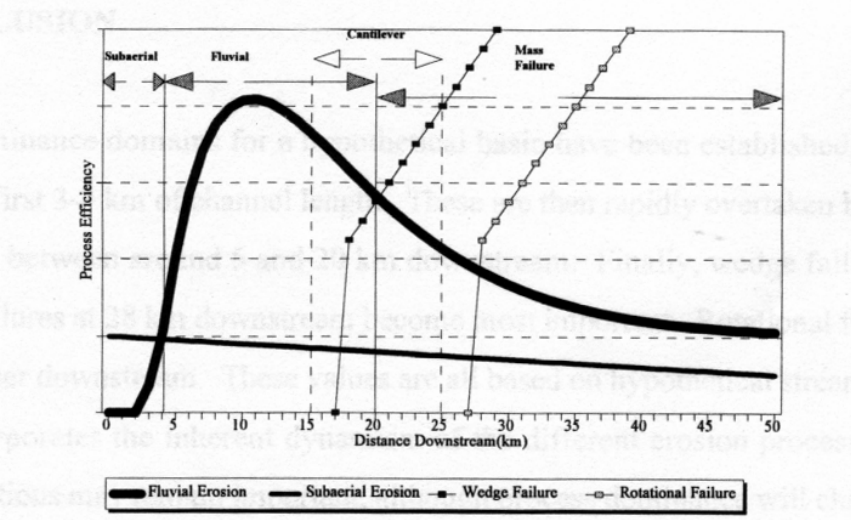

Figure 7.14 Development of Lawler's (1992a) hypothetical downstream change in process-intensity dominance domains (Harris, 1996).

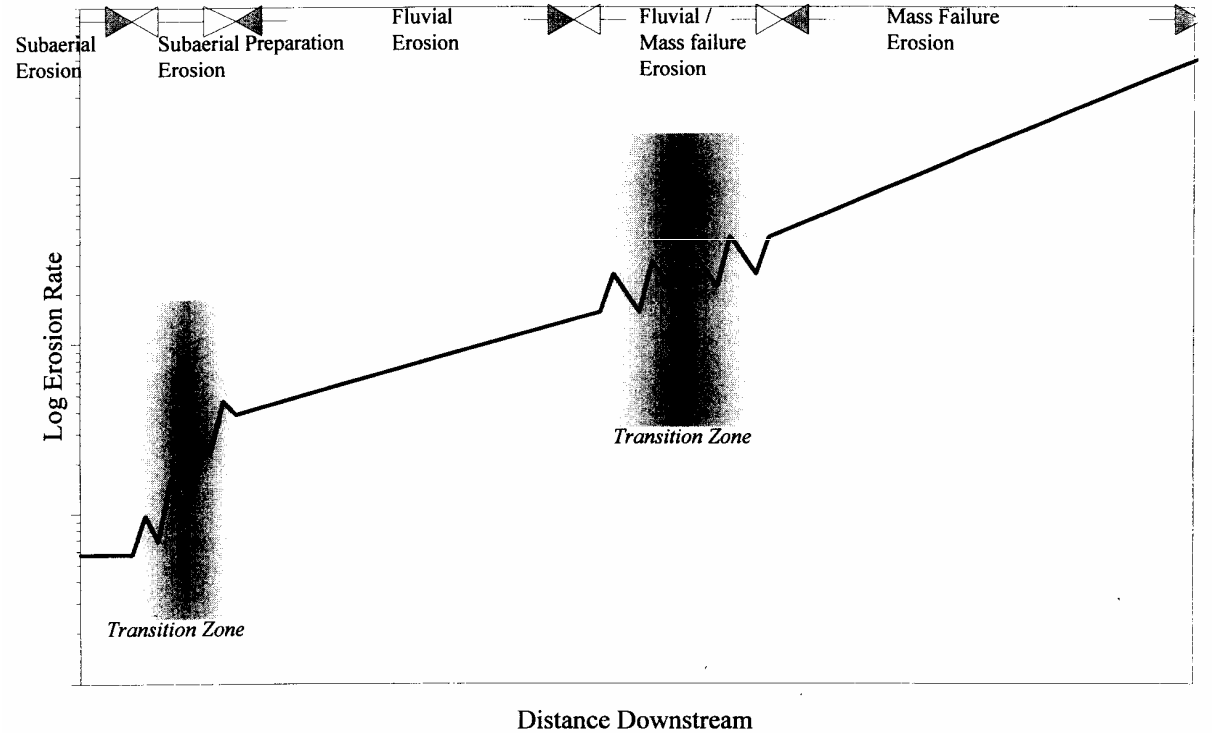

Figure 7.15 Downstream change in erosion rates and dominant erosion processes (Harris, 1996).

The suggested distances of process influence (Figure 7.14) are similar to those found in the Swale. Subaerial erosion did dominate in the upper 2.6 km; however, fluvial processes dominated from 2.6 – 87.4 km downstream with mass failures only having the greatest efficacy 104.4 km downstream. Fluvial/ Mass failures, in the form of cantilever failures, were thought to occur upstream of the mid-catchment zone because of the composite nature of the bank material (Figures 7.1 and 7.2).

Other studies of bank erosion process change and rates of channel change tend to be based around a disturbance within the drainage system, with the recovery of the river producing differing processes (Hupp and Simon, 1986; Brierley and Murn, 1997; Page and Carden, 1998; Rinaldi and Casagali, 1999; Ritter *et al.*, 1999). Whilst the impact of mining along the Swale river system (Raistrick, 1975) has clearly altered the landscape, whether the hydrology and sedimentology are currently 'recovering' from this disturbance is unclear. Work by Coultard (pers. comm.) has focused in the movement of sediment slugs through the River Swale catchment, and these may influence the bank sedimentology, river slope, and be influenced by bank erosion.

Brierley and Murn (1997) researched the impact of the European settlement (around 1830) on the Cobargo catchment in New South Wales, Australia. Although temporally detailed monitoring was not undertaken, the geomorphic changes through the catchment were examined, and related to differing processes of erosion. Six geomorphic process zones were defined and based on the ability of the river to transfer sediment (specifically bedload). They concluded that the settlement disturbance had resulted in a greater percentage of actively eroding sites upstream, while in the mid-catchment the increased amount of sediment had created bar deposits that were causing impinging flow against the bank. This had allowed fluvial entrainment, which undercut the bank. The furthest downstream reaches were sediment accumulation zones with little present day erosion: approximately 10 % of the banks were actively eroding. This may have implications on the results of disturbance to the 'natural' background catchment process distribution.

7.6 SUMMARY

1. For the Swale study, preparation processes were found to decrease in efficacy from a maximum in the upper catchment. They then increased in efficacy at the downstream sites because of the reduced efficacy of other processes, and the increasing influence of desiccation (Figures 7.1 – 7.2).
2. Fluid entrainment peaked in the mid-catchment (Figure 7.1), at the second peak of stream power (Figure 4.10J). It was, however, difficult to distinguish the difference between mass failure and entrainment at the lower catchment sites.
3. Mass failures were observed from Reeth (Site 5) downstream to Topcliffe (Site 9). The magnitude of the failures increased downstream, as the bank heights increased and the sediment became more cohesive. The frequency of the failures was thought to decrease downstream, this would explain the decreasing rates of erosion (Figure 4.1 and 4.2) and channel activity classification (Figure 4.4).
4. The downstream change in process dominance also allowed the differences in erosion seasonality to be identified. As more erosion processes became active downstream the length of the eroison season was extended.
5. A comparison with other studies of bank erosion allowed the Swale study to be put in context. The rates of erosion measured a different DBA values were similar for the Swale and the compilation of other research.
6. Processes of erosion identified by other researchers were placed in 5 categories (Subaerial Erosion, Subaerial Preparation, Fluvial Entrainment, Fluid Entrainment/Mass Failure, Mass Failure) which were proposed by Harris (1996). The scales of DBA that each process category was active over were compared with each other, and with the results from the Swale study. The downstream trends in erosion process categories for the bibliographic database showed the same trend of Subaerial activity at small DBA values, Fluvial Entrainment at intermediate DBA values, and Mass Failure in studies with a high DBA.
7. A comparison with other studies, on changes in erosion process domains at the catchment scale, revealed a general agreement with the downstream change (from Subaerial Processes changing to Fluvial Entrainment and then to Mass Failure) identified in the Swale study.
8. The compilation of all the data allows a summary of erosion processes trends downstream and recommendations for further research in Chapter 8.

CHAPTER 8

CONCLUSIONS

8.1 INTRODUCTION

Studying the rates and processes of erosion at nine sites throughout a river catchment, alongside their hydrogeomorphological characteristics, allowed the following conclusions to be reached:

1. Frost action only dominated at the most upstream site, 2.56 km downstream (Table 8.1).
2. Fluvial entrainment, both directly from the riverbanks and of material prepared by subaerial and mass failure processes, increased to a maximum in the mid-catchment. This was not, as theorised by Lawler (1992a; 1995), simply caused by the peaking of stream power in the catchment. It was instead a combination of high stream powers and the initiation of mass failures.
3. Mass failures increased in size at the downstream sites (29.9 – 104.4 km downstream) as the bank heights increased. The frequency of the failures did not increase downstream and they were not the dominant erosion process until the potential for fluid entrainment had substantially decreased at Site 9 (Table 8.1).
4. Cantilever failures, piping and sapping processes did not follow the trends suggested by Lawler (1992a; 1995) for subaerial preparation, fluid entrainment, or mass failures and were more significantly controlled by the bank sedimentology. These processes were at their most effective in the upper-mid catchment.

A summary of the work leading to these conclusions will be presented in the following chapter, as will the implications of these findings and suggestions for further work.

SITE NAME	DISTANCE DOWNSTREAM FROM RIVER SOURCE (km)	DRAINAGE BASIN AREA (km^2)	AVERAGE ANNUAL EROSION RATE ($m\ a^{-1}$) *29/02/96-13/03/98*	EROSION PROCESSES IDENTIFIED
1. Beck Meetings	2.56	4.2	0.07	Frost Action, Fluvial Entrainment, Cantilever Failures
2. Hoggarths	8.8	52.4	0.14	Frost Action, Fluvial Entrainment, Cantilever Failures
3. Muker	15.2	82.6	0.26	Frost Action, Fluvial Entrainment, Cantilever Failures
4. Low Row	23.4	141	0.09	Frost Action, Fluvial Entrainment, Piping, Cantilever Failures
5. Reeth	29.9	183	0.62	Frost Action, Fluvial Entrainment, Slab Failures, Cantilever Failures, Pop-out Failures
6. Easby	49.5	399	*3.58	Fluvial Entrainment, Cantilever Failures, (possibly Wet Flow)
7. Morton-on-Swale	74.7	593	0.35	Frost Action, Fluvial Entrainment, Piping, Slab Failures, Cantilever Failures, Pop-out Failures
8. Greystone Farm	87.4	748	0.41	Frost Action, Desiccation, Fluvial Entrainment, Slab Failures, Cantilever Failures, Wet Flow
9. Topcliffe	104.4	1282	0.13	Frost Action, Desiccation, Fluvial Entrainment, Slab Failures, Cantilever Failures, Translational Failures

Table 8.1 A summary of the distance downstream, drainage basin area, annual rate of erosion, and erosion processes at each of the monitoring site. * = Erosion from 16/01/07-13/03/98.

8.2 MAIN PROJECT FINDINGS

8.3.1 Erosion Process Spatial Domains

Lawler (1992a; 1995) suggested a downstream change in the dominant erosion process domains (Figure 1.1) for catchment scale riverbank erosion in a temperate region. Subaerial preparation processes, in particular frost action, dominated upstream. Fluid entrainment was most efficient in the mid-catchment, and mass failures were dominant in the lower catchment reaches. Abernethy and Rutherfurd (1998) came to a similar conclusion for the Latrobe River, Australia, with subaerial processes dominating upstream, fluvial processes mid-catchment, and slumping combined with fluvial processes in the lower catchment.

This study came to the conclusion that the main process groupings were similar but the theoretical basis for Lawler's (1992a, 1995) predictions did not hold under extensive field testing.

Subaerial Preparation

1. Subaerial preparation dominated over a relatively small catchment area in the upstream reaches, with fluvial entrainment and cantilever failures rapidly becoming more efficient.
2. Desiccation only became effective in the lower reaches rather than operating throughout the catchment. The banks becoming drier for a longer period, combined with a slight increase in the sediment fine fraction, may have caused this.
3. The overall distribution of subaerial preparation processes was not a gradual decline throughout the catchment as suggested by Figure 1.1. Instead the increasing efficacy of mass failure and fluvial processes mid-catchment, and their subsequent decline downstream, meant that subaerial processes were lowest in efficacy mid-catchment but increased in the lower reaches.

Fluid Entrainment

The efficacy of fluid entrainment did not match the distribution of stream power throughout the catchment. The rates of entrainment may have increased in a similar manner to the estimated stream powers; however, the mid-catchment secondary peak in stream power overlapped with the commencement of mass failures.

The main peak in stream power was not in the mid-catchment but in the upper reaches. The sedimentology of this reach may have affected the stream power predictions by supplying coarse grained basal sediment to the channel. The coarse material may also have restricted the amount of entrainment.

Mass Failures

Bank height was not the sole determining factor in the distribution of mass failure processes. Sites upstream of a similar height to those in the mid-catchment did not fail through mass failure. A change in sedimentology and flood hydrograph shape is thought to be responsible.

The efficacy of mass failure did not increase downstream from its commencement mid-catchment. The rapidity of removal by fluid entrainment in the mid-catchment meant that the rate of erosion and efficacy of mass failures was increased, as the basal region was continually at a state of excess basal capacity (Section 2.3.4).

Piping, Sapping, Cantilever, and Pop-out Failures

1. Cantilever failures are less dependent on the height of the bank than other mass failures, and will occur with a greater likelihood where the banks are composite and near to the catchment stream power maximum, probably just upstream.
2. Piping, sapping, and pop-out failures should occur near to the stream power peak. This theoretically would be an area where sandy lenses are incorporated within silty-sand sediment, allowing rapid infiltration on the steep rising limb of the flood hydrograph. The sediment would also allow preferential drainage through the bank on the steeply falling limb of the hydrograph.

8.2.2 Erosion Process Temporal Domains

The downstream change in bank erosion process efficacy throughout the catchment was linked to variations in the timing of erosion events. This explains the change in seasonal erosion rates identified during erosion pin epoch data from upstream to downstream (Figure 5.1). Whilst the efficacy of all the processes, except subaerial preparation (frost action and desiccation), may decline downstream every process still remains active in the lower catchment. This resulted in a gradually increasing number of processes becoming active throughout the river system, from upstream to downstream. The zonation of different erosion processes over an annual period resulted in a temporal model of erosion (Section 7.3) that consisted of:

1. Upstream the winter periods dominating annual erosion. This was due to the significance to frost action in preparing the bank material, which was removed during the winter/spring flood season;
2. Mid-catchment entrainment caused a rapid removal of failed/prepared material in the main period of flooding. This resulted in both erosion of subaerially prepared sediment early in the year followed by direct entrainment later in the spring. The removal of fallen debris from mass failures during high flows meant that the basal area of the bank was left prone to direct entrainment for a longer period;
3. The lower catchment sites were prone to desiccation, which meant that the erosion season was extended into the summer months. The influence of mass failures at the downstream sites also meant that the erosion season was extended. Summer floods had the ability to trigger mass failures that may have been weakened/prepared during the main flood season. This meant that they were almost seasonally independent. The continuation of frost action downstream also allowed erosion to occur during the winter months.

8.2.3 Catchment Geomorphological Characteristics

The morphological and sedimentary characteristics of the River Swale (Table 8.2) allowed the physical restraints on erosion processes to be assessed, and placed in context against other studies.

Few studies have researched the downstream change in bank sedimentology (Harris, 1996), especially in relation to bank erosion dynamics. A decreasing particle size with distance downstream was expected, and was the case for Sites 1 – 4 (Figure 4.5). The mid-catchment bank sediment variability, at the monitoring sites, could be a due to the historical mining industry in Swaledale (Raistrick, 1975). A pulse of sediment released during mining activity could have propagated to the mid-catchment, since the cessation of mining activity, possibly indicated by the lead rich layers in the sediment (Macklin *et al.*, 1994). The downstream stability of silt and sand contents, with only a small increase in clay percentage weights, was not predicted. This may be a product of overbank accretion only occurring during high flow events, which become more infrequent in a downstream direction.

GEOMORPHOLOGICAL CHARACTERISTICS	DOWNSTREAM TREND FROM CATCHMENT SOURCE
Channel Longitudinal Slope (m m^{-1}) ***(Figure 4.10 C)***	A general downstream decline in slope from 0.027 m m^{-1} at Site 1 to 0.001 m m^{-1} at Site 9. There are two exceptions to this trend, with elevated gradients of 0.017 m m^{-1} and 0.005 m m^{-1} at Sites 3 and 9.
Hydraulic Radius (m) ***(Figure 4.10 F)***	The catchment minimum of 0.50 m was at Site 1, increasing up to 2.94 m at Site 9. The radius rapidly decreased from 1.48 m at Site 4 to to 0.79 m at Site 5, then increased again downstream.
River Bank Sedimentology ***(Figures 4.5-4.8)***	There were similar trends in the upper and lower bank sedimentology, but more variability mid-catchment in the mid-bank. The general trend was decreasing gravel and sand contents, alongside increasing silt and clay contents. In the mid-catchment there was a silt content peak and sand content trough. Downstream silt and sand contents remained reasonably stable, whilst the gravel content decrease, and clay content increased.
River Bed Clast Size (mm) ***(Figure 4.10 G)***	The overall trend was for decreasing sediment b-axis size downstream; however, the D_{84} dimensions increased rapidly from 86.0-mm at Site 1 to 132.3-mm at Site 2. The size remained almost constant until a decline to 54.5-mm at Site 5. The maximum clast size of 140.8-mm was at Site 6, decreasing downstream to approximately 10.0-mm at Sites 7-9.
Stream Power (W m^{-1}) ***(Figure 4.10 J)***	There were two peaks in gross stream power. At Site 3 the catchment peak value of 39081 W m^{-1}, Sites 2 and 4 had values of around 11000 W m^{-1}. The second peak was of 4521 W m^{-1} was at Site 6. The peaks may have been caused by bedrock reaches upstream.
Riparian Vegetation ***(Table 4.7)***	There was a mid-catchment peak, at Site 6, in herbaceous species diversity. This may be indicative of more dynamic channel change in this region. Grazing, the dominant land-use at all but Site 6, could also be responsible for decreased diversity at the other sites.

Table 8.2 A summary of the geomorphological trends throughout the study catchment.

The two peaks in stream power, at Sites 3 and 6 (Table 8.2), were probably related to the bedrock reaches upstream of the monitoring sites (Section 7.2.4). Upstream bedrock may also have influenced the increased channel slope at Site 3. Sites 3 and 6 were also regions with a composite bank stratigraphy, and a large uncohesive lower bank structure. The basal bank material could be responsible for supplying larger than expected sediment to the channel, increasing the estimated stream power (Section 4.4.4).

8.2.4 Catchment Trends in Rates of Erosion

Previous work on bank erosion rates, in several basins world-wide, has shown a trend of increasing rates with DBA (Hooke, 1980) (Section 7.4.1). The results from this study (Figures 4.1 and 4.2) did not agree with this general trend and were modelled with simple quadratic functions (Equations 4.1 – 4.3). This was probably a result of the systematic monitoring within a single catchment.

The rates of erosion from this study were within the same range of DBA values as the rates compiled from erosion studies world-wide (Section 7.4.1), even though the overall trends were different. The measurement requirements for this work meant that highly eroding sites had to be selected for monitoring (Section 3.4.2). The bibliographic database has been built up from a variety of studies that use both highly eroding sites and maps to determine planform change (Lawler, 1993a), the remapping may give lower annual rates of erosion. Despite the difference in techniques in the literature the results from this study, in terms of rates and processes at different DBA values, were in general agreement with the bibliographic database (Section 7.4).

8.3 IMPLICATIONS OF THE STUDY

In terms of instrumentation and operational procedures the following recommendations may be made from this study:

1. The PEEP sensors were inadequate for distinguishing between all the process types that were being researched. For erosion caused by subaerial processes they worked well, although the disturbance of the bank when the sensor is inserted may cause disruption of the sediment surrounding the sensor. With small amounts of material being eroded this could be a significant problem, especially at sites with very unconsolidated fine sediment. The sensors did not work when submerged because of the turbid nature of the river water, from an upland peat catchment source. This meant that fluvial entrainment could not be monitored directly, and values were calculated by comparing the signals before and after the event. This may be a period of several days if river levels remained high. The monitoring length of the sensor, approximately 100 mm, was not suitable for mass failure events. These failures usually left the sensor hanging out of the bank, often in an inoperable state. The rapid

initiation of failures as the river levels receded frequently meant that the sensors were either in darkness, submerged, or covered in debris when failures occurred, producing indecipherable data.

Management of the PEEP data was not a simple procedure. Cleaning the data to remove the many spurious values, including much of the dawn and dusk periods, meant that more gaps were put into the dataset on top of those already present from when the sensors were malfunctioning.

2. The erosion pins were limited by the frequency of remeasurement and were again not suitable for mass failure monitoring as the length had to be short enough not to support the bank, and therefore whole pins were removed even in small failures. They could also not be placed in sediment containing large clasts. Bank top resurveys were limited in the amount of three-dimensional data that could be collected both spatially and temporally. It is hoped that advances in photogrammetry (Lane *et al.*, 2000) will allow erosion to be measured accurately enough to be analytically useful. The system at the moment is not accurate enough to achieve millimetre accuracy, and is expensive in terms of equipment and the amount of data produced. A critique of the method is presented in Lawler (1993a). No alternative methods are currently available to monitor bank erosion during submergence.
3. The measurement of bankface temperature using the TinyTalk thermistor dataloggers was convenient because of the lack of cabling needed. Problems of retrieval when submerged, and the length of data that could be stored, need to be addressed if this system was to be used again.

The exact thresholds for each process domain could not be identified because of the distance between monitoring sites. Regions of erosion process dominance can be suggested. These may vary between catchments due to the land-use, climatology, geology, and geomorphology of the particular river system. Despite this the results may be adapted or used as a guide for:

1. The implementation of bank erosion protection (Hemphill and Bramley, 1989). The distinction between zones that require hard or soft technology, and where the most prone areas of the bank are in the vertical and horizontal planes, may be made.

2. The assessment of potential riverbank contained pollutant release into the suspended sediment load, and solution. The timing and amount of sediment released from natural and anthropogenic contaminates within the bank sediment, such as heavy metals, could be estimated using a knowledge of the pollutant situation within the catchment (Grove and Sedgwick, 1998). This would allow an assessment of potential drinking water supply problems, and the effect of re-deposition on the floodplain downstream of the source (Sedgwick, 2000).
3. The planning of sediment budgets for reservoirs. The rate and seasonality of the sediment input from riverbanks could be approximated if the position of the reservoir within the catchment was known; especially in relation to the stream power peak, bank sedimentology and climate. Walling *et al.* (1999) estimated the riverbanks in the Swale catchment to contribute 28.2% of the suspended sediment budget (November 1994-February 1997), making banks a significant source of sediment.

8.4 FUTURE RESEARCH SUGGESTIONS

The bibliographic research into published work on erosion rates and processes revealed a lack of large-scale studies within the U.K., i.e. with DBAs above 1000 km^2 (Section 7.4). Comparative work on other catchments is needed to validate the models produced on the River Swale. Some suggestions are provided to aid the establishment of similar research projects (Table 8.3).

Process monitoring studies tend to be of one or two year duration and/or in areas that are known to be prone to erosion. In order to fully understand the influence of process dynamics in a river system monitoring needs to be undertaken over a longer time span on both rapidly and gradually eroding sites throughout a catchment, similar to that undertaken by Stott (1999).

There is a wealth of research into temperate catchments but few detailed studies in semi-arid or arctic regions (Harris, 1996). The application of photogrammetry (Lane *et al.*, 2000) in arctic systems, where insertion of equipment into the frozen sediment is both difficult and produces high errors due to preferential heating, would be desirable. The growth of thermo-erosion niches (Scott, 1978), and erosional patterns during a river melt-out cycle would aid the understanding of arctic river systems.

Work has already been undertaken on the linkages between bank erosion and heavy metal remobilization within the Swale catchment (Grove and Sedgwick, 1998). A more detailed study including the event based monitoring of both bank erosion events and heavy metal concentrations in suspended sediments would be useful in terms of managing water supplies from polluted catchments.

The understanding of pop-out failures mechanisms requires a geotechnical investigation of the interaction between the bank sediment and river water. A detailed monitoring of soil moisture contents in sediment suitable for these failures is needed.

A Initial Desktop Study

- Determine the longitudinal profile of the study river(s).
- Locate gauging stations (determine frequency and type of measurements).
  If possible create a downstream distribution of bankfull stream power using available gauging station data.
- Locate meteorological stations (determine frequency and type of measurements).
- Assess the above and below surface geology within the catchment.
- Map riparian vegetation characteristics (using local authority information, or river corridor surveys).
- Map land-use, especially riparian industries with their associated abstractions, discharges, and reservoirs. Include research into past land-use such as mining.
- Use aerial photographs to provide an indication of mass failure domains and unvegetated steep banks

B Site Reconnaissance

The reconnaissance (Thorne, 1993) of the riverbank should be used to assess the riverbanks at equal intervals down the catchment and/or at areas selected in the desktop study. The purpose of this would be to identify:

- Where actively eroding, near vertical unvegetated banks are located, which would be suitable for erosion pin and PEEP insertion.
- Where composite banks occur, indicating the likelihood of cantilever failures.

The critical region of bank heights which are sufficient to cause mass failures.

Table 8.3 A recommended research strategy for comparable catchment bank erosion studies.

C Instrumentation
❑ Erosion pins would be recommended for installation at as many sites as is feasible to compare fluvial entrainment and subaerial erosion as they are cheap and simple, recommendations on instrumentation can be found in Lawler (1993a). ❑ PEEPs would be most beneficial in the upstream reaches to monitor subaerial processes, giving comparable rates of frost heaving. Sensors could be distributed through the catchment to provide comparable data on subaerial processes, this is not recommended because of the constraints of the equipment (Section 8.3). ❑ Photogrammetric techniques (Lane *et al.*, 2000) would be usefully applied to study the concept of a downstream increase in mass failure magnitude, but decrease in frequency. This non-invasive technique would resolve the problem of pins and PEEPs being removed, or supporting the failure. ❑ Moisture sensors placed vertically in the bank profile would be advantageous in the zones of potential piping, sapping and pop-out failures to determine the thresholds moisture conditions of these processes. ❑ Stage and meteorological monitoring would need to be installed to augment or substitute the existing measurements.
D After Monitoring Completion
❑ Shear box samples could be taken around the threshold bank height of mass failures. This would allow a critical evaluation of current physical models that suggest the bank conditions needed for failures to occur (Chen, 1975; Darby *et al.*, 2000). ❑ Samples of bank sediment should be taken to determine the longitudinal profile of sediment sizes, and the bank material composition around pins and PEEPs.

Table 8.3 continued A recommended research strategy for comparable catchment scale bank erosion studies.

REFERENCES

ABAM, T.K.S. (1997) Genesis of channel bank overhangs in the Niger Delta and analysis of mechanisms of failure. Geomorphology, **18**, 151-164.

ABERNETHY, B. and RUTHERFURD, I.D. (1998) Where along a river's length will vegetation most effectively stabilise stream banks. Geomorphology, **23**, 55-75.

AHNERT, F. (1994) Equilibrium, scale and inheritance in geomorphology. Geomorphology, **11**, 125-140.

AINSWORTH, A.M., and GOULDER, R. (2000) Downstream change in leucine aminopeptidase activity and leucine assimilation by epilithic microbiota along the River Swale, northern England. Science of the Total Environment, **251/252**, 191-204.

ALLISON, J.W. and HARTNUP, R. (1981) Soils in North Yorkshire VI: sheet SE 39, Northallerton. Soil Survey of Great Britain, Harpenden, Hertfordshire.

ANDREWS, E.D. (1982) Bank stability and channel width adjustment, East Fork River, Wyoming. Water Resources Research, **18**, 1184-1192.

ANNANDALE, G.W. (1995) Erodibility. Journal of Hydraulic Research, **33**(4), 471-494.

ANNANDALE, G.W. and PARKHILL, D.L. (1995) Stream bank erosion: application of the erodibility index method. In ESPEY, W.H., and COMBS, P.G. (Eds), The First International Conference of Water Resources Engineering, American Society of Civil Engineers, San Antonio, TX, 1570-1574.

ASHBRIDGE, D. (1995) Processes of river bank erosion and their contribution to the suspended sediment load of the River Culm. In FOSTER, I.D.L., GURNELL, A.M. and WEBB, B.W. (Eds), Sediment and Water Quality in River Catchments, Wiley, Chichester, 229-245.

ASHWORTH, P.J. and FERGUSON, R.I. (1986) Interrelationships of channel processes, changes and sediments in a proglacial river. Geographiska Annaler, **68A**, 361-371.

BAGNOLD, R.A. (1960) Sediment discharge and stream power: a preliminary announcement. US Geological Survey Circular, **421**.

BAGNOLD, R.A. (1966) An approach to the sediment transport problem from general physics. U.S. Geological Survey Professional Paper, **422-I**, 37 pp.

BATHURST, J.C. (1997) Environmental river flow hydraulics. In THORNE, C.R., NEWSON, M. and HEY, R.D. (Eds) Guidebook of Applied Fluvial Geomorphology for River Engineering and Management, Wiley, Chichester.

BELLO, A., DAY, D., DOUGLAS, J., FIELD, J., LAM, K. and SOH, Z.B.H.A. (1978) Field experiments to analyze runoff, sediment and solute production in the New England region of Australia. Zeitschrift für Geomorphologie N.F. Suppl. Bd., **29**, 180-190.

BISHOP, A.W. (1955) The use of the slip circle in the stability analysis of slopes. Geotechnique, **5**, 7-17.

BLUCK, B.J. (1971) Sedimentation in the meandering River Endrick. Scottish Journal of Geology, **7**(2), 93-138.

BOARDMAN, J. (1990) Soil erosion of the South Downs: a review. In BOARDMAN, J., FOSTER, I.D.L. and DEARING, J.A. (Eds), Soil Erosion of Agricultural Land. John Wiley & Sons Ltd, Chichester, 87-105.

BOARDMAN, J. (1995) Damage to property by runoff from agricultural land, South Downs, southern England. Geographical Journal, **161**, 177-191.

BOARDMAN, J., LIGNEAU, L., DE ROO, A., and VANDAELE, K. (1994) Flooding of property by runoff from agricultural land in northwestern Europe. Geomorphology, **10**, 183-196.

BRANDT, S.A. (2000) Classification of geomorphological effects downstream of dams. Catena, **40**(4), 375-401.

BRANSON, J. (1992) Soil erosion and transport by needle ice: a laboratory investigation, Unpublished Ph.D. Thesis, University of Birmingham.

BRANSON, J., LAWLER, D.M. and GLEN, J.W. (1992) The laboratory simulation of needle ice. In N. MAENO and T. HONDOH (Eds), Proceedings of the International Symposium on the Physics and Chemistry of Ice, Sapporo, Japan, September, 1991, Hokkaido University Press, Sapporo, Japan, 1992.

BRANSON, J., LAWLER, D.M. and GLEN, J.W. (1996) Sediment inclusion events during needle-ice growth: a laboratory investigation of the role of soil moisture and temperature fluctuations. Water Resources Research, **32**, 459-466.

BRAY, D.I. (1987) A study of channel changes in a reach of the North Nashwaaksis stream, New Brunswick, Canada. Earth Surface Processes and Landforms, **12**, 151-165.

BRICE, J.C. (1973) Meandering pattern of the White River in Indiana – an analysis. In Morisawa, M. (Ed), Fluvial Geomorphology, State University, New York, Binghampton, 178-200.

BRIERLEY, G.J. and MURN, C.P. (1997) European impacts on downstream sediment transfer and bank erosion in the Combargo catchment, New South Wales, Australia. Catena, **31**, 119-136.

BRITISH RAINFALL ORGANISATION (1989) British Rainfall. Stanford, London.

BRITISH STANDARDS INSTITUTION (1975) Methods of testing soils for civil engineering purposes. BS1377, London: British Standards Institution.

BRUNSDEN, D. and KESEL, R. (1973) Slope development on a Mississippi River bluff in historic time. Journal of Geology, **81**, 576-587.

BULL, L.J. (1996) Dynamics of Fluvial Suspended Sediment Transport and River Bank Sediment Supply, Unpublished Ph.D. Thesis, University of Birmingham, 276 pp.

BULL, L.J. (1997) Magnitude and variation in the contribution of bank erosion to the suspended sediment load of the River Severn, U.K. Earth Surface Processes and Landforms, **22**, 1109-1123.

BURT, T.P., ADAMSON, J.K. and LANE, A.M. (1998) Long-term rainfall and streamflow records for north central England: putting the Environmental Change Network site at Moor House, Upper Teesdale, in context. Hydrological Sciences, **43**(5), 775-787.

CARLING, P.A. (1986) Peat slides in Teesdale and Weardale, Northern Pennines, July 1983: description and failure mechanisms. Earth Surface Processes and Landforms, **11**, 193-206.

CARROLL, R.W.H., WARRWICK, J.J., HIEM, K.J., BONZONGO, J.C., MILLER, J.R. and LYONS, W.B. (2000) Simulation of mercury transport and fate in the Carson River, Nevada. Ecological Modelling. **125**(2-3), 255-278.

CARSON, M.A. (1971) Mechanics of Erosion. Pion, London, 145 pp.

CARTER, C.E., GREER, J.D., BRAUD, H.J. and FLOYD, J.M. (1974) Raindrop characteristics in south central United States. Transactions of the ASAE, **17**, 1033-1037.

CASAGLI, N., RINALDI, M., GARGINI, A. and CURINI, A. (1999) Pore water pressure and streambank stability: results from a monitoring site on the Sieve River, Italy. Earth Surface Processes and Landforms, **24**, 1095-1114.

CHANG, H.H. (1979) Minimum stream power and river channel patterns. Journal of Hydrology, **41**, 303-327.

CHEN, W. (1975) Limit Analysis and Soil Plasticity. Elsevier, Amsterdam, 638 pp.

CHERRY-GARRARD, A. (1994) The Worst Journey in the World. Picador, London.

CHRISTMAS, M. (1998) Phosphorus dynamics in the Swale-Ouse river system. Unpublished Ph.D. Thesis, University of Durham.

CHURCH, M.A., MCLEAN, D.G. and WOLCOTT, J.F. (1987) River bed gravels: sampling and analysis. In THORNE, C.R., BATHURST, J.C. and HEY, R.D. (Eds), Sediment Transport in Gravel-bed Rivers, John Wiley & Sons, Chichester, 43-88.

CHURCH, M. and SLAYMAKER, O. (1989) Disequilibrium of Holocene sediment yield in glaciated British Columbia. Nature, **337**, 452-454.

COLEMAN, J.M. (1969) Brahmaputra River: channel processes and sedimentation. Sedimentary Geology, **3**, 129-239.

COUPERTHWAITE, J.S. (1997) Downstream Change in Channel Hydraulics Along the River Severn, Unpublished Ph.D. Thesis, University of Birmingham. 240 pp.

CUMMINS, W.A. and POTTER, H.R. (1972) Rates of erosion in the catchment area of Cropstone Reservoir, Charnwood Forest, Leicestershire. Mercian Geologist, **4**, 149-157.

DARBY, S.E. (1998) Modelling width adjustment in straight alluvial channels. Hydrological Processes, **12**(8), 1299-1321.

DARBY, S.E. and THORNE, C.R. (1994) Prediction of tension crack location and riverbank erosion hazards along destabilised channels, Earth Surface Processes and Landforms, **19**, 233-247.

DARBY, S.E. and THORNE, C.R. (1996) Stability analysis for steep, eroding, cohesive riverbanks. A.S.C.E. Journal of Hydraulic Engineering, **122**(8), 443-454.

DARBY, S.E., GESSLER, D. and THORNE, C.R. (2000) Computer program stability analysis of steep, cohesive riverbanks. Earth Surface Processes and Landforms, **25**(2), 175-190.

DAVIS, R.J. and GREGORY, K.J. (1994) A new distinct mechanism of river bank erosion in a forested catchment. Journal of Hydrology, **157**, 1-11.

DERBYSHIRE, E., GREGORY, K.J. and HAILS, J.R. (1980) Geomorphological Processes. Butterworths, London.

DOWNS, P.W. and THORNE, C.R. (1998) Design principles and suitability testing for rehabilitation in a flood defence channel: The River Idle, Nottingham, UK. Aquatic Conservation, **8**(1), 17-38.

DRAPER, N. and SMITH, H. (1966) Applied Regression Analysis. Wiley, New York.

DREWITT, A. (1991) The Vegetation of the Yorkshire Dales National Park. Yorkshire Dales National Park Committee, Skipton

DUIJSING, J.J.H.M. (1987) A sediment budget for a forested catchment in Luxembourg and its implications for channel development. Earth Surface Processes and Landforms, **12**, 173-184.

DUNAWAY, D, SWANSON, S.R. WENDEL, J. and CLARY, W. (1994) The effect of herbaceous plant communities and soil textures on particle erosion of alluvial streambanks. Geomorphology, **9**, 47-56.

DUNNET, N. (1994) Riverbank erosion and protection survey, of stretches of the River Swale and the River Wharfe, which are accessible by public right of way, within the Yorkshire Dales National Park. Yorkshire Dales National Park Authority, Grassington.

DUYSINGS, J.J.H.M. (1986) The sediment supply by streambank erosion in a forested catchment. Zeitschrift für Geomorphologie Suppl. Bd, **60**, 233-244.

EFROYMSON, M.A. (1960) Multiple Regression Analysis. In RALSTON, A. and WILF, H.S. (Eds), Mathematical Methods for Digital Computers, Vol. 1, 191-203.

ENVIRONMENT AGENCY (1988) The State of the Environment of England and Wales: Fresh Water. The Stationary Office, London.

ENVIRONMENT AGENCY (1996) The Middle Swale Restoration Project. North East Region Office, Leeds.

ENVIRONMENT AGENCY (1997) Local Environment Agency Plan: Swale, Ure and Ouse. Consultation Report, June 1997. Environment Agency, North East Region, Rivers House, Leeds.

EVANS, R. and COOK, S. (1986) Soil Erosion in Britain. SEESOIL, **3**, 28-58.

FLEMING, A. (1998) Swaledale: valley of the wild river. Edinburgh University Press, Edinburgh.

FERGUSON, R. (1977) Linear regression in geography. Geo Abstracts, Norwich.

FERGUSON, R.I. (1981) Channel form and channel changes. In Lewin, J. (Ed), British Rivers, Allen and Unwin, London, 90-125.

FRIPP, J.B. and DIPLAS, P. (1993) Surface sampling in gravel streams. Journal of Hydraulic Engineering, **119**, 473-490.

GARCIA-RUIZ, R., PATTINSON, S.N. and WHITTON, B.A. (1999) Nitrous oxide production in the River Swale-Ouse, North-east England. Water Research, **33**(5), 1231-1237.

GARDINER, T. (1983) Some factors promoting channel bank erosion, River Lagan, County Down. J. Earth Sci. R. Dudl. Soc., **5**, 231-239.

GILVEAR, D.J. (1999) Fluvial geomorphology and river engineering: future roles utilizing a fluvial hydrosystems framework. Geomorphology, **31**, 229-245.

GRAF, W.L. (1982) Spatial variations of fluvial processes in semi-arid lands. In, Thorn, C.E. (Ed) Space and Time in Geomorphology, Allen and Unwin, 193-217.

GRAF, W.L. (1983) Downstream changes in stream power in the Henry Mountains, Utah. Annals of the Association of American Geographers, **73**, 373-387.

GREEN, T.R., BEAVIS, S.G., DIETRICH, C.R. and JAKEMAN, A.J. (1999) Relating stream-bank erosion to in-stream transport of suspended sediment. Hydrological Processes, **13**(5), 777-787.

GREGORY, K.J. and WALLING, D.E. (1973) Drainage Basin Form and Process. Arnold, Avon, 458 pp.

GRISSINGER, E.H. (1982) Bank erosion of cohesive materials. In HEY, R.D., BATHURST, J.C. and THORNE, C.R. (Eds), Gravel Bed Rivers, Wiley, 273-287.

GROVE, J.R. and SEDGWICK, C. (1998) Downstream spatial and temporal remobilisation of heavy metal contaminated sediments in the River Swale, England. In IRTCES (Ed), Proc. International Symposium on Comprehensive Watershed Management, Patent Documentation, Beijing, September 1998, 505-512.

GURNELL, A.M. and SWEET, R. (1998) the distribution of large woody debris accumulations and pools in relation to woodland stream management in a small, low-gradient stream. Earth Surface Processes and Landforms, **23**(12), 1101-1121.

HAGERTY, D.J. (1991a) Piping and sapping erosion I: basic considerations. A.S.C.E. Journal of Hydraulic Engineering, **117**(8), 991-1008.

HAGERTY, D.J. (1991b) Piping and sapping erosion II: identification-diagnosis. A.S.C.E. Journal of Hydraulic Engineering, **117**(8), 1009-1025.

HAGERTY, D.J., SPOOR, M.F. and ULLRICH, C.R. (1981) Bank failure and erosion on the Ohio River, Engineering Geology, **17**, 141-158.

HARRIS, N.M. (1996) The impact of scale on river bank erosion processes, Unpublished M.Phil. Thesis, University of Birmingham. 194 pp.

HARRY, D.G. (1986) Ground Ice. The Canadian Geographer, **30**(4), 362-363.

HASLAM, S.M. (1978) River plants. Cambridge University Press, Cambridge.

HAUSER, D.P. (1974) Some problems in the use of step-wise regression techniques in geographical research. The Canadian Geographer, **18**, 148-58.

HAYNES, R.J. and SWIFT, R.S. (1990) Stability of soil aggregates in relation to organic constituents and soil water content. Journal of Soil Science, **41**, 73-83.

HEMPHILL, R.W. and BRAMLEY, M.E. (1989) Protection of River and Canal Banks. Construction Industry Research and Information Association, Butterworths, London.

HEY, R.D. and THORNE, C.R. (1984) Flow processes and river channel morphology. In BURT, T.P. and WALLING, D.E. (Eds), Catchment Experiments in Fluvial Geomorphology, Geobooks, Norwich, 489-514.

HICKIN, E.J. and NANSON, G.C. (1975) The character of channel migration on the Beatton River, Northeast British Columbia, Canada. Geological Society of America Bulletin, **86**, 487-494.

HICKIN, E.J. and NANSON, G.C. (1984) Lateral migration rates of river bends. A.S.C.E. Journal of Hydraulic Engineering, **110**, (HY11), 1557-156.

HILL, A.R. (1973) Erosion of river banks composed of glacial till near Belfast, Northern Ireland. Zeitschrift für Geomorphologie, **17**(4), 428-442.

HOLMES, N.T.H. and WHITTON, B.A. (1977) Macrophytic vegetation of the River Swale, Yorkshire. Freshwater Biology, **7**, 545-558.

HOOKE, J.M. (1979) An analysis of the processes of river bank erosion. Journal of Hydrology, **42**, 39-62.

HOOKE, J.M. (1980) Magnitude and distribution of rates of river bank erosion. Earth Surface Processes and Landforms, **5**, 143-157.

HOOKE, J.M. (1987) Changes in meander morphology. In GARDINER, V. (Ed), International Geomorphology 1986 Part 1, Wiley, Chichester, 591-609.

HOOKE, J.M. (1995) Processes of channel planform change on meandering channels in the U.K. In GURNELL, A.M. AND PETTS, G.E. (Eds), Changing River Channels, Wiley, Chichester, 87-115.

HUANG, H.Q. and NANSON, G.C. (1997) Vegetation and channel variation; a case study of four small streams in southeastern Australia. Geomorphology, **18**, 237-249.

HUDSON, N.W. (1965) The influence of rainfall mechanics on soil erosion. Unpublished M.Sc. Thesis. Cape Town University.

HUGHES, D.J. (1977) Rates of erosion on meander arcs. In GREGORY, K.J. (Ed), River Channel Changes, Wiley, 193-205.

HUPP, C.R. and SIMON, A. (1986) Vegetation and bank-slope development. Proceedings, 4th Federal Interagency Sedimentation Conference, Las Vegas.

IMESON, A.C. and JUNGERIUS, P.D. (1977) The widening of valley incisions by soil fall in a forested Keuper area, Luxembourg. Earth Surface Processes and Landforms, **2**, 141-152.

INSTITUTE OF HYDROLOGY (1995) Hydrological data UK: 1995 Yearbook. Institute of Hydrology, Wallingford.

JARVIE, H.P., NEAL, C.N., and ROBSON, A.J. (1997) The Geography of the Humber catchment. Science of the Total Environment, **194/195**, 87-99.

JONES, J.A.A. (1981) The nature of soil piping: a review of research. BGRG research monograph, **3**, Geo Abstracts, Norwich.

KESEL, R.H. and BAUMANN, R.H. (1981) Bluff erosion of a Mississippi River meander at Port Hudson, Louisiana. Physical Geography, 2(1), 62-82.

KESEL, R.H., DUNNE, K.C., MCDONALD, R.C, ALLISON, K.R. and SPICER, B.E. (1974) Lateral erosion and overbank deposition on the Mississippi River in Louisiana caused by 1973 flooding. Geology, **2**, 461-464.

KLIMEK, K. (1974) The retreat of alluvial river banks in the Wisloka valley (South Poland). Geographica Polonica, **28**, 59-76.

KNIGHTON, A.D. (1973) Riverbank erosion in relation to streamflow conditions, River Bollin-Dean, Cheshire. East Midlands Geographer, **5**, 416-426.

KNIGHTON, A.D. (1987) River channel adjustment – the downstream dimension. In Richards, K.S. (Ed), River Channels, Wiley, Chichester, 95-128.

KNIGHTON, A.D. (1998) Fluvial forms and processes: a new perspective. Arnold, London.

KNIGHTON, A.D. (1999) Downstream variation in stream power. Geomorphology, **29**, 293-306.

KONDOLF, G.M. and CURRY, R.R. (1986) Channel erosion along the Carmel River, Monterey County, California. Earth Surface Processes and Landforms, **11**, 307-319.

LACZAY, I.A. (1977) Channel pattern changes of Hungarian rivers: the example of the Hernad River. In Gregory, K.J. (Ed), River Channel Changes, Wiley, 185-192.

LANE, S.N., BIRON, P.M., BRADBROOK, K.F., BUTLER, J.B., CHANDLER, J.H., CROWELL, M.D., MCLELLAND, S.J., RICHARDS, K.S. and ROY, A.G. (1998) Three-dimensional measurement of river channel flow processes using acoustic doppler velocimetry. Earth Surface Processes and Landforms, **23**, 1247-1267.

LANE, S.N., JAMES, T.D. and CROMWELL, M.D. (2000) Application of digital photogrammetry to complex topography for geomorphological research. Photogrammetric Record, **16**(95), 793-821.

LAPOINTE, M.F. and CARSON, M.A. (1986) Migration of an asymmetric meandering river, the Rouge River, Quebec. Water Resources Research, **22**(5), 731-743.

LAUBEL, A., SVENDSEN, L.M., KRONVANG, B., and LARSEN, S.E. (1999) Bank erosion in a Danish lowland stream system. Hydrobiologia, **410**, 279-285.

LAURY, R.L. (1971) Stream bank failure and rotational slumping: preservation and significance in the geological record. Geological Society of America Bulletin, **82**, 1251-1266.

LAW, M., WASS, P. and GRIMSHAW, D. (1997) The hydrology of the Humber catchment. The Science of the Total Environment, **194/195**, 119-128.

LAWLER, D.M. (1978) The use of erosion pins in river banks. Swansea Geographer, **16**, 9-18.

LAWLER, D.M. (1984) Processes of river bank erosion: the River Ilston, South Wales, U.K. Unpublished Ph.D. Thesis, University of Wales, 518 pp.

LAWLER, D.M. (1986) River bank erosion and the influence of frost: a statistical examination. Transactions of the Institute of British Geographers, NS **11**, 227-242.

LAWLER, D.M. (1987a) Spatial variability in the climate of the Severn Basin: a palaeohydrological perspective. In GREGORY, K.J., LEWIN, J. and THORNES, J.B. (Eds), Palaeohydrology in Practice, Wiley, Chichester, 49-78.

LAWLER, D.M. (1987b) Bank erosion and frost action: an example from South Wales. In Gardiner, V. (Ed), International Geomorphology, 1986, part 1, Wiley, Chichester, 575-590.

LAWLER, D.M. (1988a) Environmental limits of needle ice: a global survey. Arctic and Alpine Research, **20**, 137-159.

LAWLER, D.M. (1988b) A bibliography of needle ice. Cold Regions Science and Technology, **15**, 295-310.

LAWLER, D.M. (1989) Some new developments in erosion monitoring: 1. The potential of optoelectronic techniques. School of Geography Working Paper Series, **No. 47**, University of Birmingham, 44 pp.

LAWLER, D.M. (1991) A new technique for the automatic monitoring of erosion and deposition rates. Water Resources Research, **27**(8), 2125-2128.

LAWLER, D.M. (1992a) Process dominance in bank erosion systems. In CARLING, P. and PETTS, G.E. (Eds), Lowland Floodplain Rivers: Geomorphological Perspectives, Wiley, Chichester, 117-143.

LAWLER, D.M. (1992b) Design and installation of a novel automatic erosion monitoring system. Earth Surface Processes and Landforms, **17**, 455-463.

LAWLER, D.M. (1993a) The measurement of river bank erosion and lateral channel change: a review. Earth Surface Processes and Landforms, **18**, 777-821.

LAWLER, D.M. (1993b) Needle ice processes and sediment mobilization on river banks: the River Ilston, West Glamorgan, U.K. Journal of Hydrology, **150**, 81-114.

LAWLER, D.M. (1994) Temporal variability in streambank response to individual flow events: the River Arrow, Warwickshire, UK. In OLIVE, L.J., LOUGHRAN, R.J. and KESBY, J.A. (Eds), Variability in Stream Erosion and Sediment Transport, Proc. Canberra Symposium. I.A.H.S. Publ., **224**, 171-180.

LAWLER, D.M. (1995) The impact of scale on the processes of channel side sediment supply: a conceptual model. In OSTERCAMP, W.R. (Ed), Effects of Scale on the Interpretation and Management of Sediment and Water Quality, IAHS, **226**, 175-185.

LAWLER, D.M. and LEEKS, G.J.L. (1992) River bank erosion events on the Upper Severn detected by the Photo-Electronic Erosion Pins (PEEP) system. In BOGEN, J., WALLING, D.E. AND DAY, T.J. (Eds), Erosion and Sediment Transport Monitoring Programmes in River Basins, Proc. Oslo Symp., I.A.H.S. Publ., **210**, 95-105.

LAWLER, D.M., THORNE, C.R. and HOOKE, J.M. (1997) Bank erosion and instability. In THORNE, C.R., NEWSON, M. and HEY, R.D. (Eds), Guidebook of Applied Fluvial Geomorphology for River Engineering and Management, Wiley, Chichester.

LAWLER, D.M., GROVE, J.R., COUPERTHWAITE, J.S. and LEEKS, G.J.L. (1999) Downstream change in river bank erosion rates in the Swale-Ouse system, northern England. Hydrological Processes, **13**, 977-992.

LECCE, S.A. (1997) Nonlinear downstream changes in stream power on Wisconsin's Blue River. Annals of the Association of American Geographers, **87**(3), 471-486.

LECCE, S.A. and PAVLOWSKY, R.T. (1997) Storage of mining-related zinc in floodplain sediments, Blue River, Winsconsin. Physical Geography, **18**, 424-439.

LEEKS, G.J., LEWIN, J. and NEWSON, M.D. (1988) Channel change, fluvial geomorphology and river engineering: the case of the Afon Trannon, Mid-Wales. Earth Surface Processes and Landforms, **13**, 207-223.

LEEKS, G.J. and NEWSON, M.D. (1989) Responses of the sediment system of a regulated river. Regulated Rivers: Research and Management, **3**, 207-233.

LEOPOLD, L.B. (1973) River channel change with time: an example. Geol. Soc. Am. Bull., **84**, 1845-1860.

LEOPOLD, L.B. and MADDOCK, T. (1953) The hydraulic geometry of stream channels and some physiographic implications. U.S. Geological Survey Professional Paper, **252**, 57 pp.

LEOPOLD, L.B., WOLMAN, M.G. and MILLER, J.P. (1964) Fluvial Processes in Geomorphology. W.H. Freeman & Co., 522 pp.

LEOPOLD, L.B., EMMETT, W.W. and MYRICK, R.H. (1966) Channel and hillslope processes in a semi arid area, New Mexico. U.S. Geological Survey Professional Paper, 352-G.

LEWIN, J. (1972) Later stage meander growth. Nature, **240**, 116.

LEWIN, J. (1982) British Floodplains. In ADLAM, B.H., FENN, C.R. and MORRIS, L. (Eds), Papers in Earth Studies, Geo Books, Norwich, UK.

LEWIN, J. (1983) Changes of channel patterns and floodplains. In GREGORY, K.J. (Ed) Background to Palaeohydrology, Wiley, New York.

LEWIN, J. (1987) Historical river channel changes. In GREGORY, K.J., LEWIN, J. and THORNES, J.B. (Eds) Palaeohydrology in Practice, Wiley, Chichester, 161-175.

LEWIN, J., CRYER, R., and HARRISON, D.I. (1974) Sources for sediments and solutes in Mid-Wales. Institute of British Geographers Special Publication, **6**, 73-85.

LEWIN, J., DAVIS, B.E. and WOLFENDEN, P.J. (1977) Interactions between channel change and historic mining sediments. In Gregory, K.J. (Ed), River Channel Changes, John Wiley & Sons, New York, 353-368.

LIMERINOS, J.T. (1970) Determination of the Manning roughness coefficient from bed roughness in natural channels. United States Geological Survey Water Supply Paper, 1898-B.

LITTLE, W.C., THORNE, C.R. and MURPHEY, J.B. (1982) Mass bank failure analysis of selected Yazoo basin streams. Transactions A.S.A.E., **25**(5), 1321-1328.

LOHNES, R. and HANDY, R.L. (1968) Slope angles in friable loess. Journal of Geology, **76**, 247-258.

LONGFIELD, S.A. (1994) Historical River Channel Change at the Piedmont-Lowland Transition Zone: The River Swale, Northern England. Unpublished BSc.(Hons) Dissertation, University of Newcastle Upon Tyne.

LONGFIELD, S.A. and MACKLIN, M.G. (1999) The influence of recent environmental change on flooding and sediment fluxes in the Yorkshire Ouse basin. Hydrological Processes, **13**, 1051-1066.

MACKLIN, M.G., RIDGWAY, J., PASSMORE, D.G., and RUMSBY, B.T. (1994) The use of overbank sediment for geochemical mapping and contamination assessment: results from selected English and Welsh floodplains. Applied Geochemistry, **9**, 689-700.

MACKLIN, M.G., HUDSON-EDWARDS, K.A. and DAWSON, E.J. (1997) The significance of pollution from historic metal mining in the Pennine orefields on river sediment contaminant fluxes to the North Sea. Science of the Total Environment, **194/195**, 391-197.

MACKLIN, M.G. and LEWIN, J. (1997) Channel, Floodplain and Drainage Basin Response to Environmental Change. In THORNE, C.R., NEWSON, M. and HEY, R.D. (Eds). Guidebook of Applied Fluvial Geomorphology for River Engineering and Management, Wiley, Chichester.

MAGILLIGAN, F.J. (1992) Thresholds and the spatial variability of flood power during extreme floods. Geomorphology, **5**, 373-390.

MALVERN INSTRUMENTS (1994) Mastersizer Micro User Manual, Malvern, Worcester, U.K.

MARKHAM, A.J. and THORNE, C.R. (1992) Geomorphology of gravel-bed river bends. In BILLI, P., HEY, R.D., THORNE, C.R. and TACCONI, P. (Eds), Dynamics of Gravel-bed Rivers, Wiley, Chichester, 433-450.

MCEWEN, L.J. (1994) Channel planform adjustment and stream power variations on the middle River Coe, Western Grampian Highland, Scotland. Catena, **21**, 357-374.

MCGREAL, W.S. and GARDINER, T. (1977) Short-term measurements of erosion from a marine and a fluvial environment in County Down, Northern Ireland. Area, **9**, 285-289.

MCGREGOR, K.C. AND MUTCHLER, C.K. (1976) Status of the *R* factor in northern Mississippi soil erosion: prediction and control. Soil Conservation Society of America, 135-142.

MCKENNEY, R., JACOBSEN, R.B. and WERTHEIMER, R.L. (1995) Woody vegetation and channel morphogenesis in low gradient, gravel-bed streams in the Ozark Plateaus, Missouri and Arkansas, Geomorphology, **13**, 175-198.

MCRAE, S.G. (1988) Practical pedology: studying soils in the field. Ellis Horwood, Chichester.

MEERTEMEYER, V. and ZIPPIN, J. (1981) Soil moisture and texture controls of selected parameters of needle ice growth. Earth Surface Processes and Landforms, **6**, 113-125.

MILES, M. (1976) An investigation of riverbank erosion, Banks Island, District of Franklin. Geological Survey of Canada Paper, **76-A**, 195-200.

MILLAR, R.G. and QUICK, M.C. (1997) Stable width and depth of gravel-bed rivers with cohesive banks. ASCE Journal of Hydraulic Engineering, **124**(10), 1005-1013.

MORISAWA, M. (1985) Rivers: form and process. Longman, London, 220 pp.

MOSELEY, M.P. (1973) Rainsplash and the convexity of badland divides. Zeitschrift für Geomorphologie, supp. band **18**, 10-25.

MOSLEY, M.P. (1975) Channel changes on the River Bollin, Cheshire, 1872-1973. East Midland Geographer, **42**, 185-199.

MOSSELMAN, E. (1992) Mathematical Modelling of Morphological Processes in Rivers with Erodible Banks. Unpublished Ph.D. Thesis, Delft University of Technology, 134 pp.

MURGATROYD, A.L. and TERNAN, J.L. (1983) The impact of afforestation on stream bank and channel form. Earth Surface Processes and Landforms, **8**, 357-369.

NANSON, G.C. and BEACH, H.F. (1977) Forest succession and sedimentation on a meandering-river floodplain, northeast British Columbia, Canada. Journal of Biogeography, **4**, 229-251.

NANSON, G.C. and HEAN, D. (1985) The West Dapto flood of February 1984: rainfall characteristics and channel changes. Australian Geographer, **16**, 249-258.

NATIONAL RIVERS AUTHORITY (1995a) Understanding Riverbank erosion from a Conservation Perspective. NRA Publication NY-4/95-2.k-E-ANFQ, National Rivers Authority, 21 pp.

NATIONAL RIVERS AUTHORITY (1995b) Rivers Swale, Ure and Ouse Catchment Management Plan: Final Plan. NRA Publication NY-01/95-2K-E-AMXD, National Rivers Authority, York, 28 pp.

NATIONAL RIVERS AUTHORITY (1996) Rivers Swale, Ure and Ouse Catchment Management Plan Annual Review. NRA Publication NY-1/96-0.6k-E-AQKV, National Rivers Authority, York, 29 pp.

NEWSON, M. and PADMORE, C. (1995) Fluvial geomorphology, physical habitat and channel maintenance: problems of the Kiplin Hall reach, River Swale, North Yorkshire. Department of Geography, University of Newcastle upon Tyne.

ODGAARD, A.J. (1987) Streambank erosion along two rivers in Iowa. Water Resources Research, **23**(7), 1225-1236.

OSMAN, A.M. and THORNE, C.R. (1988) Riverbank stability analysis I: theory. A.S.C.E. Journal of Hydraulic Engineering, **114**, (HY2), 134-150.

OUTCALT, S.I. (1971) An algorithm for needle ice growth. Water Resources Research, **7**, 394-400.

PAGE, K.J. and CARDEN, Y.R. (1998) Channel Adjustment Following the Crossing of a Threshold: Tarcutta Creek, Southeastern Australia. Australian Geographical Studies, **36**(3), 289-311.

PARKER, G., DIPLAS, P. and AKIYAMA, J. (1983) Meander bends of high amplitude. A.S.C.E. Journal of Hydraulic Engineering, **109**, (HY10), 1323-1337.

PENTZ, S.B. and KOSTSCHUK, R.A. (1999) Effect of placer mining on suspended sediment in reaches of sensitive fish habitat. Environmental Geology, **37**(1-2), 78-89.

PETIT, F. and PAUQUET, A. (1997) Bankfull discharge recurrence interval in gravel-bed rivers. Earth Surface Processes and Landforms, **22**(7), 685-693.

PETKOVIC, S., DRAGOVIC, N. and MARKOVIC, S. (1998) Fluvial processes on the Juzna Morava River. In IRTCES (Ed), Proc. International Symposium on Comprehensive Watershed Management, Patent Documentation, Beijing, September 1998, 357-364.

PETTS, G.E. (1980) Morphological changes of river channels consequent upon headwater impoundments. Journal of the Institution of Water Engineers and Scientists, **34**, 374-382.

PETTS, G.E. (1983) Sources and Methods in Geography: Rivers. Butterworths, London.

PETTS, G., ARMITAGE, P. and CASTELLA, E. (1993) Physical habitat changes and macroinvertibrate response to river regulation – the River Rede, UK. Regulated Rivers – Research and Management, **8**(1-2), 167-178.

PIZZUTO, J.E. (1982) Channel-forming processes of straight sandbed streams. Unpublished Ph.D. Thesis, University of Minnesota, 190 pp.

PIZZUTO, J.E. (1984) Bank erodibility of shallow sandbed streams. Earth Surface Processes and Landforms, **9**, 113-124.

PIZZUTO, J.E. (1990) Numerical simulation of gravel river widening. Water Resources Research, 26(9), 1971-1980.

PIZZUTO, J.E. and MECKELNBURG, T.S. (1989) Evaluation of a linear bank erosion equation. Water Resources Research, **25**, 1005-1013.

PRESTEGAARD, K.L. (1988) Morphological controls on sediment delivery pathways. In Bordas, M.P. and Walling, D.E. (Eds), Sediment Budgets Proc. Porto Alegre Symposium 1988, I.A.H.S. Publ. **174**, 533-540.

PUGH, J.C. (1975) Surveying for field scientists. Methuen, London.

RADLEY, J. and SIMMS, C. (1971) Yorkshire Flooding – Some Effects on Man and Nature. Ebor Press, York.

RAISTRICK, A. (1975) The lead industry of Wensleydale and Swaledale – Vol. 1: The Mines. Moorland Publishing Co., Buxton.

RAWLINGS, J.O. (1988) Applied regression analysis: a research tool. Wadsworth & Brooks, Pacific Grove, California.

RHOADS, B.L. (1987) Stream power terminology. Professional Geographer, **39**, 189-195.

RICHARDS, K.S. (1982) Rivers: form and process in alluvial channels. Methuen, London, 358 pp.

RICHTER, B.D., BAUMGARTNER, J.V., BRAUN, D.P., and POWELL, J. (1998) A spatial assessment of hydraulic alteration within a river network. Regulated Rivers: Research and Management, **14**(4), 329-340.

RINALDI, M. and CASAGLI, N. (1999) Stability of streambanks formed in partially saturated soils and effects of negative pore water pressures: the Sieve River (Italy). Geomorphology, **26**, 253-277.

RITTER, D.F., KOCHEL, R.C. and MILLAR, J.R. (1999) The disruption of Grassy Creek: implications concerning catastrophic events and thresholds. Geomorphology, **29**(3-4), 323-338.

ROBINSON, M. (1990) Impact of Improved Land Drainage on River Flows. Institute of Hydrology Report No. 113, Institute of Hydrology, Wallingford, 226 pp.

ROSEWELL, C.J. (1986) Rainfall kinetic energy in eastern Australia. Journal of Climate and Applied Meteorology, **25**, 1695-1701.

RYDER, P.F. (1975) Phreatic Network Caves in the Swaledale Area. Yorkshire, Trans. British Cave Research Assoc. **2** (4), 177-192.

SALLES, C. and POESEN, J. (2000) Rain properties controlling soil splash detachment. Hydrological Processes, **14**(2), 271-282.

SANSOM, A. (1996) Floods and sheep – is there a link? Bulletin of the British Ecolological Society, **1**, 27-32.

SCHUMM, S. A. (1994) Erroneous perceptions of fluvial hazards. Geomorphology, **10**(1-4), 129-138.

SCOTT, K.M. (1978) Effects of permafrost on stream channel behaviour in Arctic Alaska, U.S. Geological Survey Professional Paper, **1068**, 19 pp.

SCOTT, K.M. (1982) Erosion and sedimentation in the Kenai River, Alaska. U.S. Geological Survey Professional Paper, **1235**, 35pp.

SEBER, G.A.F. (1977) Linear regression analysis. Wiley, New York.

SEDGWICK, C. (2000) Impacts of Environmental Change on Re-mobilisation of Sediment-Associated Contaminants in Flood Plains. Unpublished Ph.D. Thesis, University of Leeds.

SELBY, M.J. (1982) Hillslope materials and processes. Oxford University Press, Oxford.

SIDLE, R.C. (1991) A conceptual-model of changes in root cohesion in response to vegetation management. Journal of Environmental Quality, **20**(1), 43-52.

SIMON, A. (1989) A model of channel response in disturbed alluvial channels. Earth Surface Processes and Landforms, **14**, 11-26.

SIMON, A. AND HUPP (1990) The recovery of alluvial systems in response to imposed channel modifications, West Tennessee, USA. In Thornes, J.B. (Ed), Vegetation and erosion, processes and environments, John Wiley & Sons, Chichester.

SIMON, A., WOLFE, W.J. and MOLINAS, A. (1991) Mass-wasting algorithms in an alluvial channel model. Proc. Fifth Federal Interagency Sedimentation Conference, Las Vegas, 2: 8-22 to 8-29.

SIMON, A. AND HUPP (1992) Geomorphic and vegetative recovery processes along modified stream channels of West Tennesee. US. Geological Survey Open-File Report **91-502**, Nashville, Tennessee.

SIMON, A. and DARBY, S.E. (1997) Process-form interactions in unstable sand-bed river channels: numerical modelling approach. Geomorphology, **21**(2), 85-106.

SMITH, D.G. (1976) Effect of vegetation on lateral migration of anastomosed channels of a glacier meltwater river. Geological Society of America Bulletin, **77**, 859-866.

STANLEY, D.J., KRINITZKY, E.L. and COMPTON, J.R. (1966) Mississippi River bank failure, Fort Jackson, Louisiana. Geological Society of America Bulletin, **77**, 859-866.

STEBBING, A.R.D, HUNTLEY, D. and LEEKS, G.J.L. (1998) Integrated riverine, estuarine and coastal research in the UK Land-Ocean Interaction Study (LOIS). Introduction to the Land-Ocean Interaction Study. Marine Pollution Bulletin, **37**(3-7), 115-121.

STOTT, T. (1997) A comparison of stream bank erosion processes on forested and moorland streams in the Balquihidder catchments, central Scotland. Earth Surface Processes and Landforms, **22**, 383-399.

STOTT, T. (1999) Stream Bank and Forest Ditch Erosion: Preliminary Responses to Timber Harvesting in Mid-Wales. In BROWN, A.G. and QUINE, T.A. (Eds), Fluvial Processes and Environmental Change, John Wiley & Sons, 47-70.

STOTT, T.A.., FERGUSON, R.I., JOHNSON, R.C. and NEWSON, M.D. (1986) Sediment budgets in forested and unforested basins in upland Scotland. In HADLEY, R.F. (Ed), Drainage Basin Sediment Delivery, International Association of Hydrological Sciences Publication, **159**, 57-68.

SUNDBORG, A. (1956) The River Klaralven, a study of fluvial processes. Geografiska Annaler, **38**, 127-316.

TABACCHI, E., PLANTY, A.M., SALINAS, M.J. and DECAMPS, H. (1996) Landscape structure and diversity in riparian plant communities: A longitudinal comparative study. Regulated Rivers – Research and Management, **12**(4-5), 367-390.

TALCOTT, D.V. (1936) Report of the Company. Harrison Smith and Robert Haas, New York.

TAYLOR, D.W. (1948) Fundamentals of Soil Mechanics, John Wiley & Son, New York.

THORNE, C.R. (1978) Processes of bank erosion in river channels, Unpublished Ph.D. Thesis, University of East Anglia, 477 pp.

THORNE, C.R. (1981) Field measurements of rates of bank erosion and bank material strength. Proc. Florence Symposium, I.A.H.S. publ., **133**, 503-512.

THORNE, C.R. (1982) Processes and mechanisms of river bank erosion. In HEY, R.D., BATHURST, J.C. and THORNE, C.R. (Eds), Gravel Bed Rivers, Wiley, Chichester, 227-259.

THORNE, C.R. (1990) Effects of vegetation on riverbank erosion and stability. In THORNES, J.B. (Ed), Vegetation and Erosion, Wiley, Chichester, 125-144.

THORNE, C.R. (1991) Bank erosion and meander migration of the Red and Mississippi Rivers, U.S.A. Hydrology for the Water Management of Large River Basins, Proc. of the Vienna Symposium, August 1991, I.A.H.S. Publ., **201**, 301-313.

THORNE, C.R. (1993) Guidelines for the Use of Stream Reconnaissance Record Sheets in the Field. Final Report to U.S. Army European Research Office, Contract Report HL-93-2.

THORNE, C.R. (1998) Stream Reconnaissance Guidebook: Geomorphological Investigation and Analysis of River Channels. John Wiley & Sons, Chichester.

THORNE, C.R. and LEWIN, J. (1979) Bank processes, bed material movement and planform development in a meandering river. In RHODES, D.D. and WILLIAMS, G.P. (Eds), Adjustments of the Fluvial System, Kendall/Hunt Publication Co. Dubuque, Iowa, 117-137.

THORNE, C.R. and TOVEY, N.K. (1981) Stability of composite river banks. Earth Surface Processes and Landforms, **6**, 469-484.

THORNE, C.R. and OSMAN, A.M. (1988) The influence of bank stability on regime geometry of natural channels. In White, W.R. (Ed), International Conference on River Regime, 18-20 May 1988, Wiley, Chichester, 135-147.

THORNE, C.R. and ABT, S.R. (1993) Analysis of riverbank instability due to toe scour and lateral erosion. Earth Surface Processes and Landforms, **18**, 835-843.

THORNE, C.R., DARBY, S.E., KNIGHT, D.K., WATSON, C.C., QUICK, M., PIZZUTO, J.E., DIPLAS, P., STEVENTS, M. and LI, L. (1998) Task Committee on River Width Adjustment, I: Processes and Mechanisms , (C.R. THORNE – Chair), Journal of Hydraulic Engineering, **124**(9), 881-902.

TRIMBLE, S.W. (1994) Erosional effects of cattle on streambanks in Tennessee, U.S.A. Earth Surface Processes and Landforms, **19**, 451-464.

TRIMBLE, S.W. (1995) Catchment Sediment Budgets and Change. In Gurnell, A. and Petts, G. (Eds), Changing River Channels, John Wiley & Sons, Chichester.

TRIMBLE, S.W. and MENDEL, A.C. (1995) The cow as a geomorphic agent – a critical review. Geomorphology, **13**, 233-253.

TWIDALE, C.R. (1964) Erosion of an alluvial bank at Birdwood, South Australia. Zeitschrift für Geomorphologie, **8**, 189-211.

WALKER, J., ARNBORG, L. and PEIPPO, J. (1987) Riverbank erosion in the Colville Delta, Alaska. Geographiska Annaler, **69A**, 61-70.

WALLING, D.E., OWENS, P.N., WATERFALL, B.D., LEEKS, G.J.L. and WASS, P.D. (1999) The particle size characteristics of fluvial suspended sediment in the Humber and Tweed catchments, UK. Science of the Total Environment, **251/252**, 205-222.

WEBSTER, R. and OLIVER, M.A. (1990) Statistical Methods in Soil and Land Resource Survey. Oxford University Press, Oxford.

WILLIAMS, D.R., ROMERIL, P.M. and MITCHELL, R.J. (1979) Riverbank erosion and recession in the Ottawa area. Canadian Geotechnical Journal, **16**, 641-650.

WILKINSON, W.B., LEEKS, G.J.L., MORRIS, A. and WALLING, D.E. (1997) Rivers and coastal research in the Land Ocean Interaction Study. Science of the Total Environment, **194**, 5-14.

WILSON, P. and HEGARTY, C. (1993) Morphology and causes of recent peat slides on Skerry Hill, County Antrim, Northern Ireland. Earth Surface Processes and Landforms, **18**, 593-601.

WOLMAN, M.G. (1954) A method of sampling coarse river-bed material. Transactions of the American Geophysical Union, **14**, 951-956.

WOLMAN, M.G. (1959) Factors influencing erosion of a cohesive river bank. American Journal of Science, **257**, 204-216.

WOLMAN, M.G. and LEOPOLD, L.B. (1957) River flood plains; some observations on their formation. U.S. Geological Survey Professional Paper, 282C.

WRIGHT, G.N. (1977) The Yorkshire Dales. David and Charles, Newton Abbot.

ZANCHI, C. AND TORRI, D. (1980) Evaluation of rainfall energy in central Italy. In DE BOODT, M. AND GABRIELS, D. (Eds) Assessment of Erosion. Wiley, Toronto, 133-142.

APPENDIX I

Grove, J.R. and Sedgwick, C. (1998) Downstream spatial and temporal remobilisation of heavy metal contaminated sediments in the River Swale, England. In IRTCES (Ed), Proc. International Symposium on Comprehensive Watershed Management, Patent Documentation, Beijing, September 1998, 505-512.

APPENDIX II

Lawler, D.M., Grove, J.R., Couperthwaite, J.S. and Leeks, G.J.L. (1999) Downstream change in river bank erosion rates in the Swale-Ouse system, northern England. Hydrological Processes, 13, 977-992.